SCHOOL OF ENGINEERING

ASSESSMENT OF SUSTAINABILITY OF PAPYRUS-BASED WETLAND WATER RESOURCES IN UGANDA

By

Alem Oyarmoi

A thesis submitted for the degree of *Doctor of Philosophy* at Newcastle University

July 2024

To my late dad, Okello Oyarmoi*,*

My mum, Lamaci Martina Oyarmoi*, and*

My beloved Uncle, Hon. Justice Alphonse Owiny-Dollo Chigamoy

ACKNOWLEDGEMENTS

Reflecting on the last four years, I see that my tenacity and many people's enormous guidance and support made this PhD study possible.

Firstly, I thank my supervisors, Caspar Hewett, Stephen Birkinshaw, and Hayley Fowler, who immensely contributed, each with their expertise, to the success of this work. I couldn’t have wished for better! Special thanks to Caspar, my principal supervisor, for accepting me as a PhD student and for his wholehearted support and patience. Thank you, Stephen, for wholeheartedly teaching me the art of hydrological modelling. Hayley, you made me think differently and critically every time we had a supervisory meeting. Thank you!

I wouldn't have pursued this PhD without the UK Commonwealth Scholarship Commission's (CSC) financial support. Thus, I thank the UK government and the technical and administrative staff of the CSC, Programme Officers in particular, for assisting me with all practicalities.

As a student at Newcastle University, I could access non-academic guidance from the Cassie Building reception Team. In a particular way, I thank Melissa Ware for her help during my study.

I want to thank colleagues in the PGR room, Cassie Building, for making the office enjoyable. I am forever grateful to my buddies, Sven Berendsen, for teaching me coding in Python, Daryl Hughes, for making me feel at home in Newcastle, and Farzana Mohuya for being a good friend.

Finally, I thank my family for their patience and emotional support. God bless you all.

TABLE OF CONTENTS

ACKNOWLEDGEMENTS ii
ABSTRACT ix
PUBLICATIONS x
ACRONYMS AND ABBREVIATIONS xi
LIST OF FIGURES xiii
LIST OF TABLES xvii
CHAPTER 1: INTRODUCTION 1
Study Motivation 1
Case Study 1
Study Goal and Research Questions 4
Thesis Structure 5
CHAPTER 2: BACKGROUND 7
Climatology of the Region 7
Wetland Classification in the Mpologoma Catchment 8
Overview of Effects of Irrigated Agriculture on Wetlands 9
Overview of Effects of Climate Change on Wetland Ecosystems 14
Selection of Catchment Modelling Tool 15
CHAPTER 3: THE SHETRAN MODELLING SYSTEM 17
Overview of the SHETRAN Catchment Modelling Tool 17
Overland and River Flow Processes 18
3.1.1 Canopy interception of rainfall 18
3.1.2 Plant evapotranspiration 20
3.1.3 Overland and channel flow 21
3.1.4 Selection of channel dimension and bed elevation 23
3.1.5 Land cover/use categorisation in SHETRAN 23
3.1.6 Lake representation in SHETRAN 23

Unsaturated and Saturated Flow 24
3.1.7 Channel-groundwater interaction 25
CHAPTER 4: THE EFFECT OF PAPYRUS WETLANDS ON FLOW REGULATION IN A TROPICAL RIVER CATCHMENT 27
Abstract 27
Introduction 27
Materials and Methods 30
4.1.1 Study Area 30
4.1.2 Data Sources and Processing 31
4.1.3 Selection and Evaluation of Rainfall Products 32
4.1.4 Estimation of Potential Evapotranspiration (PET) 33
4.1.5 Measured Flow Data 33
4.1.6 Land Surface Representation 34
4.1.7 Land Cover and Land Use Layer 34
4.1.8 Soil and Lithology 35
Modelling Approach 35
Impacts of Wetlands on Catchment Discharge 37
4.1.9 Impacts of Wetlands on Baseflow and Quickflow 38
4.1.10 Impacts of Wetlands on Future Flood and Low Flows 39
Results 41
4.1.11 Model Calibration and Validation Results 41
4.1.12 Overall Impacts of Wetlands on Historical Catchment Hydrology 45
4.1.13 Impacts of Wetlands on Historical Baseflow and Quickflow 46
4.1.14 The Overall Impact of Wetlands on Future Catchment Hydrology 47
4.1.15 Impacts of Wetlands on Future Flood and Low Flows 48
Discussion 51
4.1.16 Historical Impacts of Wetlands on Catchment Hydrology 51

4.1.17 Impacts of Wetlands on Future Catchment Hydrology 52
Implications and Limitations 53
Conclusions 55
CHAPTER 5: LINKING THE FLOW REGIME OF PAPYRUS WETLANDS TO BIOLOGICALLY-RELEVANT HYDROLOGIC ATTRIBUTES 57
Abstract 57
Introduction 58
Study Area 62
Papyrus Wetlands as a Habitat 63
Methods and Materials 64
5.1.1 Illustrations of drivers of ecological change 64
5.1.2 Assessing hydrologic alteration 65
5.1.3 Hydrological modelling 67
5.1.4 Estimation of irrigation demand 69
Results 72
5.1.5 Naigombwa wetland illustration of drivers of ecological change 72
5.1.6 Overall effects of irrigation on wetland inflow 73
5.1.7 Hydrologic alterations due to irrigation 75
5.1.8 Effect of irrigation command area on hydrologic alteration 82
Linking Altered Flow Regimes to Papyrus Wetland's Biologically-Relevant Hydrologic Attributes 85
5.1.9 Effect of altered flow regimes on seed dispersal 85
5.1.10 Effect of altered flow regimes on seed germination and establishment 86
5.1.11 Effect of altered flow regimes on rhizome spreading 87
5.1.12 Effect of altered flow regimes on papyrus distribution across riverine transects 87
5.1.13 Effect of altered flow regimes on dispersal of floating mats 88

5.1.14 Effect of altered flow regimes on sustaining wetland habitats..... 89

Conclusions 89

CHAPTER 6: EFFECTS OF LOWLAND RICE IRRIGATION ON THE PAPYRI WETLAND FLOW REGIME UNDER A FUTURE CLIMATE..... 90

Abstract..... 90

Introduction 90

Materials and Methods..... 93

6.1.1 Study area 93

6.1.2 Hydrological modelling..... 94

6.1.3 Irrigation schedule and demand..... 95

6.1.4 Assessment of hydrological alteration..... 98

6.1.5 Estimation of the degree of alteration 99

Results..... 101

6.1.6 Overall hydrological prediction of the effects of irrigation and climate change wetland inflow 101

6.1.7 Effects of future climate on the Naigombwa wetland inflow regime 104

6.1.8 Effects of irrigation on the Naigombwa wetland inflow regime 105

6.1.9 The combined effects of irrigation and future change on wetland inflow 105

6.1.10 Effects of irrigation and climate change on the frequency and duration of high and low pulses..... 106

6.1.11 Effects of irrigation and climate change on rate and frequency of water condition changes 107

6.1.12 Effects of irrigation and climate change on the magnitude of monthly water conditions 109

6.1.13 Effects of irrigation and climate change on annual extreme water conditions 110

Discussion..... 112

Conclusions 114
CHAPTER 7: DISCUSSION, CONCLUSIONS AND RECOMMENDATIONS 116
Discussion 116
Main Caveats of the Research 120
7.1.1 How the use of a different distributed hydrological model could influence the study 120
7.1.2 Modelling limitation due to the use of GCM ensemble mean estimate 121
7.1.3 The effect of the modelled vegetation's static nature on the modelling results' validity 122
7.1.4 Uncalibrated language/terms used to represent different magnitudes of change in IHA indices 122
Conclusions 123
Recommendations for Future Research 125
BIBLIOGRAPHY 127
APPENDIX 1: SUPPLEMENTARY FIGURES 157
APPENDIX 2: SUPPLEMENTARY TABLES 162
APPENDIX 3: SUPPLEMENTARY EQUATIONS 172
APPENDIX 4: EVALUATION OF SATELLITE PRECIPITATION PRODUCTS (SPPs) WITH GAUGE DATA 173
Quality control of rain gauge data 173
Accuracy of SPPs in Daily Rainfall Identification 176
Accuracy of SPPs in Capturing Daily and Monthly Rainfall Totals 176
APPENDIX 5: MODEL SENSITIVITY ANALYSIS 178
Results of Model Sensitivity Analysis 179
APPENDIX 6: QUALITY CONTROL OF MEASURED FLOW DATA 180
APPENDIX 7: PROCESSING OF FUTURE PRECIPITATION PRODUCTS 182
Selection of suitable bias correction approach 182
Framework for evaluation of the success/appropriateness of bias correction 184

ABSTRACT

Wetlands contribute up to 43.5% of the value of earthly natural biomes, yet they cover only 3% of the planet's surface. The largest area of these wetlands, which is of international importance, is Africa, where they mainly occur as papyrus-dominated marshes. Studies on these wetlands seldom cover their flow regulation services, with none at the catchment scale. This has hindered their economic valuation and conservation. This study quantified their flow regulation service in a tropical catchment and linked its flow regime to its biologically relevant hydrologic attributes.

Results show that papyrus wetlands are at least four times better at regulating quickflow than baseflow. Predictions at 2 and 4°C global warming levels (GWLs) indicate they will play critical roles in mitigating flood risks by lowering future mean flood magnitude and halving the average number of flood events in a year. However, the future mean flood duration is expected to increase.

Their Environmental Flow Components (EFCs) can be broadly categorised into large floods, small floods, high flows, low (base) flows, and extreme low flows. These EFCs are significantly altered for the irrigated area to catchment area ratio greater than approximately 1:150 (i.e., irrigated area of 1,100 ha to catchment area of 1,680 km^2). The result, however, is subject to uncertainty in hydrological model parameter estimation and flow simulation, mainly due to inherent errors in the satellite-based precipitation product used. Large-scale river water abstraction and land use change are mostly linked to agriculture and are the leading cause of wetland loss in the developing world. In the case of papyrus wetlands, lowland rice cultivation considerably alters the magnitude, duration, timing and rate of change of EFCs. These modified EFCs directly impact papyrus's ability to reproduce (sexually and asexually), access groundwater during extreme low flows, and resist invasive species.

In general, the findings in this study can help policymakers and authorities in papyrus-dominated catchments plan for the protection and conservation of papyri wetlands, a keystone species on which wetland biodiversity depends.

PUBLICATIONS

The following people and institutions contributed to this thesis's publications.

Candidate: Alem Oyarmoi, Newcastle University

Author 1: Stephen Birkinshaw, Newcastle University (Supervisor)

Author 2: Caspar Hewett, Newcastle University (Primary Supervisor)

Author 3: Hayley Fowler, Newcastle University (Supervisor)

Paper 1: Oyarmoi, A.; Birkinshaw, S.; Hewett, C.J.M.; Fowler, H.J. (2023). The Effect of Papyrus Wetlands on Flow Regulation in a Tropical River Catchment. *Land*, 12, 2158. https://doi.org/10.3390/land12122158.

Paper 2: Oyarmoi**,** A**.**, Birkinshaw, S., Hewett, C. J. M, & Fowler, H. J. (under review). Linking the flow regime of papyrus wetlands to biologically-relevant hydrologic attributes. *Journal of Ecohydrology*, under review.

ACRONYMS AND ABBREVIATIONS

AET	Actual evapotranspiration
AWD	Alternate wetting and drying
BF	Baseflow
BL	Baseline
CCI	Climate Change Initiative
CF	Continuous flooding
CFSR	Climate Forecast System Reanalysis
CHIRPS	Rainfall Estimates from Rain Gauge and Satellite Observations
D	Degree of alteration
DEM	Digital elevation model
Do	Overall degree of alteration for each IHA group
Don	Overall degree of alteration of all IHA metrics
EFC	Environmental flow component
E_{ff}	Overall irrigation efficiency
EFR	Environmental flow regime
ESA	European Space Agency
FAR	False alarm ratio
FB	Frequency bias
GCM	Global climate model
GWL	Global warming level
GWL2	2 °C Global warming level
GWL4	4 °C Global warming level
HSS	Heidke skill score
I_{gross}	Gross irrigation requirement for crops other than rice
$I_{grossRice}$	Rice gross irrigation requirement
IHA	Indicators of Hydrologic Alteration
I_{net}	Net irrigation requirement
MAAIF	Ministry of Agriculture, Animal Industry and Fisheries
MSWEP	Multi-Source Weighted-Ensemble Precipitation
MWE	Ministry of Water and Environment
NSE	Nash-Sutcliffe efficiency
NUR	Rice nursery irrigation demand
Pbias	Percent bias
PET	Potential evapotranspiration
POD	Probability of detection
QF	Quickflow
R	Refers to "correlation coefficient" unless explicitly stated in the thesis
RQ	Research question
RSR	Root mean square error standard deviation ratio
RVA	Range of Variability Approach
SAT	Rice field puddling irrigation demand
SDGs	Sustainable Development Goals

SPP	Satellite-based precipitation products
TAMSAT	Tropical Applications of Meteorology using SATellite
WSI	Wetland Specific Impact

LIST OF FIGURES

Figure 1 - 1: Map of Mpologoma catchment and Naigombwa sub-catchment in Uganda, including the location of wetlands and the proposed irrigation scheme. 3

Figure 4 - 1: Mpologoma catchment elevation, rainfall zones, land cover and soil types. The rainfall zones were delineated and defined by Basalirwa (1995). 31
Figure 4 - 2: SHETRAN masks for Phase 1 (sub-catchment 82212) and Phase 2 (Mpologoma catchment) models, including the locations of river channels, lakes, and wetlands. 37
Figure 4 - 3: Daily timestep calibration (left column) and validation (right column) results at station 82212. The date format is in Day Month Year. 43
Figure 4 - 4: Monthly timestep calibration (left column) and validation (right column) results at station 82212. Months with data gaps in measured flow are not included. The date format is in Month Year. 44
Figure 4 - 5: Daily and monthly timestep calibration at station 82217 (top row) and validation at station 82218 (bottom row) results. For the monthly plots, months with data gaps in measured flow are not included. The date format is in Day Month Year for the daily plots and Month Year for the monthly plots. 45
Figure 4 - 6: Monthly and annual wetland-specific impact (WSI) on baseflow (left column) and quickflow (right column) at the catchment outlet. Computations are over 30 years (1984 to 2013). The boxplots show the mean (triangles), median, and interquartile range. The whiskers show the upper and lower limits, excluding any outliers (indicated as circles). 47
Figure 4 - 7: Violin plots of flood (top row) and low (bottom row) flow indices for the situation with and without wetlands. Flow duration and magnitude plots depict mean annual values, whereas frequency depicts the number of events in a year. The triangles indicate the average flow index over 30 years. 50
Figure 4 - 8: Hydrograph of baseflow and total flow for the water years 1985 (left column) and 2010 (right column). 52
Figure 4 - 9: Schematisation of steps followed in the study. 157
Figure 4 - 10: Scatter plots of daily rainfall total of SPPs and rain gauge data at Tororo (columns 1 and 3) and Buginyanya (columns 2 and 4). The dashed line shows the perfect fit that could be attained if the gauge and SPP data were equal. 158

Figure 4 - 11: Bar graphs of percent bias (column 1), mean absolute error (column 2), and Nash-Sutcliffe efficiency (column 3) at daily timescale for the various SPPs at Tororo and Buginyanya. 158
Figure 4 - 12: Scatter plots of monthly rainfall totals (satellite products against gauge) at Tororo (columns 1 and 3) and Buginyanya (columns 2 and 4). The dashed line shows the perfect fit that could be attained if the gauge and SPP data were equal. 159
Figure 4 - 13: Bar graphs of percent bias (column 1), mean absolute error (column 2), and Nash-Sutcliffe efficiency (column 3) at monthly timescale for the various SPPs at Tororo and Buginyanya. 160
Figure 4 - 14: Scatter plots of model response to changes in key parameters. Inset is the sensitivity index (SI). 160
Figure 4 - 15: 30-year ensemble mean of 'observed' (MSWEP and CFSR) and bias-corrected CMIP6 models over the Mpologoma catchment. The plots show mean monthly rainfall and potential evapotranspiration (PET) at baseline (BL, top left), global warming level 2 (GWL2, top right), and global warming level 4 (GWL2, bottom left). 161
Figure 4 - 16: Climatic rainfall zones in Uganda as defined by Basalirwa (1995, 1991), including locations of rain gauges in and at the vicinity of the Mpologoma catchment. 174
Figure 4 - 17: Double-mass curve of rain gauge data at Buginyanya, Jinja, Tororo and Kiige. 174
Figure 4 - 18: Impacts-centric evaluation framework for assessing bias correction methods (source: Vogel et al. (2023)). 186

Figure 5 - 1: Study area including catchment elevation, soils, land cover, proposed irrigation command area and dam location. 63
Figure 5 - 2: Schematic of a papyrus wetland cross-section. Inset is papyrus growth stages (A, B, C, D and E) and body parts (Adapted from Gaudet (1975)). 64
Figure 5 - 3: SHETRAN model domain showing the location of crucial catchment features (wetlands, lakes, irrigated area, and the reservoir). 69
Figure 5 - 4: Annual rice irrigation demand for continuous flooding (CF) and alternate wetting and drying (AWD) irrigation scheduling. The top row shows results for rice fields

in the upper part of the command area in Figure 5 - 3; the bottom row shows results for downstream rice fields. The difference in precipitation levels between these regions is the reason for the contrast. 72
Figure 5 - 5: Illustration of the linkage between ecosystem drivers and ecological attributes relevant to papyrus wetlands in the Naigombwa catchment. 73
Figure 5 - 6: Papyrus wetland inflow for scenarios with and without irrigation. The top row is Continuous Flooding (CF) irrigation. The bottom row is Alternate Wetting and Drying (AWD) irrigation...... 74
Figure 5 - 7: Time series of Naigombwa wetland inflow from the water year 1983 to the water year 2012 showing Environmental Flow Components for the situation with and without irrigation. Extreme low flow threshold = 0.72 m^3/s; high flow start threshold for rising limb = 2.38 m^3/s; low flow start threshold for falling limp = 1.21 m^3/s; small flood minimum peak flow = 5.26 m^3/s; large flood minimum peak flow = 10.04 m^3/s. 80

Figure 6 - 1: Naigombwa catchment boundary, soils, land cover, the planned irrigation command area, and the location of the irrigation reservoir. 94
Figure 6 - 2: Papyrus wetland inflow for scenarios with and without irrigation at baseline (BL) and global warming level 2 (GWL2). The top row is Continuous Flooding (CF) at BL and GWL2. The bottom row is Alternate Wetting and Drying (AWD) at BL and GWL2. 102
Figure 6 - 3: Papyrus wetland inflow for scenarios with and without irrigation at baseline (BL) and global warming level 4 (GWL4). The top row is Continuous Flooding (CF) at BL and GWL4. The bottom row is Alternate Wetting and Drying (AWD) at BL and GWL4. 102
Figure 6 - 4: Alterations in the annual frequency (top row) and median yearly duration (bottom row) of low (left column) and high (right column) flow pulses due to the combined effect of irrigation and climate change...... 107
Figure 6 - 5: Alterations in the median annual rate of change (hydrograph rise (left column) and fall (right column) rates) of flow conditions due to the combined effect of irrigation and climate change...... 108
Figure 6 - 6: Alterations in the median monthly flow magnitude due to the combined effect of irrigation and climate change. The water year in the study area is from March (top left graph) to February (bottom right graph)...... 110

Figure 6 - 7: Alterations in the median annual extreme flows (1-, 3-, 7-, 30-, and 90-day minimum (left column) and maximum (right column) values) due to the combined effect of irrigation and climate change. 111
Figure 6 - 8: 30-year median monthly wetland inflow for situations with and without irrigation at GWL2 (left column) and GWL4 (right column). 114

LIST OF TABLES

Table 2 - 1: Examples of riverine/lake systems catastrophically impacted by irrigation water extraction. 12

Table 3 - 1: Summary of SHETRAN water flow processes (Source: Ewen et al. (2000)). 17

Table 4 - 1: Lithological depths in Mpologoma catchment. 35
Table 4 - 2: List of models (with and without wetlands) simulated/forced with 'observed' (i.e., MSWEP and CFSR) and CMIP6 climatic datasets. BL, GWL2 and GWL4 refer to Baseline, Global Warming Level 2, and Global Warming Level 4, respectively. 41
Table 4 - 3: Mean annual precipitation, actual evapotranspiration, and catchment discharge over 30 years (1984 to 2013) for the situation with and without wetlands. Models were driven with MSWEP and CFSR precipitation and PET datasets, respectively. 46
Table 4 - 4: Mean annual precipitation, actual evapotranspiration, and catchment discharge over 30 years for the situation with and without wetlands. The models were forced with bias-corrected GCM precipitation and PET datasets; however, the results are based on an ensemble average. 48
Table 4 - 5: Mean and range of flow indices (duration, magnitude, and frequency) for the situation with (w) and without (wo) wetlands over 30 years. Results are based on an ensemble average. 50
Table 4 - 6: Key satellite-based precipitation products (SPPs) often applied over Africa. 162
Table 4 - 7: FAR, POD, FB and HSS at Tororo and Buginyanya rain gauge stations over January 2001 and December 2016. 163
Table 4 - 8: List of best-performing CMIP6 GCM models over the Uganda region. The list is based on the findings of Ayugi, Zhihong, et al. (2021) and Ngoma et al. (2021). 164
Table 4 - 9: Rain gauge annual precipitation for the double mass curve. The analysis is restricted to years with no missing data. 175
Table 4 - 10: Number of months at each station with complete daily flow records. 181

Table 4 - 11: Evaluation approaches for bias correction methods (source: Vogel et al. (2023)). 186

Table 5 - 1: Summary of the 33 hydrological parameters used in the Indicators of Hydrologic Alteration (source: The Nature Conservancy (2009)). 67
Table 5 - 2: Summary of the 34 Environmental Flow Components (EFC) used in the IHA software (source: The Nature Conservancy (2009)). 67
Table 5 - 3: Irrigation demand categories and schedules for rice and poly-crops for the study area. 71
Table 5 - 4: Mean annual water balance at irrigated sites for conditions with irrigation (continuous flooding (CF) and alternate wetting and drying (AWD)) and without irrigation. 75
Table 5 - 5: Results of IHA analysis over 30 years (1984 - 2013) at the inflow to papyrus wetlands for scenarios with and without irrigation. 77
Table 5 - 6: Median annual values of EFC analysis over 30 years (1984 - 2013) at the inflow to papyrus wetlands for scenarios with and without irrigation. 79
Table 5 - 7: Summary of EFCs altered due to flow diversion. 81
Table 5 - 8: Effect of irrigated area and location of irrigation command area on the IHA group average. US, MS and DS imply upstream, midstream and downstream, respectively. 84

Table 6 - 1: List of models (with and without irrigation) forced with CMIP6 climatic datasets. 95
Table 6 - 2: Irrigation demand categories and schedules for rice and poly-crops for the study area. 98
Table 6 - 3: 30-year mean annual irrigation demand in the Naigombwa catchment at baseline (BL) and global warming levels 2 (GWL2) and 4 (GWL4). Results are based on an ensemble average. 98
Table 6 - 4: The 33 IHA indices used to study flow regime alterations (from The Nature Conservancy (2009)). 99
Table 6 - 5: Median annual water balance at the irrigated sites at BL, GWL2 and GWL4. Results are based on an ensemble average. 103

Table 6 - 6: 30-year overall degree of alteration for baseline conditions with and without. Results are based on an ensemble average. 105
Table 6 - 7: IHA-RVA analysis over 30 years showing the degrees of climate- and irrigation-induced alterations with no irrigation in the baseline. Results are based on an ensemble average. 165
Table 6 - 8: IHA-RVA analysis over 30 years showing the degrees of climate- and irrigation-induced alterations with irrigation in the baseline. Results are based on an ensemble average. 167

Table 7 - 1: How wetlands achieve select SDGs (Adapted from Ramsar Convention Secretariat (2018)). 169

CHAPTER 1: INTRODUCTION

Study Motivation

Wetlands cover approximately 3% of the earth's surface (Davidson & Finlayson, 2018); however, they contribute up to Int$47.4 trillion annually towards ecosystem services, equivalent to 43.5% of the value of natural biomes globally (Davidson et al., 2019). Critical ecosystem services include flow and climate regulation, water quality regulation, protection of biodiversity, food supply, and carbon storage (Convention on Wetlands, 2021; Salimi et al., 2021).

Most (77%) of these wetlands are inland surface-water-dependent natural wetlands dominated by three broad wetland classes: peatlands, natural lakes, and marshes and swamps on alluvial soils (Davidson & Finlayson, 2018). Tropical freshwater swamps and marshes are primarily found in Africa (Davidson & Finlayson, 2018) and have the largest area of wetlands of international importance (T. Xu et al., 2019). The most prevalent species for many of these wetlands is the giant Cyperus papyrus L. (*Cyperaceae*) (Pacini et al., 2018). As a keystone species adapted to inundated conditions, papyrus provides breeding and feeding grounds for unique flora and fauna (Chapman et al., 2001).

Studies on these wetlands mainly cover their provisioning services, biodiversity and reproduction, water purification, and carbon storage (Pacini et al., 2018; Van Dam et al., 2014; Kayendeke & French, 2019). Few (e.g., (Kayendeke & French, 2019; Kayendeke et al., 2018; Sutcliffe & Parks, 1989)) have quantified their flow regulation services (Van Dam et al., 2014), with none at the catchment scale. Further, no study has attempted to link its flow regime to its biologically relevant hydrologic attributes, which has generally hindered papyrus wetlands' economic valuation and conservation (Van Dam et al., 2014), especially for catchments experiencing the effects of global change.

Case Study

As in most African economies (Ludi, 2009), agriculture is the backbone of Uganda, providing a livelihood for more than 69% of the population (World Bank, 2013, 2016; UBOS, 2015). However, farming systems are vulnerable to the impacts of climate change, given the reliance on rainfed production (Wanyama et al. 2017; APP 2012;

Cooper et al. 2008). The ever-increasing population further compounds the pressure on farming systems, triggering wetland encroachment, given that they provide moist soils year-round (Dixon & Wood, 2003).

Over the years, the Uganda government established vital programmes, such as the National Rice Development Strategy, to enhance the country's food security (MWE and UN-WWAP, 2006). Cereal production is estimated to increase by 70% through intensified irrigated farming, including wetland utilisation. The framework for the Naigombwa Irrigation Project in the vicinity of the Naigombwa wetland in the Naigombwa catchment of the Mpologoma catchment (Figure 1 - 1) was formalised in 2013, with smallholder farmers as the main stakeholders (Namutebi & Sekanjako, 2013; MAAIF, 2019). A feasibility study and detailed design for Phase 1 of the Naigombwa Irrigation Project were carried out in 2021 (MAAIF, 2021), with construction planned to commence in 2023. Water for irrigation will be abstracted directly from the proposed Namiganda Dam. At a target command area of about 2,300 hectares, the scheme will benefit farmer groups at Busowa Traders and Farmers' Cooperative Society and Pearl Rice Limited (MAAIF, 2021). The challenge, however, is that water abstraction for irrigation can impair the functioning of the immediate downstream papyrus wetland system. Impacts on wetlands, particularly those that alter flow regimes, affect ecosystem functioning, degrade wetlands, and ultimately cause a state change (Brinson, 2011). The pictures in Plate 1 - 1 and Plate 1 - 2 show papyri-dominated wetlands (floodplain and floating) in the study area.

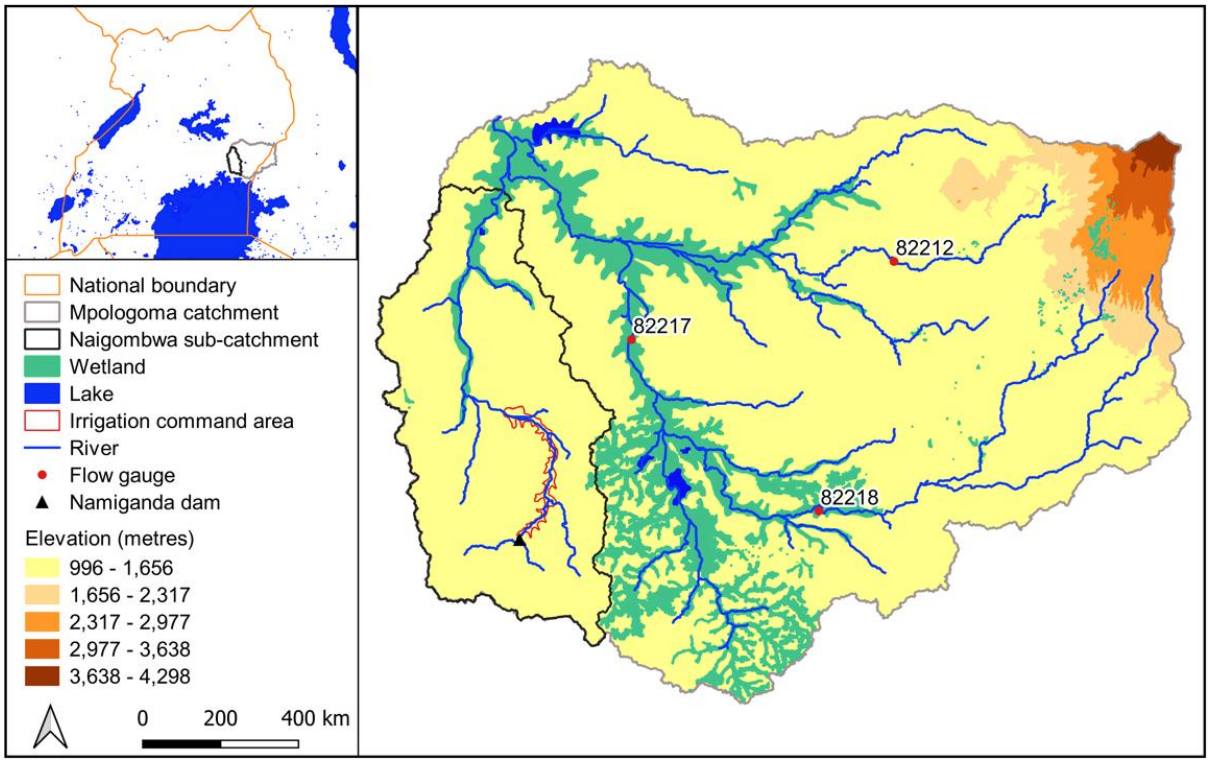

Figure 1 - 1: Map of Mpologoma catchment and Naigombwa sub-catchment in Uganda, including the location of wetlands and the proposed irrigation scheme.

Plate 1 - 1: Floodplain papyrus immediately downstream of flow gauge 82217. Picture taken during low flow.

Plate 1 - 2: Floating and floodplain papyrus in Naigombwa catchment. Picture taken during low flow.

Study Goal and Research Questions

Papyrus wetlands are known to regulate flows; however, their catchment scale effects are unknown. A detailed understanding of its catchment scale effects on flows can offer opportunities to link its flow regime to the biologically relevant hydrologic attributes, aiding its conservation and protection. This study, therefore, assessed and quantified the catchment-scale flow regulation roles of these wetlands, including the impacts of lowland rice irrigation and climate change on their flow regime, to provide sustainable management options. Five key research questions (RQ) guided the study.

RQ1: How do papyrus wetlands regulate baseflow and quickflow in the Mpologoma catchment? (Addressed in Chapter 4)

RQ2: What roles will papyrus wetlands play in regulating future extreme flows (flood and low flows) in the Mpologoma catchment? (Addressed in Chapter 4)

RQ3: How does lowland rice irrigation affect the Naigombwa wetland inflow regime, and how are the regime changes, if any, linked to the biologically relevant hydrologic attributes of papyrus wetlands? (Addressed in Chapter 5)

RQ4: How will lowland rice irrigation and climate change influence the wetland inflow regime in the Naigombwa catchment? (Addressed in Chapter 6)

RQ5: What are the sustainable management options to minimise the impacts of land use change and climate warming in the Mpologoma catchment? (Addressed in Chapter 7, Section 0)

Thesis Structure

The thesis comprises six chapters following this introduction. The analyses and results, Chapters 4, 5, and 6, are written as journal articles; thus, they have their independent introduction, results, discussion, and conclusion sections. The thesis includes a general literature review (Chapters 2 and 3) and an overall discussion, conclusions, and recommendations (Chapter 7).

Chapter 2 categorises papyrus wetlands in the Mpologoma catchment and reviews the effects of irrigated agriculture on wetlands, particularly in the developing world. Finally, it examines the approach to model selection for catchment-scale study of wetland hydrology. **Chapter 3** reviews the SHETRAN hydrological modelling tool, focusing on the significant water flow processes.

Chapter 4 investigates the catchment scale roles of papyrus wetlands on flow regulation in a tropical river catchment. Until the submission of this work, no studies have attempted to quantify papyrus flow regulatory services at the catchment scale. The study reveals vital regulatory functions on high flows compared to low flows and has been published in MDPI's Land Journal (see Oyarmoi et al. (2023)).

Chapter 5 explores the linkage between papyrus wetlands' flow regimes and their biologically-relevant hydrologic attributes. Similar to its catchment scale flow regulatory services, no study other than this work has attempted to link papyrus wetlands' flow regimes to their biologically-relevant hydrologic attributes. The study examined the effects of lowland rice irrigation, a critical land use in wetland-dominated tropics, on the inflow regime of papyrus wetlands. Results show that the magnitude, duration, timing, and rate of change of flow regimes are most affected, inhibiting sexual and asexual reproduction in papyri. This chapter is under review for the *Journal of Ecohydrology*.

Chapter 6 examines the effects of lowland rice irrigation on the papyri wetland inflow regime under a future climate. Results indicate that climate change, due to the projected increase in precipitation over the East African region, will significantly influence wetland inflow more than irrigation.

Chapter 7 discusses the thesis results, focusing on sustainable management options for minimising the impacts of rice irrigation and climate warming. Finally, conclusions and suggestions for further research are drawn.

CHAPTER 2: BACKGROUND

Climatology of the Region

Uganda, a landlocked country in East Africa, lies within latitudes 5° N to 2° S and longitudes 29° E to 36° E. Its climatic zones (Figure 2 - 1), like in most tropical regions, are mainly dependent on rainfall, which also determines the spatial distribution of natural resources and land use (Basalirwa, 1995).

Given its location along the equator, Uganda's rainfall is determined to a large extent by the movement of the Inter-tropical Convergence Zone (ITCZ), giving two main rain seasons in a year - the abundant long rains (March to May) and the highly variable short rains (October to December) (Mutai et al., 1998). Rain sources include the Indian Ocean, the Red Sea, and the coastal waters off South Africa (Gimeno et al., 2010; Basalirwa, 1991). These rains are often modulated locally by complex topographies and lakes, with the highest totals occurring in the mountainous south, west, east, and vicinity of Lake Victoria (Maidment et al., 2013; Basalirwa, 1991). Over parts of central and northern Uganda, the two wet seasons merge to form one long rain season - March to November (Basalirwa, 1991).

The now-defunct East African Meteorological Department categorised seasonal rainfall distribution within East Africa into four broad seasons (Basalirwa, 1995). The generally dry first season lasts from December of the preceding year to the end of February, corresponding to the period when the ITCZ is south of the equator and outside the domain of East Africa. Thus, any rains realised during this period are primarily a result of localised features (e.g., rains around the shores of Lake Victoria). The second season is wet and longest (March to May), coinciding with the presence of ITCZ in the region. The third season (June to August) is dry in other parts of Uganda except the north and corresponds with ITCZ being north of the equator and outside the domain of East Africa. Rains in this period are related to the moist, westerly Congo air mass (Basalirwa, 1991). The fourth season (September to November) is wet throughout the country and coincides with the presence of ITCZ in the region.

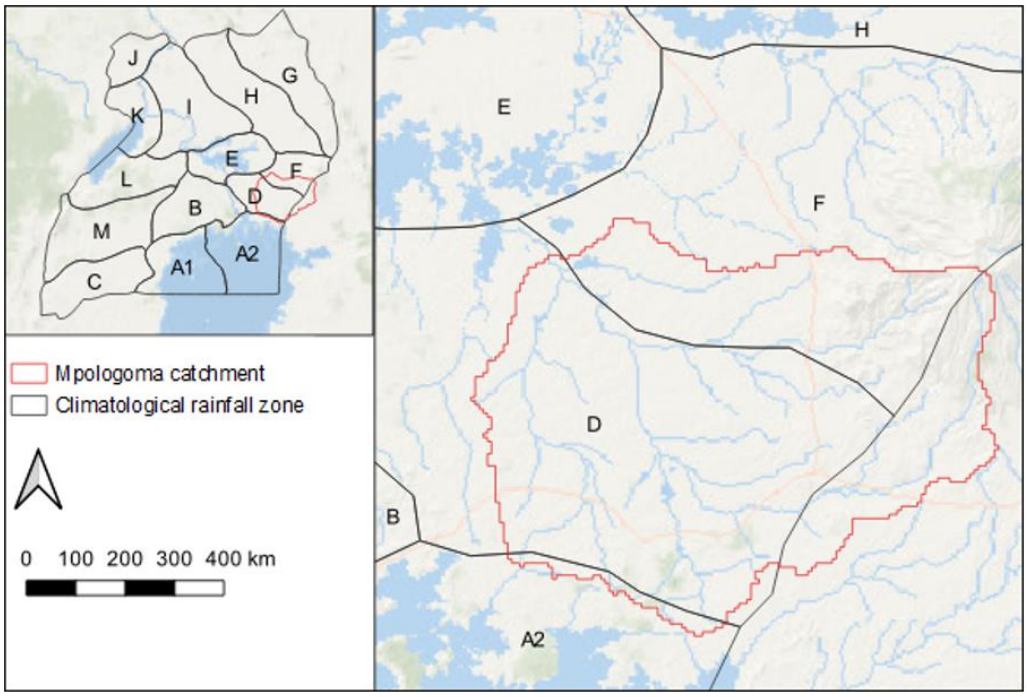

Figure 2 - 1: Climatological rainfall zones in Uganda and Mpologoma catchment. Adapted from Basalirwa (1995).

Wetland Classification in the Mpologoma Catchment

The Ramsar Convention (1971) broadly defines wetlands as “areas of marsh, fen, peatland or water, whether natural or artificial, permanent or temporary, with water that is static or flowing, fresh, brackish or salt including areas of marine water, the depth of which at low tide does not exceed 6 meters”. This definition, however, does not uniquely classify wetlands. A systemic classification is fundamental for compiling a national or regional inventory of wetlands (Semeniuk & Semeniuk, 1997). Over time, several classification systems emerged in different parts of the world. These classifications broadly categorise wetlands based on their structure (what wetlands look like), function (what wetlands do), or utility (how they are managed) (Brinson, 2011). The structural approach categorises wetlands based on vegetation (i.e., swamp, marsh, bog or fen (Keddy, 2010)) or landform (e.g., basins, channels, flats and slopes/highlands (Semeniuk & Semeniuk, 1995, 1997, 2011) and is generally suited for wetland mapping and inventory (Brinson, 2011); thus, it was adopted to describe the Mpologoma catchment wetlands. The challenge, however, is that plants don’t respond so much to landform shape as they do to the climate, local conditions of wetness, nutrient supply, and disturbances (Brinson, 2011). This leads to ambiguity in wetland categorisation. Semeniuk & Semeniuk (1995, 1997, 2011) geomorphic

approach, which is a structural method, overcomes this by delineating wetlands based on landform type and hydro-period (permanently inundated, seasonally inundated, intermittently inundated, or seasonally waterlogged), resulting in 13 main wetland types, irrespective of the climatic setting and vegetation.

Regarding vegetation, papyrus wetlands are often called swamps; however, they are marshes due to their herbaceous rather than forested vegetation (Kipkemboi & Van Dam, 2018). Thus, following Semeniuk & Semeniuk (1997, 1995), papyrus wetlands in the Mpologoma catchment are marshes that occur in flat landforms (i.e., floodplains), channel landforms (i.e., rivers and creeks), and basin landforms (i.e., lakes), with hydroperiods characterised by permanent inundation (such as in lakes, permanent rivers and permanently flooded floodplains) or seasonal inundation (such as in creeks and seasonally flooded rivers and floodplains).

Overview of Effects of Irrigated Agriculture on Wetlands

The relationship between irrigated agriculture and wetland ecosystems is a trade-off between food supply and environmental health (Galbraith et al., 2005), which calls for a balance between societal demands, tolerable side effects, and a sustainable environment (Hargreaves, 2000). However, often, the exploitation of water resources, surface water in particular, is poorly (or not) regulated, causing detrimental changes in aquatic and riparian ecosystems (Al-Quraishi & Kaplan, 2021; Gaybullaev et al., 2012; Kihwele et al., 2018; Steinfeld et al., 2020). These changes range from short-term and mild to long-term and severe, with extreme cases often causing wetland submergence (in the case of irrigation dams) or replacement by upland vegetation (or bare land) (Galbraith et al., 2005). Some extreme cases with significant impacts on downstream wetlands are in Table 2 - 1. Most of the wetlands in these surface water systems experienced dewatering and drying either permanently or intermittently. The Aral Sea, in particular, remains the worst case to date, with some of its formerly vegetated wetlands transformed into bare land due to salt accumulation in soils (Gaybullaev et al., 2012; UNESCO, 2000; White, 2013). Its annual inflow declined from 31.5 km^3 in 1998 to 5.2 km^3 in 2009 (Gaybullaev et al., 2012) due to unsustainable cotton cultivation (White, 2013).

The key factors determining irrigated agriculture's impacts are the scheme size and irrigation activity (i.e., irrigation method and crops grown) (Galbraith et al., 2005).

Large schemes often result in diverting significant wetland inflows, with impact zones ranging from the vicinity of the irrigated area to a long distance downstream. For example, the Waza Logone floodplain, in the vicinity of the Semry irrigation scheme in Cameroon, experienced a 30% (964 km^2) reduction in its area as a result of a 70% shortage in inflow (IUCN, 2003). The Nile Delta, 800 km downstream of diversion works at Aswan dam in Egypt, shifted to a destructive phase due to disruption of sediment influx, erosive effects of coastal processes, and subsidence (Stanley & Warne, 1998).

Globally, surface irrigation is most widespread (ICID, 2022), given its low capital investment, low energy requirement, adaptability to all crops, and acclimatisation to sediments (Brouwer et al., 1987). However, they are least efficient (typically 50 to 60%) in comparison to drip and sprinkler methods (75 to 90%) that allow for precision irrigation through automation (Savva & Frenken, 2002). Surface irrigation is a significant component of most of the irrigation schemes of the riverine systems listed in Table 2 - 1 (Galbraith et al., 2005).

As a rule of thumb, farmers tend to restrict irrigation to high-value crops such as rice, cotton, and wheat. Most irrigation schemes in the above-listed riverine systems (Table 2 - 1) target these crops, yet they are the highest water consumers. Cotton, rice, and wheat require about 15,897, 1,673, and 1,828 litres of water per kilogram, respectively (Mekonnen & Hoekstra, 2010), compared to low-value crops such as potatoes, cabbage, and tomato at less than 300 litres per kilogram (IME, 2013).

Besides scheme size and irrigation activity, poor (or lack of) planning and implementation of sustainable management and monitoring systems have contributed to the ecological failure in irrigated catchments. Often, management plans are anticipated or developed before construction works; however, they are localised and limited in scope (Galbraith et al., 2005). Cases in point are Iraqi marshlands and the Great Ruaha River wetlands. The Euphrates River that feeds the marshes in Iraq is a transboundary resource. The environmental disasters in the swamps of the Euphrates River were compounded by the lack of coordination between the water authorities in Turkey, Syria, and Iraq (Al-Quraishi & Kaplan, 2021). Meanwhile, the Great Ruaha River is a non-transboundary resource; however, local authorities developed irrigation schemes without considering downstream impacts (RUBADA, 2001).

Overall, irrigated agriculture in developing nations is often established without robust studies ensuring the coexistence of ecological resources and societal needs (Galbraith et al., 2005). This is primarily due to the absence of data, funding limitations, and political interference. Data availability and funding challenges can be overcome by transferring studies from similar regions; however, catchment-scale factors (e.g., land use, geology, rainfall, etc.) are specific to each watershed (Acreman & Holden, 2013; Kadykalo & Findlay, 2016; Rains et al., 2016) which necessitates catchment-specific studies.

Table 2 - 1: Examples of riverine/lake systems catastrophically impacted by irrigation water extraction.

S. No.	Riverine/lake system	Country	Comments	Reference
1	The Aral Sea and its tributaries (Amu Darya and Syr Darya rivers)	Kazakhstan, Kyrgyzstan, Tajikistan, Turkmenistan, Uzbekistan, and Afghanistan	The annual inflow of the Aral Sea declined from 31.5 km^3 in 1998 to 5.2 km^3 in 2009 due primarily to irrigated cotton, with some vegetated wetlands turning into bare land due to salt accumulation.	Gaybullaev et al. (2012); White (2013)
2	Euphrates River	Turkey, Syria, and Iraq	The monthly average flow of the Euphrates River declined by 51% between 1986 and 1992 due to the proliferation of dams and water diversion for irrigation in Turkey, Syria, and Iraq, causing a 47% reduction in the Al-Hammar marshland in Iraq.	Al-Quraishi & Kaplan (2021)
3	The Murray River and its tributaries (Gwydir River and Macquarie River)	Australia	Multiple dams and flow diversion works reduced the mean annual discharge of the Murray River to the sea by 61%, from 12,233 to 4,723 million m^3, affecting multitudes of ecosystems and wetlands in the lower reaches of the Murray-Darling Basin.	Mallen-Cooper & Zampatti (2018); Steinfeld et al. (2020)

S. No.	Riverine/lake system	Country	Comments	Reference
4	The Great Ruaha River	Tanzania	The dry season wetland coverage of the Usangu wetlands shrunk from 160 km^2 to 93 km^2 between 1958 and 2004, with wetland outflows ceasing at some points.	Kashaigili et al. (2009); Kihwele et al. (2018)
5	Logone River	Cameroon	The Waza Logone floodplain shrunk by 30% (964 km^2) due to a 70% shortage in inflow.	Scholte et al. (2000); IUCN (2003)
6	Hadejia-Nguru wetland complex	Nigeria	Inflow to wetlands was reduced by 17% due to damming and irrigation, affecting migratory birds and wetland-based plants.	Lemly et al. (2000)
7	The Nile Delta	Egypt	Diversion works at the Aswan dam disrupted sediment influx, thus exacerbating coastal erosion and subsidence of the Nile Delta.	Penvenne (1996); Stanley & Warne (1998)
8	The Colorado River Delta	Mexico	The Colorado River Delta, initially at 7,780 km^2 and a habitat for plants, birds and marine life, has been reduced to tiny remnants due to a proliferation of dams that divert water to cities and irrigation farms since the 1960s.	Glenn et al. (1996); Raise the River (2013)

Overview of Effects of Climate Change on Wetland Ecosystems

Recognising the need to reduce the risks and impacts of climate change significantly, 196 Parties at the 2015 UN Climate Change Conference (COP21) in Paris adopted the overarching goal of keeping the global average temperature well below 2°C above pre-industrial levels, with a preferred limit of 1.5°C (UNFCCC, 2015). However, given the current trend of greenhouse gas emissions, which is synonymous with high population growth, low technology development, and high energy consumption (Friedlingstein et al., 2022; Nikulin et al., 2018), the planet is on track to reach the 1.5 and 2ºC average by the 2030s and 2050s, respectively (IPCC, 2023), and warming of 3 to 4°C by the end of the century (IPCC, 2018a).

The unmistakable evidence of climate change, including elevated temperatures and shifts in precipitation patterns, is already evident, leading to tangible impacts on ecosystems, biodiversity, and human populations (Shivanna, 2022). In the case of wetland-dominated catchments, climate change affects ecosystem services that communities primarily depend on. Further, the effects of climate change are projected to worsen as temperature rises and precipitation becomes more unpredictable (IPCC, 2023). The risks to ecosystem services depend on the magnitude and rate of warming, geographic location, levels of development and vulnerability, and the choices and implementation of adaptation and mitigation options (IPCC, 2018b).

Projections over the East African region indicate increasing rainfall (Makula & Zhou, 2022; Ayugi et al., 2022; Almazroui et al., 2020) with more frequent hot days and nights (Das et al., 2023; Almazroui et al., 2020). Increased temperature impacts ecosystems by shifting species' distributional range and phenological events (i.e., the timing of recurring seasonal events) (Shivanna, 2022). Plants and animals tend to move to higher altitudes as temperatures get warmer (Ramalho et al., 2023; Couet et al., 2022). However, species that may be unable to keep pace with the changing climate lag behind, leading to their eventual extinction (Shivanna, 2022). The threat of extinction is more potent for protected areas such as wetlands as they hold many species with small distributional ranges (Velásquez-Tibatá et al., 2013).

Phenological events are based on environmental cues such as temperature, light, and precipitation (Shivanna, 2022). Climate change alters species phenology by changing the length of the growing season, the timing of flowering and fruiting in plants (including

their intensity and longevity), the migration of animals, the timing of egg laying, and the development of the larva, pupa, and adult in insects, etc. Given that some plants and animals mutually coexist, the change in the phenology of a particular species could affect the timing of events of other species. For example, in flowering plants, flowering is associated with pollinators, and fruiting is related to the availability of seed dispersers and favourable conditions for seed germination and the establishment of seedlings.

Selection of Catchment Modelling Tool

Model selection for watershed modelling typically starts with conceptualising critical catchment processes (Barnes & Bonell, 2005). In the case of wetlands, the conceptual model should characterise both wetland water transfer mechanisms and watershed hydrologic and hydraulic processes (Golden et al., 2014; Acreman & Miller, 2007). Wetland mechanisms are principally based on the hydrology of flooding and associated soil saturation (Fitz & Hughes, 2008) and include combinations of precipitation input, surface water and groundwater flows, and evapotranspiration losses (Acreman, 2004). Understanding the dynamics of wetland systems requires "getting the water right" (Fitz & Hughes, 2008), which calls for the employment of models with explicit representations of the various transfer processes (Acreman & Miller, 2007).

Three different forms of mechanistic modelling (watershed, groundwater, or coupled surface-subsurface) can be adopted depending on the critical hydrologic component of interest (i.e., surface water, shallow subsurface water, groundwater, or surface water groundwater interactions) (Golden et al., 2014). Kayendeke & French (2019) showed that surface fluxes dominate papyrus wetland flows in the Naigombwa catchment, with negligible contribution from groundwater. This study, therefore, assumes that surface water is the dominant hydrologic flux in wetlands. However, catchment scale factors, including surface and groundwater processes, influence wetland ecosystem services (Cohen et al., 2016) as this affects the wetland's water. Thus, the study employed the surface-subsurface modelling approach, given that small dams and irrigation need to be considered.

SHETRAN (Ewen et al., 2000; Birkinshaw et al., 2010; Birkinshaw, 2010), a physically based spatially distributed (PBSD) watershed model, was chosen for the study. Unlike other PBSD models such as MIKE SHE, SHETRAN is a freeware (Birkinshaw, 2018)

capable of modelling floodplain flow at a level relevant to catchment modelling (Birkinshaw, 2008b). PBSD watershed models have the strength of linking surface and subsurface flow mechanisms. These models can realistically quantify the influence of surface conditions (e.g., soil saturation and infiltration rate) on groundwater flows. Similarly, they can quantify the effect of groundwater conditions, such as water levels and flows, on surface conditions (Ewen et al., 2000). SHETRAN has also demonstrated good capabilities in representing catchment water management scenarios such as reservoirs and irrigation (Rangecroft et al. 2018).

CHAPTER 3: THE SHETRAN MODELLING SYSTEM

Since SHETRAN is the chosen catchment modelling tool for the study (see Section 0), it is imperative to understand its modelling concepts. This chapter introduces its main modelling concepts, including assumptions and limitations.

Overview of the SHETRAN Catchment Modelling Tool

SHETRAN discretises catchments into orthogonal grids in the plan view, with each grid column consisting of lithological layers. The rivers/streams run along the edges of the grid columns. Three types of elements describe the finite difference representation of a catchment (basic elements, bank elements, and channel links), with each element having four faces, numbered 1 (east), 2 (north), 3 (west), and 4 (south). Basic elements, called grid elements or grid squares, are each grid column's (stacked) cells. The grid elements' distributed data (e.g., land use/cover category, soil category, ground-surface elevation, lakes, etc.) are held in grid arrays.

Each river channel, running along the edge of a grid square, is called a channel link and has a defined cross-section, bed elevation, and bank-full elevation. Bank elements, narrow strips of land at either channel side, were not used in this study because they are not well defined in the relatively flat Mpologoma catchment.

Water flow in SHETRAN consists of two essential pathways: overland and stream/river flow and unsaturated and saturated flow, which comprises variably saturated lithologies and aquifers (Ewen et al., 2000). These pathways consist of several processes (Table 3 - 1). These processes are modelled by finite difference representations of the partial differential equations of mass, momentum, and energy conservation and by empirical equations described in the following subsections.

Table 3 - 1: Summary of SHETRAN water flow processes (Source: Ewen et al. (2000)).

Flow pathway	Flow processes
Overland and stream/river flow	• Rainfall canopy interception • Evaporation and transpiration • Overland, overbank, and channel flow • River augmentation and abstraction • Irrigation and reservoirs/dams
Unsaturated and saturated flow	• Infiltration • Variably saturated subsurface flow and storage

Flow pathway	Flow processes
	• Flow and storage in confined, unconfined, and perched aquifers • Subsurface and river interchange • Spring flow from groundwater seepage • Well / borehole abstraction

Overland and River Flow Processes

Precipitation is often a fundamental flux in hydrological models (Essou et al., 2016). In SHETRAN, net precipitation is estimated by making adjustments, where applicable, for interception, evaporation, and drainage from vegetation canopies (WRSRU/TR/9510/61.0, 2001). Surface water, comprising overland storage and runoff, is generated from net precipitation either as infiltration excess or saturation excess. Runoff is routed as overland flow into streams and rivers. At the same time, infiltration can occur during runoff and channelisation, depending on the soil moisture condition. Similarly, groundwater can be discharged on land, streams, and rivers, depending on the groundwater table.

Besides evaporation of intercepted rainfall from vegetation canopies, evaporation can occur from free water surfaces, bare soil, and dry river beds. Further, water uptake by plants from the root zone and eventual transpiration are computed.

3.1.1 Canopy interception of rainfall

Interception in SHETRAN is determined using the Rutter et al. (1971; 1975) model (Equation 3 - 1) that was initially developed for forest canopies (WRSRU/TR/9510/61.0, 2001). In the model, rainfall fills a canopy of known storage capacity (S), depicted as the minimum depth of water needed to wet all surfaces. The stored water is depleted through evaporation and drainage to the ground surface. The amount of rainfall intercepted is a function of canopy coverage (ratio of canopy area to total ground area, also referred to as Plant Area Index (PLAI)), which varies seasonally but has a maximum value p such that (1 - p) is bare ground. PLAI ranges from zero for no plant cover to 1 when plants shade the ground surface.

On the other hand, canopy evaporation, assumed to occur from all leaf surfaces, is a function of total leaf area (including leaves below others) to the ground covered by vegetation, also referred to as Canopy Leaf Area Index (CLAI). CLAI often varies seasonally. Values above 1 indicate overlapping leaves (the presence of leaves below others), at which point interception and eventual evaporation of intercepted rainfall

become generally constrained. Thus, the fixed value of one is used in SHETRAN when CLAI exceeds it (Equation 3 - 4). Further, the evaporation rate is assumed to equal the product of the potential rate (*Ep*) and the ratio *C/S* when *C* (water stored on the canopy at a particular time) is less than *S* (Equation 3 - 2); otherwise, it is equal to *Ep* (Equation 3 - 3).

$$\frac{\partial C}{\partial t} = Q - ke^{b(C-S)}$$

Equation 3 - 1

where *C* = depth of water on the canopy [mm]; *S* = canopy storage capacity [mm]; *k* = drainage parameter corresponding to the rate of drainage when the canopy is at storage capacity [mm/s]; *b* = drainage parameter that describes how drainage rate falls as the canopy dries [mm^{-1}]); *t* = time [s]; and *Q* = drainage to ground surface or net precipitation such that:

$$Q = pp'\left(P - E_p\frac{C}{S}\right) \quad when\ C \leq S$$

Equation 3 - 2

$$Q = pp'\left(P - E_p\right) \quad when\ C > S$$

Equation 3 - 3

Also:

$$pp' = pp' \ \ when\ p' \leq 1$$

$$pp' = p \ \ when\ p' > 1$$

Equation 3 - 4

where *P* = rainfall rate [mm/s]; *p* = fraction of ground in the horizontal plane covered by vegetation at its maximum extent; *p′* = Canopy Leaf Area Index; *Ep* = potential evaporation rate [mm/s].

3.1.2 Plant evapotranspiration

Actual evapotranspiration (AET, [mm/s]) in SHETRAN is determined either by using the inbuilt Penman-Monteith equation (Monteith, 1965), which requires complete meteorological data and aerodynamic and canopy resistance parameters of the various surfaces or by supplying the model with potential evapotranspiration (PET, [mm/s]) values prepared beforehand (Birkinshaw, 2008a). In the latter option, the model calculates AET by modifying the supplied PET [mm/s] using surface-specific (e.g., plant) and soil water coefficients (Equation 3 - 5).

$$AET = K_c \times K_s(\theta) \times ET_o$$

Equation 3 - 5

where K_c = surface specific coefficient and $K_s(\theta)$ = soil water coefficient.

Climatological gauges have continually shrank in Africa (Hughes, 2006; Amaning et al., 2012), and where they exist, they are often sparse in coverage (Behrangi et al., 2011; Bitew & Gebremichael, 2011) and have discrepancies and data gaps (Koutsouris et al., 2015). Thus, PET estimation methods that rely solely on temperature data (e.g., Hargreaves' method (Hargreaves & Samani, 1985)) are recommended for regions with limited data (Allen et al., 1998). This is because temperature measurements are often more spatially representative than other meteorological measurements, as the temperature is generally less variable, especially in flat regions (Orlowsky & Seneviratne, 2014).

Hargreaves' method uses minimum and maximum air temperature fields to calculate PET. Di Vittorio & Georgakakos (2021) showed that it performs similarly to the Penman equation over the papyrus-dominated Sudd wetlands in South Sudan.

As a critical meteorological product, the Climate Forecast System Reanalysis (CFSR) daily temperature fields have been shown to perform similarly to observed temperature in hydrological models over the East African region (Duan et al., 2019). Thus, the study employed Hargreaves' PET values in SHETRAN in calculating AET, as shown in Equation 3 - 5.

3.1.3 Overland and channel flow

Overland and channel flow in SHETRAN are based on the diffusive wave approximation to the full St. Venant equations, which also calculate backwater effects, including water surface slope (WRSRU/TR/9510/61.0, 2001). The model computes both the depth and rates of flow. Depths of water are calculated on the ground surface and in channels. Similarly, flow rates are estimated for fluxes on the ground surface and river links, including riverbanks.

The continuity equation for surface water processes in an element (grid square, bank element, or channel link) is shown in Equation 3 - 6.

$$\frac{\partial h_o}{\partial t} = \frac{1}{A}\left[\sum_{i=1}^{4} Q_i + Q_R\right]$$

Equation 3 - 6

Where h_o = water depth above ground in the element; A = surface area of the element; Q_i = lateral influxes in the north, east, south, and west directions (i = 1, 2, 3, or 4), which is considered positive into the element; and Q_R = net vertical input into the element, which consists of net precipitation and groundwater discharge, less infiltration and evaporation.

From the conservation of momentum, surface water depths and fluxes are computed for each direction of overland and channel flow. Equations for overland flow in the x (east and west) and y (north and south) directions of a grid square or bank element are shown in Equation 3 - 7 and Equation 3 - 8. Similarly, channel flow in a link element is calculated as shown in Equation 3 - 9.

$$Q_x = u_x h_o w_x - K_x \left[-\frac{\partial\left(z_g + h_o\right)}{\partial x}\right]^{1/2} w_x h_o^{5/3} - \frac{K_x w_x h_o^{5/3}}{L_x^{1/2}}\left[z_u - z_d\right]^{1/2}$$

Equation 3 - 7

$$Q_y = u_y h_o w_y - K_y \left[-\frac{\partial\left(z_g + h_o\right)}{\partial y}\right]^{1/2} w_y h_o^{5/3} - \frac{K_y w_y h_o^{5/3}}{L_y^{1/2}}\left[z_u - z_d\right]^{1/2}$$

Equation 3 - 8

$$Q_l = u_l A_l = K_l A_l \left[-\frac{\partial(z_g + h_o)}{\partial l} \right]^{1/2} h_o^{2/3} - \frac{K_l A_l h_o^{2/3}}{L_l^{1/2}} [z_u - z_d]^{1/2}$$

Equation 3 - 9

where Q_x and Q_y = grid overland flow in x and y directions; Q_l = channel flow; u_x, u_y, and u_l = flow velocities in the x, y, and l directions; w_x and w_y = element width across x and y directions; K_x, K_y, and K_l = Strickler coefficient, the inverse of Manning coefficient, in respective directions; z_g = ground or channel bed level; L_x, L_y, and L_l = distances between the centres of the two elements whose flows are interacting; z_u and z_d = water surface elevations in the upstream and downstream elements; and A_l = cross-sectional area of the channel, which is a function of h_o (Equation 3 - 6).

Equation 3 - 7 to Equation 3 - 9 apply to flows between similar elements (overland flow elements or channel links). Flows between non-similar elements (e.g., grid or bank element and channel link, and vice versa) can occur. In SHETRAN, this flow interaction can be one of three possible types:

a) Adjacent grid or bank element discharging into a channel link is typical when the bank-full level in the channel link is below the discharging grid or bank element elevation.
b) Overbank flow from the channel link to the grid or bank element applies when the water level in the adjacent grid or bank element is below the channel's water level.
c) There is no flow between the adjacent grid and the channel link when the adjacent element ground level is lower than the bank-full elevation of the channel link, and the channel does not overflow.

A resistance equation accounts for flow in type (a) above, which also applies to type (b) for the condition that the adjacent element ground level is higher than the channel bank elevation (i.e., channel-full elevation). Otherwise, the broad-crested weir standard flow equation applies if the channel bank elevation exceeds the adjacent ground level, which allows computation of non-drowned flow (when the channel water level is low compared with the bank elevation) and drowned flow (when the channel water level is comparable with the bank elevation).

3.1.4 Selection of channel dimension and bed elevation

SHETRAN uses input data on channel dimension and bed level. Channel cross-sections are either trapezoidal or rectangular, and a unique cross-section can be assigned individually to each channel link. For this study, all channels were assumed to be rectangular. The Google Earth satellite imagery was used to extract channel widths. Channel and lake depths were defined based on fieldwork data collected by interviewing local communities and conducting spot checks at infrastructure sites (bridges and flow gauging stations). Overall, channel depths varied from 1.5 to 2 m in the upstream parts of the catchment and 2 to 6 m in the mid and downstream parts of the catchment. Bed elevations were defined relative to the ground level, described by a digital elevation model (DEM).

3.1.5 Land cover/use categorisation in SHETRAN

As explained in Sections 3.1.1, 3.1.2, and 3.1.3, SHETRAN uses the Rutter et al. (1971; 1975) model (Equation 3 - 1) to compute interception, the momentum equation (Equation 3 - 7 and Equation 3 - 8) to compute surface water depths and fluxes, and surface-specific (i.e., plant and soil water) coefficients (Equation 3 - 10) to compute evapotranspiration. Thus, the critical variables that SHETRAN uses to distinguish unique land cover/use types are the Plant Area Index, the Canopy Leaf Area Index, Canopy storage capacity, canopy drainage parameters, the Strickler coefficient, the root zone distribution, and soil water coefficients. The soil water coefficients are computed by SHETRAN as described in Section 0, depending on the soil type, water availability, and plant evaporative demand.

Papyrus are perennial plants with dense structures (Chapman et al., 2001) and heights of up to 5 to 6 m (Kipkemboi & Van Dam, 2018). Thus, they were assumed to function hydrologically as needle-leafed forests.

3.1.6 Lake representation in SHETRAN

Although model computational expense improves with grid resolution (Zhang, 2015), the SHETRAN grid size has to reasonably represent critical land cover features, such as lakes and wetlands. Google satellite imagery indicates a minimum wetland width of 1 km in the Mpologoma catchment, less extensive than most miniature lakes in the study area (Figure 4 - 2). Thus, the 1 km grid size was adopted for the study, as detailed in Section 4.1.6.

The SHETRAN automatic river generator does not recognise lakes and reservoirs; thus, generated channel Links along the edges of lake grid cells are manually removed, except those that flow in and out of the lakes as depicted by the physical catchment. Further, the elevation of lake grids is modified to match the bed elevations of lakes in the physical catchment.

The flow between lake grid cells and inflow/outflow channel links relies on overbank flows, whereby water spills over the bank between the grid element and channel link. The flow is calculated using a broad-crested weir equation over the length of the channel. Thus, the lakes act as reservoirs that delay outflow while enhancing evaporation and percolation.

Unsaturated and Saturated Flow

The variably saturated subsurface (VSS) module in SHETRAN allows for infiltration and deep percolation from net precipitation or surface water (overland or in channels) (WRSRU/TR/9510/61.0, 2001). Soil moisture content and tension distributions in the unsaturated zone and recharge to the saturated zone are calculated in the VSS module. Plant transpiration, calculated in the evapotranspiration/interception model, is extracted from the VSS module as a sink term. Further, groundwater can discharge overland or into channels. Equation 3 - 11 (Parkin, 1996) shows the basic VSS 3D model for a heterogeneous, anisotropic medium.

$$\eta \frac{\partial \psi}{\partial t} = \frac{\partial}{\partial x}\left[K_x k_r \frac{\partial \psi}{\partial x}\right] + \frac{\partial}{\partial y}\left[K_y k_r \frac{\partial \psi}{\partial y}\right] + \frac{\partial}{\partial z}\left[K_z k_r \frac{\partial \psi}{\partial z}\right] + \frac{\partial (K_z k_r)}{\partial z} - q$$

Equation 3 - 11

where Ψ = pressure potential; t = time; K_x, K_y, and K_z = saturated hydraulic conductivity in the x, y, and z dimensions; k_r = relative hydraulic conductivity; η = storage coefficient as defined in Equation 3 - 12; and q = specific volumetric flow rate (volumetric flow rate per unit volume of medium) out of the medium as expressed in Equation 3 - 13.

$$\eta = \frac{\theta S_s}{n} + \frac{d\theta}{d\psi}$$

Equation 3 - 12

$$q = q_w + q_{sp} + q_t$$

Equation 3 - 13

where θ = volumetric soil water content; S_s = specific storage; n = porosity; q_w, $q_{sp,}$ and q_t = well abstraction, spring discharges, and transpiration losses, respectively.

3.1.7 Channel-groundwater interaction

In SHETRAN, flow interchange between an aquifer and a channel consists of, where applicable, flow through the channel bed and walls (WRSRU/TR/9510/61.0, 2001). Bed infiltration or exfiltration is computed the same way as in overland. A dry bed corresponds to a flux boundary, while a channel with water is considered a ponded boundary. At the channel walls, flow is calculated based on pressure distribution, which varies with time and acts as a lateral head boundary condition (h).

$$h = z_s \quad for \quad z_{gs} < z < z_s$$

Equation 3 - 14

And:

$$h = z \quad for \quad z_s < z < z_p$$

Equation 3 - 15

where z_{gs} = elevation of the channel bed above datum; z_s = elevation of the channel water surface above datum; z_p = elevation of the top of the channel seepage face above datum.

The specific volumetric flow rate into the channel (q_{ex}) through the channel walls is expressed as:

$$q_{ex} = K_{ex}^{eff} k_r \Delta h$$

Equation 3 - 16

where k_r = relative hydraulic conductivity; K_{ex}^{eff} = effective hydraulic conductivity (weighted harmonic mean of the conductivities in the adjacent element and the channel sediments) as expressed below.

$$K_{ex}^{eff} = \frac{(d_x + d_B)K_a K_B}{d_x K_B + d_B K_a}$$

where d_x = distance from the channel side to the adjacent computational node; K_a = saturated hydraulic conductivity of the aquifer (K_x or K_y, depending on channel orientation); d_B = thickness of channel bed sediments; and K_B = saturated hydraulic conductivity of channel bed sediments.

CHAPTER 4: THE EFFECT OF PAPYRUS WETLANDS ON FLOW REGULATION IN A TROPICAL RIVER CATCHMENT

This chapter is a publication in MDPI's Land Journal (see Oyarmoi et al. (2023)). The numbering of sections and figures has been adapted to ensure the consistency of the overall thesis.

Abstract

Africa has the largest area of wetlands of international importance, and papyrus constitutes the most dominant species for many of these wetlands. This hydrological modelling study assesses and quantifies the impacts of these papyrus wetlands on historical baseflow and quickflow, as well as future flood and low flows in the Mpologoma catchment in Uganda. Assessment over the historic period shows that wetlands strongly attenuate quickflow while moderately enhancing baseflow. They play a moderating role in most months, except for the first dry season (June and July), due to the reversal of flows between wetlands and rivers that often occur during this period. Annual estimates show that wetlands are four times better at regulating quickflow than baseflow. Examination of changes at 2 and 4 °C global warming levels (GWLs) indicate that wetlands will play critical roles in mitigating flood risks, with a lesser role in supporting low flows. Wetlands are predicted to lower future mean flood magnitude by 5.2 and 7.8% at GWL2 and GWL4, respectively, as well as halving the average number of flood events in a year, irrespective of the warming level. This work shows that papyrus-dominated wetlands strongly influence catchment hydrology, with significant roles on quickflow, including floods, and highlights the need for their conservation and protection.

Introduction

Wetland loss has been estimated at 64 to 71% since 1900 (Davidson, 2014). This is a major issue given their contribution to ecosystem services, including maintaining the hydrological cycle, regulating climate, and protecting biodiversity (Hu et al., 2017). Among the continents, Africa has the most extensive wetlands of international importance (T. Xu et al., 2019), covering an impressive 7% of the continent (Junk et al., 2013). Despite their vast scale, African wetlands are continually under pressure

(Tockner, 2002). Up to 42% of wetlands were lost between 1970 and 2015 (Darrah et al., 2019). Threats to wetlands often stem from political and social debates on whether wetland areas are at their highest economic use, which fuels negative sentiments about them (Woodward & Wui, 2001). Threats to these wetlands include population pressure and agricultural expansion (Davidson, 2014; Kashaigili et al., 2009; Pacini et al., 2018), river regulation (Kashaigili et al., 2009), and climate change (Van Dam et al., 2014; Pacini et al., 2018). High population growth rates and food shortages often trigger wetland encroachment for crop production, given that they provide year-round moist soil conditions (Dixon & Wood, 2003).

The giant sedge *Cyperus papyrus* L. (Cyperaceae), the largest of the 400 tropical sedge species within the genus, constitutes the most widespread dominant species for many of the African wetlands (Pacini et al., 2018). At 5–6 m in height, papyrus exists as rooted or floating marshes in riverine and lacustrine landscapes (Kipkemboi & Van Dam, 2018). Their hydro-periods are characterised by permanent inundation (such as in rivers and lakes) or seasonal inundation (such as in floodplains and creeks) (Kipkemboi & Van Dam, 2018). In Uganda, wetland coverage is 11 to 13%, with papyrus being the dominant or co-dominant plant (Kipkemboi & Van Dam, 2018). Major papyrus wetlands include those in the shorelines of lakes such as Victoria, Albert, and Kyoga and riverine systems such as Mpologoma, Nabajuzzi, and Namatala. Like wetland trends in Africa, papyrus wetlands in Uganda are under pressure. Loss rates are estimated at 0.5 to 5% per annum, although few studies have been undertaken (Van Dam et al., 2014).

The two primary ecosystem services of papyrus wetlands are provisioning and regulating services. Provisioning services include carbon storage, fisheries, papyrus biomass, and wetland reproduction (Gaudet, 1975; Emerton et al., 1999; Kansiime & Nalubega, 1999; Jones & Humphries, 2002; Kiwango & Wolanski, 2008; Opio et al., 2014; Saunders et al., 2014; Ssanyu et al., 2014; Terer et al., 2014). Regulating services include storing floodwaters and maintaining surface water flow during dry periods (Hurst, 1933; Sutcliffe & Parks, 1989; Kayendeke & French, 2019; Kayendeke et al., 2018; Sutcliffe & Parks, 1987; Howell et al., 2009; Di Vittorio & Georgakakos, 2021). Van Dam et al. (2014) provided research and policy priorities for papyrus wetlands, emphasising the need for improved understanding and modelling of the often alluded to but rarely quantified regulating services. These regulating services hold a

far more significant advantage than provisioning services but are difficult to evaluate (Pacini et al., 2018), thus hindering the economic valuation and conservation of papyrus wetlands (Van Dam et al., 2014). Studies in Uganda that quantified the microscale papyrus regulating services include Kayendeke et al. (2018) and Kayendeke & French (2019), who, respectively, assessed the response of papyrus root mats to changing water levels and the seasonal variations in papyrus wetland water balance. Elsewhere in Africa, Di Vittorio & Georgakakos (2021), Howell et al. (2009), Hurst (1933), and Sutcliffe & Parks (1989, 1987) described the regulation services of papyrus wetland complexes at the Sudd and Okavango wetlands in South Sudan and Botswana. Wetland ecosystem services emanate from the aggregated effects of wetlands (Cohen et al., 2016); however, no studies have attempted to quantify papyrus flow regulatory services at the catchment scale. Catchment scale studies incorporate the dynamic effects of wetlands, which can mitigate the risks of adverse policies, engineering, and management solutions emanating from single wetland studies (Thorslund et al., 2017).

As a transition zone between terrestrial and aquatic ecosystems, wetlands play an essential role in climate change. Although generally resistant to change (Salimi et al., 2021), wetlands are susceptible to temporal dynamics, especially if thresholds (e.g., seasonal variations in hydrology) are exceeded (Langan et al., 2018). As temperature increases, the rate of wetland evapotranspiration increases (Salimi et al., 2021; Wang et al., 2006), which could lower the water levels, particularly during dry seasons (Salimi et al., 2021). Meanwhile, changes in the timing and amount of precipitation can result in flow regime changes. Extremes in temperature and flow regimes lead to changes in wetland biogeochemistry (Salimi et al., 2021) and biodiversity (Salimi et al., 2021; Döll & Zhang, 2010). Research that helps predict wetlands' role in mitigating future impacts of climate-induced changes in hydrology is valuable.

Models are crucial to developing insights into the dynamics of wetland ecosystem services (Langan et al., 2018). Their selection, however, requires a conceptualisation of the critical processes to be modelled (Barnes & Bonell, 2005). At the catchment scale, these processes include hydrologic and hydraulic fluxes (Golden et al., 2014; Acreman & Miller, 2007), such as precipitation, evapotranspiration, surface water, and groundwater. 'Getting the water right' is a prerequisite to understanding the dynamics of wetland systems (Fitz & Hughes, 2008), which require the use of models that have

an explicit representation of the various water transfer mechanisms (Acreman & Miller, 2007), with the coupled surface-groundwater flows a critical component (Golden et al., 2014). SHETRAN (Ewen et al., 2000) is a suitable model, as it is a physically based, spatially distributed catchment modelling tool that simulates surface-groundwater flows and can quantify the effects of wetlands. It is freeware and has also successfully been applied globally in land use and climate change studies in predominantly rural catchments (e.g., (Birkinshaw et al., 2017; Op de Hipt et al., 2019; Zhang et al., 2019)).

This paper investigates the impacts of papyrus-dominated wetlands on catchment hydrology under climate change, focusing on the climate data-limited Mpologoma catchment. It is worth noting that human comprehension of catchment systems is underpinned by the availability and level of confidence in observational data (Dembélé et al., 2020; Hughes, 2006), of which atmospheric data are most critical (Wilby et al., 2017). This study, therefore, focuses on addressing the following research questions. (a) What are the limitations of freely available global precipitation datasets in developing a catchment model in the study region? (b) How do papyrus wetlands regulate baseflow and quickflow in the Mpologoma catchment? (c) What roles will papyrus wetlands play in regulating future extreme flows (flood and low flows) in the Mpologoma catchment?

Materials and Methods

4.1.1 Study Area

The Mpologoma catchment, located between longitude 33.4–33.6° E and latitude 0.3–1.3° N, is a transboundary watershed between Uganda and Kenya (Figure 4 - 1) with over 80% of its area in Uganda. Covering 8989 km^2 (MWE, 2018), its highest peak, Mount Elgon, is to the northeast and at approximately 4298 m above sea level (a.s.l). A more significant part of the catchment (over 80%) lies between 996 and 1150 m a.s.l, the former being the mean lake level at Lake Kyoga, Mpologoma's outlet. Key tributaries include Namatala, Manafwa, Malaba, and Naigombwa. The region's rainfall regime is bimodal (peak months of March to May and August to November) (Basalirwa, 1991), with a mean annual rainfall of 1215 to 1660 mm (Basalirwa, 1991; Chombo et al., 2018). Following Köppen–Geiger's climate classification (Kottek et al., 2006), the catchment can be categorised as wet Equatorial Monsoonal. Subsistence farming is the main economic activity, with major crops being rice, maize, beans, groundnuts, cassava, sugarcane, etc. Seven unique land use and cover types were identified in

2019 (Bunyangha et al., 2021). These include woodland (6.2%), grassland (5.2%), built-up areas (11.6%), subsistence crops (53.2%), wetland (21.5%), open water (1.9%), and commercial farms (0.5%).

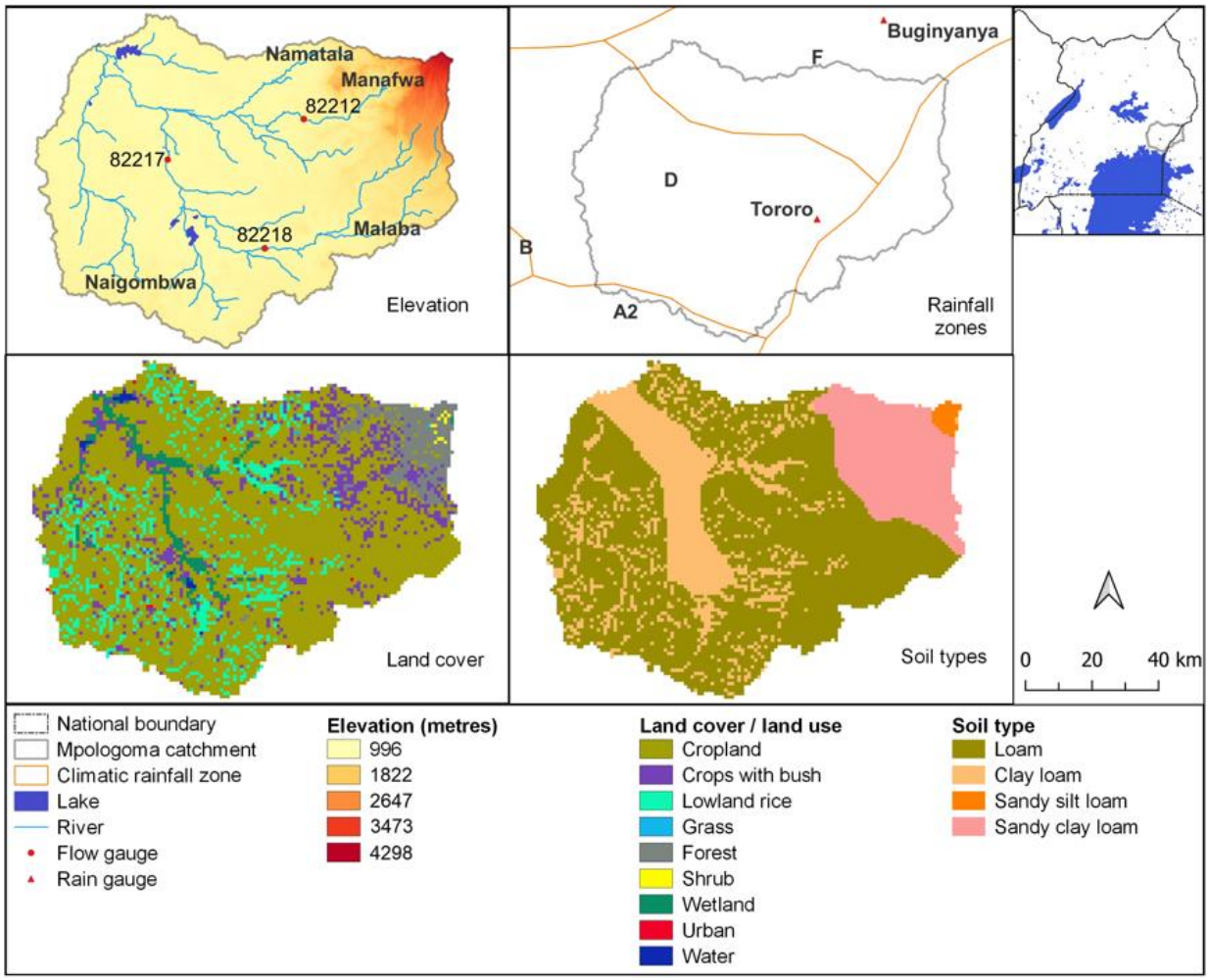

Figure 4 - 1: Mpologoma catchment elevation, rainfall zones, land cover and soil types. The rainfall zones were delineated and defined by Basalirwa (1995).

4.1.2 Data Sources and Processing

Hydrological modelling in SHETRAN requires spatially explicit input datasets of climate (precipitation and potential evapotranspiration), land surface topography, land use, land cover, and soil and lithological distribution. Measured surface flow and/or groundwater levels are also required for model calibration and validation. The following subsections describe the selection and preparation of these datasets. Figure 4 - 9 in APPENDIX 1 shows a schematisation of the steps followed in the study.

4.1.3 Selection and Evaluation of Rainfall Products

Satellite-based and reanalysis rainfall products have often been favoured for hydrological modelling in regions with low rain gauge networks, such as Sub-Saharan Africa (Bitew et al., 2012; Fuka et al., 2013). However, the rainfall fields of reanalysis products are less accurate in the tropics compared to satellite estimates (Maidment et al., 2013). As the predominant rainfall over inland East Africa is convective (Mutai & Ward, 2000), satellite products may provide more accurate data. The essential satellite-based precipitation products (SPPs) that have been applied over Africa include TAMSAT, CHIRPS, ARC, RFE, MSWEP, PERSIANN, CMORPH, and TRMM 3B42 (Table 4 - 6, APPENDIX 2).

This study evaluated the SPPs mentioned above by ground truthing (i.e., direct comparison with rain gauge data) followed by hydrological modelling. Point-to-pixel ground-truthing, with gauges at the point scale and SPPs at the grid scale, was carried out for climatological rainfall zones D and F (Figure 4 - 1) at daily and monthly time scales, which was preceded by quality control of gauge data, as outlined in Maidment et al. (2013). The point-to-pixel comparison was used to eliminate interpolation error, which is a concern for regions with sparse gauge networks (Gumindoga et al., 2019). Given that RFE2.0 and MSWEP2.2 start and end, respectively, in January 2001 and October 2017, evaluations were limited to January 2001 and December 2016. Overall, 0.79% and 12.25% of gauge records for Tororo and Buginyanya, respectively (Figure 4 - 1), were not included in the assessment due to missing data.

Following other studies on Africa (e.g., Dembélé & Zwart (2016); Dinku et al. (2018)), the point-to-pixel evaluation comprised assessment for accuracy in daily rainfall identification and daily and monthly rainfall totals. The extent of rainfall identification was assessed through measures of False Alarm Ratio (FAR), Probability of Detection (POD), Frequency Bias (FB), and Heidke skill score (HSS) (see Equation 4 - 2 to Equation 4 - 5 in APPENDIX 3). In contrast, rainfall totals were assessed through correlation coefficient (R) and Nash–Sutcliffe efficiency (NSE). FAR represents the fraction of satellite-estimated rain days not captured by the gauge, and POD is the fraction of gauge rainfall days identified by the satellite product. FB is the ratio of total rain days in the satellite product to that of the gauge. It ranges from 0 to ∞, with values less (greater) than one indicating under (over) estimation of rain days. HSS, on the other hand, assesses the overall skill of a satellite product's rain-day detection while

accounting for random chance. Its value ranges from −∞ to 1, with zero indicating that the satellite product cannot detect rain days. A value less than zero implies that random chance is better than the product, whereas one denotes perfect skill.

Given that SPPs underestimate short-duration and low-intensity precipitation (Koutsouris et al., 2015), a threshold of 1 mm/day, similar to studies by Diem et al. (2014) and Dinku et al. (2018) in the East African region, was used to discriminate between rain and non-rain days. This was applied to both the gauge and the satellite products. However, it could lower rain days in the gauge data relative to the satellite products (Dinku et al., 2018).

MSWEP, TAMSAT, and CHIRPS performed best at the monthly timescale (see results in APPENDIX 4). These SPPs were then hydrologically assessed to select the best SPP for the study area.

4.1.4 Estimation of Potential Evapotranspiration (PET)

Duan et al. (2019) evaluated the performance of Climate Forecast System Reanalysis (CFSR) daily temperature fields over the eastern African region of Ethiopia. They concluded they are as good as the observed temperature when employed in hydrological models. Hargreaves' method (Hargreaves & Samani, 1985) uses temperature values for PET estimation, and it is recommended for regions with limited data (Allen et al., 1998). Di Vittorio & Georgakakos (2021) estimated monthly evapotranspiration rates over the Sudd wetlands in South Sudan using four different methods, including Hargreaves'. Hargreaves' procedure performed best, with results similar to those generated using the Penman equation. Thus, this study used the CFSR daily minimum and maximum air temperature fields to calculate PET.

4.1.5 Measured Flow Data

Water level time series recorded at 08:00 and 16:00 h for 17 years (2000 to 2016) were acquired from the Ministry of Water and Environment (MWE), Uganda. The datasets comprised measurements for rivers Manafwa (Station 82212), Malaba (Station 82218), and Mpologoma (Station 82217), Figure 4 - 1. Rating curves for each station, also supplied by MWE, were used to derive daily average flows. Given that a quality check of flow measurements is essential in hydrological modelling, the minimum steps recommended by Crochemore et al. (2020) were adopted as described in APPENDIX 6. These include analysis of data availability (in terms of length and spatial distribution

of time series) and quality checks for outliers, homogeneity, and trend. The above steps were preceded by a visual inspection of hydrographs for suspicious records (e.g., negative values, wrongly recorded missing data and out-of-the-ordinary hydrograph patterns of variation). Data preprocessing can lower hydrologic data uncertainty by up to 10%, minimising bias and incorrect conclusions (McMillan et al., 2018).

4.1.6 Land Surface Representation

Coarse grids are often adopted in physically based, spatially distributed models to lower unknowns and execution time (Wildemeersch et al., 2014), which increases prediction uncertainty (Sreedevi & Eldho, 2021). However, 0.5 to 4 km grid scales are generally acceptable for flow prediction in large catchments. For example, Sreedevi & Eldho (2021) simulated discharge and sediment yield at 1 and 4 km grid scales based on effective parameters of a 2 km SHETRAN model. No significant difference was detected in the monthly flow predictions. Similarly, Zhang (2015) compared the SHETRAN model performance at 0.5, 1, and 2 km grid scales. Performance generally improved with grid resolution. Nonetheless, the 1 and 2 km grids gave good results. Although DEM resampling techniques do not significantly influence streamflow modelling (Tan et al., 2015), resampling to coarser grids greater than 1 km could substantially affect the spatial distribution of land use, soil types, and river links, which can affect model performance in capturing peak flows and runoff volumes (Zhang, 2015). Thus, for this study, the Advanced Space-borne Thermal Emission and Reflection Radiometer (ASTER) Global Digital Elevation Model (DEM) Version 3 (NASA/Japan Space Systems, 2018), initially at 30 m × 30 m grid resolution, was resampled to 1 km × 1 km grid size and used in defining catchment boundary, ground surface elevations, and generating river flow paths.

4.1.7 Land Cover and Land Use Layer

The European Space Agency (ESA) Climate Change Initiative (CCI) land cover map (Defourny et al., 2017) was used to categorise land use/cover in the study area. ESA CCI provides annual global land cover layers at 300 m spatial resolution from 1992 to recent times, with accuracies varying from 71% to 97% depending on the land use/cover type (Defourny et al., 2017). No significant change in permanent (i.e., papyrus-dominated) wetland areas was detected from 2000 to 2020. Thus, model calibration and validation used the 2007 land cover layer (Figure 4 - 1). Detailed

information on ESA CCI land cover layers is online at https://www.esa-landcover-cci.org/.

4.1.8 Soil and Lithology

The FAO/UNESCO Digital Soil Map of the World version 3.6 (FAO/UNESCO, 2007) was used to define soil categories. However, soils in some wetland areas and small water bodies were not correctly categorised. The topsoil in these areas is mostly clay loam (MWE, 2018). Thus, the land cover map was used to identify these locations, and the soil category was reclassified accordingly. As with the DEM, the soil layer was resampled to a 1 km × 1 km grid. Four soil types (loam, clay loam, sandy silt loam, and sandy clay loam) were identified in the catchment (Figure 4 - 1).

Lithological depths were estimated from borehole log data for the study area (1986 in total). Analysis of the records indicates 1668, 195, and 123 logs in the regions dominated by loam, clay loam, and sandy clay loam, respectively. No log data were available for the area dominated by sandy silt loam. Thus, its lithological depths were assumed to be the same as the soil category closest to it, sandy clay loam. In addition, sandy silt loam covers less than 1% of the catchment. Overall, three critical lithological layers (topsoil, weathered rock, and base rock) were identified from the log data (Table 4 - 1).

Table 4 - 1: Lithological depths in Mpologoma catchment.

Topsoil type	**Mean bottom depth from the ground surface (m)**		
	Topsoil	**weathered rock**	**base rock**
Loam	3.893	12.553	30
Clay loam	3.857	12.943	30
Sandy silt loam / sandy clay loam	5.226	14.16	30

Modelling Approach

SHETRAN (Ewen et al., 2000) is a 3D integrated surface and subsurface finite difference modelling system for water flow, sediment transport, and contaminant transport in catchments. Its water flow components comprise interception and evapotranspiration, overland and channel flow, variably saturated lithology and aquifers, and channel–aquifer interactions. The model's xy grid was set at 1 km × 1 km, with 35 cells in each grid column. The lithological cells ranged from 0.1 to 0.2 m in the topsoils but were set to 5 m in the rock layers. The selection of the number of cells

is a trade-off between accuracy and simulation time. Generally, the cells are smaller nearer the surface (as the flow is more variable) and larger as you go down the column. Although models were driven with daily data (precipitation and evapotranspiration), the simulation timestep was set to 1 hour. Detailed information on SHETRAN can be accessed at https://research.ncl.ac.uk/shetran/.

Model calibration and validation, preceded by sensitivity analysis (APPENDIX 5), were carried out manually in two phases, using the 'one parameter at a time' method. In Phase 1, the second step for precipitation product evaluation (i.e., hydrological evaluation of SPPs), SHETRAN was calibrated and validated on the sub-catchment gauged at station 82212 (Figure 4 - 2). The calibration and validation were carried out independently for each SPP (i.e., MSWEP, TAMSAT, and CHIRPS) that performed relatively well in the ground-truth evaluation. The sub-catchment gauged at 82212 has an insignificant wetland coverage. Thus, it enabled model parameterisation for catchments without wetlands in the region.

In Phase 2, the entire Mpologoma catchment was simulated, with parameters initially set to the effective values attained in Phase 1. The Phase 2 model was set up only for the precipitation product that performed best in Phase 1. Recalibration and revalidation on stations 82217 and 82218, respectively, were carried out with parameter adjustments limited to locations with wetlands.

River channels in the SHETRAN model flow along the edge of grid squares and are automatically created from the DEM. However, due to weaknesses in the SHETRAN automatic river generator in the flatter wetland areas, they were manually adjusted to follow the actual river network. River channels were removed where there are lakes, and the elevations of grid squares in lake locations were changed to depict average lake depths. The modified files were used in SHETRAN (version 4.4.5). Model performances were assessed statistically by quantifying the Nash–Sutcliffe efficiency (NSE), percent bias (Pbias), and the root mean square error standard deviation ratio (RSR). These metrics are generally recommended for model performance assessment in hydrology (Moriasi et al., 2007).

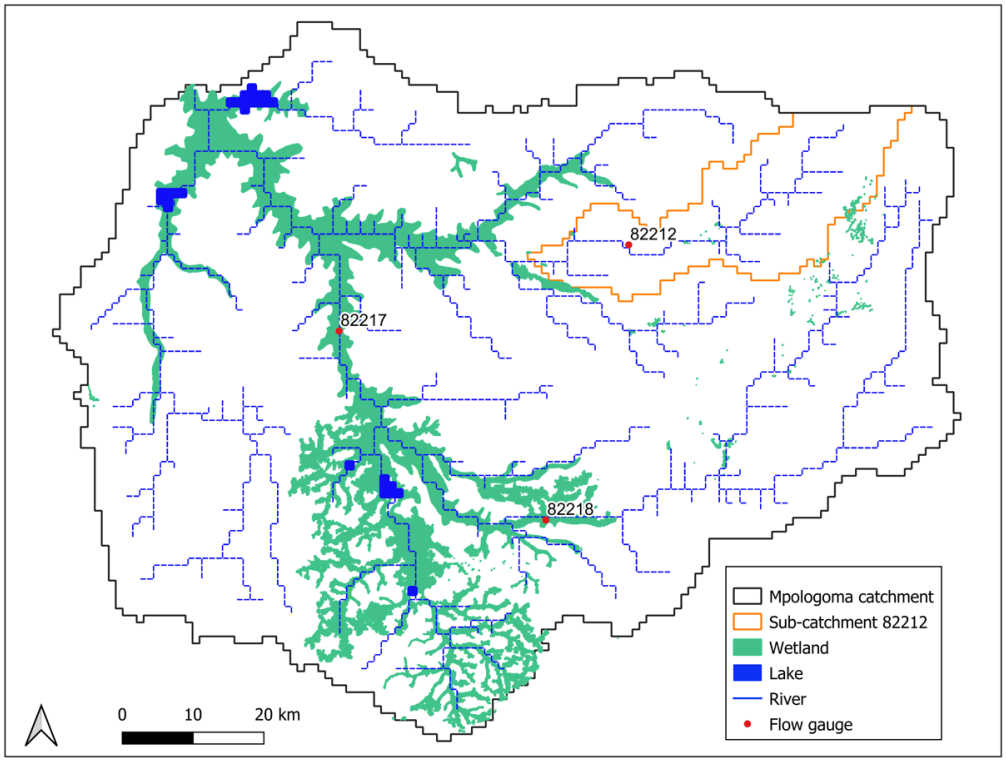

Figure 4 - 2: SHETRAN masks for Phase 1 (sub-catchment 82212) and Phase 2 (Mpologoma catchment) models, including the locations of river channels, lakes, and wetlands.

Impacts of Wetlands on Catchment Discharge

Wetland flow regulating functions can be assessed if a reference condition is defined, against which flow changes associated with the wetland are quantified (Smakhtin & Batchelor, 2005). Bullock & Acreman (2003) documented the most used approaches for inferring wetland flow regulating functions. The 'with/without' approach, restricted to model-based studies, compares the same catchment with and without wetlands. The model is typically calibrated and validated for a 'with' or 'without' scenario. Simulations are then carried out with the alternate scenario, and any difference between the model outputs is attributed to the existence of wetlands. Papyrus plants are perennial herbaceous vegetation. Although communities around them harvest papyri in the dry season, they quickly regenerate at the onset of rains (Kipkemboi & Van Dam, 2018). This study assumed that papyri stand remains the same all year round.

Furthermore, hydrological measures (flow indices) are employed in quantifying wetland flow regulating functions. These measures can be broadly classified into five groupings

(Bullock & Acreman, 2003): gross water balance, groundwater recharge, baseflow and low flows, flood response, and river flow variability. In this study, the historical impacts of wetlands on catchment flow were assessed using indices of baseflow and quickflow. In contrast, future effects were evaluated using flood and low flow indices. Quickflow is the part of precipitation that reaches the river fastest through surface runoff and interflow and is mainly responsible for floods. Thus, baseflow and quickflow are good indicators of how wetlands respond to slow and fast flow processes. However, a more holistic approach to catchment management requires the characterisation of flows in terms of flood/low flow indices (e.g., magnitude, duration, frequency, etc.) (Postel & Richter, 2003); thus, it was adopted for the future period.

4.1.9 Impacts of Wetlands on Baseflow and Quickflow

The Wetland Specific Impact (WSI) metric (Fossey et al., 2016) was employed in quantifying wetland flow regulating functions. It normalises the hydrological impact, which is an increase or decrease in flow metrics with respect to the wetland area (Equation 4 - 1).

$$WSI_{BF/QF} = \frac{R_{BFw/QFw} - R_{BFwo/QFwo}}{A}$$

Equation 4 - 1

where WSI ($m^3/s/km^2$) is the index of wetland impact expressed as a flow parameter (baseflow (BF) or quickflow (QF)) per unit area of wetland; R (m^3/s) is discharge (baseflow or quickflow) for the situation with (w) and without (wo) wetlands; and A (km^2) is the total wetland area.

The hydrological impacts of wetlands are highly dependent on climatic conditions, leading to seasonal and inter-annual variability (Fossey et al., 2016); thus, WSI values were computed at monthly and annual timescales. Boxplots showing the mean, median, and interquartile range and upper and lower limits were employed to illustrate this variability. However, only the mean WSI values and non-outlying WSI range (upper and lower limits) were used to describe wetlands' roles. WSI values were computed over 30 years (1984 to 2013) for the model outputs forced with 'observed' climatic data (i.e., MSWEP and CFSR, Table 4 - 2). Baseflow and quickflow components were extracted from total flows using WETSPRO, a flow filtering tool based on the extended

Chapman filter (Willems, 2009) and available online at https://bwk.kuleuven.be/hydr/pwtools.htm#Wetspro (accessed on 10 August 2022).

4.1.10 Impacts of Wetlands on Future Flood and Low Flows

This study assessed climate change impacts using the first ensemble (r1i1p1f1) daily climate variables from the Coupled Model Intercomparison Project phase 6 (CMIP6). Given that suitable corrections can only be attained if the scale gap between the model and observational data is plausible (Maraun & Widmann, 2018), the CMIP6 models were restricted to 100 km nominal resolution. Thus, only four (GFDL-ESM4, CESM2-WACCM, MRI-ESM2-0, and NorESM2-MM) of the nine CMIP6 models (Table 4 - 8, APPENDIX 2) recommended for application over the East African region were selected. Ayugi, Zhihong, et al. (2021) and Ngoma et al. (2021) evaluated the nine CMIP6 models against the gauge-based Climatic Research Unit precipitation product (Harris et al., 2020) and the gauge-corrected CHIRPS SPP. The models were assessed based on the ability to reproduce the annual climatology, seasonal rainfall distribution, and trend, including mean and extreme precipitation over the East African region.

As of July 2022, CESM2-WACCM had no historical minimum and maximum temperature at the official CMIP6 web portal (https://esgf-node.llnl.gov/projects/cmip6/). Thus, GFDL-ESM4, MRI-ESM2-0, and NorESM2-MM were the only Global Climate Models (GCMs) used. These GCMs were bias-corrected using the Quantile Delta Mapping (QDM) method in RStudio's 'MBC' package (Cannon, 2020), with daily MSWEP and CFSR as observed precipitation and temperature fields, respectively. The reason for selecting the QDM method is described in APPENDIX 7.

The focus was on the impacts of representative concentration pathway 8.5 (RCP8.5), given that current greenhouse gas emissions are closer to it than the other RCPs (Friedlingstein et al., 2022). Although there is consensus to limit warming to 2 °C (UNFCCC, 2013), Intergovernmental Panel on Climate Change (IPCC) predictions indicate end-of-century warming of up to 4 °C if the current emission trend continues (Arias et al., 2021). Thus, this study assessed climate change impacts at 2 and 4 °C global warming levels (GWLs), with NOAA GISS Surface Temperature Analysis (GISTEMP, 2022) global observational data as a reference. A collection of 30-year

windows corresponding to 2 and 4 °C GWLs were extracted for each GCM, following the method in Vautard et al. (2014). The global warming levels are relative to pre-industrial (1880 to 1909), and the GCM baseline (BL) period (1984 to 2013) was used for the SHETRAN present-day simulations.

Following X. Xu et al. (2019), the mitigating effects of wetlands on future flood flows were assessed using flow duration, magnitude, and frequency indices by analysing model outputs with and without wetlands. These were similarly adapted for low flows. Table 4 - 2 shows the total number of simulations carried out with the various CMIP6 datasets at the baseline (BL), GWL2, and GWL4. A 2-year return period flood and low flow threshold of the baseline scenario were used to detect the occurrence of flood and low flows, assuming that river cross sections do not change at GWL2 and GWL4. The 2-year threshold is often used as an estimate of bank-full discharge (Wu et al., 2022), thus a proxy for flood flow (i.e., starting point of inundation). Further, the wetland-dominated parts of the Mpologoma catchment are flat, with water levels often close to bank-full (Plate 1 - 1 and Plate 1 - 2). The same return period was chosen for low flow as a review of droughts over Africa showed that, in the worst case, droughts occur every two years in Uganda (Masih et al., 2014). A flood event was considered one or more consecutive days when the daily flow was larger than the bank-full flow. Similarly, a low flow event is one or more consecutive days when daily flow is less than or equal to the low flow threshold. The estimated 2-year return period flood and low flow threshold of the baseline scenario are 33.2 and 11.5 m^3/s, respectively.

The various flow indices were calculated over the water year (March to February). Flow duration was calculated as the average of individual events in a water year. The average per event was calculated before averaging over a year for flow magnitude. Flow frequency is the number of flood or low flow events yearly. The analysis assumed the same wetland size for baseline and future scenarios.

Table 4 - 2: List of models (with and without wetlands) simulated/forced with 'observed' (i.e., MSWEP and CFSR) and CMIP6 climatic datasets. BL, GWL2 and GWL4 refer to Baseline, Global Warming Level 2, and Global Warming Level 4, respectively.

S. No.	Climatic datasets	Simulation period (model warmup)	Wetlands present or not
1	MSWEP rainfall and CFSR PET	1979 - 2013 (1979 - 1983)	Yes
2			No
3	GFDL-ESM4 at BL	1979 - 2013 (1979 - 1983)	Yes
4			No
5	MRI-ESM2-0 at BL	1979 - 2013 (1979 - 1983)	Yes
6			No
7	NorESM2-MM at BL	1979 - 2013 (1979 - 1983)	Yes
8			No
9	GFDL-ESM4 at GWL2	2028 - 2063 (2028 - 2032)	Yes
10			No
11	MRI-ESM2-0 at GWL2	2030 - 2065 (2030 - 2034)	Yes
12			No
13	NorESM2-MM at GWL2	2025 - 2060 (2025 - 2029)	Yes
14			No
15	GFDL-ESM4 at GWL4	2059 - 2094 (2059 - 2063)	Yes
16			No
17	MRI-ESM2-0 at GWL4	2051 - 2086 (2051 - 2055)	Yes
18			No
19	NorESM2-MM at GWL4	2049 - 2084 (2049 - 2053)	Yes
20			No

Results

4.1.11 Model Calibration and Validation Results

Phase 1 model calibration and validation results for the best-performing SPPs (MSWEP, TAMSAT, and CHIRPS) are shown in Figure 4 - 3 and Figure 4 - 4 for daily and monthly timesteps, respectively. Overall, MSWEP performed best with a daily NSE (Pbias/RSR) and monthly NSE (Pbias/RSR) of 0.47 (−11.4%/0.73) and 0.73 (−5.15%/0.52) at calibration and 0.44 (−0.68%/0.75) and 0.87 (−3.39%/0.36) at validation. CHIRPS followed this at 0.24 (10.31%/0.87) and 0.55 (−6.95%/0.67) for calibration and 0.45 (−4.68%/0.74) and 0.86 (−7.17%/0.38) for validation. Meanwhile, TAMSAT attained −0.33 (1.28%/1.16) and 0.39 (1.34%/0.78) at calibration and −0.07 (−0.44%/1.03) and 0.18 (−4.02%/0.9) at validation. Model performance generally improves with timestep and concurs with studies over Africa (e.g., Dembélé et al. (2020; Bisselink et al. (2016)) that recommend hydrological performance assessment of SPPs at longer timescales (e.g., monthly instead of daily). This is because validation

errors in SPPs are often offset upon spatial and temporal integration at the catchment scale (Stisen & Sandholt, 2010). In addition, real-time control, design, and management of most catchment systems (such as irrigation and water supply, reservoirs, land use change, climate change, and environmental impact studies) can be achieved with monthly hydrological model estimates (Blöschl & Sivapalan, 1995). Mutenyo et al. (2013) modelled the catchment gauged at 82212 using SWAT, a semi-distributed hydrological model, with daily gauge rainfall data from 1955 to 1961. The model performed best at the monthly timescale with NSE values (Pbias) of 0.72 (−0.49%) and 0.64 (20.5%) for calibration and validation, respectively, which are similar to the results obtained in this study.

Given its superiority in this study, MSWEP was further used in Phase 2 of model calibration and validation, focusing on the recalibration of channel Strickler coefficient (Krc) in locations with wetlands. Strickler coefficient is the inverse of Mannings coefficient. An optimal Krc of 7 $m^{1/3}/s$, from an initial value of 30 $m^{1/3}/s$ (Phase 1), denoting a 76.6% change in Strickler coefficient, was attained, with daily and monthly NSE (Pbias/RSR) of 0.52 (−2.46%/0.69) and 0.64 (−6.04%/0.6) at calibration and 0.55 (−13.67%/0.69) and 0.59 (−13.66%/0.64) at validation, respectively (Figure 4 - 5). To ensure the robustness of the Phase 2 model, calibration and validation were carried out at two different sites (82217 for calibration and 82218 for validation). Due to uneven data gaps in the records of the two gauging stations, calibration was carried out from January 2011 to November 2013, whereas validation was from January 2000 to December 2003.

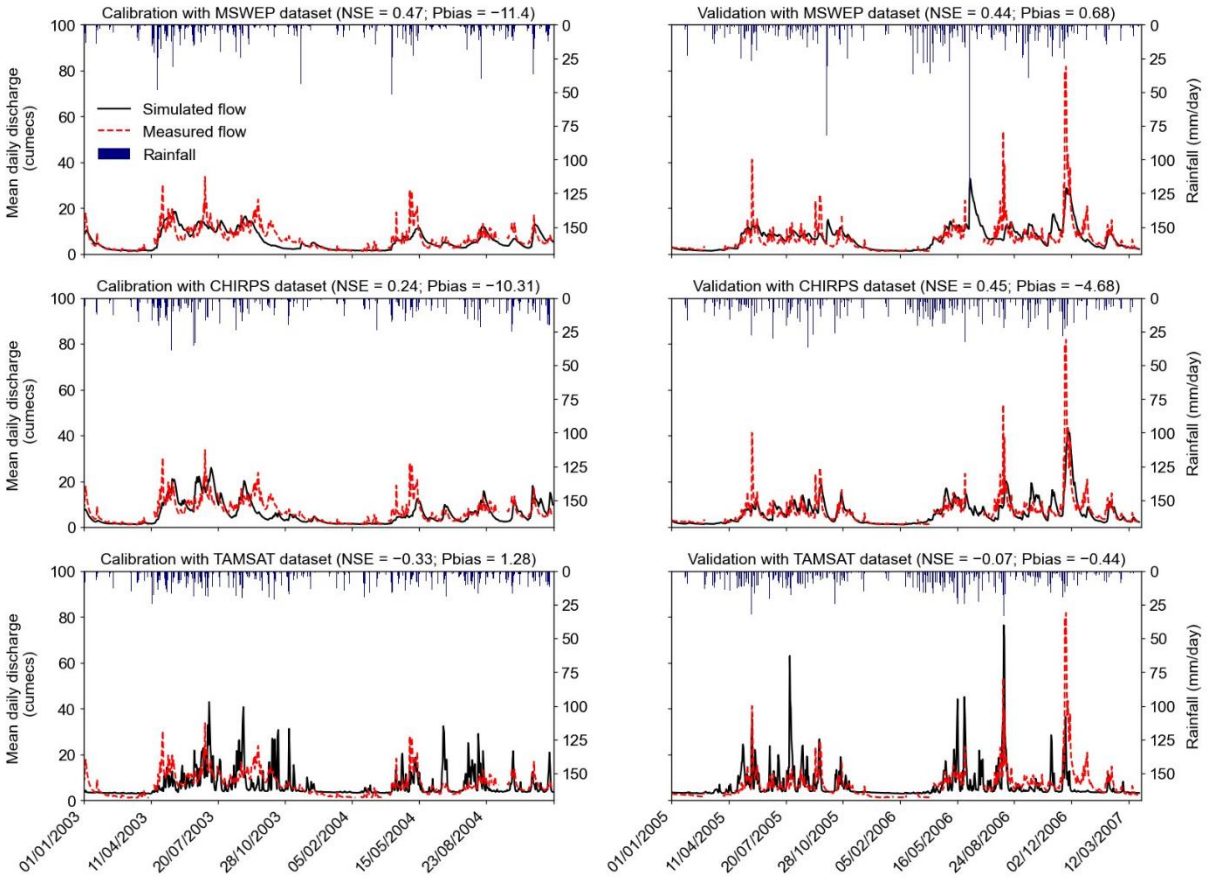

Figure 4 - 3: Daily timestep calibration (left column) and validation (right column) results at station 82212. The date format is in Day Month Year.

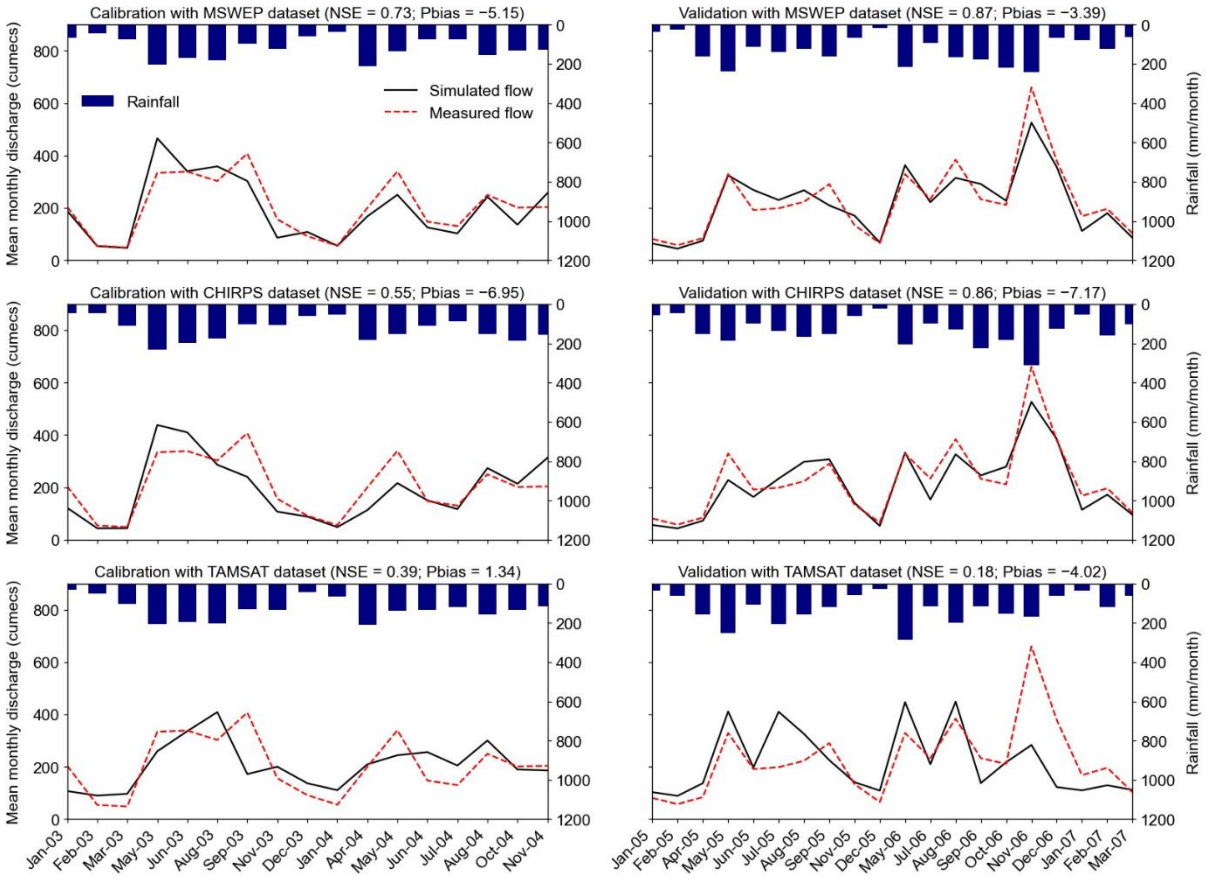

Figure 4 - 4: Monthly timestep calibration (left column) and validation (right column) results at station 82212. Months with data gaps in measured flow are not included. The date format is in Month Year.

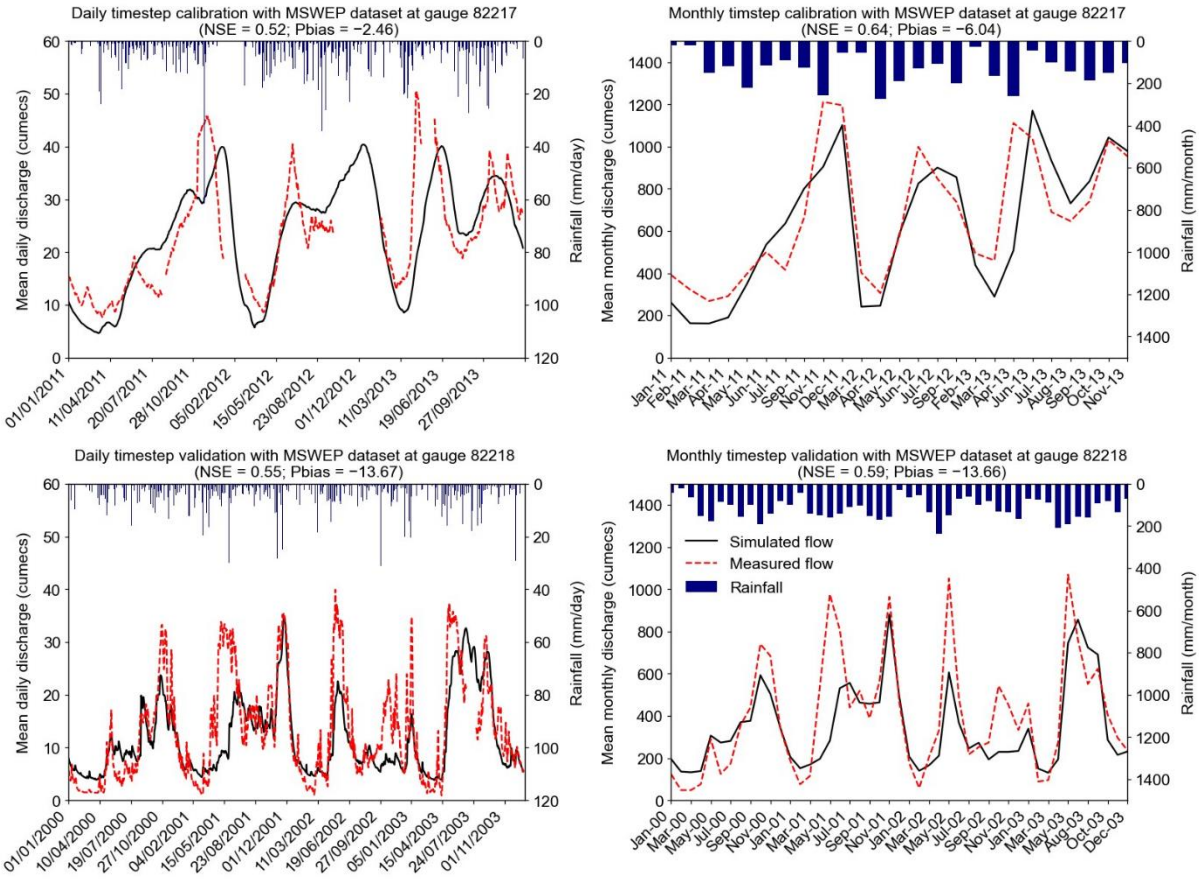

Figure 4 - 5: Daily and monthly timestep calibration at station 82217 (top row) and validation at station 82218 (bottom row) results. For the monthly plots, months with data gaps in measured flow are not included. The date format is in Day Month Year for the daily plots and Month Year for the monthly plots.

4.1.12 Overall Impacts of Wetlands on Historical Catchment Hydrology

The mean annual water balance components over the Mpologoma catchment are shown in Table 4 - 3. Precipitation (P), actual evapotranspiration (AET), and catchment outflow (Q) were extracted from the SHETRAN model output for the situation with and without wetlands over the period 1984 to 2013 (30 years). The models were driven with MSWEP and CFSR precipitation and PET datasets. Overall, wetlands modulate river flow in the Mpologoma catchment by decreasing annual discharge by 5.5% on average. In contrast, evapotranspiration is enhanced annually by 0.4% on average.

Table 4 - 3: Mean annual precipitation, actual evapotranspiration, and catchment discharge over 30 years (1984 to 2013) for the situation with and without wetlands. Models were driven with MSWEP and CFSR precipitation and PET datasets, respectively.

Water balance component	Without wetlands	With wetlands	Relative change (%)
Precipitation (mm)	1,299.3	1,299.3	
Actual evapotranspiration (mm)	1,218.2	1,222.5	0.4
Catchment outflow (mm)	78.6	74.3	-5.5

4.1.13 Impacts of Wetlands on Historical Baseflow and Quickflow

Based on mean WSI values (Figure 4 - 6), wetlands moderately support baseflow at the catchment scale in most months of the year except June (WSI of −0.02 $m^3/s/km^2$). Quickflow is suppressed in most months, except July and February (positive WSI of 0.16 and 0.01 $m^3/s/km^2$, respectively). Negative baseflow and positive quickflow WSI values indicate a reversal of the supportive role of wetlands towards these flow components, whereas zero implies a null response. The critical periods during which baseflow is often positively impacted are from March to May (WSI of 0.13, 0.12 and 0.05 $m^3/s/km^2$, respectively) and from October to February (WSI of 0.05, 0.05, 0.05, 0.08 and 0.1 $m^3/s/km^2$, respectively). Meanwhile, the corresponding periods for quickflow are from April to June (WSI of −0.48, −1.21 and −0.43 $m^3/s/km^2$, respectively) and September to November (WSI of −0.25, −0.16 and −0.36 $m^3/s/km^2$, respectively).

At the annual timescale, wetlands generally enhance baseflow (mean WSI = 0.68 $m^3/s/km^2$) and attenuate quickflow (mean WSI = −3 $m^3/s/km^2$). However, the yearly WSI non-outlying range shows that wetlands significantly reduced quickflow (−5.19 to −0.71 $m^3/s/km^2$) compared to enhanced baseflow (−1.31 to 2.7 $m^3/s/km^2$).

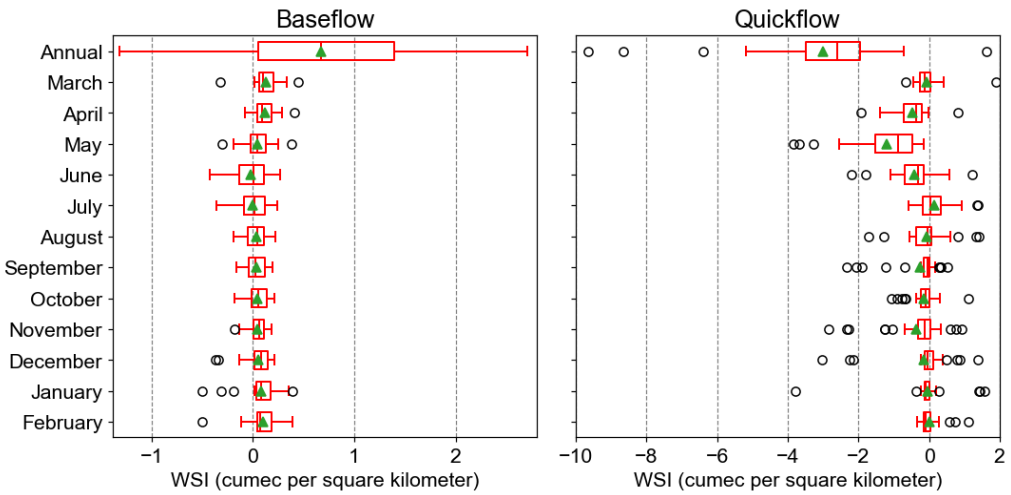

Figure 4 - 6: Monthly and annual wetland-specific impact (WSI) on baseflow (left column) and quickflow (right column) at the catchment outlet. Computations are over 30 years (1984 to 2013). The boxplots show the mean (triangles), median, and interquartile range. The whiskers show the upper and lower limits, excluding any outliers (indicated as circles).

4.1.14 The Overall Impact of Wetlands on Future Catchment Hydrology

The mean annual water balance components over the Mpologoma catchment for the ensemble baseline (BL), GWL2 and GWL4 are summarised in Table 4 - 4. Like the water balance for the models driven by MSWEP and CFSR precipitation and PET products (Table 4 - 3), water balance components were extracted over 30 years, with the baseline period set from 1984 to 2013. GWL2 and GWL4 water balance components are tied to a future 30-year period with a mid-point at 2 and 4 °C global warming levels, respectively. As the various individual GCM products were bias-corrected with MSWEP and CFSR datasets, model simulations for the BL are similar to those driven by MSWEP and CFSR. Wetlands in the BL modulate river flow by decreasing annual discharge (−6.6%) while enhancing evapotranspiration (0.4%) on average. These effects continue with warming but with a reduced impact on discharge.

Table 4 - 4: Mean annual precipitation, actual evapotranspiration, and catchment discharge over 30 years for the situation with and without wetlands. The models were forced with bias-corrected GCM precipitation and PET datasets; however, the results are based on an ensemble average.

Water balance component	Without wetlands	With wetlands	Relative change (%)
Model ensemble - baseline period			
Precipitation (mm)	1,294.9	1,294.9	
Actual evapotranspiration (mm)	1,212.7	1,217.0	0.4
Catchment discharge (mm)	82.4	77.0	-6.6
Model ensemble - GWL2			
Precipitation (mm)	1,403.4	1,403.4	
Actual evapotranspiration (mm)	1,298.8	1,304.3	0.4
Catchment discharge (mm)	111.8	107.0	-4.3
Model ensemble - GWL4			
Precipitation (mm)	1,456.9	1,456.9	
Actual evapotranspiration (mm)	1,361.8	1,367.4	0.4
Catchment discharge (mm)	105.7	100.5	-5.0

4.1.15 Impacts of Wetlands on Future Flood and Low Flows

Figure 4 - 7 shows violin plots of flood and low flow indices for the situation with and without wetlands. For flood flows and a particular catchment treatment (i.e., with or without wetlands), the 30-year mean value (Table 4 - 5) indicates that both duration and magnitude increase with warming. However, the difference between GWL2 and GWL4 indices is minimal. For the situation with wetlands, the mean flood duration per event increases from 85 days at BL to 128 and 110 days at GWL2 and GWL4, respectively. Similarly, for the situation without wetlands, the duration increases from 46 days at BL to 72 and 61 days at GWL2 and GWL4, respectively. The mean flood magnitude per event, for the situation with wetlands, increases from 37.65 m^3/s at BL to 42.87 and 41.21 m^3/s at GWL2 and GWL4, respectively. For the case without wetlands, the magnitude per event increases from 42.23 m^3/s at BL to 45.21 and 44.7 m^3/s at GWL2 and GWL4, respectively. In general, wetlands in the Mpologoma catchment are predicted to increase the mean flood duration by 77.8% (56 days) and 80.3% (49 days) at GWL2 and GWL4, respectively, and lower the mean flood magnitude by 5.2 and 7.8%.

From Table 4 - 5, the estimated mean flood frequency is constant, irrespective of warming level, at 1 and 2 flood events per year for the situation with and without

wetlands, respectively. However, the potential for a larger number of flood events in a year (the range) increases with warming. For example, for the situation with wetlands, annual flood events increase from the BL range of 0–2 flood events to 0–3 and 0–4 events at GWL2 and GWL4, respectively. For the situation without wetlands, the range increases from 0–4 to 0–5 at both GWL2 and GWL4.

Unlike flood flows, the impacts of warming levels on low flows are generally heterogeneous. For example, for the situation with wetlands, the mean low flow duration at GWL2 (33 days) is the same as that at BL (32 days) but increases to 48 days at GWL4. However, the range of low flow duration per event increases with warming from 3–59 days at BL to 14–65 and 15–97 days at GWL2 and GWL4, respectively. Similarly, for the situation without wetlands, the mean low flow duration at GWL2 (19 days) is the same as that at BL (22 days) but increases to 27 days at GWL4. The range, however, increases with warming from 2–53 days at BL to 5–61 and 3–88 days at GWL2 and GWL4, respectively. In general, wetlands are projected to increase future mean low flow duration by 73.7% (14 days) and 77.8% (21 days) at GWL2 and GWL4, respectively.

For the case of low flow magnitude, there is no significant change in the 30-year mean flow value, irrespective of catchment treatment. For example, for the situation with wetlands, the mean flow magnitude per event increases and drops minimally from 10.42 m^3/s at BL to 10.6 and 10.04 m^3/s at GWL2 and GWL4, respectively. Similarly, for the situation without wetlands, it increases and drops minimally from 10.47 to 10.71 and 10.45 m^3/s, respectively. No significant change can be seen in the range of low flow values, except for GWL4 with wetlands. The range of low flow magnitude increases from 8.91–11.4 m^3/s at BL to 7.4–11.17 m^3/s at GWL4. In general, though not significant, projections suggest that wetlands will reduce future mean low flow magnitude by 1 and 3.9% at GWL2 and GWL4, respectively. However, a considerable decline of 21.2% is expected in the lower limit of low flow at GWL4.

The mean low flow frequency is generally constant, irrespective of the warming level. On average, one low flow event occurs per year regardless of catchment treatment. However, the range of low flow events is lower for the situation with wetlands. Events vary from 0–2 and 0–4 at GWL2 and GWL4, respectively, compared to 0–7 and 0–6 for the situation without wetlands. Overall, though wetlands are predicted to negatively

impact future low flow magnitude and duration, they are expected to positively impact low flow frequencies by lowering the range of events in a year by 71.4 and 33.3% at GWL2 and GWL4, respectively.

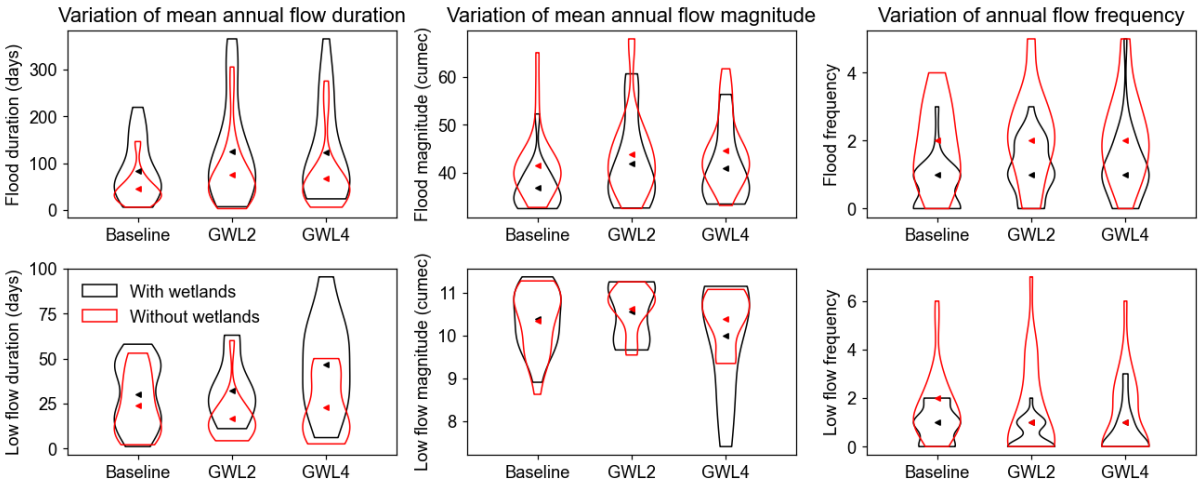

Figure 4 - 7: Violin plots of flood (top row) and low (bottom row) flow indices for the situation with and without wetlands. Flow duration and magnitude plots depict mean annual values, whereas frequency depicts the number of events in a year. The triangles indicate the average flow index over 30 years.

Table 4 - 5: Mean and range of flow indices (duration, magnitude, and frequency) for the situation with (w) and without (wo) wetlands over 30 years. Results are based on an ensemble average.

Scenario	Flow duration (days)		Flow magnitude (m^3/s)		Event frequency	
	Mean	Range	Mean	Range	Mean	Range
Flood flows						
BLw	85	3 - 216	37.65	33.27 - 52.70	1	0 - 2
GWL2w	128	9 - 365	42.87	34.14 - 60.68	1	0 - 3
GWL4w	110	21 - 295	41.21	33.70 - 56.78	1	0 - 4
BLwo	46	3 - 144	42.23	33.37 - 65.43	2	0 - 4
GWL2wo	72	16 - 250	45.21	35.35 - 68.29	2	0 - 5
GWL4wo	61	8 - 272	44.70	33.92 - 59.92	2	0 - 5
Low flows						
BLw	32	3 - 59	10.42	8.91 - 11.40	1	0 - 2
GWL2w	33	14 - 65	10.60	9.69 - 11.30	1	0 - 2
GWL4w	48	15 - 97	10.04	7.40 - 11.17	1	0 - 4
BLwo	22	2 - 53	10.47	8.62 - 11.54	2	0 - 5
GWL2wo	19	5 - 61	10.71	9.56 - 11.27	1	0 - 7
GWL4wo	27	3 - 88	10.45	9.39 - 11.32	1	0 - 6

Discussion

4.1.16 Historical Impacts of Wetlands on Catchment Hydrology

The catchment water balance (Table 4 - 3) shows that the Mpologoma floodplain wetlands reduce annual average river flow, increase evapotranspiration compared to most land types, and enhance groundwater recharge. The response is typical of wetlands, depending on the underlying lithology (Bullock & Acreman, 2003). Additionally, the mean annual WSI, depicting enhanced baseflow and attenuated quickflow, show that wetlands regulate flow variability at the catchment scale (Quin & Destouni, 2018). Past studies in Africa, although restricted to wetland complexes (e.g., the Sudd wetland in South Sudan (Hurst, 1933; Sutcliffe & Parks, 1989) and the Okavango Delta in Botswana (Sutcliffe & Parks, 1989)), have also shown that papyrus-based riparian wetlands play significant roles in dampening flow variability. The greater impact on quickflow compared to baseflow, as seen in this study's WSI non-outlying range, concurs with the work by Kadykalo & Findlay (2016), who concluded that wetlands perform better in flood mitigation than low flow augmentation. Overall, the mean annual WSI values show that wetlands in the Mpologoma catchment are at least four times better at attenuating quickflow than enhancing baseflow. Like the mean annual WSI values, the mean monthly WSI results show that papyrus wetlands are most effective in curtailing quickflow. The periods in which quickflow is suppressed coincide with the region's wet seasons (March to May and September to November).

Although the mean monthly WSI shows baseflow enhancement in most months, reversal of the supportive role of wetlands occurs in the first dry season (June to July). One would expect baseflow enhancement and nearly zero quickflow WSI during the first dry season (June to July), as seen in the second dry season (December to February). The disparity between the two dry periods could be due to the different antecedent conditions. Both dry periods start immediately after a wet period; however, the first rainy season is much wetter than the second, and the second dry spell is much drier (Basalirwa, 1991). This affects storage and connectivity pathways between wetlands and rivers. Hydraulic gradients and hydrological connectivity in riparian wetlands, typical of those in the Mpologoma catchment, depend on adequate water levels in both the river and wetlands, thus influencing discharge to or recharge from rivers (Fossey et al., 2016). This exchange of fluxes between wetlands and rivers is driven by catchment scale factors such as rainfall (intensity and duration), landscape

(topography, soil and geology, drainage area, land use, and land cover), and initial conditions (Kadykalo & Findlay, 2016; Acreman & Holden, 2013; Rains et al., 2016). Kayendeke & French (2019) showed that, for a microsite of 0.18 km^2 in the Naigombwa sub-catchment of the Mpologoma catchment, papyrus wetland flows are dominated by surface inflows, with negligible contribution from groundwater (i.e., wetland soils are mostly heavy clay loam). The lack of baseflow support from wetlands in June–July may result from a reversal in hydrological dynamics between rivers and wetlands, as shown in Figure 4 - 8. The figure shows hydrographs of baseflow and total flow for water years 1985 and 2010 when wetlands reduced baseflow by the largest amount in June and July. For these two years, baseflow with wetlands was, respectively, 0.61 and 0.64 of the baseflow with no wetlands for June and 0.69 and 0.72 for July. Figure 4 - 8 indicates that the wetland's supportive role of providing baseflow discharge to rivers was reversed between May and September. This reversal was also observed by Kayendeke & French (2019) for the site mentioned above between July 2015 and January 2016. Overall, wetland interconnections are complex at the catchment scale due to the aggregation effects of multiple wetlands on flow regimes and the influences of various flow paths (Thorslund et al., 2017).

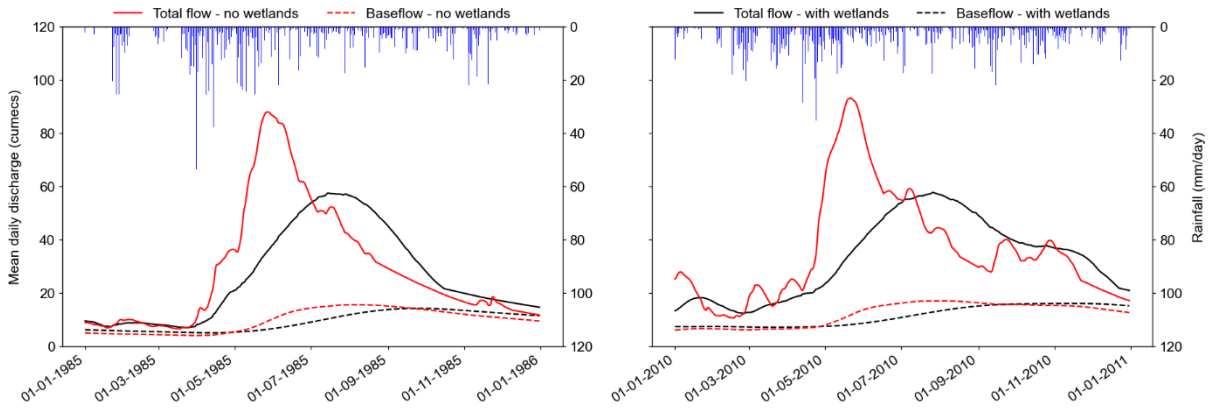

Figure 4 - 8: Hydrograph of baseflow and total flow for the water years 1985 (left column) and 2010 (right column).

4.1.17 Impacts of Wetlands on Future Catchment Hydrology

The projected catchment water balance (Table 4 - 4) shows that wetlands will decrease discharge at GWL2 and GWL4 but at rates lower than BL. CMIP6 models project increased precipitation over East Africa (Makula & Zhou, 2022; Ayugi et al., 2022), as seen in the 30-year ensemble mean of the GCMs used in this study (Table 4 - 4 and

Figure 4 - 15 in APPENDIX 1). Thus, it explains the expected reduced effect of wetlands on the future annual discharge and the predicted increase, irrespective of catchment treatment (i.e., with or without wetlands), in the 30-year mean flood duration and magnitude and the range of flood frequencies in a year (Table 4 - 5).

Although the mean flood magnitude and the range of flood frequencies increase at GWL2 and GWL4, they are lower for the situation with wetlands. Meanwhile, the predicted mean flood duration is more significant in the case of wetlands. This agrees with other studies that show that floodplain wetlands lower flood magnitude, reduce the frequency of flooding, increase time to peak (flood duration), and delay floods (Kadykalo & Findlay, 2016; Bullock & Acreman, 2003).

Future predictions show that wetlands will worsen low flow's mean duration and magnitude. Warmer climates accelerate wetland water loss through evapotranspiration (Salimi et al., 2021), leading to a decline in dry season flows, particularly during severe drought (Fossey et al., 2016). Floodplain wetlands in other parts of Africa, such as Sierra Leone and South Africa, have been shown to negatively impact dry season river flow due to high evapotranspiration rates (Bullock & Acreman, 2003). Meanwhile, wetlands in the Mpologoma catchment will positively impact future low flow frequencies by lowering the range of frequencies in a year. The predicted reduction could be associated with water storage and slow water release wetland services. Acting like a 'sponge', wetlands store water during the wet season and release it in the dry period (Bucher et al., 1993), thus minimising low flow episodes.

Implications and Limitations

Findings show that wetlands greatly influence the hydrological footprint (i.e., the influence of watershed features on downstream discharge) of the Mpologoma catchment. However, increased wetland conversion for crop production, the most significant driver of wetland loss in rural catchments in Uganda (Turyahabwe et al., 2013), poses threats to sustainable catchment management. Changing climates characterised by increased precipitation, typical of the East African region (Makula & Zhou, 2022; Ayugi et al., 2022), coupled with large-scale wetland loss, are predicted to aggravate flood risk (Gulbin et al., 2019). Bunyangha et al. (2021) estimated a wetland loss rate of 0.6% per annum between 1986 and 2019 in the Mpologoma catchment, with a predicted loss rate of 0.2% between 2019 and 2039. This calls for

restoration and conservation measures, given that most urban centres and rural communities in the Mpologoma catchment rely on natural systems (upstream wetlands) for flood management. The importance of wetland restoration for flow regulation services has been exemplified in several studies, such as Acreman et al. (2003), Mitsch & Day (2006), Wu et al. (2020), and Yang et al. (2010). Furthermore, Gulbin et al. (2019) demonstrated that, even if a significant change to flow regulation is not achieved upon wetland restoration under the current climate, it could provide a future complementary measure for mitigating the negative impacts of existing flood management strategies. For example, current adequate flood protection structures such as dikes could fail due to increased precipitation. Thus, restored wetlands can play important supplementary roles.

Looking at the broader impact of climate change, irrespective of catchment treatment (i.e., with or without wetlands), projections indicate increased flood and low flow risks, a trend similar to global projections (Thompson et al., 2021). The broader impact of flood risk in the Mpologoma catchment is projected to manifest through increased mean flood magnitude and duration and increased variability in flood frequency. Low flow risks are expected to manifest primarily in the form of increased variability in duration and number of events in a year. Although mean low flow magnitude may not significantly change with warming, extreme warming (i.e., at GWL4) is predicted to significantly reduce low flows and increase their variability. These findings on the broader impact of climate change are similar to other studies in Uganda, with indications of increased future flood magnitude (Nyenje & Batelaan, 2009; Bahati et al., 2021; Gabiri et al., 2020; Mehdi et al., 2021; Mileham et al., 2009) and occurrence of drought flows (Nyenje & Batelaan, 2009). Thus, there is a need for the development of sustainable catchment flood and low flow management plans.

Table 4 - 3 and Table 4 - 4 show that wetlands lower catchment outflow by 4.3 to 6.6%, but the model PBIAS for the model calibrated on MSWEP precipitation is larger than this (i.e., up to 11.4% at the daily timescale (Figure 4 - 3) and 5.2% at the monthly timescale (Figure 4 - 4)). This does not mean the results are invalid. Still, some people might interpret the result as meaning that the beneficial effects of wetlands are marginal or negligible when compared to model error and uncertainty. This illustrates the challenges in producing a ‘model of everywhere’ when there is so much uncertainty in model parameterisations and parameters (Beven, 2007; Blair et al., 2019). A core

motivation of ‘models of everywhere’ is to constrain uncertainty, exploiting as much knowledge as is available about a particular place (Blair et al., 2019). Often, the model domain only includes known hydrological processes (Buechel et al., 2023). Unincluded or undiscovered processes may significantly affect hydrological impacts unknown to the modeller (Beven et al., 2011). Furthermore, processes within the model may inaccurately be implemented numerically or physically (Hrachowitz & Clark, 2017). Therefore, inadequate process representation and implementation could potentially affect results. Nonetheless, modellers often produce the best model they can (baseline model) and any change compared to the baseline is assumed to be realistic.

This paper provides valuable information for wetland managers and policymakers on the supportive roles played by papyrus-based wetland systems, indicating a need for their restoration and conservation. However, results should be treated with caution, given that modelling studies on flow regulation services of wetlands tend to predict larger impacts compared to empirical studies (Kadykalo & Findlay, 2016). Future climate data generally contribute the most significant uncertainty to hydrologic studies (Prudhomme et al., 2003). Lee et al. (2021) assessed the impacts of uncertainties arising from climate change data on the streamflow of a catchment with wetlands. They concluded that the variability of GCM projections was the most significant contributor to flow prediction uncertainty. Nine CMIP6 GCMs were initially identified for this study, but only three were used due to limitations on resolution. Thus, the use of a larger GCM or regional climate model ensemble to lower prediction uncertainty is recommended. This is because convective rainfall dominates inland East Africa (Mutai & Ward, 2000), and climate models do not accurately represent them due to the low spatial resolution and representation of sub-grid processes (Bosilovich et al., 2008; Betts et al., 2006). Other causes of uncertainty include assumptions in model physics, model parameter uncertainty, and errors in ingested data.

Conclusions

This study investigated the effects of papyrus-dominated wetlands on baseflow and quickflow, including future flood and low flows within the Mpologoma catchment in Uganda. With the aid of the physically based, spatially distributed catchment modelling tool SHETRAN, the study quantified the catchment-scale flow regulating roles of papyrus wetlands. Findings show that papyrus wetlands wield a strong influence on catchment hydrology. They significantly affect quickflow (including floods), with a minor

role on baseflow and most low flow indices. This indicates that wetland management is integral to water resources and flood management, particularly in tropical Africa, where papyrus wetlands naturally occur. These wetlands provide nature-based solutions against floods to several communities in the developing nations of Africa, thus providing solutions to challenges faced by flood engineers and water resources managers.

The modelled high wetland evapotranspiration rates with increased risks of low flows, especially in dry years, indicate an exaggeration of water scarcity. However, conservation decisions on whether papyrus wetlands are essential despite water scarcity risks should be taken in the broader context, depending on other wetland functions (e.g., biodiversity, human health and food, flood mitigation, recreation, etc.).

CHAPTER 5: LINKING THE FLOW REGIME OF PAPYRUS WETLANDS TO BIOLOGICALLY-RELEVANT HYDROLOGIC ATTRIBUTES

This chapter is under review for the Journal of Ecohydrology. The numbering of sections and figures has been adapted for the consistency of the overall thesis.

Abstract

The dominant plant species in many African wetlands is Cyperus papyrus. Its adaption to saturated and low oxygen conditions and its dense structure and height provide breeding and feeding grounds for unique flora and fauna. As a keystone species adapted to local hydrology, the flow regime of papyrus offers the full range of hydrologic conditions and events essential to ecosystem health. However, no study has attempted to link papyrus wetlands' flow regimes to their biologically-relevant hydrologic attributes. The Indicators of Hydrologic Alteration (IHA) enable the evaluation of changes to flow regimes by examining hydrologic records and linking them to biologically-relevant hydrologic characteristics through the Environmental Flow Components (EFCs) approach. This study assesses hydrologic alterations of a papyrus wetland's flow regime due to rice irrigation. Illustrations of drivers of ecological change linking papyrus to hydrologic attributes are developed to determine the consequences of changed EFCs (extreme low flows, base flow, high flow pulses, and small and large floods) on papyrus as a habitat. Results show that agricultural water management considerably alters the magnitude, duration, timing, and rate of change of EFCs for the irrigated area to catchment area ratio greater than approximately 1:150 (i.e., irrigated area of 1,100 ha to catchment area of 1,680 km^2), affecting both sexual and asexual reproduction in papyri plants. The result, however, is subject to uncertainty in hydrological model parameter estimation and flow simulation, mainly due to inherent errors in the satellite-based precipitation product used. Overall, a better understanding of the threats of water diversion for agriculture is made by linking papyrus' flow regimes to biologically-relevant hydrologic attributes. Knowledge of the roles of the various EFCs could provide opportunities for conserving and protecting papyrus wetlands, especially for systems at risk of altered flows.

Introduction

Irrigated agriculture is estimated to cover 18 - 20% of global cultivated land, yet it consumes the largest share of freshwater resources (UNESCO-WWAP, 2012; Fischer et al., 2007). The sector accounts for 70% of water withdrawals (Fischer et al., 2007), of which 62% is surface water (Siebert et al., 2013). Intense exploitation of surface water resources such as lakes, rivers, and wetlands for irrigation has resulted in changes in natural flow regimes and, in some cases, catastrophic damage to aquatic and riparian ecosystems (Al-Quraishi & Kaplan, 2021; Gaybullaev et al., 2012; Kihwele et al., 2018; Steinfeld et al., 2020). Given that freshwater biotas are typically adapted to local hydrology, the risk to habitats and biodiversity increases the farther river flows deviate from natural regimes (Poff et al., 1997, 2010). Wetland and riparian ecosystems are particularly sensitive to deviations in hydroperiods (i.e., the timing, duration, frequency, and rate of change of inundation) (Cole et al., 1997; Ward et al., 2013), with water diversions often leading to a change in hydrological connectivity (Higgisson et al., 2020) and loss of habitats (Mitsch & Gosselink, 2000). These changes in connectivity can alter wetland vegetation communities (Higgisson et al., 2020), which can affect connectivity even after flow restoration (Li et al., 2020) due to the flow regulatory roles of different types and densities of vegetation (Valyrakis et al., 2021). Some of the vital surface water resources and ecosystems that have been adversely impacted by irrigation include the Aral Sea and its tributaries (Gaybullaev et al., 2012); the Euphrates River in Turkey, Syria, and Iraq (Al-Quraishi & Kaplan, 2021); the Yangtze River in China (Sun et al., 2020); the Gwydir and Macquarie rivers in Australia (Mallen-Cooper & Zampatti, 2018); and the Great Ruaha River in Tanzania (Kashaigili et al., 2009; Kihwele et al., 2018).

After a nearly 30-year hiatus in public irrigation development in Sub-Saharan Africa, governments have renewed their interest in investment in large-scale irrigation schemes (Higginbottom et al., 2021; Woodhouse et al., 2017). Due to population pressure and food shortage, wetlands are often viewed as wasted land, especially by local communities (Mwakubo & Obare, 2009; Woodhouse et al., 2017). As a livelihood provision to farming communities, public authorities have often converted these fragile landscapes into irrigation schemes by developing flow regulation structures (Dixon & Wood, 2003). For example, Doho, Kibimba and Olweny rice schemes were developed in wetlands in Uganda during the 1960s and 1970s (Kaggwa et al., 2009). More

recently, Uganda's Ministry of Agriculture, Animal Industry and Fisheries (MAAIF) established the national rice development strategy as a major intervention to enhance the country's food security. Cereal production is targeted to increase by 70% through intensified irrigated farming, including wetland development and utilisation (MWE and UN-WWAP, 2006). To this end, MAAIF laid the framework for the Naigombwa wetland rice irrigation project in eastern Uganda, with smallholder farmers as stakeholders (Namutebi & Sekanjako, 2013; MAAIF, 2019). The feasibility study and detailed design for Phase 1 of the project were completed in 2021 (MAAIF, 2021), with construction slated to commence in 2023. The scheme will cover about 2,300 hectares and benefit farmer groups at the Busowa Traders and Farmers' Cooperative Society and Pearl Rice Limited (MAAIF, 2021).

Despite the well-known impacts on habitats and ecosystems, irrigation projects in the region are often designed and operated without robust environmental flow management plans (Galbraith et al., 2005). A case in point is the Great Ruaha River in Tanzania, which includes the Usangu wetlands - a papyrus-dominated marshland (Kipkemboi & Van Dam, 2018) - and the Ruaha National Park (a habitat for wildlife including lions, cheetahs, leopards, elephants, giraffes, hippos, buffalos, etc.). Its changing flow regime, primarily due to water diversions for rice cultivation, from perennial to intermittent (Kihwele et al., 2018; Kashaigili et al., 2009), led to dry season inflows to the Usangu wetlands declining by about 70% between 1958 and 2004 (Kashaigili et al., 2009). Further, Usangu's dry season wetland coverage declined from about 160 km^2 to approximately 93 km^2 (Kashaigili et al., 2009), and its outflows ceased for extended periods in the last decades (Kashaigili et al., 2009; Kihwele et al., 2018), with wetlands drying up in 2000, 2002 and 2005 (Kihwele et al., 2018). To sustain the ecological condition of the Ruaha River, Kashaigili et al. (2009) recommended a minimum Usangu wetland dry season inflow and outflow of 7 and 0.6 m^3/s, respectively. However, maintaining freshwater habitats requires more than a minimum low-flow rule. Instead, it is necessary to establish a pattern that emulates the natural pulsed regime (Poff et al., 2010) regarding the amount and timing of water flows needed to support ecosystem health (Mathews & Richter, 2007).

Environmental flow regimes (EFRs) describe the volumes, timing, and quality of flows needed to sustain ecosystems and human livelihoods (Winrock International, 2018). By examining daily hydrologic records and linking them to biologically-relevant

hydrologic attributes, the Indicators of Hydrologic Alteration (IHA) facilitate the evaluation of human-induced changes to flow regimes (Richter et al., 1996; Mathews & Richter, 2007). To allow hydrograph characterisation to represent key flow-ecology relationships, five Environmental Flow Components (EFCs) complement the IHA (Mathews & Richter, 2007; The Nature Conservancy, 2009). These include extreme low flows, low (base) flows, high flow pulses, and small and large floods. Mathews & Richter (2007) describe these EFC events. Extreme low flows occur during drought and are characterised by the drying of floodplains and reduced connectivity, which restricts the movement of aquatic organisms. High flow pulses occur when water levels rise above low (base) flow levels but do not exceed bank full flow, typically during or after rain events. Small floods depict the main channel flows that overtop banks and occur frequently (every 2 - 10 years). They provide recharge for floodplain hyporheic zones, thus supporting macroinvertebrates and riparian plants. They also allow mobile organisms (such as fish) to access floodplain habitats, offer access to significant food resources and sites for spawning and rearing, and provide suitable water chemistry and characteristics (e.g., flow rates, temperature, etc.). Large floods, on the other hand, are rare but play critical roles in aquatic and floodplain ecosystems, such as moving significant amounts of sediment, organic matter and large woody debris, refreshing water quality, forming new habitats, and dispersing organisms (including riverbank vegetation) downstream.

These EFCs are ecologically relevant in a broad spectrum of hydro-climatic regions, provide a heuristic means for describing organism responses to flow variability, and are used in some of the commonly applied holistic methodologies for establishing environmental flows (Mathews & Richter, 2007). Some of the frequently utilised approaches that employ the EFCs include the Holistic Method (Arthington et al., 1992), the Building Block Methodology (King & Louw, 1998), Benchmarking (Brizga et al., 2002), and DRIFT (King et al., 2003). To apply the IHA concept, specific EFCs influencing organisms are identified by examining the life stages of organisms and linking them to flows. The IHA is then used to characterise the EFCs' magnitude, duration, timing, frequency, and rate of change (Mathews & Richter, 2007). Overall, IHA provides a detailed representation of the hydrologic statistics commonly used in the characterisation of ecologically relevant features of flow regimes (Richter et al., 1996, 1997; Principato & Viggiani, 2012). It is the most widely used index system (Zhou

et al., 2020) from more than 200 hydrologic indicators developed (Sheikh et al., 2022) and has been applied in numerous studies in the Americas (e.g., George et al., 2021; Jardim et al., 2020), Africa (e.g., Martínez-Capel et al., 2017; Taylor et al., 2003), Asia (e.g., Zhou et al., 2020; Zolfagharpour et al., 2022), and Europe (e.g., Fernández et al., 2012; Pardo-Loaiza et al., 2021).

Flow-ecology hypotheses in IHA-based studies are developed using illustrative drivers of ecological change or quantitative ecological models (Mathews & Richter, 2007). Quantitative models use mathematical and statistical concepts to describe and forecast the behaviour of systems, which could produce better conservation management than expertise-based actions (García-Díaz et al., 2019). However, they are prohibitively expensive in terms of data requirement and computational time, which limits the prospect of their application in ecosystem management studies in developing nations. On the other hand, illustrations of drivers of ecological change are expert-based and developed by reviewing data and knowledge about the river-floodplain system, native species, and their flow regime dependencies on low, high, and flood flows (Richter et al., 2006). The content of the review work, however, depends on how extensively the river environment has been studied, the type and amount of information gathered, and the availability of studies on similar ecosystems. The review work can be targeted to a specific species, especially if it is a keystone species such that its flow needs are representative of an ecological guild (Richter et al., 2006).

The giant sedge Cyperus papyrus L. (Cyperaceae) is the most widespread dominant species in many African wetlands (Pacini et al., 2018). Its dense structure and height, coupled with the environs in which it prospers, provide breeding and feeding grounds for unique fauna, including vertebrates (amphibians, reptiles, fish, birds, and mammals), insects, and aquatic invertebrates (Chapman et al., 2001). Some of these faunas, such as the white-winged scrub-warbler, greater swamp warbler, papyrus canary, papyrus yellow warbler, Carruthers's cisticola, and the papyrus gonolek, are endemic or near-endemic to papyrus wetlands (Donaldson et al., 2016). As a keystone species adapted to local hydrology, the flow regime of papyrus plants can provide the full range of hydrologic conditions and events needed to sustain ecosystem health in papyrus-based wetlands. However, no study has attempted to link its EFR to biologically-relevant hydrologic attributes. Knowledge of the roles of the various EFCs in the flow regime of papyrus wetlands could provide opportunities for its

conservation and protection, particularly for systems experiencing or at risk of altered flows.

This paper assesses hydrologic alterations of papyrus wetland EFRs due to rice irrigation. Illustrations of drivers of ecological change linking papyrus as a species to its biologically-relevant hydrologic attributes are developed and used to identify the effects of altered EFCs on papyrus as a habitat. The ecological change illustrations are tested on an irrigation scheme planned for the Naigombwa catchment in Uganda. The hydrologic changes are modelled in detail using a 3D integrated surface and subsurface hydrological model. Thus, by linking the papyrus wetland EFRs to biologically-relevant hydrologic attributes, a better understanding of the threats resulting from changes in EFCs is made.

Study Area

Naigombwa catchment, covering an area of about 1,680 km^2, forms part of Uganda's Mpologoma catchment (Figure 5 - 1). The climate in the region is Equatorial Monsoonal as per Köppen-Geiger's climate classification (Kottek et al., 2006), with a mean annual rainfall of 1,216 to 1,660 mm (Basalirwa, 1991). Along its path, the Naigombwa River travels mostly through low-gradient valleys, with broad floodplains forming wetlands in the middle and lower parts of the catchment. Its wetland channels are slightly meandering, with low gradients and high width-to-depth ratios (Kayendeke et al., 2018). Based on the European Space Agency land cover maps (Defourny et al., 2017), permanent wetlands (i.e., papyrus-dominated areas) showed no discernible change in coverage between 2000 and 2020. They cover about 31 km^2 (2%) of the catchment and are primarily located in the lower parts of the Naigombwa catchment.

As a rural catchment, the main economic activities comprise cultivation (lowland rice, maize, beans, groundnuts, cassava, sugarcane, etc.), livestock rearing and wetland-based fishing. The proposed Naigombwa irrigation scheme, including the reservoir (i.e., Namiganda dam), is located in the middle and upper parts of the catchment. The reservoir, designed at a capacity of 22.9 million m^3, will irrigate 2,200 and 100 hectares of lowland rice and polycrops (maize, beans, watermelon, etc.), respectively (MAAIF, 2021).

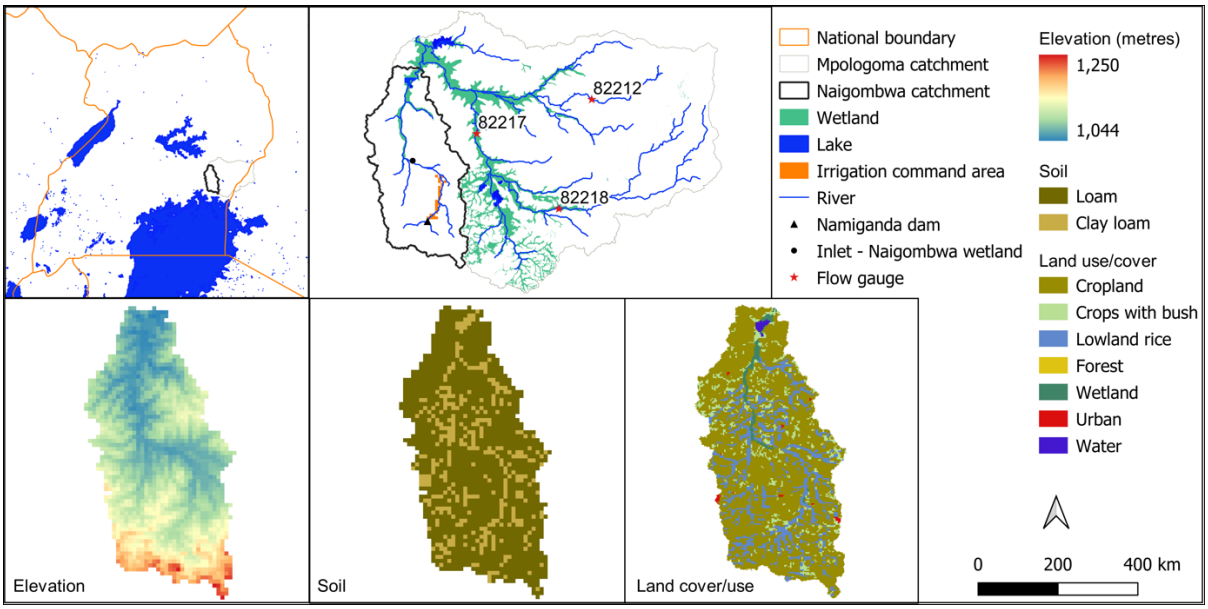

Figure 5 - 1: Study area including catchment elevation, soils, land cover, proposed irrigation command area and dam location.

Papyrus Wetlands as a Habitat

Papyrus wetlands are marshes occurring in flat, channel, or basin landforms, with hydroperiods characterised by permanent inundation (such as in rivers and lakes) or seasonal inundation (such as in floodplains and creeks) (Kipkemboi & Van Dam, 2018). The large intercellular air cavities of their culms provide efficient oxygen transport to rhizomes and roots, enabling adaptation to low oxygen conditions (Li & Jones, 1995). Culms (Figure 5 - 2) have umbels at the top and scale leaves where they meet rhizomes anchored in a dense mat-like mass of debris (Gaudet, 1975). The growth cycle comprises five key stages (Kayendeke, 2018): Stage A - germination or shoot growth from the rhizome; Stage B - establishment of the culm with closed umbels; Stage C - opening of the umbels; Stage D - fully open umbels; and Stage E - senescence. Shoots typically take 6 to 9 months to mature from rhizomes that have already formed or seeds that have germinated (Mburu et al., 2015). However, shorter growth times have been registered at productive sites. For example, 147 days (about five months) were measured at Lake George in Uganda from the emergence of a new stem to its senescence (Vaughan, 2011). These shoots can reach 5 - 6 m at maturity (Kipkemboi & Van Dam, 2018).

As a habitat, papyrus wetlands provide sanctuary to several species of flora and fauna. Fallen stems and the tall structural complexity of live papyrus provide a habitat for the

growth of numerous vines (Chapman et al., 2001). These non-papyrus plants generally occur as pockets of monoculture stands, with a distinct difference in floral diversity between permanently- and seasonally-flooded areas (Kipkemboi & Van Dam, 2018). Some fauna, such as fish, worms and insect larvae, live in the lower, water-saturated area, whereas others, such as birds, occupy the canopy (Kipkemboi & Van Dam, 2018). Other animals in these wetlands include swamp antelopes, hippos, otters, pythons, monitor lizards, frogs, toads, etc.

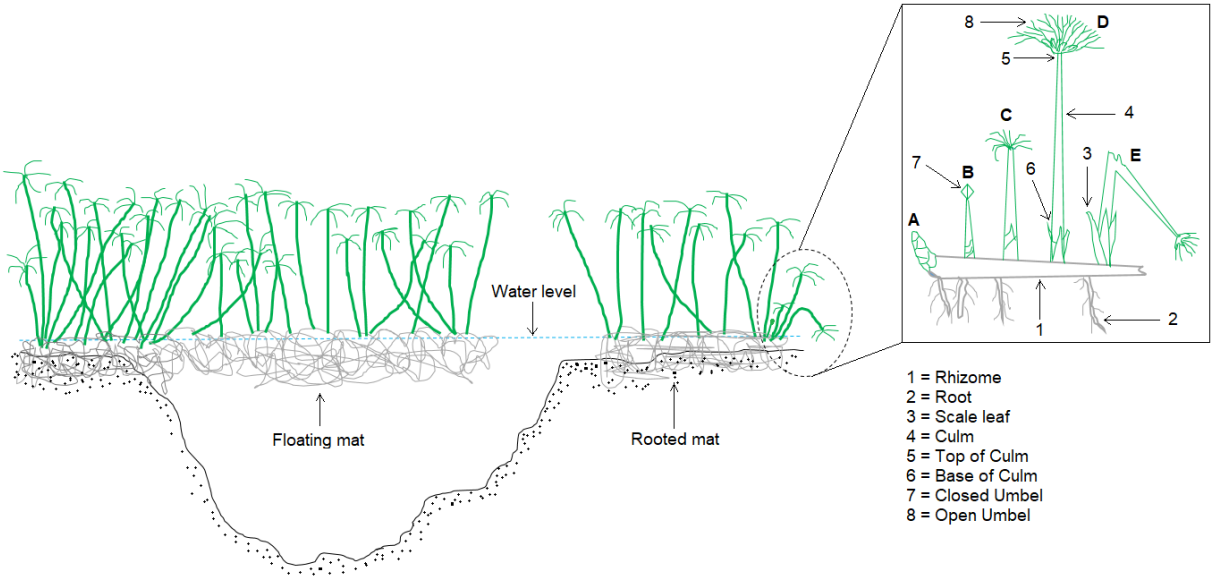

Figure 5 - 2: Schematic of a papyrus wetland cross-section. Inset is papyrus growth stages (A, B, C, D and E) and body parts (Adapted from Gaudet (1975)).

Methods and Materials

5.1.1 Illustrations of drivers of ecological change

Illustrations showing drivers of ecological change are valuable for organising and summarising knowledge on ecosystem structure and functions (Heemskerk et al., 2003). By linking ecosystem drivers and stressors to ecological effects and attributes, they communicate scientific thought, ecological outcomes, and their relationship to specific habitat components that management can purposely manipulate (Mushet et al., 2012). Ogden et al. (2005) describe the key features of the ecological illustration. Ecosystem drivers are natural and anthropogenic forces outside a system with large-scale influence on the system (e.g., climate cycles, catchment water management, etc.); ecosystem stressors are driver-induced changes to the physical and chemical conditions, patterns, and relationships of biological components in natural systems

(e.g., droughts, floods, etc.); ecological effects are the physical, chemical and biological responses caused by stressors (e.g., altered water depths, altered hydroperiods, etc.); and ecological attributes are the impacted ecosystem's biological elements or components linked to system sustainability (e.g., reproduction, dispersal, etc.).

For this study, the two-stage process described by Mushet et al. (2012) was used in developing the papyrus wetland Illustrations of drivers of ecological change. As a first step, existing literature was used to identify critical papyrus habitat components and ecological attributes affected by water availability. Finally, with the identified ecological attributes as endpoints, a linkage was made to catchment agricultural water management as an ecosystem driver by identifying ecosystem stressors and their ecological effects. The result is an illustration that visualises the linkages between ecosystem drivers and stressors and ecological effects and attributes.

5.1.2 Assessing hydrologic alteration

The effects of irrigated agriculture on flow regimes were assessed using the IHA software (version 7.1). The IHA software (The Nature Conservancy, 2009) computes up to 33 hydrologic indicators (Table 5 - 1) characterising intra- and inter-annual variability in hydrologic conditions. These hydrologic indicators define the magnitude, frequency, duration, timing, and rate of change of flows or water levels. They can be employed in impact analysis using data from before and after alterations. This study did not use the metric describing the ‘number of zero-flow days’ because data before and after alterations contained no zero-flow days.

Although helpful in describing human-induced changes to flow regimes, the hydrologic indicators do not tell users if alterations are within acceptable limits. Further, due to the relatively large number of parameter sets, water managers can feel overwhelmed when presented with 33 different environmental flow targets, such as in the “Range of Variability Approach” of Richter et al. (1997) (Mathews & Richter, 2007). To overcome this challenge, The Nature Conservancy added 34 parameters to the IHA software that quantify the five Environmental Flow Components (EFCs) (Table 5 - 2). Each EFC influences the amount and characteristics (e.g., connectivity, flow rate, temperature, pH, etc.) of aquatic and riparian habitats available throughout the year, thus triggering responses in organisms. The reaction of these organisms to the EFCs leads to species

persistence through reproduction or mortality during stressful times (Mathews & Richter, 2007).

The IHA-EFC concept was applied in two steps. In step 1, hydrologic alterations were analysed by comparing altered and unaltered flows. In step 2, the IHA analyses were linked to the EFCs to determine altered flow regimes. Generally, 20 years of daily data is recommended to account for natural climatic variability in IHA analyses (The Nature Conservancy, 2009). Thus, this study used 30 years (1983 to 2012) of discharge data for each altered and unaltered flow condition. Because hydrological data are often non-normal (Helsel & Hirsch, 2002), non-parametric (percentile) statistics were used in the IHA-EFC analyses.

The IHA group alteration index, computed as the mean of all deviations (in absolute values) within the group (i.e., the group average), can be classified into four categories: low (0 - 0.25%), mild (0.25 - 0.5%), moderate (0.5 - 0.75%), and high (0.75 - 1%) (Kuriqi et al., 2019). One limitation of using the group average is that it underestimates the impact of highly altered indicators (Xue et al., 2017). Thus, this study classified the alteration index of indicators within each group. The above classification, however, was developed for a run-of-river hydropower scheme. Unlike irrigation schemes, which lose a large proportion of diverted water through evapotranspiration and percolation, leading to detrimental changes in wetland ecosystems (Galbraith et al., 2005), run-of-river schemes return much of the diverted water to the river. Thus, to better capture the influence of large-scale water diversion on critical ecosystems such as wetlands, this study modified the above classification by proposing conservative classification categories. The IHA deviation of less than 10% is considered weak, 10 to 20% is moderate, and greater than 20% is strong. A similar classification was adopted for the EFCs; however, moderate alterations were further subdivided into slight-moderate (deviation of 10 to 14%) and moderate (deviation of 15 to 20%). This enabled better categorisation of alterations in EFCs.

Table 5 - 1: Summary of the 33 hydrological parameters used in the Indicators of Hydrologic Alteration (source: The Nature Conservancy (2009)).

IHA group/parameter	Regime characteristics	Number of indicators
Group 1: Magnitude of monthly water conditions	Magnitude and Timing	12
Group 2: Magnitude and duration of annual extreme water conditions	Magnitude and Duration	12
Group 3: Timing of annual extreme water conditions	Timing	2
Group 4: Frequency and duration of high and low pulses	Frequency and Duration	4
Group 5: Rate and frequency of water condition changes	Rates of Change and Frequency	3

Table 5 - 2: Summary of the 34 Environmental Flow Components (EFC) used in the IHA software (source: The Nature Conservancy (2009)).

EFC group/parameter	Regime characteristics	Number of parameters
Group 1: Monthly low (base) flows	Magnitude and Timing	12
Group 2: Annual extreme low flows	Magnitude, Duration, Timing and Frequency	4
Group 3: Annual high flow pulses	Magnitude, Duration, Timing, Frequency and Rate of Change	6
Group 4: Annual small floods	Magnitude, Duration, Timing, Frequency and Rate of Change	6
Group 5: Annual large floods	Magnitude, Duration, Timing, Frequency and Rate of Change	6

5.1.3 Hydrological modelling

Given that the irrigation command area is upstream of the Naigombwa wetland (Figure 5 - 1), the effects of the irrigation scheme on the wetland's flow regime are best evaluated by analysing inflow to the wetland. However, the Naigombwa River is ungauged. Thus, the inflow to wetlands was generated using the SHETRAN catchment modelling tool. SHETRAN (Ewen et al., 2000; Birkinshaw et al., 2010; Birkinshaw, 2010) is a 3D integrated surface and subsurface finite difference modelling system for water flow, sediment transport, and contaminant transport in catchments. It can simulate the influence of different land covers, including wetlands and catchment water

management scenarios, such as irrigation and reservoirs (Rangecroft et al., 2018; Oyarmoi et al., 2023). The SHETRAN catchment model for the Mpologoma catchment, including the Naigombwa catchment, for current conditions (i.e., without irrigation) was calibrated and validated on flow gauge stations 82212, 82217, and 82218 (Figure 5 - 1) by Oyarmoi et al. (2023). Naigombwa wetland's inflow time series were extracted from the model output. Wetland inflows for the situation with irrigation were also extracted from a modified model of the Mpologoma catchment. The model was modified to include the irrigation scheme and the Namiganda reservoir. The dam crest was set in the model by raising (i.e., increasing) the elevation of grid cells at the dam location to depict its design height of 11 m (MAAIF, 2021), thus creating a reservoir at the immediate upstream of the dam. In the model, water was abstracted only for irrigation from the reservoir based on a predetermined irrigation schedule and added to irrigation grids (Figure 5 - 3).

Irrigation schedules were prepared for the two main types of lowland rice water management - the traditional water-intensive continuous flooding (CF) technique (Orasen et al., 2019; Carrijo et al., 2017) and the less-intensive alternate wetting and drying (AWD) irrigation scheduling method developed by the International Rice Research Institute (IRRI, 2013). Rice fields are continuously ponded under CF, except for a brief period for weed control, until just before harvest when the water is drained. Due to the higher water demand of lowland rice compared with other cereal crops (Pimentel et al., 2004), in addition to the effects of global warming and competing water needs (Wassmann et al., 2009), CF is only feasible when both environmental and socio-economic requirements are satisfied (Orasen et al., 2019). AWD attempts to improve the sustainability of irrigated rice systems by lowering water use and greenhouse gas emissions (IRRI, 2013). AWD is known to lower water use and emission in rice systems by up to 30 and 48%, respectively, without significantly affecting yield (Richards & Sander, 2014).

Lowland rice is typically grown in fields with bunds that retain ponded water of a particular height. This was modelled in SHETRAN by restricting overland flow in rice grids when the water level is less than or equal to 25 cm (depicting bund height). The model was set to lower the overland Strickler coefficient from the calibration value of 0.0469 $m^{1/3}/s$ for rice fields (Oyarmoi et al., 2023) to 0.0001 $m^{1/3}/s$ when the irrigated grid water level is less than or equal to the bund height. Thus, effectively stopping

overland flow but still allowing infiltration. As discussed in the section on model sensitivity analysis, APPENDIX 5, the overland Strickler coefficient (Kro) is one of the most sensitive parameters in the SHETRAN model of the Mpologoma catchment, with a sensitivity index of 0.72. Strickler coefficient in ricefield and grassland experimental plots generally ranges from 1.03 to 6.25 $m^{1/3}/s$ (Weltz et al., 1992; Engman, 1986; Ree et al., 1977). However, due to uncertainty in models (e.g., assumptions in model physics and structure, data limitations, and errors in input datasets), the calibrated model parameters usually differ from experimental values (Singh et al., 2017; Seibert & McDonnell, 2002; Cerdan et al., 2004). Some SHETRAN data files are set out in fixed format (e.g., Kro is input in a 7-character format). Further, the Kro value of 0.0000 $m^{1/3}/s$ is hardcoded in SHETRAN, such that it directs the model to use Kro values from a different location in the input files. Thus, the reason for choosing the minimal value of 0.0001 $m^{1/3}/s$.

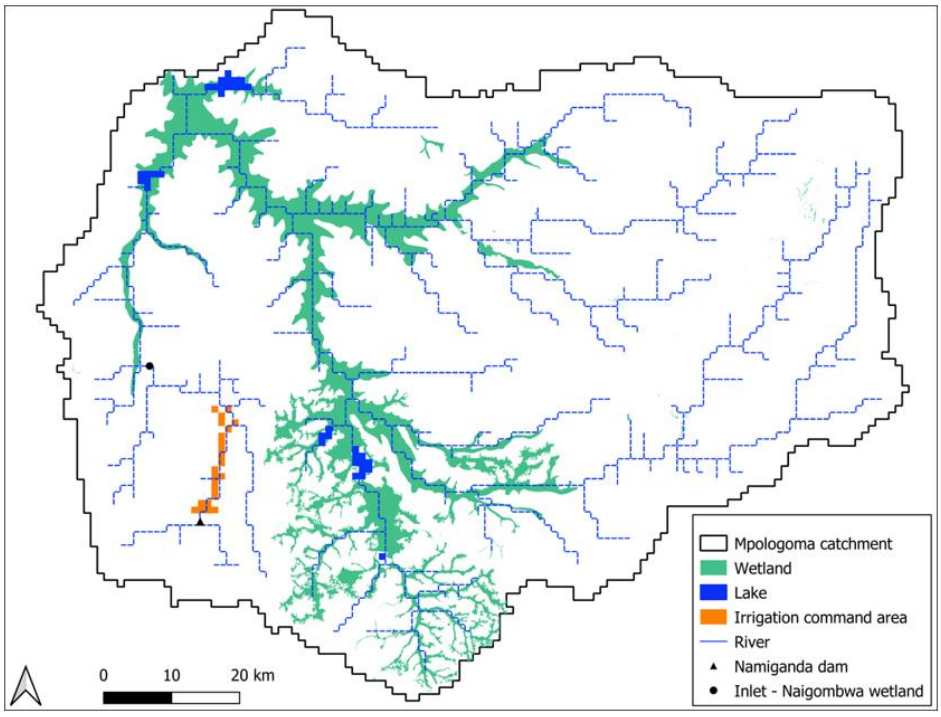

Figure 5 - 3: SHETRAN model domain showing the location of crucial catchment features (wetlands, lakes, irrigated area, and the reservoir).

5.1.4 Estimation of irrigation demand

As a means of minimising irrigation water use and the cost of management and operation of irrigation infrastructure, farmers often align the crop lifecycle with rainy seasons. This way, irrigation is used only to supplement precipitation (Oweis, 1997).

There are two rainy seasons a year in the study area - March to May and August to November. The first cropping season is from March to June/July, and the second is from August to November/December. Table 5 - 3 shows a typical cropping calendar for rice and polycrops (represented as beans in this study). Rice is often transplanted, while polycrops are dry-seeded. Thus, the only irrigation demand category for beans is the daily gross irrigation requirement from planting (dry-seeding) to maturity (1st March/August to 17th June/November). The gross irrigation requirement (I_{gross}) was calculated from the net irrigation using Equation 5 - 1, where I_{net} is the net irrigation, and E_{ff} = 60% (MAAIF, 2021) is the scheme's overall irrigation efficiency. I_{net} was calculated using the Food and Agriculture Organization's crop growth model, AquaCrop version 7. AquaCrop (FAO, 2009; Raes et al., 2022), a field scale model calibrated for various crops (including rice and beans), calculates net irrigation while accounting for rainfall, field conditions, and soil moisture balance (Raes, 2022). For this study, the daily net irrigation for beans was estimated with soil moisture maintained at field capacity.

$$I_{gross} = \frac{I_{net}}{E_{ff}}$$

Equation 5 - 1

For rice, the demand categories include supply to nursery beds (Nur), field puddling requirement for transplanting rice seedlings (SAT), and the irrigation requirement from the time of transplant to maturity (I_{net}/E_{ff}), Equation 5 - 2.

$$I_{grossRice} = Nur + SAT + \frac{I_{net}}{E_{ff}}$$

Equation 5 - 2

The nursery demand is about 120 mm per season (Bin et al., 2003). Nurseries cover approximately a tenth of the area to be transplanted and take about 15 to 20 days to mature (IRRI, 2007). Thus, the irrigation demand for nurseries was applied over 20 days (1st March/August to 20th March/August) at a 6 mm/day peak rate while monitoring the above-ground water level in each rice field. The nursery demand is calculated as the difference between the peak demand and the day's average field water level. A parallel SHETRAN model with bunds but no irrigation was used to generate daily field

water levels. Farmers typically use 150 to 250 mm of water for land preparation for rice transplant (Guerra et al., 1998). This study assumed the soil puddling requirement was 200 mm per season and applied over seven days (15th March/August to 21st March/August). Thus, a peak demand of 28 mm/day was applied, depending on the day's above-ground water level. Like beans, the daily net irrigation requirement for rice was calculated using AquaCrop with soil moisture maintained at field capacity; however, the estimation was from the time of transplant (25th March/August) to maturity (3rd July/December). Rice field bunds were also set in AquaCrop to account for ponded water. The rice gross irrigation requirement from the time of transplant to maturity was calculated from the net irrigation using the overall irrigation efficiency (E_{ff}) of 60% (MAAIF, 2021) and 78% for CF and AWD, respectively. AWD lowers infield water use by up to 30% (Richards & Sander, 2014); thus, the E_{ff} was adjusted from 60% to 78%.

Figure 5 - 4 shows the estimated annual rice irrigation demand under CF and AWD irrigation scheduling. The mean yearly irrigation demand is 1,197 and 1,013 mm, respectively, denoting an 18% difference.

Table 5 - 3: Irrigation demand categories and schedules for rice and poly-crops for the study area.

Crop type	Irrigation demand category	Cropping calendar		Irrigation duty	
		Season 1	Season 2	Season 1	Season 2
Lowland rice	Rice seedlings watering	1st March to 20th March	1st August to 20th August	120 mm per season (Bin et al., 2003)	
	Land preparation for transplanting	15th March to 21st March	15th August to 21st August	200 mm per season (Brouwer & Heibloem, 1986)	
	Net/gross irrigation demand	25th March to 3rd July	25th August to 3rd December	Net irrigation was calculated using AquaCrop software; gross irrigation was calculated using an overall irrigation efficiency of 60% for CF and 78% for AWD.	
Polycrop (beans)	Net/gross irrigation demand	1st March to 17th June	1st August to 17th November	Net irrigation was calculated using AquaCrop software; gross irrigation was calculated using an overall irrigation efficiency of 60%.	

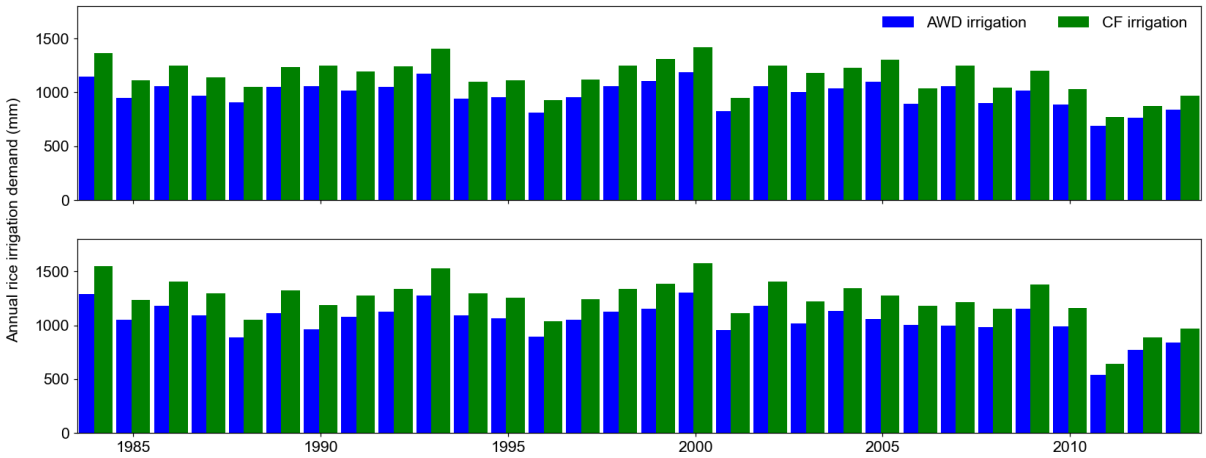

Figure 5 - 4: Annual rice irrigation demand for continuous flooding (CF) and alternate wetting and drying (AWD) irrigation scheduling. The top row shows results for rice fields in the upper part of the command area in Figure 5 - 3; the bottom row shows results for downstream rice fields. The difference in precipitation levels between these regions is the reason for the contrast.

Results

5.1.5 Naigombwa wetland illustration of drivers of ecological change

Figure 5 - 5 shows the linkage between ecosystem drivers and ecological attributes in the Naigombwa catchment. The model links agricultural water management as the primary ecosystem driver to the identified ecological attributes of recharging and maintaining the floodplain water table, deposition of nutrients in floodplains, flushing wastes and debris in wetlands, shaping physical wetland habitats through erosion and deposition of sediments and debris, creating secondary channels and oxbow lakes linking wetlands to main river channels, reproduction and survival of papyrus plants, dispersal and recolonisation, and purging invasive plant and animal species from papyrus wetlands (Boar, 2006; Kipkemboi & Van Dam, 2018; Thompson & Grime, 1979; Vaughan, 2011; Terer et al., 2014; Azza et al., 2000; Kayendeke et al., 2018; Richter et al., 2006). These ecological attributes are responsible for sustaining papyrus populations. The primary ecosystem stressors and ecological effects linked to these attributes are water diversions to farmland, increased seepage, evapotranspiration and runoff in rice fields, and altered river flow regimes and wetland hydroperiods, respectively.

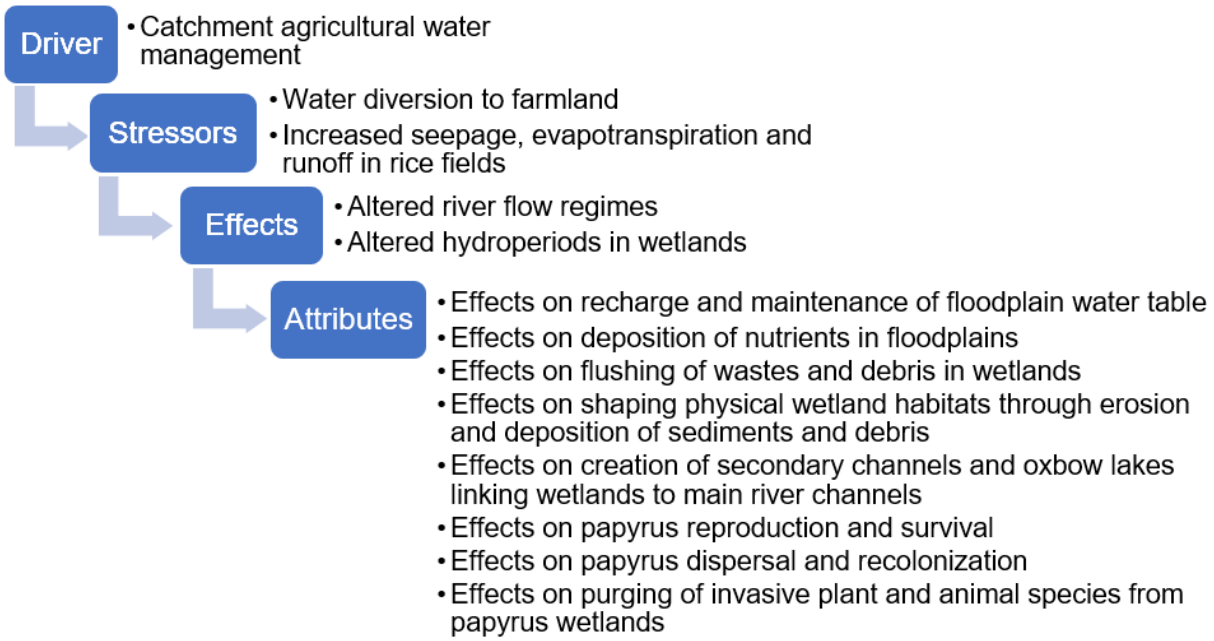

Figure 5 - 5: Illustration of the linkage between ecosystem drivers and ecological attributes relevant to papyrus wetlands in the Naigombwa catchment.

5.1.6 Overall effects of irrigation on wetland inflow

The 30-year hydrographs at the inlet to the papyrus wetlands (Figure 5 - 6) and the mean annual water balance at the irrigated sites (Table 5 - 4) for the scenarios with and without irrigation clearly show the effects of water diversions on catchment water balance. Both low and high flows are altered, with the peaks most affected (Figure 5 - 6). However, the difference between the irrigation-scenario (CF and AWD) hydrographs appears negligible except for 1994-1995, 1997-1999 and 2007-2008. The daily average flow, at 2.05 m^3/s under no irrigation, remains very similar at 2.07 m^3/s under continuous flooding (CF) and alternate wetting and drying (AWD) irrigation scheduling. However, the maximum and minimum flows are lowered from 23.9 and 0.51 m^3/s under no irrigation to 15.36 and 0.2 m^3/s under CF and AWD. The minimal difference in the effects of CF and AWD on the overall catchment water balance can be seen in the average annual flow volume. The average yearly wetland inflow under CF (65.69 million m^3) is similar to that under AWD (65.74 million m^3).

Seepage in rice fields contributes to rising water tables during the rice-growing season, with very shallow groundwater levels typically 0.2 to 1.6 m below the ground surface (Goitom et al., 2016; Bin et al., 2003). These water levels usually recede quickly after harvest. Measurements by Bin et al. (2003) show that the water table's influence area

is up to 400 m from rice fields, with logging often occurring in areas within 200 m. The Naigombwa rice scheme command area is within the Naigombwa River floodplain (Figure 5 - 1); thus, the easily generated runoff in these saturated riparian zones, following rain events, reaches the river quickly. This explains the increased flashiness during low flows (Figure 5 - 6).

As expected, the mean annual evapotranspiration increases under CF and AWD irrigation (3.3 and 3.2%, respectively, Table 5 - 4), with transpiration rates most affected. The annual mean transpiration rate at irrigated sites increases by 12.1 and 11.8%, while soil evaporation decreases by 1.1% and 1%, respectively. The rice canopy strongly shields and impedes soil evaporation after the initial growth stage (Yoshida, 1979; Tsuchiya et al., 2018). For this study, it was assumed that rice plants cover the entire irrigated field; however, the ratio of the total leaf area to the ground covered by vegetation is set to the SHETRAN model calibrated value of 50% (Oyarmoi et al., 2023). The effect is seen in the reduced soil evaporation rates. Canopy evaporation is unaltered, given that irrigation water is applied on the soil surface. Meanwhile, the water lost to percolation and surface runoff increases by 314.2% and 274%, respectively.

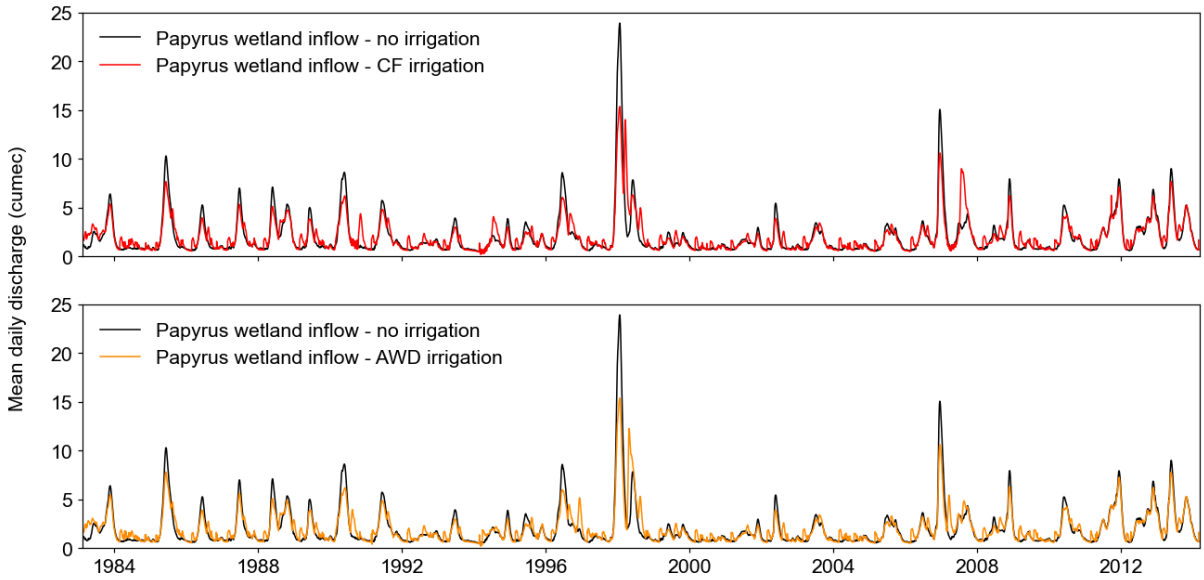

Figure 5 - 6: Papyrus wetland inflow for scenarios with and without irrigation. The top row is Continuous Flooding (CF) irrigation. The bottom row is Alternate Wetting and Drying (AWD) irrigation.

Table 5 - 4: Mean annual water balance at irrigated sites for conditions with irrigation (continuous flooding (CF) and alternate wetting and drying (AWD)) and without irrigation.

Water balance component	No irrigation	CF irrigation (relative change %)	AWD irrigation (relative change %)
Precipitation (mm)	1,313	1,313	1,313
Irrigation water (mm)	0	1,359	1,188
Canopy evaporation (mm)	367	367 (0)	367 (0)
Transpiration (mm)	266	298 (12.1)	297 (11.8)
Soil evaporation (mm)	257	254.13 (-1.1)	254.44 (-1.0)
Actual evapotranspiration (mm)	890	919 (3.3)	918 (3.2)
Percolation and runoff (mm)	423	1,753 (314.2)	1,582 (274.0)

5.1.7 Hydrologic alterations due to irrigation

Given the insignificant difference in wetland inflows for conditions of continuous flooding (CF) and alternate wetting and drying (AWD) irrigation scheduling, the Indicators of Hydrologic Alteration (IHA) analysis was based only on the SHETRAN model results with CF irrigation. Table 5 - 5 summarises the IHA analysis for the situation with and without irrigation. The flow deviation for each IHA group is captured in the group average. A large group average indicates a significant change in flow, as depicted by the hydrologic indicators within the group. The group average of Group 1 (magnitude of median monthly flow, 28.2%), Group 4 (frequency and duration of high and low flow pulses, 20.4%), and Group 5 (rate and frequency of change in conditions, 26.6%) are generally larger than those of Group 2 (magnitude and duration of median annual extremes, 11.7%) and Group 3 (median timing of annual extremes, 4%).

Based on the individual attributes in each group, all of the hydrologic attributes in Group 1, except for during May, November, and December, indicate moderate to strong alterations (-10.2 to 149.7%) in the magnitude of median monthly flows. Significant flow reductions occur in June, July, January, and February (-10.2 to -12.3%), while increases are experienced in March, April, August, September, and October (11.3 to 149.7%). The reduced flow periods coincide with the region's dry seasons (June to July and December to February). Meanwhile, the increased flow periods (March to April and August to September) coincide with the water-intensive land preparation for rice transplanting in March and August for the first and second crop cycles, respectively. Most Group 2 attributes are weakly altered, except for the baseflow index

and the 1-day, 3-day, 7-day, and 30-day maximum flows. The median values of these annual flow extremes are moderately lowered in the 17.2 to 19.6% range. However, the timing of these extremes, as indicated by the Group 3 attributes, remains largely unaltered (0 to -7.9%). For Group 4, the frequency and duration of high flow pulses are largely unaltered; however, the low flow pulses are strongly altered in frequency (-33.3%) and duration (41.1%). Finally, for Group 5, although the number of reversals between hydrograph rise and fall is weakly altered (-1.8%), the rate of change in flow conditions (hydrograph rise and fall rates) are moderately (17.9%) and strongly (60.2%) altered, respectively.

The influence of the above-identified alterations on flow components (extreme low flows, low (base) flows, high flow pulses, small floods, and large floods) are summarised in the Environmental Flow Component (EFC) analysis results in Table 5 - 6. The EFC hydrographs and thresholds are defined in Figure 5 - *7*. From Table 5 - 6, the magnitude of median annual low (base) flows is weakly altered in most months, except for March (0.76 to 1.1 m^3/s, 44.2%), April (0.86 to 1.04 m^3/s, 20.8%) and June (1.7 to 1.52 m^3/s, -10.3%). For extreme low flows, the median annual peak magnitude and the frequency of occurrence are weakly altered (-5.3 and 0%, respectively). However, the median flow duration per event is strongly enhanced from 8 to 19 days (137.5%). Similarly, the timing of the lowest flow in a year is strongly altered (-14.7%). The lowest flow occurs 11 days earlier.

All the hydrological regimes of high flow pulses are significantly altered. The median annual magnitude, duration, frequency, rise rate, and fall rate are strongly modified by -49.5, -76.3, 100, 471.5, and 99.6%, respectively. Meanwhile, the timing is moderately altered by -17% (i.e., occurring earlier by 31 days). The median annual peak flow value and duration per event are lowered from 3.53 to 1.78 m^3/s and 93 to 22 days, respectively, and the rise and fall rates increase from 0.048 to 0.275 m^3/s and -0.026 to -0.051 m^3/s, respectively. Nonetheless, the median yearly occurrences of high flow pulses increase from nearly zero to at least 2.

Small floods are weakly affected in duration and frequency. However, the peak flow, timing and rates of change are significantly altered. Small floods' peak flow, timing, and fall rate are moderately adjusted by -11.1, 15.9, and -10.4%, respectively, while the rate of rise is strongly reduced by -47.3%. The median annual peak, rise rate, and fall

rate are reduced from 7 to 6.22 m^3/s, 0.096 to 0.051 m^3/s, and -0.064 to -0.057 m^3/s, respectively. The timing, meanwhile, increases by 27 days.

Large floods, on the other hand, are weakly altered in timing, frequency, and fall rate. However, they are significantly affected in magnitude, duration and rise rate. The peak flow is moderately altered (-13.8%), while the duration (29.5%) and rise rate (-23.9) are strongly modified. The median annual peak and rise rate are reduced from 15.06 to 12.98 m^3/s and 0.349 to 0.266 m^3/s, while the duration increases from 161 to 209 days.

Table 5 - 7 summarises the above-identified changes in EFCs, with moderate alterations further subdivided into slight-moderate (deviation of 10 to 14%) and moderate (deviation of 15 to 20%). Flow regimes most affected by water diversion for irrigation are flow magnitude, duration, timing, and rate of change. The frequency of occurrence of the various EFCs, except for high flow pulses, are least affected. The EFCs significantly altered in magnitude include floods (large and small), high flow pulses, and low (base) flows in March, April, and June. Those greatly affected in duration include extreme low flows, high flow pulses, and large floods. The EFCs extensively modified in the timing of their occurrence include extreme low flows, high flow pulses and small floods. Meanwhile, the rates of change of the various EFCs are significantly altered only for the higher flows (high flow pulses, small floods, and large floods).

Table 5 - 5: Results of IHA analysis over 30 years (1984 - 2013) at the inflow to papyrus wetlands for scenarios with and without irrigation.

IHA group		Median value		Deviation (%)
		No irrigation	CF irrigation	
Group 1: Magnitude (m^3/s) of monthly flow	Median March flow	0.71	1.78	149.7
	Median April flow	0.87	1.14	31.5
	Median May flow	1.67	1.55	-7.1
	Median June flow	3.09	2.76	-10.8
	Median July flow	2.67	2.34	-12.3
	Median August flow	1.65	2.72	64.4
	Median September flow	1.37	1.67	22.5
	Median October flow	1.16	1.29	11.3
	Median November flow	1.49	1.46	-2.5
	Median December flow	1.16	1.21	3.6

IHA group		Median value		Deviation (%)
		No irrigation	CF irrigation	
	Median January flow	0.87	0.78	-10.2
	Median February flow	0.76	0.67	-12.3
	Group average[1] (%)			**28.2**
Group 2: Magnitude (m^3/s) and duration (days) of annual extremes	1-day minimum flow	0.67	0.61	-7.7
	3-day minimum flow	0.67	0.62	-7.2
	7-day minimum flow	0.68	0.63	-7.0
	30-day minimum flow	0.71	0.67	-5.8
	90-day minimum flow	0.83	0.88	5.6
	1-day maximum flow	5.27	4.25	-19.3
	3-day maximum flow	5.27	4.25	-19.4
	7-day maximum flow	5.26	4.23	-19.6
	30-day maximum flow	4.98	4.05	-18.6
	90-day maximum flow	3.56	3.61	1.2
	Base flow index	0.37	0.31	-17.2
	Group average[1] (%)			**11.7**
Group 3: Timing of annual extremes	Julian's date of 1-day minimum flow[2]	63	58	-7.9
	Julian's date of 1-day maximum flow	178	178	0.0
	Group average[1] (%)			**4.0**
Group 4: Frequency and duration of high and low flows[3, 4, 5]	The annual number of low pulses	3	2	-33.3
	The annual low pulse duration (days)	14	20	41.1
	The annual number of high pulses	1	1	0
	The annual high pulse duration (days)	72	67	-7.3
	Group average[1] (%)			**20.4**
Group 5: Rate	Rise rate[6]	0.026	0.031	17.9
	Fall rate	-0.018	-0.028	60.2

[1] Mean of all deviations (in absolute values) within the group.
[2] Julian dates are calendar dates by integer values, starting with 1 on January 1 and ending with 366 on December 31 - the earliest date is used if there are many days with the same flow value in a water year.
[3] the metrics that define the low and high flow pulse frequencies and durations were estimated for the periods during which the daily flow dropped or exceeded the 25 and 75th percentiles, respectively.
[4] low pulse threshold = 0.82 m^3/s.
[5] high pulse threshold = 2.38 m^3/s.
[6] calculated as differences between consecutive daily values after dividing data in each water year into "rising" (positive) and "falling" (negative) periods. Unit is m^3/s.

IHA group		Median value		Deviation (%)
		No irrigation	CF irrigation	
(m^3/s) and frequency of change in conditions	Number of reversals[7]	56	55	-1.8
	Group average[1] (%)			**26.6**

Table 5 - 6: Median annual values of EFC analysis over 30 years (1984 - 2013) at the inflow to papyrus wetlands for scenarios with and without irrigation.

EFC parameters		Median value		Deviation (%)
		No irrigation	CF irrigation	
Annual low (base) flows[8]	March low flow	0.76	1.10	44.2
	April low flow	0.86	1.04	20.8
	May low flow	1.40	1.39	-0.7
	June low flow	1.70	1.52	-10.3
	July low flow	1.07	0.99	-6.9
	August low flow	1.07	1.16	8.5
	September low flow	0.96	1.02	6.2
	October low flow	0.99	1.05	5.4
	November low flow	1.09	1.10	1.6
	December low flow	0.97	0.94	-3.1
	January low flow	0.87	0.85	-2.2
	February low flow	0.78	0.77	-0.6
Annual extreme low flows	Extreme low peak[8]	0.69	0.65	-5.3
	Extreme low duration[9]	8	19	137.5
	Extreme low timing[10]	78	56	-28.2[11]
	Extreme low frequency	2	2	0
Annual high	High flow peak[8]	3.53	1.78	-49.5
	High flow duration[9]	93	22	-76.3

[7] the number of times that flow switches from one type of period to another (i.e., rise to fall and vice versa).
[8] Flow value in m^3/s.
[9] duration in days.
[10] timing is in Julian's date (calendar dates by integer values, starting with 1 on January 1 and ending with 366 on December 31).
[11] because of the difficulties in calculating statistics for periodic variables (e.g., time), the median dates are placed into quarterly bins (1-91, 92-183, 184-275, and 276-366) before calculating the deviation. If the median timings before and after alteration are in the same bin or the second and third bins, the deviation is computed as the difference between them. If the median timing before and after alteration are in the fourth and first bins, respectively, and vice versa, 366 is added to the date in the first bin before computing the deviation.

EFC parameters		Median value		Deviation (%)
		No irrigation	CF irrigation	
flow pulses	High flow timing[10]	185	154	-17[11]
	High flow frequency	0	2	100.0
	High flow rise rate[12]	0.048	0.275	471.5
	High flow fall rate[12]	-0.026	-0.051	99.6
Annual small floods	Small flood peak[8]	7.00	6.22	-11.1
	Small flood duration[9]	215	213	-0.9
	Small flood timing[10]	167	194	15.9[11]
	Small flood frequency	0	0	0
	Small flood rise rate[12]	0.096	0.051	-47.3
	Small flood fall rate[12]	-0.064	-0.057	-10.4
Annual large floods	Large flood peak[8]	15.06	12.98	-13.8
	Large flood duration[9]	161	209	29.5
	Large flood timing[10]	354	6	5.1[11]
	Large flood frequency	0	0	0
	Large flood rise rate[12]	0.349	0.266	-23.9
	Large flood fall rate[12]	-0.097	-0.088	-8.7

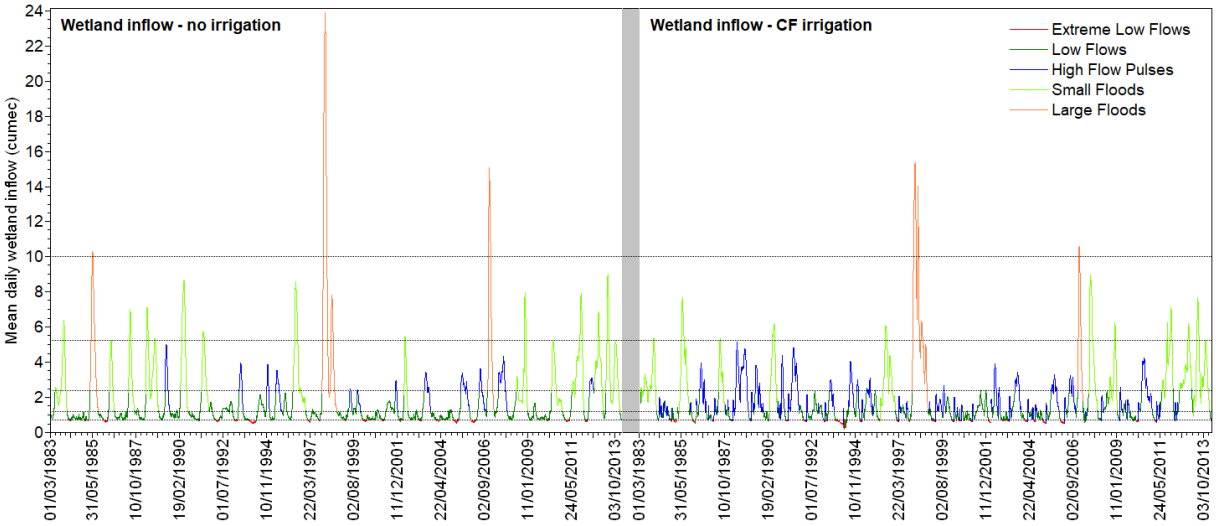

Figure 5 - 7: Time series of Naigombwa wetland inflow from the water year 1983 to the water year 2012 showing Environmental Flow Components for the situation with and without irrigation. Extreme low flow threshold = 0.72 m^3/s; high flow start threshold for rising limb = 2.38 m^3/s; low flow start threshold for falling limp = 1.21 m^3/s; small flood minimum peak flow = 5.26 m^3/s; large flood minimum peak flow = 10.04 m^3/s.

[12] calculated as differences between consecutive daily values after dividing data in each water year into "rising" (positive) and "falling" (negative) periods. Unit is m^3/s.

Table 5 - 7: Summary of EFCs altered due to flow diversion.

EFC parameter	Degree of flow alteration			
	Negligible	**Slight-moderate**	**Moderate**	**Strong**
Magnitude				
Extreme low flows				
Low (base) flows	In most months except March, April and June	-10.3% (1.7 to 1.52 m^3/s) in June		44.2% (0.76 to 1.1 m^3/s) in March and 20.8% (0.86 to 1.04 m^3/s) in April
High flow pulse				-49.5% (3.53 to 1.78 m^3/s)
Small floods		-11.1% (7 to 6.22 m^3/s)		
Large floods		-13.8% (15.06 to 12.98 m^3/s)		
Duration				
Extreme low flows				137.5% (8 to 19 days)
High flow pulse				-76.3% (93 to 22 days)
Small floods				
Large floods				29.5% (161 to 209 days)
Timing				
Extreme low flows				-28.2% (Julian day 78 to Julian day 56)
High flow pulse			-17% (Julian Day 185 to Julian Day 154)	
Small floods			15.9% (Julian Day 167 to Julian Day 194)	
Large floods				
Frequency				
Extreme low flows				
High flow pulse				100% (from nearly 0 to 2 events in a year)
Small floods				
Large floods				
Rate of change				

EFC parameter	Degree of flow alteration			
	Negligible	Slight-moderate	Moderate	Strong
High flow pulse				Rise rate: 471.5% (0.048 to 0.275 m^3/s); fall rate: 99.6% (-0.026 to -0.051 m^3/s)
Small floods		Fall rate: -10.4% (-0.064 to -0.057 m^3/s)		Rise rate: -47.3% (0.096 to 0.051 m^3/s)
Large floods				Rise rate: -23.9 (0.349 to 0.266 m^3/s)

5.1.8 Effect of irrigation command area on hydrologic alteration

Table 5 - 8 shows the impact of the irrigation command area and the location of the irrigated area on the IHA group averages (i.e., the mean of all deviations - in absolute values - within each group). Group averages were calculated for the conditions of the dam present but no irrigation, Phase 1 target irrigated area (2,300 ha), about half of the target irrigated area (1,100 ha) in the upstream (US) or downstream (DS), about a quarter of the target irrigated area (500 ha) in the US, midstream (MS) or DS, and 100 ha in the US, MS or DS.

Group 3 metrics (timing of annual extremes) are least affected (group average of 0.3 to 1.1%) for all conditions. Meanwhile, Group 4 (frequency and duration of high and low flows) are most impacted (20.4 to 61%). Significant deviations (i.e., group averages > 10%) occur in Group 1, Group 2, and Group 4 when only the dam is present but no irrigation. Negligible alterations in wetland inflow for the conditions with irrigation occur for most IHA groups except Group 4, as long as the irrigated area is less than or equal to 1,100 ha. Flood irrigation in rice fields enhances groundwater recharge (Negri et al., 2020; Essaid & Caldwell, 2017) and discharge to rivers (Essaid & Caldwell, 2017). In the case of the Naigombwa catchment, the release to rivers offsets reservoir storage and the delayed release at the dam. However, the influence of flood irrigation in mitigating the regulatory effects of the dam is mainly within the limits of the natural pulsed regime when the irrigated area is about 1,100 ha at most, equivalent to the irrigated area (1,100 ha) to catchment area (1,680 km^2) ratio in the order of 1:150. It is worth noting that the result is subject to uncertainty in hydrological model parameter estimation and flow simulation, mainly due to inherent errors in the satellite-based

precipitation product (see Section 4.1.11) used in forcing the SHETRAN and AquaCrop models.

Table 5 - 8: Effect of irrigated area and location of irrigation command area on the IHA group average. US, MS and DS imply upstream, midstream and downstream, respectively.

Area irrigated (ha)	Dam only (no irrigation)	2,300 (Phase 1 target area)	1,100		500			100		
Location of irrigated area			US	DS	US	MS	DS	US	MS	DS
Group average (%)										
IHA Group 1: Magnitude of monthly flow	12.9	28.2	4.2	5.2	6.3	4.3	4.3	6.5	6.8	4.9
IHA Group 2: Magnitude and duration of annual extremes	15.7	11.7	8.5	7.7	9.2	8.6	8.6	9.6	9.9	8.6
IHA Group 3: Timing of annual extremes	0.8	4.0	0.5	1.1	0.3	0.5	0.5	0.3	0.3	0.5
IHA Group 4: Frequency and duration of high and low flows	61.0	20.4	38.2	43.8	33.2	38.2	38.2	26.6	33.3	53.2
IHA Group 5: Rate and frequency of change in conditions	8.6	26.6	10.3	7.6	9.3	11.3	11.9	7.6	7.3	7.5

Linking Altered Flow Regimes to Papyrus Wetland's Biologically-Relevant Hydrologic Attributes

Complemented with ecologically relevant statistics (IHA-EFC analyses), this hydrological modelling study assessed and quantified hydrologic alterations of a papyrus wetland's environmental flow regime due to agricultural water management (i.e., rice irrigation). By linking catchment-scale agricultural water management, an ecosystem driver acting outside the wetland system but with large-scale influence on the wetland, to its ecological attributes on the wetland (Section 5.1.1), a connection can be developed between the hydrologic alterations and papyrus wetland's biologically-relevant hydrologic attributes. The following subsections (i.e., Sections 5.1.9 to 5.1.14) discuss the relation between the altered flow regimes and the biologically-relevant hydrologic attributes. However, due to modelling uncertainties (e.g., the mismatch in scale between SHETRAN and AquaCrop as discussed in the second last paragraph of Section 0, inherent errors in the satellite-based precipitation product used (see Section 4.1.11), etc.) and the fact that catchments have unique landscapes (i.e., topography, soil and geology, drainage area, and land use/cover) (Rains et al., 2016), the discussion on the link between the altered flow regimes and the biologically-relevant hydrologic attributes is limited to the Naigombwa catchment and for the irrigated area of 2,300 hectares. Nonetheless, the identified biologically-relevant hydrologic attributes apply to most papyrus-dominated catchments. However, the scale of the effects of water diversion will vary depending on catchment characteristics (i.e., landscape, precipitation, and potential evapotranspiration) and irrigation acreage.

5.1.9 Effect of altered flow regimes on seed dispersal

Papyri plants reproduce sexually through seed germination or asexually through shoots sprouting from rhizomes (Kipkemboi & Van Dam, 2018; Boar, 2006). Although asexual reproduction is the most common (Boar, 2006), sexual regeneration allows for faster expansion over a larger area and the exchange of genetic material among individuals, promoting genetic diversity (Kipkemboi & Van Dam, 2018). However, it entails seed dispersal and the susceptible growth stages of germination and seedling establishment (Kipkemboi & Van Dam, 2018). Seed dispersal occurs through the spreading effects of animals and water currents. In the case of water currents, flood flows play a critical role in spreading seeds in floodplains. Small floods are generally

the most effective, given that they occur at least every 2 to 10 years. Large floods, on the other hand, are rare but play the critical role of dispersing seeds over long distances. Water diversion for irrigation in the Naigombwa catchment has a negligible impact on small flood duration and frequency; however, it significantly lowers the magnitude of small and large floods (Table 5 - 7). This indicates that agricultural water management will negatively affect papyrus seed dispersal, thus impeding papyrus expansion and the exchange of genetic materials among individuals.

5.1.10 Effect of altered flow regimes on seed germination and establishment

Papyrus-dominated floodplains are adapted to a particular wetting or flood pattern that anthropogenic flow alterations can negatively impact. Germination and establishment in these floodplains are dependent on substrate characteristics such as soil moisture and organic content (Kipkemboi & Van Dam, 2018). Experiments by Boar (2006) in the Naivasha wetland in Kenya show that seeds germinate within 12 days of planting. However, only areas devoid of standing water are suitable for germination. Sites with saturated soil produced the best results, followed by locations where water levels were below but very near the soil surface (about 5 cm). The few seedlings that germinated died at the spots left to dry out. After 30 days, most seeds in the ideal sites had fully developed to 13 mm in height. Observations and germination tests showed that seeds germinated swiftly in rewetted sediment; however, swamps only formed when the water level rose gradually, allowing seedling development to keep up with the water level. Papyrus seed banks support quick germination in rewetted sediments. The seed banks are naturally accustomed to handling irregular germination occurrences resulting from unfavourable circumstances (Boar, 2006); however, they are suited to predictable seasonal fluctuations (Thompson & Grime, 1979). Thus, just like for dispersal, small floods are the most important EFC for seed germination and establishment in papyrus-dominated floodplains, given that they naturally occur at rates conducive to the success of papyrus seed banks. However, besides reduced flow magnitude, agricultural water management in the Naigombwa catchment significantly alters small floods' timing and rate of change (Table 5 - 7). The peak flow of small floods will be delayed by about a month (27 days), and its hydrograph rise and fall rates will be lowered by 47.3% and 10.4%, respectively. This indicates that papyri seed banks will need to adapt to the changed small flood regime.

5.1.11 Effect of altered flow regimes on rhizome spreading

Unlike seed germination and establishment that typically occur on newly inundated, low-gradient floodplain sediments with shallow water, asexual reproduction and rhizome spreading are favoured by deep water (Boar, 2006). For example, for the Naivasha wetland in Kenya, the littoral papyrus margin extended by rhizome spreading from floating mats into open water by around 40% of dry-year width following extreme flood events (Boar, 2006). These rhizomes, depending on water availability (Terer et al., 2014), have culms at various developmental stages, with senescence and emergence co-occurring throughout the year (Vaughan, 2011). In the Naigombwa wetland, the average dry and wet season water depth below the floating mats is about 78 and 170 cm, respectively (Kayendeke et al., 2018). Large floods are rare; thus, they may not influence rhizome spreading and asexual reproduction in floating mats as often as extreme low flows, low (base) flows, high flow pulses and small floods. The critical flow regimes (for rhizome spreading and asexual reproduction) of these commonly occurring EFCs are flow magnitude, duration and frequency. These flow regimes are altered positively and negatively (Table 5 - 7). As mentioned above, small floods are limited in magnitude. Base flow magnitudes are largely unaltered in most months, except for positive changes in March and April and a slight reduction in June. High flow pulses are positively impacted in frequency, which could enhance the survival of instream floating mats since these fluxes generally relieve aquatic flora and fauna from stressful low-flow conditions (Mathews & Richter, 2007); however, they are negatively impacted in magnitude and duration. The adverse alterations in the duration of extreme low flows will compound the influence of reduced magnitude and duration of the high flow pulses and the limited small flood magnitude. This could limit rhizome spreading and asexual reproduction in floating mats, especially in dry years.

5.1.12 Effect of altered flow regimes on papyrus distribution across riverine transects

Like reproduction, the distribution of papyrus across floodplain transects is directly linked to water availability. The distribution covers a wide range of river-floodplain/lake-floodplain flow-related gradients of magnitude, duration, and frequency ranging from the landward side to open water bodies (Azza et al., 2000). Plants are typically embedded in sediments to depths of about 1 m on the shallow water landward side (Boar, 2006) and are loosely anchored and easily detached into floating mats towards

the open water (Azza et al., 2000). The deep floodplain roots give them considerable resilience to desiccation during low water levels, enabling them to withstand shoreline recession of over 100 m in low-gradient areas (Boar, 2006). This implies that rooted papyri depend mainly on elevated groundwater levels and the frequently occurring small floods; meanwhile, floating papyri distribution depends on instream water availability. The floating mats are confined to river channels during extreme low flows, low (base) flows, and high flow pulses but can extend to floodplains during flood flows. Given that agricultural water management negatively affects extreme low flows and high flow pulses in the Naigombwa catchment (Table 5 - 7), the distribution of rooted and floating mats and other species inhabiting these wetlands could be affected. Rooted papyrus will find it increasingly challenging to access groundwater given the increased duration of extreme low flows, thus increasing the risk of invasive species. Floating papyri, meanwhile, can tolerate extreme low flow conditions due to adaptation to low-oxygen conditions (Li & Jones, 1995); however, other species in these habitats might be vulnerable. Shallow flow conditions concentrate prey species and trigger alteration of water chemistry, temperature increase, and lowering of dissolved oxygen (Mathews & Richter, 2007). On the other hand, high flow pulses, though short-term, provide much-needed relief from stressful low-flow conditions by increasing mobility through improved access to upstream/downstream areas, flushing wastes in river habitats, delivering food and organic matter, increasing dissolved oxygen, and relieving higher water temperatures (Mathews & Richter, 2007). However, the influence of high flow pulses in mitigating stressful low-flow conditions will be limited due to the reduced flow magnitude and duration and increased rate of change.

5.1.13 Effect of altered flow regimes on dispersal of floating mats

To allow for the colonisation of new sites and the creation of floating papyrus islands, floating mats frequently extend into new regions or join existing mature stands due to wind and water waves (Terer et al., 2014). Water waves are essential during flood flows; meanwhile, the wind is critical in complementing the dispersal effect of high flow pulses. Large floods are rare but crucial in dispersing floating mats over long distances. However, their impact will be hampered by irrigation water diversion, given the reduction in its flow magnitude. Nonetheless, the increased duration of these large floods could compensate for the decrease in magnitude. On the other hand, high flow

pulses will occur frequently; however, their role will be limited due to the reduction in magnitude and duration.

5.1.14 Effect of altered flow regimes on sustaining wetland habitats

Flood flows are also vital in depositing nutrients in floodplains, flushing wastes and debris in wetlands, shaping physical wetland habitats, creating channels and oxbow lakes linking wetlands to the river, and purging invasive plants and animals (Richter et al., 2006). Small floods can perform most tasks that enhance primary production (Talbot et al., 2018). However, large floods are crucial for reshaping habitats by flushing wastes and debris in wetlands, shaping physical wetland habitats, creating channels and oxbow lakes, and purging invasive plants and animals (The Nature Conservancy, 2009). The efficiency of large floods in performing some of these crucial tasks will be affected by reduced flow magnitude.

Conclusions

This study links the flow regime of papyrus wetlands to biologically-relevant hydrologic attributes, including identifying the effects of altered Environmental Flow Components (EFCs) on papyrus as a habitat. Results show that agricultural water management considerably alters the magnitude, duration, timing, and rate of change of EFCs. The altered EFCs directly affect papyri reproduction (sexual and asexual) and sustenance. However, the wetland's natural pulsed regime is maintained when the ratio of the irrigated area to the catchment area is approximately no more than 1:150.

Papyri are native to Africa, and as a growing continent, Africa faces population pressure and the effects of climate change (Pacini et al., 2018). Thus, most countries have placed irrigated agriculture on the development agenda (Woodhouse et al., 2017; Higginbottom et al., 2021), which could affect the inflow to critical habitats in papyrus-dominated catchments. This work can help catchment managers protect and conserve papyrus wetland habitats in catchments threatened by irrigated agriculture by a) guiding in developing the linkage between catchment-scale agricultural water management and its ecological attributes on wetland habitats; b) identifying critical biologically-relevant hydrologic attributes of papyrus wetlands that are affected by altered flow regimes.

CHAPTER 6: EFFECTS OF LOWLAND RICE IRRIGATION ON THE PAPYRI WETLAND FLOW REGIME UNDER A FUTURE CLIMATE

Abstract

Climate change modifies wetland biogeochemical processes through temperature increases and alteration of the hydrological regime, affecting essential wetland ecosystem services. Human activities, particularly water abstraction and land use change, which are mainly linked to agriculture, compound the effects of global warming. Lowland rice is often cultivated in catchments dominated by natural wetlands in the tropics. To date, no study has assessed the impacts of lowland rice irrigation on the most dominant wetland plant species in Africa (papyrus) under a future climate. Hydrological modelling results, complemented with ecologically relevant statistical analyses, indicate that climate change, due to the projected increase in precipitation over the Naigombwa catchment in Uganda, will significantly influence wetland inflow more than irrigation for the irrigation command area of 2,300 ha, equivalent to the irrigated area to catchment area ratio of the order 1:70. Like studies in other parts of the world, extreme flows (flood and low flows) are most affected by water diversion for agriculture. Reduced flood regimes (frequency, peak amplitude, and rate of change) affect papyrus sexual reproduction by limiting opportunities for soil rewetting, which is critical for seed germination and establishment in floodplain-dominated wetlands such as the Naigombwa catchment. Overall, the findings in this study can help catchment managers in similar ecosystems plan for conservation programmes that can enhance the productivity of papyrus plants, given that it is a keystone species on which wetland biodiversity depends.

Introduction

The World Economic Forum's 2023 Global Risks Report (WEF, 2023) ranked climate change and related environmental challenges as one of the top five global risks. Climate change affects marine, freshwater, and terrestrial ecosystems, as well as ecosystem services (Pörtner et al., 2022). Given global greenhouse gas emission rates, climate change will likely become the dominant direct driver of global biodiversity and ecosystem services loss by the end of the century (Millennium Ecosystem Assessment, 2005a). As one of the most productive ecosystems, wetlands are

particularly vulnerable to climate change (Salimi et al., 2021), and the effects of climate change on wetland processes and fluxes are considered one of the most important unanswered questions for the foreseeable future (Erwin, 2009; Salimi et al., 2021).

Wetland ecosystems maintain a delicate biogeochemical balance between soil, water, microbial, plant, and atmospheric processes (Reddy & DeLaune, 2008). Climate change modifies wetland biogeochemical processes through temperature increases and alteration of the hydrological regime (Salimi et al., 2021; Rezanezhad et al., 2020). This affects essential wetland ecosystem services such as carbon sequestration, flow regulation, biodiversity conservation and food supply. These climate-induced ecosystem changes are compounded by human activities such as river regulation, water abstraction and land use change (Döll et al., 2020). These human activities, particularly water abstraction and land use change, are mostly linked to agriculture (Fischer et al., 2007; Siebert et al., 2013; Winkler et al., 2021) and are predicted to increase due to population growth and global warming (Rosa, Chiarelli, Sangiorgio, et al., 2020; Hejazi et al., 2012; Boretti & Rosa, 2019).

The impacts of increased food demand and agricultural expansion on natural resources, including wetlands, could be minimised by adopting intensive agriculture (Rosa, 2022). Intensive agriculture focuses on increasing productivity on rainfall-constrained cropland through irrigation (Rosa, Chiarelli, Rulli, et al., 2020). However, irrigation projects often threaten habitats and ecosystems, especially if developed without robust environment management plans (Galbraith et al., 2005), which climate change could further exacerbate by significantly altering both water availability and crop water requirement (Cai et al., 2015).

Studies show that Africa, with a growing population, has the potential to meet its future food demand through irrigation (Rosa, 2022; Rosa, Chiarelli, Sangiorgio, et al., 2020), and several countries have placed irrigated agriculture on the development agenda (Woodhouse et al., 2017; Higginbottom et al., 2021). However, some countries have essential wetlands and habitats (Kingsford et al., 2021) that irrigation water abstraction and climate change could negatively impact. Thus, as one of the most critical challenges scientists face today (Salimi et al., 2021), there is a need to predict the impacts of future catchment changes on wetland habitats. However, it is challenging to predict the ecological consequences of future change, given the complexity of the

variables involved (e.g., environmental warming, alterations to hydrology and biogeochemistry, etc.) (Stewart et al., 2013; Walther, 2010) and ecological data limitation (e.g., the composition, phenology, abundance, productivity and distribution of these habitats under a future climate) (Stewart et al., 2013).

Hydrological modelling helps predict how flows change due to irrigation or climate change (Siad et al., 2019; Xia et al., 2022). However, metrics that link hydrologic regimes (i.e., the magnitude, frequency, duration, timing, and rate of change of flows) of the changed flows to biologically-relevant hydrologic attributes of ecosystems are required (Richter et al., 1996; Sheikh et al., 2022; Gao et al., 2009; Yang et al., 2012). The Indicators of Hydrologic Alteration (IHA) is a statistical approach for deriving biologically-relevant hydrologic attributes (Richter et al., 1996; Mathews & Richter, 2007) and is the most widely used metric for the characterisation of ecologically-relevant features of flow regimes (Zhou et al., 2020). The IHA uses the Range of Variability Approach (RVA) in designing 'environmentally acceptable' flow regimes (Richter et al., 1997), providing a framework for setting preliminary flow management or restoration targets for rivers where annual streamflow characteristics frequently fall outside their historical range(s) of variability (Richter et al., 1997, 1998).

As a low-cost approach to environmental flow management (Martínez-Capel et al., 2017), the IHA-RVA concept has been applied globally to assess flow regime alterations due to agricultural water abstraction (e.g., Hillman et al., 2012; Stefanidis et al., 2016; Xue et al., 2017; Yasarer et al., 2020; Wang et al., 2022). However, few, if any, have assessed the effects of lowland rice irrigation on wetlands under a future climate. This paper assesses the impact of future climate and rice irrigation on papyrus-dominated wetlands in the Naigombwa catchment in Uganda. As Uganda's central rice food basket (Barungi & Odokonyero, 2016), the wetlands in this region of Uganda continually face the challenges of agricultural encroachment mainly due to population pressure (Bunyangha et al., 2021) and the effects of climate change (Chombo et al., 2018). For example, recently, to mitigate the effects of climate change and offset the national rice food deficit, the Ministry of Agriculture, Animal Industry and Fisheries established the Naigombwa rice irrigation project (Namutebi & Sekanjako, 2013; MAAIF, 2019, 2021), with construction commencement slated for 2023. This study, therefore, has two main objectives: 1) to quantify the impacts of lowland rice irrigation and future climate on the natural inflow into papyrus-dominated wetlands; 2)

to understand how these changes to the flow regime will affect the sustainability of the wetlands.

Materials and Methods

6.1.1 Study area

The Naigombwa catchment is a part of the wetland-dominated Mpologoma catchment (MWE, 2018) and covers approximately 1,680 km^2. The Naigombwa wetland system is primarily located in the lower parts of the Naigombwa catchment (Figure 6 - 1) and covers roughly 31 km^2 (2%). Typical of wetlands in the region, the papyrus-dominated marshes occur in flat, channel, and basin landforms (e.g., floodplains, rivers, and lakes, respectively (Semeniuk & Semeniuk, 1995)), with hydroperiods characterised by seasonal inundation (such as in floodplains) and permanent inundation (such as in rivers and lakes) (Kipkemboi & Van Dam, 2018). These wetlands are habitats for several species of flora and fauna (Chapman et al., 2001). Non-papyrus plants, mainly vines that depend on the tall structural complexity of live papyrus (Chapman et al., 2001), tend to occur as pockets of monoculture stands (Kipkemboi & Van Dam, 2018). Animals, on the other hand, occupy both the lower water-saturated area (e.g., fish, worms, and insect larvae) and the upper surfaces (e.g., birds and insects) (Kipkemboi & Van Dam, 2018).

Phase 1 of the Naigombwa rice irrigation project will cover about 2,300 hectares, including 2,200 hectares of lowland rice and 100 hectares of polycrops (maize, beans, watermelon, etc.) (MAAIF, 2021). The irrigation reservoir, Namiganda Dam, at 22.9 million m^3, will be located upstream of the irrigation command area.

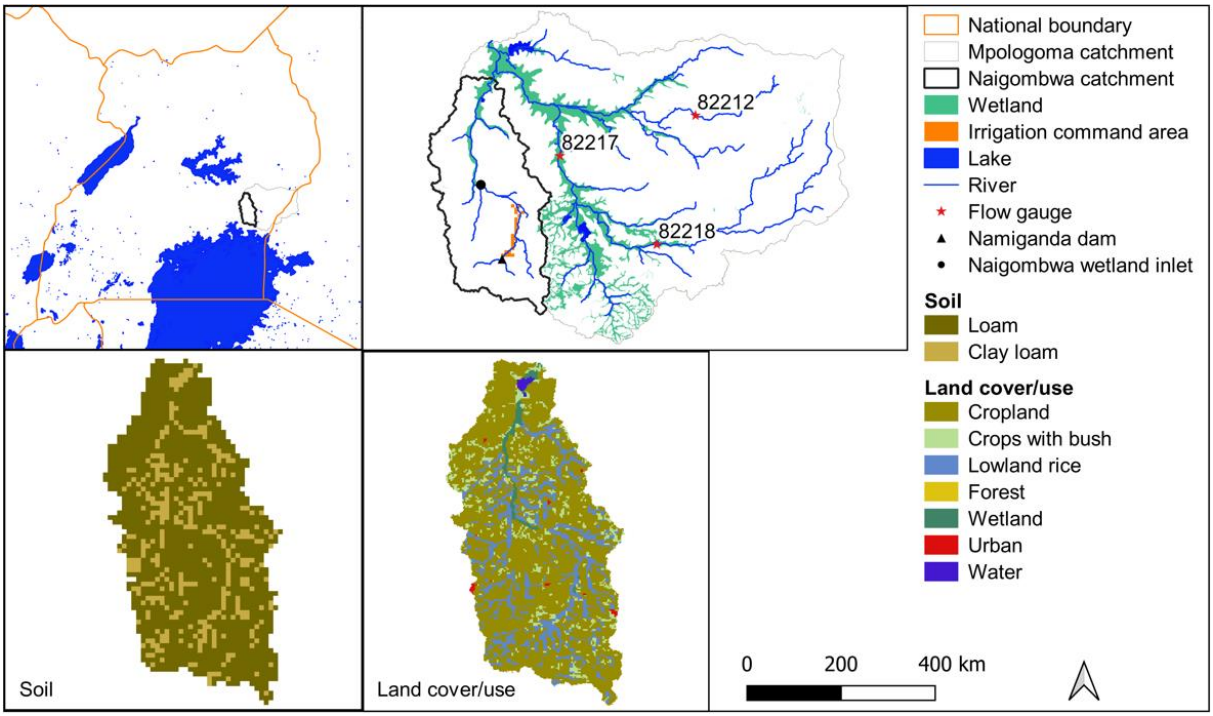

Figure 6 - 1: Naigombwa catchment boundary, soils, land cover, the planned irrigation command area, and the location of the irrigation reservoir.

6.1.2 Hydrological modelling

Hydrological modelling was carried out by forcing the calibrated SHETRAN model for the Mpologoma catchment (see Oyarmoi et al. (2023)) with rainfall and potential evapotranspiration data from the Coupled Model Intercomparison Project phase 6 (CMIP6) Global Climate Models (GCMs). Model runs were executed with and without irrigation for the baseline (BL) and the 2 and 4°C global warming levels (i.e., GWL2 and GWL4), Table 6 - 1. The selection and bias correction of the CMIP6 GCMs used in this study (i.e., GFDL-ESM4, MRI-ESM2-0 and NorESM2-MM) is described in Oyarmoi et al. (2023). The SHETRAN model with irrigation allows quantifying the combined effects of irrigation and climate change at GWL2 and GWL4. Thus, for a particular warming level, the difference between the models with and without irrigation predicts the impact of irrigation alone on the flow regime.

The calibrated SHETRAN model for the Mpologoma catchment depicts catchment characteristics for no irrigation. In the case of irrigation, the model was modified to include the irrigation scheme and the Namiganda dam (Figure 6 - 1). Lowland rice is cultivated in fields with bunds that retain ponded water. This was mimicked in SHETRAN by lowering the overland Strickler coefficient from the calibration value of

0.0469 $m^{1/3}/s$ for rice fields (Oyarmoi et al., 2023) to 0.0001 $m^{1/3}/s$ when the irrigated grid water level is less than or equal to the bund height of 25 cm. As a result, overland flow is stopped, but infiltration continues. The dam crest, meanwhile, was set in the model to depict its design height of 11 m and spillway width and depth of 46.8 and 4 m, respectively (MAAIF, 2021). The water used for irrigation was abstracted from the reservoir based on a predetermined irrigation schedule and applied to the irrigation grids in SHETRAN. Irrigation schedules were prepared for the traditional water-intensive continuous flooding (CF) (Orasen et al., 2019; Carrijo et al., 2017) and the less-intensive alternate wetting and drying (AWD) (IRRI, 2013).

Table 6 - 1: List of models (with and without irrigation) forced with CMIP6 climatic datasets.

S. No.	Climatic datasets	Simulation period (model warmup)	Irrigation present or not
1	GFDL-ESM4 at BL	1979 - 2013 (1979 - 1983)	Yes
2			No
3	MRI-ESM2-0 at BL	1979 - 2013 (1979 - 1983)	Yes
4			No
5	NorESM2-MM at BL	1979 - 2013 (1979 - 1983)	Yes
6			No
7	GFDL-ESM4 at GWL2	2028 - 2063 (2028 - 2032)	Yes
8			No
9	MRI-ESM2-0 at GWL2	2030 - 2065 (2030 - 2034)	Yes
10			No
11	NorESM2-MM at GWL2	2025 - 2060 (2025 - 2029)	Yes
12			No
13	GFDL-ESM4 at GWL4	2059 - 2094 (2059 - 2063)	Yes
14			No
15	MRI-ESM2-0 at GWL4	2051 - 2086 (2051 - 2055)	Yes
16			No
17	NorESM2-MM at GWL4	2049 - 2084 (2049 - 2053)	Yes
18			No

6.1.3 Irrigation schedule and demand

There are two rain seasons in a year in the study area. The first rainy season is from March to May, and the second is from August to November. The lifecycle of annual crops such as rice, maize, beans and watermelon are targeted to these seasons. Given that supplementary irrigation (irrigated agriculture aligned to rain seasons) minimises irrigation water use, thus lowering the cost of management and operation of irrigation systems, this study's cropping calendar was adapted to the rainy seasons (Table 6 - 2). Polycrops (represented as beans in this study) are grown from

March/August to June/November, and lowland rice from March/August to July/December.

Beans are dry-seeded; thus, the only irrigation demand category is the daily gross irrigation requirement (I_{gross}) from planting to maturity. I_{gross} was calculated from the net irrigation requirement (I_{net}) using Equation 6 - 1, where E_{ff} = 60% (MAAIF, 2021) is the scheme's overall irrigation efficiency. The daily net irrigation was estimated using the field-scale crop growth model, AquaCrop version 7 (FAO, 2009; Raes et al., 2022), with soil moisture maintained at field capacity. Calibrated for various crops (including rice and beans), AquaCrop calculates net irrigation while accounting for rainfall and soil moisture balance (Raes, 2022). Its modelling principle is based on the fundamental connection between water transpiration and carbon assimilation. It simulates the interactions between the plant and the soil, with the area immediately above the plant surface and below the topsoil (i.e., root zone) as upper and lower model boundaries. The plant extracts water and nutrients from the root zone depending on field management (e.g., soil fertility, soil salinity stress, field slope, contouring, terracing, method of planting, bunds, soil covering, irrigation, and practices affecting infiltration). The upper boundary links the plant-soil system to the atmosphere, determining rain input and evaporative demand (ETo) and supplying CO_2 and energy for crop growth. The Curve Number method determines the amount of rainwater lost as runoff. At the lower boundary, water drains from the system to the subsoil and the groundwater table. If the groundwater table is shallow, water can move upward into the root system by capillary rise.

$$I_{gross} = \frac{I_{net}}{E_{ff}}$$

Equation 6 - 1

The irrigation demand categories for rice include supply to nursery beds (Nur), field puddling requirement for transplanting rice seedlings (SAT), and the requirement for replenishing soil moisture from the time of transplant to maturity (I_{net}/E_{ff}), Equation 6 - 2.

$$I_{grossRice} = Nur + SAT + \frac{I_{net}}{E_{ff}}$$

Equation 6 - 2

Rice seedlings in nurseries occupy roughly 10% of the area designated for transplantation and mature approximately 15 to 20 days after sowing (IRRI, 2007). The seasonal demand for nurseries, estimated at 120 mm (Bin et al., 2003), was applied over 20 days (1st March/August to 20th March/August) at a 6 mm/day peak rate. The daily nursery demand was estimated as the deficit between the peak rate and the average daily field water level, which was obtained using a parallel SHETRAN model with bunds but no irrigation.

The seasonal field puddling demand is roughly 150 to 250 mm (Guerra et al., 1998), averaging 200 mm. This was applied over seven days (15th March/August to 21st March/August) at a 28 mm/day peak rate. Like the nursery demand, the daily puddling demand was estimated as the deficit between the peak rate and the average daily field water level.

Like beans, the daily net irrigation for rice was estimated using AquaCrop, with soil moisture maintained at field capacity. Rice bunds were set in AquaCrop to account for ponded water. The gross irrigation was calculated from the net irrigation using the overall irrigation efficiency (E_{ff}) of 60% (MAAIF, 2021) for CF. Since AWD lowers infield water use by up to 30% (Richards & Sander, 2014), its E_{ff} was adjusted from 60% to 78%. Table 6 - 3 shows the estimated mean annual irrigation demand in the Naigombwa catchment under the various warming levels and irrigation methods. Overall, irrigation demand increases with global warming due to increases in evapotranspiration (Vila-Traver et al., 2022).

Table 6 - 2: Irrigation demand categories and schedules for rice and poly-crops for the study area.

Crop type	Irrigation demand category	Cropping calendar		Irrigation duty	
		Season 1	Season 2	Season 1	Season 2
Lowland rice	Rice seedlings watering	1st March to 20th March	1st August to 20th August	120 mm per season (Bin et al., 2003)	
	Land preparation for transplanting	15th March to 21st March	15th August to 21st August	200 mm per season (Brouwer & Heibloem, 1986)	
	Net/gross irrigation demand	25th March to 3rd July	25th August to 3rd December	Net irrigation was calculated using AquaCrop software; gross irrigation was calculated using an overall irrigation efficiency of 60% for CF and 78% for AWD.	
Polycrop (beans)	Net/gross irrigation demand	1st March to 17th June	1st August to 17th November	Net irrigation was calculated using AquaCrop software; gross irrigation was calculated using an overall irrigation efficiency of 60%.	

Table 6 - 3: 30-year mean annual irrigation demand in the Naigombwa catchment at baseline (BL) and global warming levels 2 (GWL2) and 4 (GWL4). Results are based on an ensemble average.

BL		GWL2 (relative change)		GWL4 (relative change)	
CF	AWD	CF	AWD	CF	AWD
1,357 mm	1,145 mm	1,368 mm (0.8%)	1,153 mm (0.7%)	1,446 mm (6.6%)	1,213 mm (6.0%)

6.1.4 Assessment of hydrological alteration

The Indicators of Hydrologic Alteration (IHA), proposed by Richter et al. (1996), assess the effects of flow regime change by analysing inter- and intra-annual variability in daily hydrologic data in pre- and post-impact periods. The IHA contains 33 hydrological indices subdivided into five groups that define the magnitude, frequency, duration, timing, and rate of change of flows (*Table 6 - 4*). This study calculated the hydrological indices using the IHA software (version 7.1) developed by the Nature Conservancy (The Nature Conservancy, 2009). The software is programmed to do both parametric and non-parametric analysis. Unlike the parametric method, which assumes that the

data conforms to a particular distribution, the non-parametric approach does not rely on any assumption about the underlying distribution of the data. And given that hydrological data are often strongly non-normal (Helsel & Hirsch, 2002), the study used the non-parametric approach.

Thirty years of data were used for each pre- and post-impact period to account for natural climatic variability, given that at least 20 years of data are required (The Nature Conservancy, 2009). The post-impact periods were targeted to the 2 and 4 °C warming levels, with the baseline period (1983 to 2012) as the pre-impact. Because there were no zero-flow days in the pre- and post-impact periods, the metric that describes the "number of zero-flow days" was not used.

Table 6 - 4: The 33 IHA indices used to study flow regime alterations (from The Nature Conservancy (2009)).

IHA group/parameter	Regime characteristics	Number of indicators
Group 1: Magnitude of monthly water conditions	Magnitude and Timing	12
Group 2: Magnitude and duration of annual extreme water conditions	Magnitude and Duration	12
Group 3: Timing of annual extreme water conditions	Timing	2
Group 4: Frequency and duration of high and low pulses	Frequency and Duration	4
Group 5: Rate and frequency of water condition changes	Rates of Change and Frequency	3

6.1.5 Estimation of the degree of alteration

Like the IHA indices, the RVA metrics are programmed in the Nature Conservancy's IHA software (The Nature Conservancy, 2009). The RVA categorises all the pre-impact data of each IHA metric into three categories (Richter et al., 1997, 1998). These include low-range, middle-range and high-range. In non-parametric IHA analysis, the boundaries between the RVA categories are based on quartile values (The Nature Conservancy, 2009). These were set to the 25th and 75th quartiles to maintain IHA metrics within the middle category in 50% of the years.

The degree of alteration (D) of each of the 32 IHA metrics in the post-impact data is measured by the extent to which the RVA target range was not attained. The degree of alteration is expressed as (Richter et al., 1998):

$$D_n = \frac{N_{on} - N_{en}}{N_{en}} \times 100\%$$

Equation 6 - 3

Where n is the n^{th} IHA metric, and N_{on} and N_{en} represent the count of years of the IHA indices falling within the RVA target range (i.e. the middle category) in the post- and pre-impact periods, respectively. A positive value indicates an increase in the frequency of the flow metric values in the category from pre-impact to post-impact. In contrast, a negative value indicates a reduction in the frequency of values. Richter et al. (1998) set thresholds for D. Values less than or equal to 33% signify slight alteration, 34 to 67% represent moderate alteration, and greater than 67% as highly altered.

The degree of alteration of a single metric (D) does not reflect the overall change in the flow regime. Thus, the overall degree of alteration was calculated for each IHA group and all 32 indicators, as expressed below (Xue et al., 2017).

$$D_o = D_{on} = \sqrt{\frac{\sum_{n=1}^{N} D_n^2}{N}} \times 100\%$$

Equation 6 - 4

where D_o and D_{on} is the overall degree of alteration for each group and all metrics, respectively, and N is the number of IHA metrics. Following Xue et al. (2017), the overall degree of alteration is classified into five classes, including slight alteration (<20%), low alteration (20 to 40%), moderate alteration (40 to 60%), high alteration (60 to 80%), and severe alteration (>80%).

The outputs of the models summarised in Table 6 - 1 were used in estimating the degree of alteration (D, D_o and D_{on}) due to climate change alone (i.e., climate-induced) and the combined effects of irrigation and climate change (i.e., irrigation- and climate-induced). To estimate the influence of irrigation alone (i.e., irrigation-induced), climate-

induced D was subtracted from the corresponding climate- and irrigation-induced D. The overall degree of alteration (D_o and D_{on}) was then calculated using Equation 6 - 4.

Results

6.1.6 Overall hydrological prediction of the effects of irrigation and climate change wetland inflow

The 30-year wetland inflow hydrographs at the baseline (BL) and the 2 and 4°C global warming levels (GWLs) for the conditions with and without irrigation are shown in Figure 6 - 2 and Figure 6 - 3, respectively. It can be seen that extreme flows (flood and low flows) are the most affected by irrigation. However, for a particular warming level, the difference between the irrigation-induced hydrographs (i.e., continuous flooding (CF) and alternate wetting and drying (AWD)) is negligible. The median daily flow under CF and AWD is 1.81 and 1.82 m^3/s, respectively, at BL, 2.15 and 2.09 m^3/s at GWL2 and 2 and 2.02 m^3/s at GWL4. Meanwhile, the median daily flow for no irrigation is 1.66, 1.9 and 1.73 m^3/s at BL, GWL2 and GWL4, respectively. Lowland rice irrigation is generally known to enhance river flow (Essaid & Caldwell, 2017) due to increased groundwater recharge (Negri et al., 2020; Essaid & Caldwell, 2017).

Table 6 - 5 shows the irrigated sites' median annual water balance for the various warming levels and irrigation scenarios. The actual evapotranspiration rates are similar for a particular GWL but increase with warming due to increased evapotranspiration rates (Vila-Traver et al., 2022).

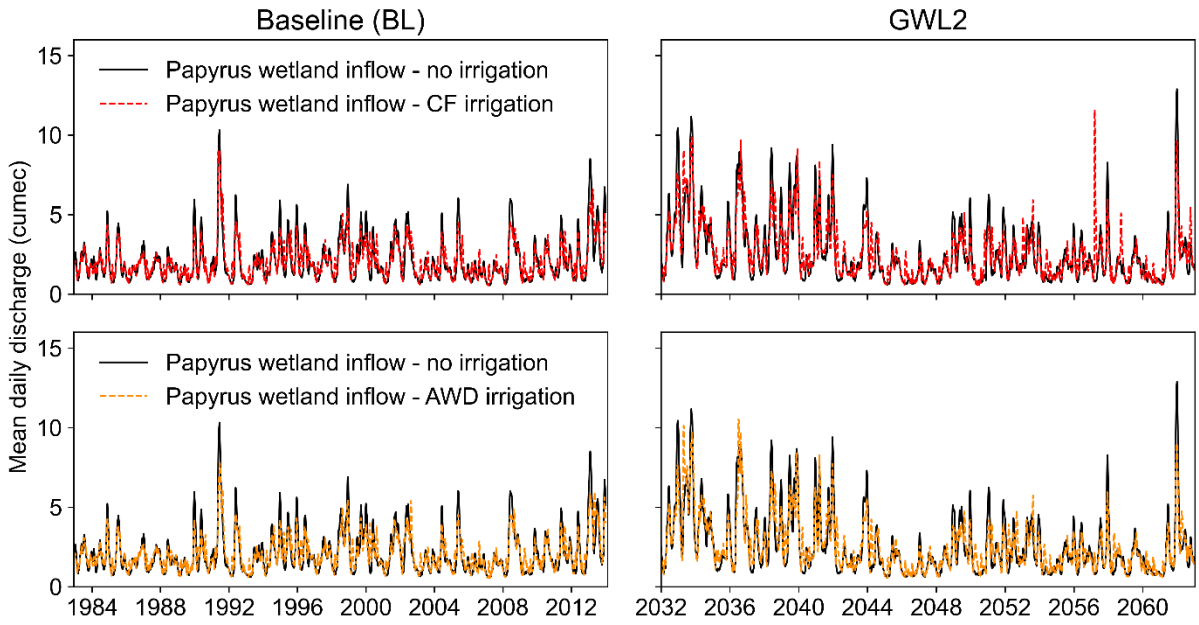

Figure 6 - 2: Papyrus wetland inflow for scenarios with and without irrigation at baseline (BL) and global warming level 2 (GWL2). The top row is Continuous Flooding (CF) at BL and GWL2. The bottom row is Alternate Wetting and Drying (AWD) at BL and GWL2.

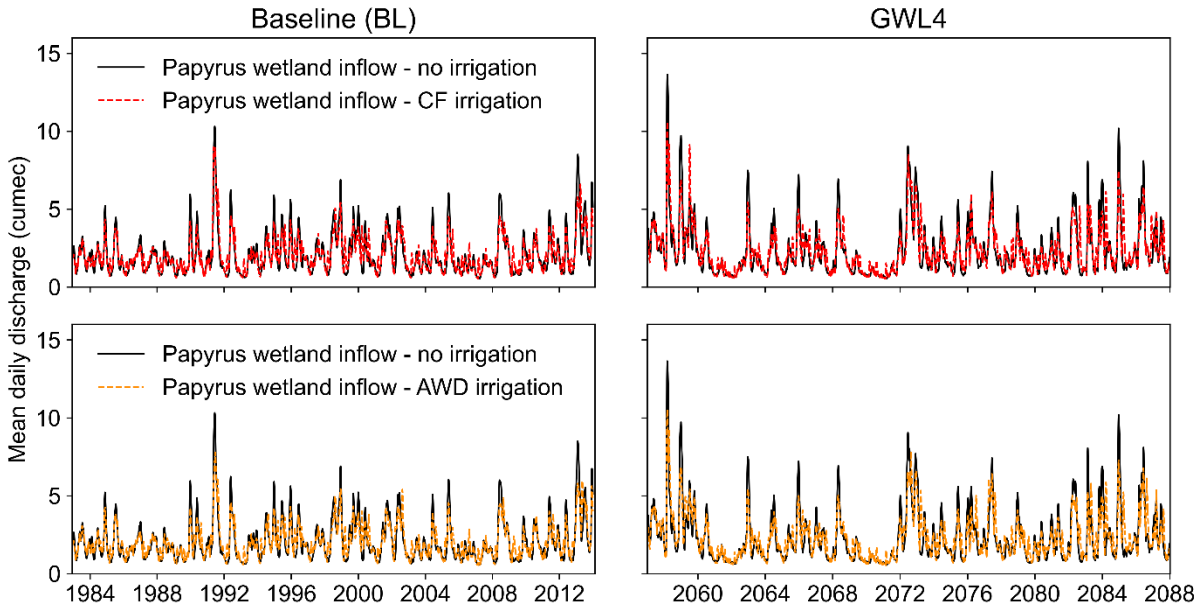

Figure 6 - 3: Papyrus wetland inflow for scenarios with and without irrigation at baseline (BL) and global warming level 4 (GWL4). The top row is Continuous Flooding (CF) at BL and GWL4. The bottom row is Alternate Wetting and Drying (AWD) at BL and GWL4.

Table 6 - 5: Median annual water balance at the irrigated sites at BL, GWL2 and GWL4. Results are based on an ensemble average.

Water balance component	Baseline (BL)		GWL2 (relative change, %)		GWL4 (relative change, %)	
	CF irrigation	AWD irrigation	CF irrigation	AWD irrigation	CF irrigation	AWD irrigation
Precipitation (mm)	1,313	1,313	1,349 (2.7)	1,349 (2.7)	1,402 (6.5)	1,402 (6.5)
Irrigation water (mm)	1,357	1,145	1,368 (0.7)	1,153 (0.7)	1,446 (6.9)	1,213 (6.3)
Total evapotranspiration (mm)	907	907	912 (0.3)	912 (0.3)	965 (6.1)	965 (6.1)
Percolation and runoff (mm)	1,762	1,550	1,805 (2.4)	1,590 (2.6)	1,883 (7.1)	1,651 (6.6)

6.1.7 Effects of future climate on the Naigombwa wetland inflow regime

The projected degree of alteration on each IHA group (D_o) and all IHA metrics (D_{on}) for the baseline conditions with and without irrigation are summarised in Table 6 - 6. Climate-induced D_o and D_{on} are generally dependent on the baseline condition. As expected, they are more prominent for the irrigated baseline condition, except for Group 3 metrics at GWL4. Climate-induced D_{on} values of 67.1 and 63.4%, indicating high alteration, are projected at GWL2 and GWL4, which are more significant than the moderate alterations of 56.2 and 53.6% for the no-irrigation baseline. Similarly, climate-induced D_o at GWL2 ranges from moderate (56.7%) to severe (100%) for the irrigated baseline and slight (19.8%) to severe (97.1%) for the unirrigated baseline. However, at GWL4, D_o ranges from low to severe irrespective of the baseline condition (i.e., 30.9 to 100% and 32.2 to 96.2%).

Overall, for the irrigated baseline, all groups are significantly affected (moderate to severe alteration) irrespective of the warming level, except for Group 3 (timing of annual extreme water conditions) at GWL4. Similarly, most groups are significantly altered for the no-irrigation baseline, except for Group 3 at GWL2 and GWL4 and Group 1 (magnitude of monthly water conditions) and Group 2 (magnitude and duration of annual extreme water conditions) at GWL4.

Table 6 - 6: 30-year overall degree of alteration for baseline conditions with and without. Results are based on an ensemble average.

IHA group	Baseline condition	The overall degree of alteration (%)					
		Climate-induced		Climate- and irrigation-induced		Irrigation-induced	
		GWL2	GWL4	GWL2	GWL4	GWL2	GWL4
Group 1 D_o	No irrigation	41.8	37.3	52.1	43.2	29.1	23.3
	With irrigation	57.2	47.8	46.7	42.5	21.3	22.4
Group 2 D_o	No irrigation	48.1	39.4	44.6	37.1	31.6	21.2
	With irrigation	56.7	55.3	59.9	42.5	29.1	21.7
Group 3 D_o	No irrigation	19.8	32.2	29.6	39.5	23.8	9.9
	With irrigation	58.1	30.9	32.2	39.5	31.9	18.2
Group 4 D_o	No irrigation	97.1	96.2	98.1	93.9	2	7
	With irrigation	100	100	99	97.8	2.1	4.5
Group 5 D_o	No irrigation	75.4	82.2	59.7	72.9	27.7	18.4
	With irrigation	89.3	94.2	83.1	88.1	11.4	8.1
D_{on} of all metrics	No irrigation	56.2	53.6	57	53.2	27.9	20.1
	With irrigation	67.1	63.4	63	57.2	23.4	19.5

6.1.8 Effects of irrigation on the Naigombwa wetland inflow regime

The projected irrigation-induced degrees of alteration (D_o and D_{on}) are summarised in Table 6 - 6. D_{on} values are generally insignificant, ranging from slight to low alteration (19.5 to 27.9%), irrespective of the baseline condition and warming level. Similarly, D_o values are negligible (slight to low alterations of 2 to 31.9%). The D_o and D_{on} values are much lower than the corresponding climate-induced degrees of alteration, indicating that climate change will be more prominent in altering wetland inflows in the Nigombwa catchment for the irrigation area considered.

6.1.9 The combined effects of irrigation and future change on wetland inflow

Table 6 - 6 summarises the climate- and irrigation-induced overall degrees of alteration (D_o and D_{on}). The alterations' significances (low to severe at GWL2 (29.6 to 99%) and

GWL4 (37.1 to 97.8%)) are generally similar to those of the climate-induced alterations (slight to severe at GWL2 (19.8 to 100%) and low to severe at GWL4 (30.9 to 100%)). As indicated by D_o, the most altered metrics (moderate to severe alteration) by the combined effects of irrigation and climate change at GWL2 for the no irrigation baseline are in Group 4 (severe alteration, 98.1%) and Groups 1, 2 and 5 (moderate alteration of 52.1, 44.6 and 59.7%). Similarly, Group 4 (severe alteration, 97.8%), Group 5 (high alteration, 72.9%), and Group 1 (moderate alteration, 43.2%) are the most altered at GWL4. Meanwhile, Groups 4 and 5 (severe alteration of 83.1 to 99%) and Groups 1 and 2 (moderate alteration of 42.5 to 59.9%) are the most altered for the irrigated baseline.

Thus, given that the climate- and irrigation-induced alterations capture the influences of irrigation and climate change and are more pronounced than the irrigation-induced alterations, the analysis of each IHA metric's projected alteration (D) is focused on the climate- and irrigation-induced modelling output.

6.1.10 Effects of irrigation and climate change on the frequency and duration of high and low pulses

The climate- and irrigation-induced degree of alteration (D) of each IHA metric in the most altered group (Group 4) indicates a future highly modified frequency and duration of high and low pulses irrespective of the baseline condition. D ranges from -87 to -100% (denoting highly altered) at GWL2 and GWL4 (Table 6 - 7 and Table 6 - 8, APPENDIX 2). The effect of the GLW2 and GWL4 is fewer pulses but a much longer duration when they occur. This results in negative D values, which indicate an increased occurrence of low and high pulses outside the domain of the baseline middle-range (i.e., the 25^{th} and 75^{th} quartiles of the baseline period). This can be seen in Figure 6 - 4, which shows the annual count of pulses and the median annual event duration for the baseline period (1983 to 2012), GWL2 (2032 to 2061) and GWL4 (2057 to 2086). Pulse counts will increase in the low-range, with the duration of occurrence falling more often in the high-range.

Overall, the 30-year median annual low pulse frequency is expected to drop from about 17 and 22 for baseline conditions with and without irrigation, respectively, to 2 at GWL2 and 1 and 2 at GWL4 (Table 6 - 7 and Table 6 - 8, APPENDIX 2). Similarly, the 30-year median annual high pulse frequency is expected to decline from about 18

and 15 to 2 at GWL2 and 3 at GWL4. Meanwhile, the 30-year median annual low pulse duration will increase from 3 and 2 days, respectively, to 12 and 24 days at GWL2 and 32 and 25 days at GWL4. The high pulse duration will increase from 2 to 45 days at GWL2 and 35 days at GWL4. Although evapotranspiration increases with warming (Vila-Traver et al., 2022; Wang et al., 2006), increased precipitation and reduced runoff can offset its effect by alleviating soil water stress (Li et al., 2023). Projections show increasing rainfall with warming over the East African region (Makula & Zhou, 2022; Ayugi et al., 2022; Almazroui et al., 2020). This could be the reason for the negligible difference in alterations at the 2 and 4 °C warming levels.

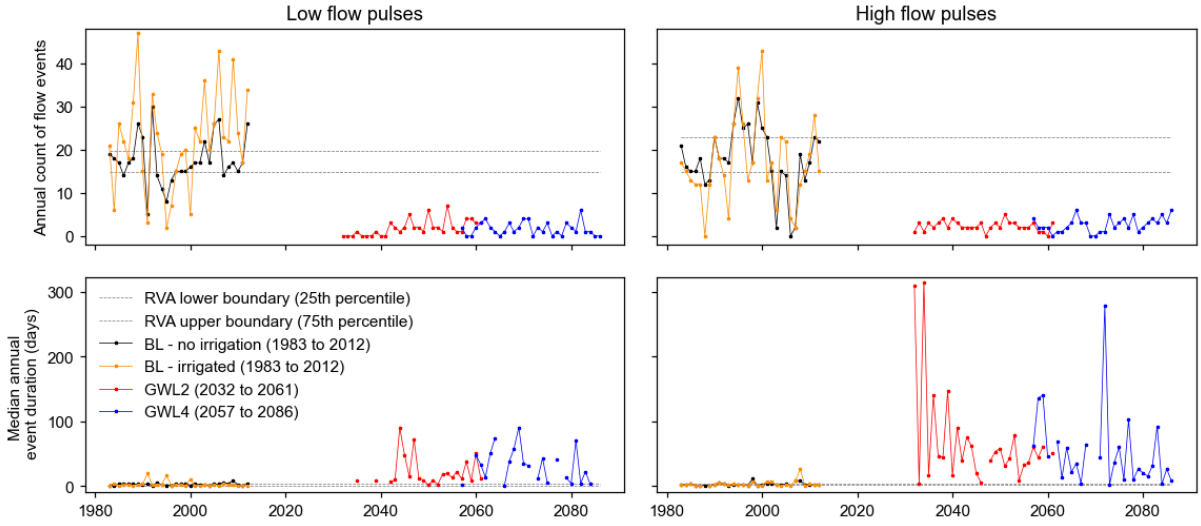

Figure 6 - 4: Alterations in the annual frequency (top row) and median yearly duration (bottom row) of low (left column) and high (right column) flow pulses due to the combined effect of irrigation and climate change.

6.1.11 Effects of irrigation and climate change on rate and frequency of water condition changes

Group 5, the second most altered IHA group by the combined effects of irrigation and climate change, quantifies changes in the rise/fall rates of high flows, including the number of reversals in the flow conditions (Mathews & Richter, 2007). Flow reversals are related to the frequency of events (Olden & Poff, 2003), which the Group 4 metrics have captured, as explained in the previous section.

As seen in the previous section, the combined effects of irrigation and climate change increase the duration of high pulses. This is likely due to the projected decline in high flow rise and fall rates (Figure 6 - 5). Although lowland rice irrigation enhances river

flow (Essaid & Caldwell, 2017), which can reduce high flow rise/fall rates due to slow flux rates of groundwater systems, the irrigation command area in this study has a negligible effect compared to future climate change. Global climate models (GCMs) commonly suffer from too much light rain with few heavy showers, yet in reality, light-rain events are low in frequency in the tropics, with moderate-to-heavy rains occurring often (Cui et al., 2022). This can result in a decline in high flow rise/fall rates in catchment models. The effect significantly alters the high flow rise and fall rates at the inlet to Naigombwa wetlands, with D ranging from -43.8 to -93.8% (denoting moderate to highly altered) for the irrigated baseline (Table 6 - 8, APPENDIX 2). Similarly, for the no irrigation baseline (Table 6 - 7, APPENDIX 2), the rise and fall rates are significantly altered by -37.5 to -75%, except for the fall rate at GWL2 (slight alteration of -18.8%). The negative D values indicate the increased occurrence of high flow rise and fall rates outside the domain of the baseline middle-range (i.e., the 25th and 75th quartiles of the baseline period), with increased occurrence in the low-range (Figure 6 - 5).

Overall, the 30-year median rise rate is predicted to decline from 0.1 and 0.06 m^3/s at BL for the condition with and without irrigation to 0.04 and 0.03 m^3/s at GWL2 and GWL4, respectively. Similarly, the 30-year median fall rate will drop from 0.04 m^3/s (for the conditions with and without irrigation) to 0.04 and 0.03 m^3/s.

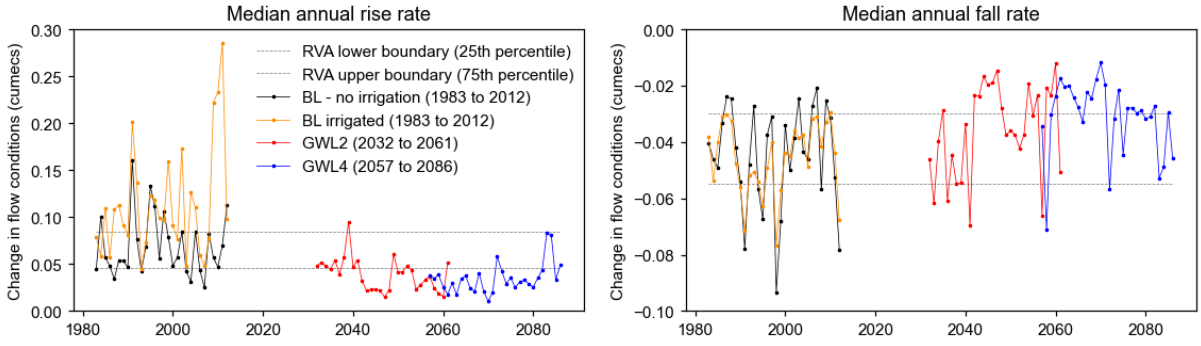

Figure 6 - 5: Alterations in the median annual rate of change (hydrograph rise (left column) and fall (right column) rates) of flow conditions due to the combined effect of irrigation and climate change.

6.1.12 Effects of irrigation and climate change on the magnitude of monthly water conditions

As the third most altered IHA group, the magnitude of monthly flows in Group 1 is significantly transformed (moderately or highly modified) in about half of the months, irrespective of the baseline (BL) condition and warming level. D ranges from -43.8 to -93.8% and -37.5 to -87.5% at GWL2 for the no irrigation and irrigated baselines, respectively (Table 6 - 7 and Table 6 - 8, APPENDIX 2). Similarly, D at GWL4 ranges from -37.5 to -93.8% and -37.5 to -68.8%. The affected months at GWL2 are March, April, August, September, November, December and January for the no-irrigation BL and March, April, July, December and January for the irrigated BL (Figure 6 - 6). The corresponding periods at GWL4 are March, April, July, November, December and February, and March, April and November to February. The least affected months for all conditions are May and June. The negative D values indicate a projected decline in the frequency of median monthly wetland inflows in the middle-range of the baseline period, with a significant increase in the high-range (Figure 6 - 6).

Although GCMs generally predict increased future rainfall over the East African region (Makula & Zhou, 2022; Ayugi et al., 2022; Almazroui et al., 2020), thus the projected increase in median monthly flows in the high-range, changes are more significant during the second rainy (August to November) compared to the first (March to May) (Ayugi, Dike, et al., 2021). This explains the insignificant flow alterations in the first dry season (May to June) compared to the second (December to February). Overall, the 30-year median monthly flows will increase from 0.86 - 2.71 m^3/s and 0.97 - 2.08 m^3/s at BL with and without irrigation, respectively, to 1.27 - 3.33 m^3/s at GWL2 and 1.39 - 2.53 m^3/s at GWL4 (Table 6 - 7 and Table 6 - 8, APPENDIX 2).

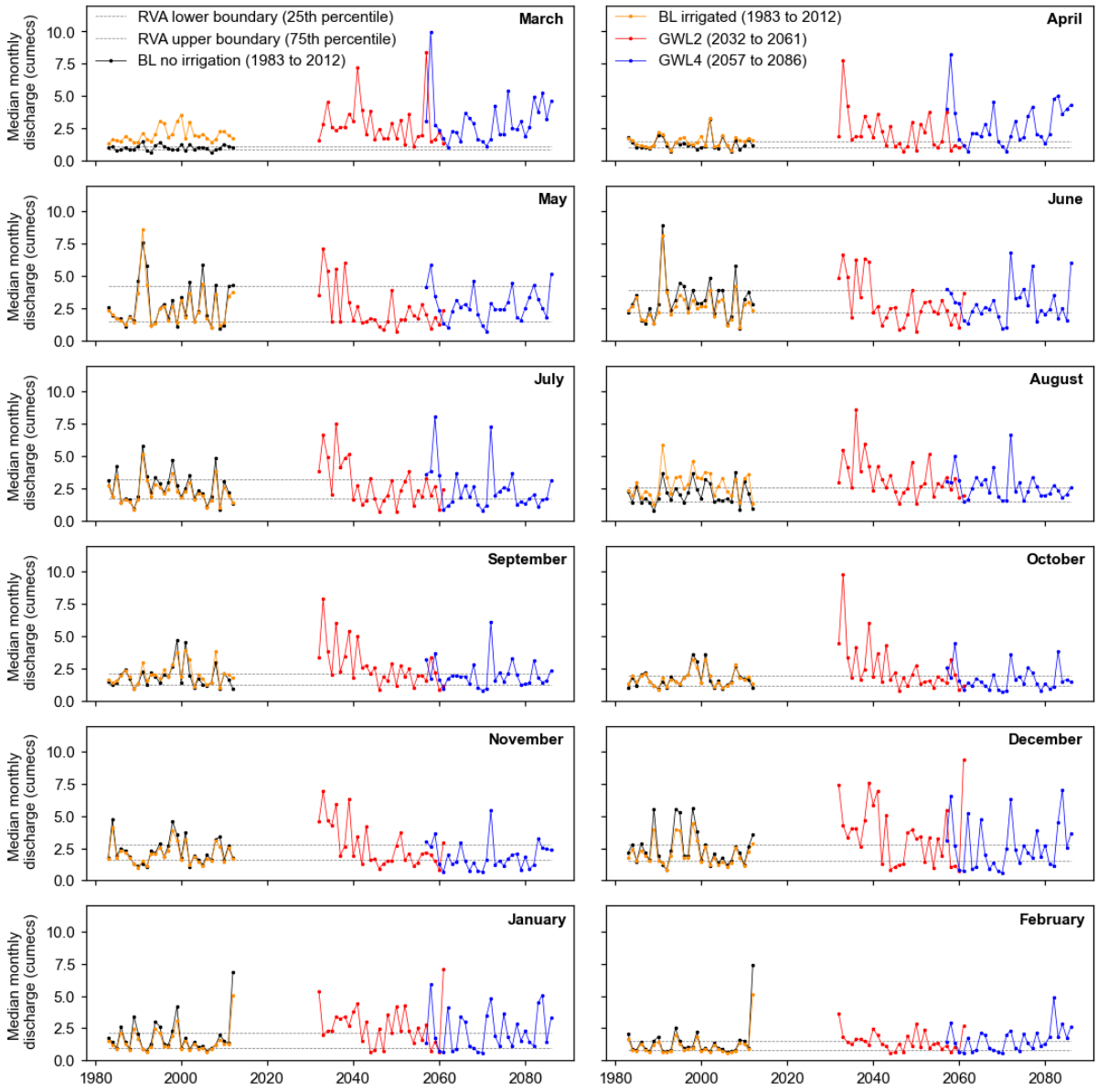

Figure 6 - 6: Alterations in the median monthly flow magnitude due to the combined effect of irrigation and climate change. The water year in the study area is from March (top left graph) to February (bottom right graph).

6.1.13 Effects of irrigation and climate change on annual extreme water conditions

The predictions of the degree of alteration (D) of the magnitude of annual extreme flows in the Group 2 metrics indicate dependence on the baseline (BL) condition. As the fourth most altered IHA group, the Group 2 metrics are more often significantly transformed (moderately or highly) for the BL condition with irrigation. All annual extremes (1-, 3-, 7-, 30-, and 90-day minimum/maximum flows) are changed

considerably at all warming levels for the irrigated BL, except for the 30-day minimum flow at GWL2 (Table 6 - 8, APPENDIX 2). Meanwhile, significant modifications for the no irrigation BL occur only in the 1-, 3-, 7- and 90-day minimum flows and the 1-day maximum flow at GWL2 and GWL4, including the 90-day maximum flow at GWL2 (Table 6 - 7, APPENDIX 2). The D alterations are projected to range from -50 to -93.8% and -37.5 to -56.3% for the conditions with and without irrigation, respectively, at GWL2. Similarly, projections at GWL4 indicate D alterations in the range of -37.5 to -62.5% and -50 to -56.3%. The negative D values indicate a projected decline in the frequency of median annual extremes in the middle-range of the baseline period, with a significant increase in the high-range (Figure 6 - 7).

Overall, the 30-year median annual minimum discharge is predicted to increase from 0.72 - 1.46 m^3/s and 0.74 - 1.42 m^3/s at BL with and without irrigation to 0.89 - 1.51 m^3/s and 0.84 - 1.29 m^3/s at GWL2 and GWL4, respectively (Table 6 - 7 and Table 6 - 8, APPENDIX 2). Similarly, the 30-year median annual maximum flow will increase from 2.63 - 4.24 m^3/s and 2.9 - 5.2 m^3/s to 3.5 - 4.8 m^3/s and 3.3 - 4.6 m^3/s.

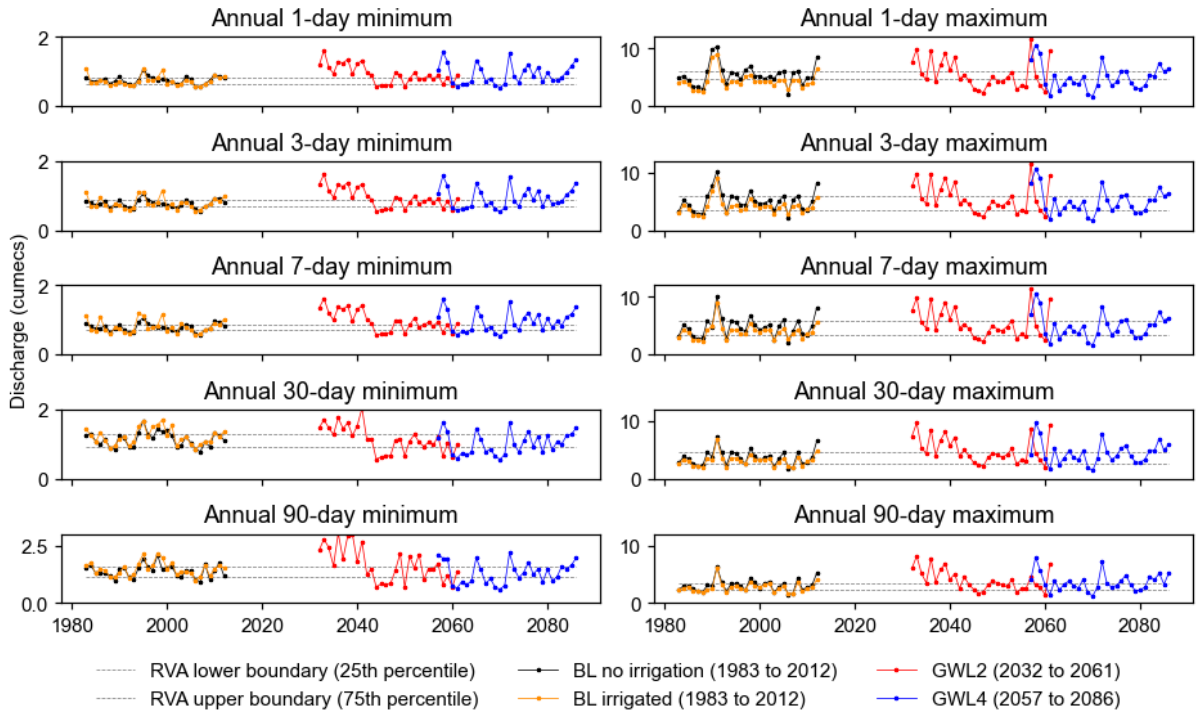

Figure 6 - 7: Alterations in the median annual extreme flows (1-, 3-, 7-, 30-, and 90-day minimum (left column) and maximum (right column) values) due to the combined effect of irrigation and climate change.

Discussion

Findings suggest climate change will play a much more significant role than irrigation in influencing future wetland inflow in the Naigombwa catchment for the target lowland rice acreage of 2,200 ha. The highland and lake regions in East Africa, such as the Mpologoma catchment, are expected to experience precipitation increases (Makula & Zhou, 2022; Ayugi et al., 2022; Almazroui et al., 2020), with mean annual precipitation increases of 9.2 and 25.7% in the near (2030 - 2059) and far (2070 - 2099) future, respectively (Almazroui et al., 2020). The projected increase in precipitation is significantly higher than the predicted increase in irrigation requirement in the Naigombwa catchment. Mean annual irrigation demand under continuous flooding (CF) is estimated to increase only by 0.8 and 6.6% at the 2 °C and 4 °C warming levels, respectively (Table 6 - 3).

A number of IHA-RVA studies on the effects of irrigation water abstraction on river systems show that extreme flows are most altered (Hillman et al., 2012; Stefanidis et al., 2016; Xue et al., 2017; Yasarer et al., 2020; Wang et al., 2022). Although based on historical periods, the findings of these studies are generally similar to those in this study. In the Naigombwa catchment, extreme flows are significantly altered in the frequency and duration of low and high flows, the rate of change of flow conditions (i.e., hydrograph rise and fall rates), and the magnitude of annual extremes. These corroborate the findings by Pompeu et al. (2022) and Stefanidis et al. (2016) in Europe, Xue et al. (2017) and Wang et al. (2022) in China, and Yasarer et al. (2020) in the United States, who evidenced significant changes in the magnitude, frequency, duration, and rate of change of extremes. Findings also show that irrigation applied to supplement rainwater (i.e., when irrigated crop lifecycle is aligned to rain seasons) increases monthly river flow during rain periods but lowers flows during low rain / dry periods (Figure 6 - 8). The crop cycle in the Naigombwa catchment is from March to June/July for the first season and August to November/December for the second season. Figure 6 - 8 shows that irrigation generally enhances wetland inflow from March to May and August to October, while flows are lowered from June to July and December to February, corresponding to the first and second low rain / dry seasons in a water year. Pompeu et al. (2022) witnessed similar changes in a catchment irrigated with dam water in Spain. Summer flows significantly increased while winter flows declined. An indication that irrigation alters and can even shift seasonal flow

patterns (Pompeu et al., 2022) depending on the source water (e.g., reservoir abstraction, river diversion and groundwater withdrawal), irrigation time, and the irrigation method.

It is worth noting that the findings in this study are subject to limitations and uncertainties of the approaches taken. Firstly, AquaCrop and SHETRAN use soil-saturated hydraulic conductivity (Ksat) and soil water content at saturation (SAT) as parameters. As a field-scale model, Ksat and SAT values for AquaCrop are often determined experimentally (Haileselassie et al., 2016). Due to errors in input data (e.g., precipitation, measured water level/river flow, soil and land use/cover, etc.), in addition to assumptions in model physics and structure, the calibrated parameters of catchment-scale models such as SHETRAN usually differ from experimental values (Singh et al., 2017; Seibert & McDonnell, 2002; Cerdan et al., 2004). Thus, for this study, the field-scale values of Ksat and SAT of Saxton & Rawls (2018) were used in AquaCrop. The values were, however, adjusted in SHETRAN to attain a working model.

Secondly, this study forced the calibrated SHETRAN model for the Mpologoma catchment (see Oyarmoi et al. (2023)) with future climate data (CMIP6 rainfall and potential evapotranspiration products). The model was calibrated with the MSWEP rainfall data, a satellite-based precipitation product (SPP). SPPs have inherent errors which can lead to uncertainty in hydrological model parameter estimation and flow simulation (Dembélé et al., 2020; Bisselink et al., 2016). Thirdly, future climate data generally contribute the most significant uncertainty to hydrologic studies (Prudhomme et al., 2003), with the variability of GCM projections as the most critical contributor to flow prediction uncertainty in catchments with wetlands (Lee et al., 2021). This study used only three GCMs out of a possible nine due to limitations in resolution. Thus, using a larger GCM or regional climate model ensemble to lower prediction uncertainty is recommended.

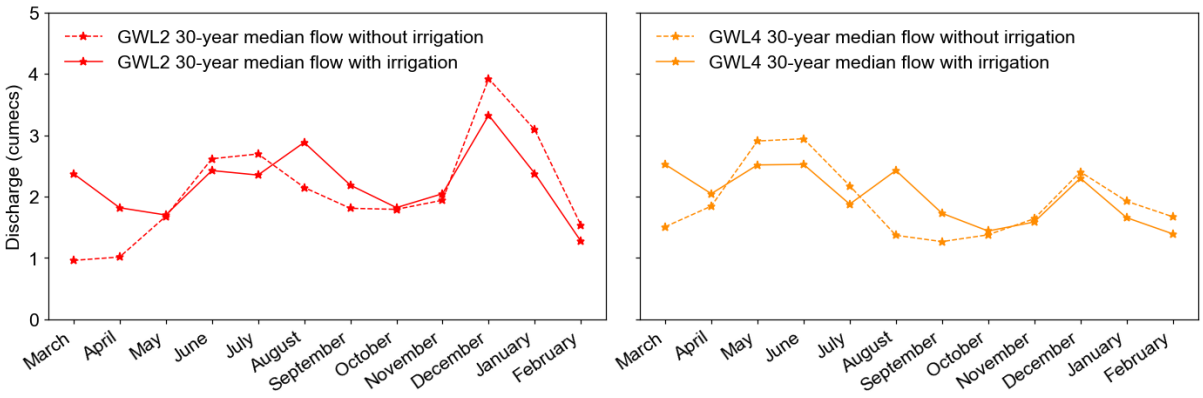

Figure 6 - 8: 30-year median monthly wetland inflow for situations with and without irrigation at GWL2 (left column) and GWL4 (right column).

Conclusions

This study identified and quantified the alterations in the flow regime of a papyrus-dominated wetland system due to the effects of global warming and irrigated agriculture. By calculating indices that define the degree of alteration between the hypothetical and the current (baseline) scenario, the impacts of lowland rice irrigation amid climate change in the Naigombwa catchment in Uganda are quantified. Results indicate that climate change, due to the projected increase in precipitation over the study area, will significantly influence wetland inflow more than irrigation for the irrigation command area of 2,300 ha, equivalent to the irrigated area to catchment area ratio of the order 1:70. Similar to studies in other parts of the world, findings show that extreme flows are most affected by water diversion for agriculture. High (flood) flows are critical for floodplain-dominated papyrus wetlands. In the Naigombwa catchment, high flows are negatively affected (i.e., reduction) in frequency, peak amplitude, and rate of change. This, ecologically, will affect papyrus sexual reproduction by limiting opportunities for soil rewetting, which is critical for seed germination and establishment. Papyrus is resilient to limitations in sexual reproduction by regenerating asexually; however, this will curtail the exchange of genetic material and promotion of genetic diversity, which is only possible through sexual reproduction. The consequence is a weaker potential to adapt, through genetic interaction, to environmental pressures associated with climate warming. Studies show that tropical wetlands, one of the richest ecosystems in the world, will be adversely affected by global warming through temperature increases and increased water abstraction for food production. Thus, the findings in this study can help

catchment managers in similar ecosystems plan for conservation programmes that can enhance the productivity of papyrus plants, given that it is a keystone species on which wetland biodiversity depends.

CHAPTER 7: DISCUSSION, CONCLUSIONS AND RECOMMENDATIONS

Discussion

This thesis has contributed to understanding the catchment-scale papyrus wetland flow regulatory services in a tropical humid climate where they naturally occur. Further, the study examined the effects of lowland rice irrigation, a critical land use in wetland-dominated tropics, on the inflow regime of papyrus wetlands. It also linked the regime changes to papyrus wetlands' biologically-relevant hydrologic attributes. This section discusses the sustainable management options for minimising the impacts of rice irrigation and climate change, thus conserving the flow regulatory roles provided by papyrus-dominated wetlands in the Mpologoma catchment.

As one of the wealthiest and most productive systems on Earth (Davidson et al., 2019), wetlands provide multiple benefits and services essential to achieving the Sustainable Development Goals (SDGs) (Ramsar Convention Secretariat, 2018). Wetlands are directly linked to 10 SDGs (i.e., SDG 1, 2, 5, 6, 8, 9,11, 13, 14 and 15) that can largely be attained by conserving and restoring wetlands. As detailed in Table 7 - 1 in APPENDIX 2, wetlands achieve the SDGs by providing the opportunity for biodiversity conservation (SDG 14 and 15), human well-being (SDG 1, 2, 5, 6, 8, 9 and 11), economic growth (SDG 8 and 9), and climate mitigation and adaptation (SDG 11 and 13).

Four broad goals supporting the achievement of the SDGs and the Convention on Biological Diversity's Aichi Targets (Coates, 2016) are identified in the Ramsar Convention's fourth Strategic Plan (2016 - 2024) (Ramsar Convention Secretariat, 2016). These include addressing the drivers of wetland loss and degradation (Goal 1), effectively conserving and managing the Ramsar Site network (Goal 2), wisely using all wetlands (Goal 3), and enhancing the implementation of Goals 1, 2 and 3 (Goal 4). Goal 1 is linked to this research study given that it focuses on addressing the drivers of wetland loss and degradation through, among others, ensuring water for wetland ecosystem needs.

By addressing RQ2 (i.e., what roles will papyrus wetlands play in regulating future extreme flows (flood and low flows) in the Mpologoma catchment?), RQ3 (i.e., how does lowland rice irrigation affect the Naigombwa wetland inflow regime, and how are

the regime changes, if any, linked to the biologically relevant hydrologic attributes of papyrus wetlands?), and RQ4 (i.e., how will lowland rice irrigation and climate change influence the wetland inflow regime in the Naigombwa catchment?), findings suggest that rice irrigation (by addressing RQ3 in Chapter 5) and climate change (by addressing RQ2 in Chapter 4 and RQ4 in Chapter 6) alter the natural pulsed regime of papyrus wetlands, affecting their reproduction and sustenance. This is because biological and hydrological processes influence water allocation between agricultural needs and wetlands in wetland-dominated catchments (Lankford & Franks, 2000). Under the current climate, the alteration is within the limits of the natural pulsed regime, provided the ratio of irrigated area to catchment area is in the order of 1:150 (Chapter 5). Wetlands under the current climate, as addressed by RQ1 (i.e., *how do papyrus wetlands regulate baseflow and quickflow in the Mpologoma catchment?*), Chapter 4, strongly attenuate quickflow while moderately enhancing baseflow. Further, annual estimates show that wetlands are four times better at regulating quickflow than baseflow. This demonstrates the roles they play in mitigating floods. For the future, projections show that climate change, due to the projected increase in precipitation over the study area, will significantly influence wetland inflow more than irrigation (Chapter 6). However, the study was limited to the irrigation command area of 2,300 ha, equivalent to the irrigated area to catchment area ratio of the order 1:70. As addressed by RQ2, wetlands are predicted to play critical roles in mitigating flood risks (by lowering the flood magnitude and the number of flood events in a year), with a lesser role in supporting low flows.

In the short and long term, the Ugandan government, through its National Development Plans (UNPA, 2020) and the National Irrigation Policy (MAAIF & MWE, 2017), has placed extensive investment in irrigated agriculture as a means of combating the effects of climate change and spurring economic development. The estimated sustainable irrigation coverage limitation of about 1:150 in the study area is a limiting factor in achieving the government's target under the current climate. Nonetheless, this may be overcome by adopting the management options discussed below, thus addressing RQ5 ("*what are the sustainable management options to minimise the impacts of land use change and climate warming in the Mpologoma catchment?*"). The options were developed following discussions with officials at the Ministry of Water and Environment (MWE), the Ministry of Agriculture, Animal Industry

and Fisheries (MAAIF), and local farming communities in the Naigombwa catchment. The discussions centred on the importance of wetlands, the link between wetlands and economic activities in the catchment, the effectiveness of current wetland management systems, and how wetlands could be protected while ensuring the economic growth of the local community. This was complemented with a literature review (e.g., MWE, 2018; MAAIF, 2009; Kayendeke, 2018; MWE, 2016) and knowledge of the study area (i.e., the researcher worked in the Naigomwa catchment for over five years as an irrigation engineer between 2010 and 2017).

a) Diversification of production systems:

   For example, lowland rice cultivation could be maintained at a sustainable acreage with non-wetland intrusive production systems (such as fishponds and aquaculture schemes) supplementing production. Fishponds are typically constructed at the periphery of wetlands and depend on overland flow to wetlands and spillages from wetlands, with river flow into wetlands untapped. The Mpologoma Catchment Management Plan (MWE, 2018) indicates a possible fishpond coverage of up to 4,000 ha in the Mpologoma catchment. Meanwhile, aquaculture, the controlled cultivation of aquatic organisms such as fish, can be carried out in the numerous surface water bodies (i.e., lakes) in the Mpologoma catchment.

b) Promotion of non-water intensive crops:

   Traditionally, farmers in the Mpologoma catchment depend on rainfed upland crops such as cassava, potatoes, maize, millet, beans, groundnuts, plantain, tomatoes, onions, etc. Rice was introduced in 1942 as a cash crop and scaled up in 1974 by constructing the first lowland rice scheme (Doho rice scheme) in the Mpologoma catchment (MAAIF, 2009). Due to its increasing market and the continual decline in soil fertility in the uplands, farmers are encouraged to invest in lowland rice production rather than traditional crops. Up to 55% of the rice harvests are sold mainly to purchase conventional food crops (Kayendeke, 2018). In order of importance, Uganda's primary food security crops are maize, cassava, plantain, millet and sorghum. Thus, the government can promote traditional upland crops by sensitizing farmers to their water use benefits and providing incentives for enhancing soil fertility and the development of irrigation infrastructure to combat the increasingly variable rains. Given their low water

consumption compared to lowland rice, the sustainable irrigated acreage under these traditional crops will be larger than that of rice.

c) Continuous mapping and monitoring of wetlands:

One of the mandates of the Wetlands Management Department of the Ministry of Water and Environment is to map and demarcate wetland boundaries. This helps protect wetlands from conversion for industrial development, settlements, agriculture, and sand and clay mining, which are critical threats to wetlands in Uganda (MWE, 2016). Uganda's National Wetlands Information System was created in 2005 and updated in 2010. However, it is inaccurate. For example, the most recent map classified degraded wetland areas as having papyrus (Kayendeke, 2018). This is an indication of weakness in wetland monitoring in Uganda. Thus, the responsible authority must ensure timely tracking of wetlands, in addition to clearly demarcating wetland boundaries (e.g., by use of tree species that naturally grow in these wetlands) and sensitizing local communities to the benefits of wetland conservation. Wetland mapping and demarcation can help foster the above-highlighted wetland water management options.

Wetlands are one of the most carbon-rich sinks on the planet. Thus, their restoration and prevention of further wetland loss are vital in limiting future emissions to meet climate goals (Moomaw et al., 2018). The Constitution of Uganda, amended in 1995, recognizes wetlands as public resources and mandates the government to hold them in trust for the common good of all the people. As a signatory to many international conventions on wetlands and freshwaters (e.g., The Ramsar Convention, UN Convention on Biological Diversity, etc.), Uganda has adequate regulatory frameworks (policies, laws, regulations, decrees and directives, guidelines and standards) for the management of wetlands. However, to be effective, they require methodological approaches and procedures for the permitting process, risk and impact assessments, ownership and use of wetland resources, and clarity of institutional mandates and roles (Naigaga, 2021). Further, the "National Policy for the Conservation and Management of Wetland Resources" (MWE, 1995), unreviewed for nearly 30 years, is weak in addressing wetland restoration orders and community participation in wetland management. Solid institutional frameworks with well-coordinated and non-overlapping mandates are needed to maintain the inflow regime and conserve the flow

regulatory roles of papyrus wetlands in the Mpologoma catchment. Additionally, restoration guidelines and incentives for the wise use and conservation of wetlands need to be developed and implemented.

Main Caveats of the Research

7.1.1 How the use of a different distributed hydrological model could influence the study

Hydrology plays a central role in applied and fundamental environmental sciences, but it suffers from an overwhelming diversity of models, mainly to simulate streamflow (Horton et al., 2022). One of the critical drivers for the pronounced model diversity in hydrology is the wide range of model applications (Weiler & Beven, 2015), given that no single valid model fits every purpose (Hämäläinen, 2015). This study modelled land use/cover change. Thus, a distributed modelling approach, in which a watershed is subdivided into grid cells or sub-watersheds, was employed to capture land surface characteristics' natural or human-induced variation. Some of the principal distributed models used in the catchment-scale study of wetlands include semi-distributed models like the Soil and Water Assessment Tool (SWAT) (G. Arnold et al., 2012), the PHYSITEL/HYDROTEL modelling platform (Fossey et al., 2015), the Soil and Water Integrated Model (SWIM), the Hydrologic Simulation Program-Fortran (HSPF), and the fully-distributed model MikeSHE (Graham & Butts, 2005).

SWAT has been widely applied among these models because of the vast support network. Its wetland modules, like those of PHYSITEL/HYDROTEL, SWIM, and HSPF, estimate the change in inundation extent (i.e., water levels) using empirical wetland-water volume-surface area relationships. Further, they often lump the effect of multiple wetlands within a sub-watershed. Thus, wetland physical processes and representation are oversimplified in a watershed context (Lee et al., 2019). On the other hand, MikeSHE and SHETRAN employ physical equations to describe wetland water flow at the grid/wetland scale, thus improving spatial processes and patterns. However, it remains unclear if enhanced model capabilities can lead to improved prediction of wetland function and dynamics because catchment-scale simulation results are often evaluated against "aggregate" hydrological variables (e.g., streamflow collected at a catchment's outlet) (Lee et al., 2019). This implies that the relative improvement in aggregated response may not offer insight into the 'internal'

hydrological processes (i.e., hydrological interactions between wetlands and surrounding areas). Thus, assessing catchment-scale modelled dynamics and wetland functions remains incomplete (Lee et al., 2019).

From the above discussion, semi-distributed hydrological models might be better suited for regional/global scale applications, given the wetland module simplifications, lower data requirements, and lower computational time. Meanwhile, fully distributed models are suited to local scale studies, given their ability to model grid-scale hydrological interactions between wetlands and surrounding areas. Thus, given their simplifications, the results of local scale (i.e., watershed scale) modelling of wetlands, such as in the Mpologoma catchment, using semi-distributed models will be different from those of fully distributed models. Further, since many climate change and land use assessments are starting to use multiple hydrological models, it makes sense to compare the results of this study (SHETRAN results) with those of similar fully distributed catchment-scale models.

7.1.2 Modelling limitation due to the use of GCM ensemble mean estimate

Global climate models (GCMs) are developed to simulate past and future climate. Their contributions to identifying regional issues and possible solutions in water resources planning/management are valued worldwide. Water resource planners, however, have criticized GCM estimates because of their significant uncertainty (Raju & Kumar, 2020). The uncertainty stems from the lack of complete information about atmospheric processes, approximations during numerical modelling, spatio-temporal scales, coarser or finer resolution, different feedback mechanisms (e.g., cloud and solar radiation, greenhouse gases, aerosols, natural and anthropogenic sources, ocean circulation, water vapour and warming, ice and snow albedo, etc.), and different perspectives (physical parameterisations, initialisations, and model structures) are the causes of uncertainties that lead to either overestimation or underestimation of climate variables. Because of this, different GCMs generate different outcomes for the same forcing. Thus, showing impact studies' upper and lower limits is standard practice (Pörtner et al., 2022) since the variability of GCM projections is the most significant contributor to flow prediction uncertainty (Lee et al., 2021).

Due to time limitations, partly contributed by the effects of COVID-19, this study used only the ensemble mean estimates of GCMs. Thus, the results will be different for individual GCMs.

7.1.3 The effect of the modelled vegetation's static nature on the modelling results' validity

Climate change is causing substantial global vegetation shifts (Gang et al., 2013), with temperature and precipitation patterns playing a crucial role in determining their distribution (Hansen et al., 2001). For instance, tree density declines and species composition changes have led to a southward shift of the savanna vegetation zone in the African Sahel and West Africa into previously more humid areas, with temperature increases and precipitation decreases most significantly explaining tree cover changes (Gonzalez et al., 2012). Further, increased woody cover in savannas has been reported across Africa, including West Africa, East Africa, and Southern Africa, due to rising temperatures and rainfall changes (Martens et al., 2021; Kimiti et al., 2020; Buitenwerf et al., 2012).

As one of the most vulnerable continents to climate change, Africa's temperature is predicted to increase within a range of 3 to 4 °C by the end of the 21st Century (Pörtner et al., 2022), affecting vegetation composition and distribution. This modelling study assumed the same land cover/use size and distribution for the baseline and future scenarios, which may not depict future reality. Thus, the results should be treated with caution, given that land cover/use distribution (vegetation in particular) is affected by climatic conditions (temperature, radiation, precipitation, carbon dioxide, etc.), human activities (grazing, fire, etc.), and the geographical environment (mountains and plains) (Sun et al., 2022).

7.1.4 Uncalibrated language/terms used to represent different magnitudes of change in IHA indices

Although the IHA indices are used in Chapters 5 and 6, the **IHA Group Alteration Index** (computed as the mean of all deviations (in absolute values) within the group) and the **IHA Alteration Index for each indicator within a group** are calculated in chapter 5. Meanwhile, the **Group Degree of Alteration** and the **Degree of Alteration of each indicator within a group** are computed in Chapter 6. These alterations (i.e., the **IHA Alteration Index** and the **Degree of Alteration**) represent different

magnitudes of change and, thus, are based on different percentage ranges. The **Degree of Alteration** measures the extent to which the pre-impact target range was not attained (i.e., how often the post-impact IHA indices fall outside the pre-impact target range). On the other hand, the **IHA Alteration Index** measures the extent to which an indicator or group of indicators are altered (i.e., the change in the post-impact, with the pre-impact as a baseline).

Conclusions

The 1971 Ramsar Convention on Wetlands advocates for 'the conservation and wise use of all wetlands through local, regional and national actions and international cooperation, as a contribution towards achieving sustainable development throughout the world' (Ramsar Convention Secretariat, 2010). The Ramsar concept of the conservation and wise use of wetlands can be rephrased as "the long-term use of one or several of the wetland's ecosystem services without degrading or losing other ecosystem services" (Van Dam et al., 2014). Thus, agriculture, the backbone of most African economies (Ludi, 2009) and a crucial threat to wetlands in rural Africa (Dixon & Wood, 2003), such as the Mpologoma catchment, can only be sustainable if it enhances all the ecosystem services of wetlands. In practice, the opposite is often the case – agriculture alters the flow regimes of wetlands in ways that damage these fragile ecosystems, as evidenced in this study.

Polarizing political and societal arguments over whether wetlands are at their best economic use fuels negative sentiments about them (Woodward & Wui, 2001). These arguments often stem from inadequate information on the monetary value of wetland services, mainly regulating services (Van Dam et al., 2014), which hold a far more significant advantage than the often-studied provisioning services (Pacini et al., 2018). Research on well-evaluated wetlands demonstrates that undisturbed wetlands have a far higher economic value than degraded or transformed wetlands (Balmford et al., 2002). This study's first two research questions (RQ1: "*how do papyrus wetlands regulate baseflow and quickflow in the Mpologoma catchment?*" and RQ2: "*what roles will papyrus wetlands play in regulating future extreme flows (flood and low flows) in the Mpologoma catchment?*") quantify papyrus wetlands' catchment scale flow regulatory roles in the Mpologoma catchment, thus supporting their economic valuation and conservation. As addressed by RQ1, papyrus wetlands strongly attenuate quickflow while moderately enhancing baseflow, with annual estimates

showing that they are four times better at regulating quickflow than baseflow. Examination of changes at 2 and 4 °C global warming levels (GWLs), as addressed by RQ2, indicate that wetlands will play critical roles in mitigating flood risks, with a lesser role on low flows. Wetlands are predicted to lower future mean flood magnitude by 6.6 and 9.3% at GWL2 and GWL4, respectively, as well as halving the average number of flood events in a year, irrespective of the warming level.

Water resources planning and management are carried out in Uganda at the catchment scale (MWE, 2019). Mpologoma catchment's management plan, drafted about five years ago (MWE, 2018), recommends the development of lowland rice irrigation schemes to support economic growth. However, this fails to take into account the risks to wetlands. This study quantifies the catchment scale effects of lowland rice irrigation on the inflow regime of papyrus wetlands and links the flow regime changes to the biologically-relevant wetland hydrologic attributes as guided by research questions 3 and 4 (i.e., RQ3: "*how does lowland rice irrigation affect the Naigombwa wetland inflow regime, and how are the regime changes, if any, linked to the biologically-relevant hydrologic attributes of papyrus wetlands?*" and RQ4: "*how will lowland rice irrigation and climate change influence the wetland inflow regime in the Naigombwa catchment?*"). This has the potential to help guide future management plans and policies, which could help conserve wetland ecosystem services. By addressing RQ3, findings show that under the current climate, irrigation-induced flow alterations are within the limits of the natural pulsed regime, provided the ratio of irrigated area to catchment area is in the order of 1:150. As addressed by RQ4, predictions show that climate change, due to the projected increase in precipitation over the study area, will significantly influence wetland inflow more than irrigation. However, the study was restricted to the 2,300 ha irrigation command area, equivalent to the irrigated area to catchment area ratio of the order 1:70.

The proposed Mpologoma catchment sustainable management options (Section 0), as guided by research question 5 ("*what are the sustainable management options to minimise the impacts of land use change and climate warming in the Mpologoma catchment?*"), provide practical approaches for sustainably spurring economic growth in the catchment. The approaches are anchored on diversification of production systems, promotion of non-water intensive crops, and continuous mapping and monitoring of wetlands.

Recommendations for Future Research

This thesis considerably advances the understanding of papyrus wetlands' catchment-scale flow regulatory services. It identifies the roles of different environmental flow components in sustaining them and how lowland rice irrigation threatens their natural flow regime. Nonetheless, further research is required to explore flow regulatory behaviour and the threats wetlands face from large-scale irrigation, as summarised below.

a) The quality of precipitation data forms the basis for sound hydrological modelling (Thiemig et al., 2013; Habib et al., 2014). Rain gauges are fundamental in estimating point precipitation and are often the preferred input data in hydrological studies. However, because of political and social instabilities and funding gaps, Uganda's gauge networks have shrunk (Basalirwa, 1991). Where they exist, they are often sparse in coverage and have discrepancies and data gaps (Asadullah et al., 2008). This affects the quality of the readily available gauge-corrected satellite-based and reanalysis precipitation products, which limits the accuracy of this study's hydrological modelling to the monthly timescale. Better-quality precipitation products would greatly enhance model predictability at the daily timescale. This would improve understanding of papyrus wetlands' flow regulatory services and the threats to their flow regime posed by irrigation.
b) Water extraction in the catchment modelling tool SHETRAN is currently limited to wells/boreholes, making it impossible to extract surface water from reservoirs directly. Therefore, irrigation water in this study was extracted from the reservoir's subsurface. This led to model instability due to the significant irrigation demand. This was overcome by increasing the saturated conductivity and specific storage of the subsurface lithology. Further, the subsurface grids neighbouring the reservoir's lithology were set to zero saturated conductivity to prevent their interaction. It would be highly beneficial to future research to improve the surface water extraction capability of SHETRAN, given that large-scale irrigation schemes often rely on surface water systems (rivers, lakes and reservoirs).
c) Fertiliser and pesticide use are essential for increasing crop yield in irrigated agriculture (De Fraiture et al., 2014). However, surface irrigation systems are

often inefficient in water and agrochemical use, increasing the risk of diffuse pollution (Fan et al., 2014; Quemada et al., 2013). Excessive use of fertilisers near or in wetlands increases nitrogen and phosphorus loading in wetland ecosystems, leading to the buildup of nutrients. This can cause ecological impacts, such as eutrophication, increased growth of invasive species, increased nutrient leaching, and shifts in the dominance and composition of species in the ecosystem (Verhoeven et al., 2006). Thus, future work should investigate agrochemical pollutants' roles in papyrus wetland habitats. Further, improved practices concerning fertiliser and pesticide use, e.g., targeted applications, smaller loadings, improved methods, etc., could be investigated.

d) CMIP6 (Coupled Model Intercomparison Project phase 6) models, unlike CMIP5, have not been dynamically downscaled over Africa and most parts of the world. Nonetheless, Ayugi et al. (2021) show that they outperform CMIP5 models in East Africa. This study used only three CMIP6 models due to resolution limitations. Future work should employ a larger ensemble of dynamically downscaled CMIP6 models to lower climate change prediction uncertainty.

BIBLIOGRAPHY

Acreman, M. & Holden, J. (2013) 'How Wetlands Affect Floods', *Wetlands*, 33(5), pp. 773–786.

Acreman, M.C. (2004) *Impact assessment of wetlands: focus on hydrological and hydrogeological issues. Phase 2 report.*

Acreman, M.C. & Miller, F. (2007) 'Hydrological impact assessment of wetlands', in C. Bergkamp and J. McKay S. Ragone, N. Hernandez-Mora, A. de la Hera (ed.) *"Hydrologic Impact Assessment of Wetlands, Held in Alicante, Spain, from 24 to 27 January 2006." In The Global Importance of Groundwater in the 21st Century: Proceedings of the International Symposium on Groundwater Sustainability*. [Online]. 2007 Ohio, USA: National Groundwater Association Press. pp. 225–255.

Acreman, M.C., Riddington, R. & Booker, D.J. (2003) 'Hydrological impacts of floodplain restoration: a case study of the River Cherwell, UK', *Hydrology and Earth System Sciences*, 7(1), pp. 75–85.

AghaKouchak, A., Mehran, A., Norouzi, H. & Behrangi, A. (2012) 'Systematic and random error components in satellite precipitation data sets', *Geophysical Research Letters*, 39(9), p. 4.

Al-Quraishi, A.K. & Kaplan, D.A. (2021) 'Connecting changes in Euphrates River flow to hydropattern of the Western Mesopotamian Marshes', *Science of The Total Environment*, 768p. 144445.

Alexandersson, H. (1986) 'A homogeneity test applied to precipitation data', *Journal of Climatology*, 6(6), pp. 661–675.

Allen, R.G., Pereira, L.S., Raes, D. & Smith, M. (1998) *Crop Evapotranspiration - guidelines for computing crop water requirements. FAO Irrigation and Drainage Paper No. 56.* Rome, Italy: Food and Agriculture Organization of the United Nations.

Almazroui, M., Saeed, F., Saeed, S., Nazrul Islam, M., Ismail, M., Klutse, N.A.B. & Siddiqui, M.H. (2020) 'Projected Change in Temperature and Precipitation Over Africa from CMIP6', *Earth Systems and Environment*, 4(3), pp. 455–475.

Amaning, A.K., Liliang, R., Kwame, A.-A.E., Kwabena, K.-Y. & Anning, A.A. (2012) 'Validation of TRMM Data in the Black Volta Basin of Ghana', *Journal of Hydrologic Engineering*, 17(5), pp. 647–654.

APP (2012) *Africa Progress Report 2012. Jobs, Justice and Equity - Seizing opportunities in times of global change. Africa Progress Panel*.

Arias, P., Bellouin, N., Coppola, E., Jones, C., Krinner, G., Marotzke, J., Naik, V., Plattner, G.-K., Rojas, M., Sillmann, J., Storelvmo, T., Thorne, P., Trewin, B., Achutarao, K., Adhikary, B., Armour, K., Bala, G., Barimalala, R., Berger, S., et al. (2021) *Climate Change 2021: The Physical Science Basis. Contribution of Working Group I to the Sixth Assessment Report of the Intergovernmental Panel on Climate Change; Technical Summary*. B. [Masson-Delmotte, V., P. Zhai, A. Pirani, S.L. Connors, C. Péan, S. Berger, N. Caud, Y. Chen, L. Goldfarb, M.I. Gomis, M. Huang, K. Leitzell, E. Lonnoy, J.B.R. Matthews, T.K. Maycock, T.

Waterfield, O. Yelekçi, R. Yu, Zhou (ed.). Cambridge, United Kingdom and New York, NY, USA: Cambridge University Press.

Arthington, A., King, J., O'keefe, J., Bunn, S., Ja, D., Pusey, B. & Tharme, R. (1992) 'Development of an holistic approach for assessing environmental flow requirements for riverine ecosystems', in *Proceedings of an International Seminar and Workshop on Water Allocation for the Environment*. [Online]. 1992 Centre for Water Policy Research, UNE, Armidale. pp. 69–76.

Asadullah, A., Mcintyre, N. & Kigobe, M. (2008) 'Evaluation of five satellite products for estimation of rainfall over Uganda', *Hydrological Sciences Journal*, 53pp. 1137–1150.

Ashouri, H., Hsu, K.-L., Sorooshian, S., Braithwaite, D.K., Knapp, K.R., Cecil, L.D., Nelson, B.R. & Prat, O.P. (2015) 'PERSIANN-CDR: Daily Precipitation Climate Data Record from Multisatellite Observations for Hydrological and Climate Studies', *Bulletin of the American Meteorological Society*, 96(1), pp. 69–83.

Ayugi, B., Dike, V., Ngoma, H., Babaousmail, H., Mumo, R. & Ongoma, V. (2021) 'Future Changes in Precipitation Extremes over East Africa Based on CMIP6 Models'. Water 13 (17).

Ayugi, B., Shilenje, Z.W., Babaousmail, H., Lim Kam Sian, K.T.C., Mumo, R., Dike, V.N., Iyakaremye, V., Chehbouni, A. & Ongoma, V. (2022) 'Projected changes in meteorological drought over East Africa inferred from bias-adjusted CMIP6 models', *Natural Hazards*, 113(2), pp. 1151–1176.

Ayugi, B., Zhihong, J., Zhu, H., Ngoma, H., Babaousmail, H., Rizwan, K. & Dike, V. (2021) 'Comparison of CMIP6 and CMIP5 models in simulating mean and extreme precipitation over East Africa', *International Journal of Climatology*, 41(15), pp. 6474–6496.

Azza, N.G.T., Kansiime, F., Nalubega, M. & Denny, P. (2000) 'Differential permeability of papyrus and Miscanthidium root mats in Nakivubo swamp, Uganda', *Aquatic Botany*, 67(3): 169.

Bahati, H.K., Ogenrwoth, A. & Sempewo, J.I. (2021) 'Quantifying the potential impacts of land-use and climate change on hydropower reliability of Muzizi hydropower plant, Uganda', *Journal of Water and Climate Change*, 12(6), pp. 2526–2554.

Balmford, A., Bruner, A., Cooper, P., Costanza, R., Farber, S., Green, R.E., Jenkins, M., Jefferiss, P., Jessamy, V. & Madden, J. (2002) 'Economic reasons for conserving wild nature', *science*, 297(5583), pp. 950–953.

Barnes, C. & Bonell, M. (2005) 'How to choose an appropriate catchment model', in L A Bruijnzeel & M Bonell (eds.) *Forests, Water and People in the Humid Tropics: Past, Present and Future Hydrological Research for Integrated Land and Water Management*. International Hydrology Series. [Online]. Cambridge: Cambridge University Press. pp. 717–741.

Barungi, M. & Odokonyero, T. (2016) *Understanding the Rice Value Chain in Uganda: Opportunities and Challenges to Increased Productivity. Research Report No. 15*.

Basalirwa, C.P.K. (1995) 'Delineation of Uganda into climatological rainfall zones using the method of principal component analysis', *Int. J. Climatol*, 15pp. 1161–

1177.

Basalirwa, C.P.K. (1991) *Raingauge network designs for Uganda*. [Online]. Nairobi University.

Beck, H.E., Wood, E.F., Pan, M., Fisher, C.K., Miralles, D.G., van Dijk, A.I.J.M., McVicar, T.R. & Adler, R.F. (2019) 'MSWEP V2 Global 3-Hourly 0.1° Precipitation: Methodology and Quantitative Assessment', *Bulletin of the American Meteorological Society*, 100(3), pp. 473–500.

Behrangi, A., Khakbaz, B., Jaw, T.C., AghaKouchak, A., Hsu, K. & Sorooshian, S. (2011) 'Hydrologic evaluation of satellite precipitation products over a mid-size basin', *Journal of Hydrology*, 397(3), pp. 225–237.

Betts, A.K., Zhao, M., Dirmeyer, P.A. & Beljaars, A.C.M. (2006) *Comparison of ERA-40 and NCEP/DOE near-surface data sets with other ISLSCP-II data sets.* 111.

Beven, K. (2007) 'Towards integrated environmental models of everywhere: uncertainty, data and modelling as a learning process', *Hydrol. Earth Syst. Sci.*, 11(1), pp. 460–467.

Beven, K. & Binley, A. (2014) 'GLUE: 20 years on', *Hydrological Processes*, 28(24), pp. 5897–5918.

Beven, K. & Binley, A. (1992) 'The future of distributed models: Model calibration and uncertainty prediction', *Hydrological Processes*, 6(3), pp. 279–298.

Beven, K., Smith, P.J. & Wood, A. (2011) 'On the colour and spin of epistemic error (and what we might do about it)', *Hydrol. Earth Syst. Sci.*, 15(10), pp. 3123–3133.

Bhatti, H.A., Rientjes, T., Haile, A.T., Habib, E. & Verhoef, W. (2016) 'Evaluation of Bias Correction Method for Satellite-Based Rainfall Data', *Sensors (Basel, Switzerland)*, 16(6), p. 884.

Bin, D., Zhichen, L., Loeve, R., Molden, D. & Baozhong, Y. (2003) 'Rice impact in Henan irrigation districts along the lower Yellow River reaches. In Yellow River Conservancy Commission.', in *1st International Yellow River Forum on River Basin Management*. [Online]. 2003 Zhengzhou, China: The Yellow River Conservancy Publishing House. pp. 105–113.

Birkinshaw, S. (2018) *SHETRAN Hydrological model*. [Online] [online]. Available from: https://research.ncl.ac.uk/shetran/index.htm (Accessed 17 October 2019).

Birkinshaw, S. (2008a) *SHETRAN Version 4: Data Requirements, Data Processing and Parameter Values*.

Birkinshaw, S. (2008b) *SHETRAN Water Flow Component, Equations and Algorithms. School of Civil Engineering and Geosciences, Newcastle University*.

Birkinshaw, S., Guerreiro, S., Nicholson, A., Liang, Q., Quinn, P., Zhang, L., He, B., Yin, J. & Fowler, H. (2017) 'Climate change impacts on Yangtze River discharge at the Three Gorges Dam', *Hydrology and Earth System Sciences*, 21pp. 1911–1927.

Birkinshaw, S.J. (2010) 'Technical Note: Automatic river network generation for a physically-based river catchment model', *Hydrology and Earth System Sciences*,

14(9), pp. 1767–1771.

Birkinshaw, S.J., James, P. & Ewen, J. (2010) ‘Graphical user interface for rapid set-up of SHETRAN physically-based river catchment model’, *Environmental Modelling & Software*, 25(4), pp. 609–610.

Bisselink, B., Zambrano-Bigiarini, M., Burek, P. & de Roo, A. (2016) ‘Assessing the role of uncertain precipitation estimates on the robustness of hydrological model parameters under highly variable climate conditions’, *Journal of Hydrology: Regional Studies*, 8pp. 112–129.

Bitew, M.M. & Gebremichael, M. (2011) ‘Assessment of satellite rainfall products for streamflow simulation in medium watersheds of the Ethiopian highlands’, *Hydrology and Earth System Sciences*, 15(4), pp. 1147–1155.

Bitew, M.M., Gebremichael, M., Ghebremichael, L.T. & Bayissa, Y.A. (2012) ‘Evaluation of high-resolution satellite rainfall products through streamflow simulation in a hydrological modeling of a small mountainous watershed in Ethiopia’, *Journal of Hydrometeorology*, 13(1), pp. 338–350.

Blair, G.S., Beven, K., Lamb, R., Bassett, R., Cauwenberghs, K., Hankin, B., Dean, G., Hunter, N., Edwards, L., Nundloll, V., Samreen, F., Simm, W. & Towe, R. (2019) ‘Models of everywhere revisited: A technological perspective’, *Environmental Modelling & Software*, 122p. 104521.

Blöschl, G. & Sivapalan, M. (1995) ‘Scale issues in hydrological modelling: A review’, *Hydrol. Process.*, 9pp. 251–290.

Boar, R.R. (2006) ‘Responses of a fringing Cyperus papyrus L. swamp to changes in water level’, *Aquatic Botany*, 84(2), pp. 85–92.

Boretti, A. & Rosa, L. (2019) ‘Reassessing the projections of the World Water Development Report’, *npj Clean Water*, 2(1), p. 15.

Borgonovo, E. & Plischke, E. (2016) ‘Sensitivity analysis: A review of recent advances’, *European Journal of Operational Research*, 248(3), pp. 869–887.

Bosilovich, M.G., Chen, J., Robertson, F.R. & Adler, R.F. (2008) ‘Evaluation of Global Precipitation in Reanalyses’, *Journal of Applied Meteorology and Climatology*, 47(9), pp. 2279–2299.

Brinson, M.M. (2011) ‘Classification of Wetlands’, in Ben A LePage (ed.) *Wetlands. Integrating Multidisciplinary Concepts*. [Online]. Dordrecht: Springer Netherlands. pp. 95–113.

Brizga, S.O., Arthington, A., Pusey, B., Kennard, M., Mackay, S., G.L, W., N.M., C. & Choy, S. (2002) *Benchmarking, a ‘top-down’ methodology for assessing environmental flows in Australian rivers*.

Brouwer, C. & Heibloem, M. (1986) *Irrigation Water Management. Training Manual No. 3 - Irrigation water needs*.

Brouwer, C., Prins, K., Kay, M. & Heibloem, M. (1987) *Irrigation Water Management. Training manual no 5. Irrigation Methods*.

Bucher, E., A, B., Boyle, T., Canevari, P., Castro, G., Huszar, P. & Stone, T. (1993)

Hidrovia: An Initial Environmental Examination of the Paraguay-Parana Waterway. Humedades para las Americas. Publicacao. Publicatio. Manomet, MA, USA: Wetlands for the Americas.

Buechel, M.E.H., Slater, L. & Dadson, S. (2023) 'Afforestation impacts on terrestrial hydrology insignificant compared to climate change in Great Britain', *Hydrology and Earth System Sciences Discussions*, 2023pp. 1–31.

Buishand, T.A. (1982) 'Some methods for testing the homogeneity of rainfall records', *Journal of Hydrology*, 58(1), pp. 11–27.

Buitenwerf, R., Bond, W.J., Stevens, N. & Trollope, W.S.W. (2012) 'Increased tree densities in South African savannas: >50 years of data suggests CO2 as a driver', *Global Change Biology*, 18(2), pp. 675–684.

Bullock, A. & Acreman, M. (2003) 'The role of wetlands in the hydrological cycle', *Hydrology and Earth System Sciences*, 7(3), pp. 358–389.

Bunyangha, J., Majaliwa, M.J.G., Muthumbi, A.W., Gichuki, N.N. & Egeru, A. (2021) 'Past and future land use/land cover changes from multi-temporal Landsat imagery in Mpologoma catchment, eastern Uganda', *The Egyptian Journal of Remote Sensing and Space Science*, 24(3, Part 2), pp. 675–685.

Cai, X., Zhang, X., Noël, P.H. & Shafiee-Jood, M. (2015) 'Impacts of climate change on agricultural water management: a review', *WIREs Water*, 2(5), pp. 439–455.

Cannon, A.J. (2020) *Package 'MBC'. Multivariate Bias Correction of Climate Model Outputs*.

Cannon, A.J. (2008) 'Probabilistic Multisite Precipitation Downscaling by an Expanded Bernoulli–Gamma Density Network', *Journal of Hydrometeorology*, 9(6), pp. 1284–1300.

Cannon, A.J., Sobie, S.R. & Murdock, T.Q. (2015) 'Bias Correction of GCM Precipitation by Quantile Mapping: How Well Do Methods Preserve Changes in Quantiles and Extremes?', *Journal of Climate*, 28(17), pp. 6938–6959.

Carrijo, D.R., Lundy, M.E. & Linquist, B.A. (2017) 'Rice yields and water use under alternate wetting and drying irrigation: A meta-analysis', *Field Crops Research*, 203pp. 173–180.

Cerdan, O., Le Bissonnais, Y., Govers, G., Lecomte, V., van Oost, K., Couturier, A., King, C. & Dubreuil, N. (2004) 'Scale effect on runoff from experimental plots to catchments in agricultural areas in Normandy', *Journal of Hydrology*, 299(1), pp. 4–14.

Chapman, L., Balirwa, J., Bugenyi, F.W.B., Chapman, C. & Crisman, T. (2001) 'Wetlands of East Africa: biodiversity, exploitation and policy perspectives', in B. Gopal, W. J. Junk, & J. A. Davis (eds.) *Biodiversity in Wetlands: Assessment, Function and Conservation. Vol. 2*. [Online]. Backhuys Publishers. pp. 101–131.

Chombo, O., Lwasa, S. & Makooma, T.M. (2018) 'Spatial Differentiation of Small Holder Farmers' Vulnerability to Climate Change in the Kyoga Plains of Uganda', *American Journal of Climate Change*, 7(04), p. 624.

Coates, D. (2016) 'Strategic Plan for Biodiversity (2011–2020) and the Aichi

Biodiversity Targets', in C Max Finlayson, Mark Everard, Kenneth Irvine, Robert J McInnes, Beth A Middleton, Anne A van Dam, & Nick C Davidson (eds.) *The Wetland Book*. [Online]. Dordrecht: Springer Netherlands. pp. 1–7.

Cohen, M.J., Creed, I.F., Alexander, L., Basu, N.B., Calhoun, A.J.K., Craft, C., D'Amico, E., DeKeyser, E., Fowler, L., Golden, H.E., Jawitz, J.W., Kalla, P., Kirkman, L.K., Lane, C.R., Lang, M., Leibowitz, S.G., Lewis, D.B., Marton, J., McLaughlin, D.L., et al. (2016) 'Do geographically isolated wetlands influence landscape functions?', *Proceedings of the National Academy of Sciences*, 113(8), pp. 1978–1986.

Cole, C.A., Brooks, R.P. & Wardrop, D.H. (1997) 'Wetland hydrology as a function of hydrogeomorphic (HGM) subclass', *Wetlands*, 17(4), pp. 456–467.

Convention on Wetlands (2021) *Global Wetland Outlook: Special Edition 2021*.

Cooper, P.J.M., Dimes, J., Rao, K.P.C., Shapiro, B., Shiferaw, B. & Twomlow, S. (2008) 'Coping better with current climatic variability in the rain-fed farming systems of sub-Saharan Africa: An essential first step in adapting to future climate change?', *Agriculture, Ecosystems and Environment*, 126(1–2), pp. 24–35.

Couet, J., Marjakangas, E.-L., Santangeli, A., Kålås, J.A., Lindström, Å. & Lehikoinen, A. (2022) 'Short-lived species move uphill faster under climate change', *Oecologia*, 198(4), pp. 877–888.

Crochemore, L., Isberg, K., Pimentel, R., Pineda, L., Hasan, A. & Arheimer, B. (2020) 'Lessons learnt from checking the quality of openly accessible river flow data worldwide', *Hydrological Sciences Journal*, 65(5), pp. 699–711.

Cui, Z., Wang, Y., Zhang, G.J., Yang, M., Liu, J. & Wei, L. (2022) 'Effects of Improved Simulation of Precipitation on Evapotranspiration and Its Partitioning Over Land', *Geophysical Research Letters*, 49(5), p. e2021GL097353.

Van Dam, A.A., Kipkemboi, J., Mazvimavi, D. & Irvine, K. (2014) 'A synthesis of past, current and future research for protection and management of papyrus (Cyperus papyrus L.) wetlands in Africa', *Wetlands Ecology and Management*, 22(2), pp. 99–114.

Darrah, S.E., Shennan-Farpón, Y., Loh, J., Davidson, N.C., Finlayson, C.M., Gardner, R.C. & Walpole, M.J. (2019) 'Improvements to the Wetland Extent Trends (WET) index as a tool for monitoring natural and human-made wetlands', *Ecological Indicators*, 99pp. 294–298.

Das, P., Zhang, Z., Ghosh, S., Lu, J., Ayugi, B., Ojara, M.A. & Guo, X. (2023) 'Historical and projected changes in Extreme High Temperature events over East Africa and associated with meteorological conditions using CMIP6 models', *Global and Planetary Change*, 222p. 104068.

Davidson, N.C. (2014) 'How much wetland has the world lost? Long-term and recent trends in global wetland area', *Marine and Freshwater Research*, 65(10), pp. 934–941.

Davidson, N.C., Van Dam, A.A., Finlayson, C.M. & McInnes, R.J. (2019) 'Worth of wetlands: revised global monetary values of coastal and inland wetland ecosystem services', *Marine and Freshwater Research*, 70(8), pp. 1189–1194.

Davidson, N.C. & Finlayson, C.M. (2018) ‘Extent, regional distribution and changes in area of different classes of wetland’, *Marine and Freshwater Research*, 69(10), pp. 1525–1533.

Defourny, P., Bontemps, S., Lamarche, C., Brockmann, C., Boettcher, M., Wevers, J. & Kirches, G. (2017) *Land Cover CCI. Product User Guide Version 2*.

Dembélé, M., Schaefli, B., van de Giesen, N. & Mariéthoz, G. (2020) ‘Suitability of 17 gridded rainfall and temperature datasets for large-scale hydrological modelling in West Africa’, *Hydrol. Earth Syst. Sci.*, 24(11), pp. 5379–5406.

Dembélé, M. & Zwart, S.J. (2016) ‘Evaluation and comparison of satellite-based rainfall products in Burkina Faso, West Africa’, *International Journal of Remote Sensing*, 37(17), pp. 3995–4014.

Diem, J.E., Hartter, J., Ryan, S.J. & Palace, M.W. (2014) ‘Validation of Satellite Rainfall Products for Western Uganda’, *Journal of Hydrometeorology*, 15(5), pp. 2030–2038.

Dinku, T., Ceccato, P., Grover-Kopec, E., Lemma, M., Connor, S.J. & Ropelewski, C.F. (2007) ‘Validation of satellite rainfall products over East Africa’s complex topography’, *International Journal of Remote Sensing*, 28(7), pp. 1503–1526.

Dinku, T., Funk, C., Peterson, P., Maidment, R., Tadesse, T., Gadain, H. & Ceccato, P. (2018) ‘Validation of the CHIRPS satellite rainfall estimates over eastern Africa’, *Quarterly Journal of the Royal Meteorological Society*, 144(S1), pp. 292–312.

Dixon, A.B. & Wood, A.P. (2003) ‘Wetland cultivation and hydrological management in eastern Africa: Matching community and hydrological needs through sustainable wetland use’, *Natural Resources Forum*, 27(2), pp. 117–129.

Döll, P., Trautmann, T., Göllner, M. & Schmied, H.M. (2020) ‘A global-scale analysis of water storage dynamics of inland wetlands: Quantifying the impacts of human water use and man-made reservoirs as well as the unavoidable and avoidable impacts of climate change’, *Ecohydrology*, 13(1), p. e2175.

Döll, P. & Zhang, J. (2010) ‘Impact of climate change on freshwater ecosystems: a global-scale analysis of ecologically relevant river flow alterations’, *Hydrology and Earth System Sciences*, 14(5), pp. 783–799.

Donaldson, L., Woodhead, A.J., Wilson, R.J. & Maclean, I.M.D. (2016) ‘Subsistence use of papyrus is compatible with wetland bird conservation’, *Biological Conservation*, 201pp. 414–422.

Dosio, A. (2016) ‘Projections of climate change indices of temperature and precipitation from an ensemble of bias-adjusted high-resolution EURO-CORDEX regional climate models’, *Journal of Geophysical Research: Atmospheres*, 121(10), pp. 5488–5511.

Duan, Z., Tuo, Y., Liu, J., Gao, H., Song, X., Zhang, Z., Yang, L. & Mekonnen, D.F. (2019) ‘Hydrological evaluation of open-access precipitation and air temperature datasets using SWAT in a poorly gauged basin in Ethiopia’, *Journal of Hydrology*, 569(March 2018), pp. 612–626.

Emerton, L., Iyango, L., Luwum, P. & Malinga, A. (1999) *The Present Economic Value of Nakivubo Urban Wetland, Uganda*.

Engman, E.T. (1986) 'ROUGHNESS COEFFICIENTS FOR ROUTING SURFACE RUNOFF', *Journal of Irrigation and Drainage Engineering - ASCE*, 112(1), pp. 39–53.

Erwin, K.L. (2009) 'Wetlands and global climate change: the role of wetland restoration in a changing world', *Wetlands Ecology and Management*, 17(1), pp. 71–84.

Essaid, H.I. & Caldwell, R.R. (2017) 'Evaluating the impact of irrigation on surface water - groundwater interaction and stream temperature in an agricultural watershed.', *The Science of the total environment*, 599–600pp. 581–596.

Essou, G.R.C., Sabarly, F., Lucas-Picher, P., Brissette, F. & Poulin, A. (2016) 'Can precipitation and temperature from meteorological reanalyses be used for hydrological modeling?', *Journal of Hydrometeorology*, 17(7), pp. 1929–1950.

Ewen, J., Geoff, P. & O'Connell, E.P. (2000) 'SHETRAN: Distributed River Basin Flow and Transport Modeling System', *Journal of Hydrologic Engineering*, 5(3), pp. 250–258.

Fan, Z., Lin, S., Zhang, X., Jiang, Z., Yang, K., Jian, D., Chen, Y., Li, J., Chen, Q. & Wang, J. (2014) 'Conventional flooding irrigation causes an overuse of nitrogen fertilizer and low nitrogen use efficiency in intensively used solar greenhouse vegetable production', *Agricultural Water Management*, 144pp. 11–19.

FAO/UNESCO (2007) *The Digital Soil Map of The World - Version 3.6*. [Online] [online]. Available from: https://data.apps.fao.org/map/catalog/srv/eng/catalog.search#/metadata/446ed430-8383-11db-b9b2-000d939bc5d8 (Accessed 5 March 2020).

FAO (2009) *AquaCrop. The crop water productivity model*.

Fernández, J.A., Martínez, C. & Magdaleno, F. (2012) 'Application of indicators of hydrologic alterations in the designation of heavily modified water bodies in Spain', *Environmental Science & Policy*, 16pp. 31–43.

Fischer, G., Tubiello, F.N., van Velthuizen, H. & Wiberg, D.A. (2007) 'Climate change impacts on irrigation water requirements: Effects of mitigation, 1990–2080', *Technological Forecasting and Social Change*, 74(7), pp. 1083–1107.

Fitz, H.C. & Hughes, N. (2008) *Wetland Ecological Models*.

Fossey, M., Rousseau, A.N., Bensalma, F., Savary, S. & Royer, A. (2015) 'Integrating isolated and riparian wetland modules in the PHYSITEL/HYDROTEL modelling platform: model performance and diagnosis', *Hydrological Processes*, 29(22), pp. 4683–4702.

Fossey, M., Rousseau, A.N. & Savary, S. (2016) 'Assessment of the impact of spatio-temporal attributes of wetlands on stream flows using a hydrological modelling framework: a theoretical case study of a watershed under temperate climatic conditions', *Hydrological Processes*, 30(11), pp. 1768–1781.

De Fraiture, C., Fayrap, A., Unver, O. & Ragab, R. (2014) 'Integrated Water Management Approaches for Sustainable Food Production', *Irrigation and*

Drainage, 63(2), pp. 221–231.

Friedlingstein, P., Jones, M.W., O'Sullivan, M., Andrew, R.M., Bakker, D.C.E., Hauck, J., Le Quéré, C., Peters, G.P., Peters, W., Pongratz, J., Sitch, S., Canadell, J.G., Ciais, P., Jackson, R.B., Alin, S.R., Anthoni, P., Bates, N.R., Becker, M., Bellouin, N., et al. (2022) 'Global Carbon Budget 2021', *Earth System Science Data*, 14(4), pp. 1917–2005.

Fuka, D.R., Walter, M.T., Macalister, C., Degaetano, A.T., Steenhuis, T.S. & Easton, Z.M. (2013) 'Using the Climate Forecast System Reanalysis as weather input data for watershed models', *Hydrological Processes*, 28(22), pp. 5613–5623.

Funk, C., Peterson, P., Landsfeld, M., Pedreros, D., Verdin, J., Shukla, S., Husak, G., Rowland, J., Harrison, L., Hoell, A. & Michaelsen, J. (2015) 'The climate hazards infrared precipitation with stations—a new environmental record for monitoring extremes', *Scientific Data*, 2(1), pp. 1–21.

G. Arnold, J., N. Moriasi, D., W. Gassman, P., C. Abbaspour, K., J. White, M., Srinivasan, R., Santhi, C., D. Harmel, R., van Griensven, A., W. Van Liew, M., Kannan, N. & K. Jha, M. (2012) 'SWAT: Model Use, Calibration, and Validation', *Transactions of the ASABE*, 55(4), pp. 1491–1508.

Gabiri, G., Diekkrüger, B., Näschen, K., Leemhuis, C., van der Linden, R., Majaliwa, J.-G.M. & Obando, J.A. (2020) 'Impact of Climate and Land Use/Land Cover Change on the Water Resources of a Tropical Inland Valley Catchment in Uganda, East Africa'. Climate 8 (7).

Galbraith, H., Amerasinghe, P. & Huber-Lee, A. (2005) *The effects of agricultural irrigation on wetland ecosystems in developing countries: a literature review*.

Gang, C., Zhou, W., Li, J., Chen, Y., Mu, S., Ren, J., Chen, J. & Groisman, P.Y. (2013) 'Assessing the Spatiotemporal Variation in Distribution, Extent and NPP of Terrestrial Ecosystems in Response to Climate Change from 1911 to 2000', *PLOS ONE*, 8(11), p. e80394.

Gao, Y., Vogel, R.M., Kroll, C.N., Poff, N.L. & Olden, J.D. (2009) 'Development of representative indicators of hydrologic alteration', *Journal of Hydrology*, 374(1), pp. 136–147.

García-Díaz, P., Prowse, T.A.A., Anderson, D.P., Lurgi, M., Binny, R.N. & Cassey, P. (2019) 'A concise guide to developing and using quantitative models in conservation management.', *Conservation science and practice*, 1(2), p. e11.

Gaudet, J.J. (1975) 'Mineral Concentrations in Papyrus in Various African Swamps', *Journal of Ecology*, 63(2), pp. 483–491.

Gaybullaev, B., Chen, S.-C. & Kuo, Y.-M. (2012) 'Large-scale desiccation of the Aral Sea due to over-exploitation after 1960', *Journal of Mountain Science*, 9(4), pp. 538–546.

Gebrechorkos, S.H., Hülsmann, S. & Bernhofer, C. (2018) 'Evaluation of multiple climate data sources for managing environmental resources in East Africa', *Hydrology and Earth System Sciences*, 22(8), pp. 4547–4564.

George, R., McManamay, R., Perry, D., Sabo, J. & Ruddell, B.L. (2021) 'Indicators of

hydro-ecological alteration for the rivers of the United States', *Ecological Indicators*, 120p. 106908.

Gimeno, L., Drumond, A., Nieto, R., Trigo, R.M. & Stohl, A. (2010) 'On the origin of continental precipitation', *Geophysical Research Letters*, 37(13), .

GISTEMP, T. (2022) *GISS Surface Temperature Analysis (GISTEMP), version 4. NASA Goddard Institute for Space Studies.* [Online] [online]. Available from: https://data.giss.nasa.gov/gistemp/ (Accessed 1 June 2022).

Glenn, E.P., Lee, C., Felger, R. & Zengel, S. (1996) 'Effects of Water Management on the Wetlands of the Colorado River Delta, Mexico', *Conservation Biology*, 10(4), pp. 1175–1186.

Goitom, B., Tripathi, R., Ogbazghi, W. & Weldeslassie, T. (2016) 'Effect of Puddling and Compaction on Water Requirements of Rice at Hamelmalo, Eritrea', *Computational Water, Energy, and Environmental Engineering*, 05pp. 27–37.

Golden, H.E., Lane, C.R., Amatya, D.M., Bandilla, K.W., Raanan Kiperwas, H., Knightes, C.D. & Ssegane, H. (2014) 'Hydrologic connectivity between geographically isolated wetlands and surface water systems: A review of select modeling methods', *Environmental Modelling & Software*, 53pp. 190–206.

Gonzalez, P., Tucker, C.J. & Sy, H. (2012) 'Tree density and species decline in the African Sahel attributable to climate', *Journal of Arid Environments*, 78pp. 55–64.

Graham, D. & Butts, M. (2005) 'Flexible, integrated watershed modelling with MIKE SHE', in *Watershed Models*. [Online]. pp. 245–272.

Van Groenendaal, W.J.H. & Kleijnen, J.P.C. (1997) 'On the assessment of economic risk: factorial design versus Monte Carlo methods', *Reliability Engineering & System Safety*, 57(1), pp. 91–102.

Gudmundsson, L., Bremnes, J.B., Haugen, J.E. & Engen-Skaugen, T. (2012) 'Technical Note: Downscaling RCM precipitation to the station scale using statistical transformations - a comparison of methods', *Hydrology and Earth System Sciences*, 16(9), pp. 3383–3390.

Guerra, L.C., Bhuiyan, S.I., Tuong, T.P. & Barker, R. (1998) *Producing more rice with less water from irrigated system*.

Gulbin, S., Kirilenko, A.P., Kharel, G. & Zhang, X. (2019) 'Wetland loss impact on long term flood risks in a closed watershed', *Environmental Science & Policy*, 94pp. 112–122.

Gumindoga, W., Rientjes, T.H.M., Haile, A.T., Makurira, H. & Reggiani, P. (2019) 'Performance of bias-correction schemes for CMORPH rainfall estimates in the Zambezi River basin', *Hydrology and Earth System Sciences*, 23(7), pp. 2915–2938.

Gutjahr, O. & Heinemann, G. (2013) 'Comparing precipitation bias correction methods for high-resolution regional climate simulations using COSMO-CLM', *Theoretical and Applied Climatology*, 114(3), pp. 511–529.

Habib, E., Haile, A., Sazib, N., Zhang, Y. & Rientjes, T. (2014) 'Effect of Bias Correction of Satellite-Rainfall Estimates on Runoff Simulations at the Source of

the Upper Blue Nile', *Remote Sensing*, 6pp. 6688–6708.

Hagemann, S., Chen, C., Haerter, J.O., Heinke, J., Gerten, D. & Piani, C. (2011) 'Impact of a Statistical Bias Correction on the Projected Hydrological Changes Obtained from Three GCMs and Two Hydrology Models', *Journal of Hydrometeorology*, 12(4), pp. 556–578.

Haileselassie, H., Araya, A., Habtu, S., Meles, K.G., Gebru, G., Kisekka, I., Girma, A., Hadgu, K.M. & Foster, A.J. (2016) 'Exploring optimal farm resources management strategy for Quncho-teff (Eragrostis tef (Zucc.) Trotter) using AquaCrop model', *Agricultural Water Management*, 178pp. 148–158.

Hämäläinen, R.P. (2015) 'Behavioural issues in environmental modelling – The missing perspective', *Environmental Modelling & Software*, 73pp. 244–253.

Hansen, A.J., Neilson, R.P., Dale, V.H., Flather, C.H., Iverson, L.R., Currie, D.J., Shafer, S., Cook, R. & Bartlein, P.J. (2001) 'Global Change in Forests: Responses of Species, Communities, and Biomes: Interactions between climate change and land use are projected to cause large shifts in biodiversity', *BioScience*, 51(9), pp. 765–779.

Hargreaves, G.H. (2000) 'Food, Water, and a Possible World Crisis', in *4th Decennial National Irrigation Symposium of the American Society of Agricultural Engineers*. [Online]. 2000 Phoenix, Arizona: .

Hargreaves, G.H. & Samani, Z.A. (1985) 'Reference crop evapotranspiration from temperature', *Applied Engineering in Agriculture*, 1(2), pp. 96–99.

Harris, I., Osborn, T.J., Jones, P. & Lister, D. (2020) 'Version 4 of the CRU TS monthly high-resolution gridded multivariate climate dataset', *Scientific Data*, 7(1), p. 109.

Heemskerk, M., Wilson, K. & Pavao-Zuckerman, M. (2003) 'Conceptual Models as Tools for Communication Across Disciplines', *Conservation Ecology*, 7(3), p. 13.

Hejazi, M.I., Edmonds, J.A. & Chaturvedi, V. (2012) 'Global irrigation demand - A holistic approach', *Irrigation and Drainage Systems Engineering*, 1(2), pp. 1–4.

Helsel, D.R. & Hirsch, R.M. (2002) 'Statistical methods in water resources', in *Statistical methods in water resources: Techniques of Water-Resources Investigations of the United States Geological Survey. Book 4, Hydrologic Analysis and Interpretation*. Version 1. [Online]. Reston, VA: U.S. Geological Survey. p. 524.

Higginbottom, T.P., Adhikari, R., Dimova, R., Redicker, S. & Foster, T. (2021) 'Performance of large-scale irrigation projects in sub-Saharan Africa', *Nature Sustainability*, 4(6), pp. 501–508.

Higgisson, W., Higgisson, B., Powell, M., Driver, P. & Dyer, F. (2020) 'Impacts of water resource development on hydrological connectivity of different floodplain habitats in a highly variable system', *River Research and Applications*, 36(4), pp. 542–552.

Hillman, B., Douglas, E.M. & Terkla, D. (2012) 'An analysis of the allocation of Yakima River water in terms of sustainability and economic efficiency', *Journal of Environmental Management*, 103pp. 102–112.

Op de Hipt, F., Diekkrüger, B., Steup, G., Yira, Y., Hoffmann, T. & Rode, M. (2017) 'Applying SHETRAN in a Tropical West African Catchment (Dano, Burkina Faso)—Calibration, Validation, Uncertainty Assessment'. Water 9 (2).

Op de Hipt, F., Diekkrüger, B., Steup, G., Yira, Y., Hoffmann, T., Rode, M. & Näschen, K. (2019) 'Modeling the effect of land use and climate change on water resources and soil erosion in a tropical West African catch-ment (Dano, Burkina Faso) using SHETRAN', *Science of The Total Environment*, 653pp. 431–445.

Holthuijzen, M., Beckage, B., Clemins, P.J., Higdon, D. & Winter, J.M. (2022) 'Robust bias-correction of precipitation extremes using a novel hybrid empirical quantile-mapping method', *Theoretical and Applied Climatology*, 149(1), pp. 863–882.

Horton, P., Schaefli, B. & Kauzlaric, M. (2022) 'Why do we have so many different hydrological models? A review based on the case of Switzerland', *WIREs Water*, 9(1), p. e1574.

Howell, P., Lock, M. & Cobb, S. (eds.) (2009) *The Jonglei Canal: Impact and Opportunity*. Cambridge University Press.

Hrachowitz, M. & Clark, M.P. (2017) 'HESS Opinions: The complementary merits of competing modelling philosophies in hydrology', *Hydrol. Earth Syst. Sci.*, 21(8), pp. 3953–3973.

Hu, S., Niu, Z., Chen, Y., Li, L. & Zhang, H. (2017) 'Global wetlands: Potential distribution, wetland loss, and status', *Science of The Total Environment*, 586pp. 319–327.

Huffman, J.G., Adler, F.R., Bolvin, T.D. & Nelkin, J.E. (2011) 'The TRMM Multi-Satellite Precipitation Analysis (TMPA)', in Mekonnen Gebremichael & Faisal Hossain (eds.) *Satellite Rainfall Applications for Surface Hydrology*. [Online]. Springer, Dordrecht. pp. 3–22.

Hughes, D.A. (2006) 'Comparison of satellite rainfall data with observations from gauging station networks', *Journal of Hydrology*, 327(3), pp. 399–410.

Hurst, H.E. (1933) 'The sudd region of the nile', *J. Roy. Soc. Arts*, 81(4205), pp. 720–736.

ICID (2022) *World scenario data on irrigation. International Commission on Irrigation and Drainage (ICID)*. [Online] [online]. Available from: https://icid-ciid.org/knowledge/icid_database (Accessed 12 January 2023).

IME (2013) *Global Food: Waste Not, Want Not. Improving the world through engineering*.

IPCC (2018a) *Global Warming of 1.5°C. An IPCC Special Report on the impacts of global warming of 1.5°C above pre-industrial levels and related global greenhouse gas emission pathways, in the context of strengthening the global response to the threat of climate change,*. V. Masson-Delmotte, P. Zhai, H.-O. Pörtner, D. Roberts, J. Skea, P.R. Shukla, A. Pirani, W. Moufouma-Okia, C. Péan, R. Pidcock, S. Connors, J.B.R. Matthews, Y. Chen, X. Zhou, M.I. Gomis, E. Lonnoy, T. Maycock, M. Tignor, & T. Waterfield (eds.). Cambridge, UK and New York, NY, USA: Cambridge University Press.

IPCC (2023) ‘Summary for Policymakers’, in IPCC Core Writing Team, H. Lee, & Romero J. (eds.) *Climate Change 2023: Synthesis Report. Contribution of Working Groups I, II and III to the Sixth Assessment Report of the Intergovernmental Panel on Climate Change*. [Online]. Geneva, Switzerland: IPCC. pp. 1–34.

IPCC (2018b) ‘Summary for Policymakers’, in V. Masson-Delmotte, P. Zhai, H.-O. Pörtner, D. Roberts, J. Skea, P.R. Shukla, A. Pirani, W. Moufouma-Okia, C. Péan, R. Pidcock, S. Connors, J.B.R. Matthews, Y. Chen, X. Zhou, M.I. Gomis, E. Lonnoy, T. Maycock, M. Tignor, & T. Waterfield (eds.) *Global Warming of 1.5°C. An IPCC Special Report on the impacts of global warming of 1.5°C above pre-industrial levels and related global greenhouse gas emission pathways, in the context of strengthening the global response to the threat of climate change,*. [Online]. Cambridge, UK and New York, NY, USA: Cambridge University Press. pp. 1–24.

IRRI (2007) *Planting the rice: nursery systems. International Rice Research Institute (IRRI)*. [Online] [online]. Available from: http://www.knowledgebank.irri.org/ericeproduction/II.5_Nursery_systems.htm (Accessed 15 February 2023).

IRRI (2013) *Rice farming: saving water through Alternate Wetting Drying (AWD) method, Indonesia*.

IUCN (2003) *Waza Logone Floodplain, Cameroon: economic benefits of wetland restoration. Case studies in wetland valuation #4*.

Jardim, P.F., Melo, M.M.M., Ribeiro, L. de C., Collischonn, W. & Paz, A.R. da (2020) ‘A Modeling Assessment of Large-Scale Hydrologic Alteration in South American Pantanal Due to Upstream Dam Operation’. Frontiers in environmental science. 8.

Johnson, F. & Sharma, A. (2011) ‘Accounting for interannual variability: A comparison of options for water resources climate change impact assessments’, *Water Resources Research*, 47(4), .

Jones, M.B. & Humphries, S.W. (2002) ‘Impacts of the C4 sedge Cyperus papyrus L. on carbon and water fluxes in an African wetland’, *Hydrobiologia*, 488(1), pp. 107–113.

Joosten, H., Sirin, A., Couwenberg, J., Laine, J. & Smith, P. (2016) ‘The role of peatlands in climate regulation’, in Aletta Bonn, Hans Joosten, Martin Evans, Rob Stoneman, & Tim Allott (eds.) *Peatland Restoration and Ecosystem Services: Science, Policy and Practice*. Ecological Reviews. [Online]. Cambridge: Cambridge University Press. pp. 63–76.

Junk, W., An, S., Finlayson, M., Gopal, B., Květ, J., Mitchell, S., Mitsch, W. & Robarts, R. (2013) ‘Current state of knowledge regarding the world’s wetlands and their future under global climate change: A synthesis’, *Aquatic Sciences*, 75.

Kadykalo, A.N. & Findlay, C.S. (2016) ‘The flow regulation services of wetlands’, *Ecosystem Services*, 20pp. 91–103.

Kaggwa, R., Hogan, R. & Hall, B. (2009) *Enhancing Wetlands’ Contribution to Growth,*

Employment and Prosperity. UNDP/NEMA/UNEP Poverty Environment Initiative.

Kansiime, F. & Nalubega, M. (1999) *Wastewater treatment by a natural wetland: the Nakivubo swamp, Uganda. Processes and implications*. [Online]. A.A. Balkema, Rotterdam.

Kashaigili, J.J., McCartney, M.P., Mahoo, H.F., Lankford, B.A., Mbilinyi, B.P. & Yawson, D.K. (2009) 'Use of a Hydrological Model for Environmental Management of the Usangu Wetlands, Tanzania'. IWMI Research Report 104

Kayendeke, E. & French, H.K. (2019) 'Characterising the Hydrological Regime of a Tropical Papyrus Wetland in the Lake Kyoga Basin, Uganda', in Yazidhi Bamutaze, Samuel Kyamanywa, Bal Ram Singh, Gorettie Nabanoga, & Rattan Lal (eds.) *Agriculture and Ecosystem Resilience in Sub Saharan Africa: Livelihood Pathways Under Changing Climate*. [Online]. Cham: Springer International Publishing. pp. 213–236.

Kayendeke, E.J. (2018) *Water storage dynamics of papyrus wetlands and land use change in the Lake Kyoga basin, Uganda*. [Online]. Norwegian University of Life Sciences.

Kayendeke, E.J., Kansiime, F., French, H.K. & Bamutaze, Y. (2018) 'Spatial and temporal variation of papyrus root mat thickness and water storage in a tropical wetland system', *Science of The Total Environment*, 642pp. 925–936.

Keddy, P. (2010) 'Wetlands: An overview', in Paul A Keddy (ed.) *Wetland Ecology: Principles and Conservation*. 2nd edition [Online]. Cambridge: Cambridge University Press. pp. 1–41.

Kendall, M. (1975) *Multivariate Analysis*. London: Charles Griffin.

Kihwele, E., Muse, E., Magomba, E., Mnaya, B., Nassoro, A., Banga, P., Murashani, E., Irmamasita, D., Kiwango, H., Birkett, C. & Wolanski, E. (2018) 'Restoring the perennial Great Ruaha River using ecohydrology, engineering and governance methods in Tanzania', *Ecohydrology & Hydrobiology*, 18(2), pp. 120–129.

Kimiti, D.W., Ganguli, A.C., Herrick, J.E. & Bailey, D.W. (2020) 'Evaluation of Restoration Success to Inform Future Restoration Efforts in Acacia reficiens Invaded Rangelands in Northern Kenya', *Ecological Restoration*, 38(2), pp. 105–113.

King, J., Brown, C. & Sabet, H. (2003) 'A scenario-based holistic approach to environmental flow assessments for rivers', *River Research and Applications*, 19(5–6), pp. 619–639.

King, J. & Louw, D. (1998) 'Instream flow assessments for regulated rivers in South Africa using the Building Block Methodology', *Aquatic Ecosystem Health & Management*, 1(2), pp. 109–124.

Kingsford, R.T., Bino, G., Finlayson, C.M., Falster, D., Fitzsimons, J.A., Gawlik, D.E., Murray, N.J., Grillas, P., Gardner, R.C., Regan, T.J., Roux, D.J. & Thomas, R.F. (2021) 'Ramsar Wetlands of International Importance–Improving Conservation Outcomes', *Frontiers in Environmental Science*, 9.

Kipkemboi, J. & Van Dam, A.A. (2018) 'Papyrus Wetlands', in C. Finlayson, G. Milton,

R. Prentice, & N. Davidson (eds.) *The Wetland Book*. [Online]. Springer, Dordrecht. pp. 183–197.

Kiwango, Y.A. & Wolanski, E. (2008) 'Papyrus wetlands, nutrients balance, fisheries collapse, food security, and Lake Victoria level decline in 2000–2006', *Wetlands Ecology and Management*, 16(2), pp. 89–96.

Kottek, M., Grieser, J., Beck, C., Rudolf, B. & Rubel, F. (2006) 'World Map of the Köppen-Geiger climate classification updated', *Meteorologische Zeitschrift*, 15(3), pp. 259–263.

Koutsouris, A., Chen, D. & Lyon, S. (2015) 'Comparing global precipitation data sets in eastern Africa: A case study of Kilombero Valley, Tanzania', *International Journal of Climatology*,

Kummerow, C. (1998) 'Beamfilling Errors in Passive Microwave Rainfall Retrievals', *Journal of Applied Meteorology*, 37(4), pp. 356–370.

Kuriqi, A., Pinheiro, A.N., Sordo-Ward, A. & Garrote, L. (2019) 'Influence of hydrologically based environmental flow methods on flow alteration and energy production in a run-of-river hydropower plant', *Journal of Cleaner Production*, 232pp. 1028–1042.

Langan, C., Farmer, J., Rivington, M. & Smith, J.U. (2018) 'Tropical wetland ecosystem service assessments in East Africa; A review of approaches and challenges', *Environmental Modelling & Software*, 102pp. 260–273.

Langbein, W.B., Hardison, C.H. & Searcy, J.K. (1960) *Double-Mass Curves. Manual of Hydrology - Part 1 - General Surface-Water Techniques, Methods and Practices of the Geological Survey*. U.S. Geological Survey water-supply paper 1541-B. Washington, D.C.: .

Lankford, B. & Franks, T. (2000) 'The Sustainable Coexistence of Wetlands and Rice Irrigation: A Case Study From Tanzania', *The Journal of Environment & Development*, 9(2), pp. 119–137.

Lee, S., Qi, J., McCarty, G.W., Yeo, I.-Y., Zhang, X., Moglen, G.E. & Du, L. (2021) 'Uncertainty assessment of multi-parameter, multi-GCM, and multi-RCP simulations for streamflow and non-floodplain wetland (NFW) water storage', *Journal of Hydrology*, 600p. 126564.

Lee, S., Yeo, I.-Y., Lang, M.W., McCarty, G.W., Sadeghi, A.M., Sharifi, A., Jin, H. & Liu, Y. (2019) 'Improving the catchment scale wetland modeling using remotely sensed data', *Environmental Modelling & Software*, 122p. 104069.

Lemly, A.D., Kingsford, R.T. & Thompson, J.R. (2000) 'Irrigated Agriculture and Wildlife Conservation: Conflict on a Global Scale.', *Environmental management*, 25(5), pp. 485–512.

Li, B., Huang, Y., Du, L. & Wang, D. (2021) 'Bias Correction for Precipitation Simulated by RegCM4 over the Upper Reaches of the Yangtze River Based on the Mixed Distribution Quantile Mapping Method'. Atmosphere 12 (12).

Li, M. & Jones, M.B. (1995) 'CO2 and O2 transport in the aerenchyma of Cyperus papyrus L.', *Aquatic Botany*, 52(1), pp. 93–106.

Li, W., Li, H., Zhou, D., Gong, Z., Zhang, L. & Wang, Q. (2020) 'Modelling Hydrological Connectivity in the Marine-Freshwater Interaction in the Yellow River Estuary of China', *Wetlands*, 40(6), pp. 2825–2835.

Li, Z., Ciais, P., Wright, J.S., Wang, Y., Liu, S., Wang, J., Li, L.Z.X., Lu, H., Huang, X., Zhu, L., Goll, D.S. & Li, W. (2023) 'Increased precipitation over land due to climate feedback of large-scale bioenergy cultivation', *Nature Communications*, 14(1), p. 4096.

Ludi, E. (2009) 'Climate change, water and food security - ODI Background Note'. ODI Background Notes (March).

MAAIF (2021) *Detailed Studies, Detailed Engineering Design and Construction Supervision for Proposed Irrigation Schemes Development of Igogero and Naigombwa in Bugiri and Bugweri Districts. Final detailed design Report - Project Works Phase 1*.

MAAIF (2019) *Enhancing National Food Security Through Increased Rice Production Project (ENRP)*. [Online] [online]. Available from: https://www.agriculture.go.ug/enhancing-national-food-security-through-increased-rice-production-project/ (Accessed 26 November 2019).

MAAIF (2009) *Uganda national rice development strategy. Government of the Republic of Uganda - Ministry of Agriculture, Animal Industry and Fisheries.*

MAAIF & MWE (2017) *National Irrigation Policy. Agricultural Transformation Through Irrigation Development*.

Maggioni, V. & Massari, C. (2018) 'On the performance of satellite precipitation products in riverine flood modeling: A review', *Journal of Hydrology*, 558pp. 214–224.

Maidment, R., Grimes, D., Allan, R., Greatrex, H., Rojas, O. & Leo, O. (2013) 'Evaluation of satellite-based and model re-analysis rainfall estimates for Uganda', *Meteorological Applications*, 20.

Maidment, R.I., Grimes, D., Black, E., Tarnavsky, E., Young, M., Greatrex, H., Allan, R.P., Stein, T., Nkonde, E., Senkunda, S. & Alcántara, E.M.U. (2017) 'A new, long-term daily satellite-based rainfall dataset for operational monitoring in Africa', *Scientific Data*, 4(1), p. 170063.

Makula, E.K. & Zhou, B. (2022) 'Coupled Model Intercomparison Project phase 6 evaluation and projection of East African precipitation', *International Journal of Climatology*, 42(4), pp. 2398–2412.

Mallen-Cooper, M. & Zampatti, B.P. (2018) 'History, hydrology and hydraulics: Rethinking the ecological management of large rivers', *Ecohydrology*, 11(5), p. e1965.

Mann, H.B. (1945) 'Nonparametric Tests Against Trend', *Econometrica*, 13(3), pp. 245–259.

Maraun, D. (2012) 'Nonstationarities of regional climate model biases in European seasonal mean temperature and precipitation sums', *Geophysical Research Letters*, 39(6), .

Maraun, D., Wetterhall, F., Ireson, A.M., Chandler, R.E., Kendon, E.J., Widmann, M., Brienen, S., Rust, H.W., Sauter, T., Themeßl, M., Venema, V.K.C., Chun, K.P., Goodess, C.M., Jones, R.G., Onof, C., Vrac, M. & Thiele-Eich, I. (2010) 'Precipitation downscaling under climate change: Recent developments to bridge the gap between dynamical models and the end user', *Reviews of Geophysics*, 48(3), .

Maraun, D. & Widmann, M. (2018) *Statistical Downscaling and Bias Correction for Climate Research*. Cambridge: Cambridge University Press.

Martens, C., Hickler, T., Davis-Reddy, C., Engelbrecht, F., Higgins, S.I., von Maltitz, G.P., Midgley, G.F., Pfeiffer, M. & Scheiter, S. (2021) 'Large uncertainties in future biome changes in Africa call for flexible climate adaptation strategies', *Global Change Biology*, 27(2), pp. 340–358.

Martínez-Capel, F., García-López, L. & Beyer, M. (2017) 'Integrating Hydrological Modelling and Ecosystem Functioning for Environmental Flows in Climate Change Scenarios in the Zambezi River (Zambezi Region, Namibia)', *River Research and Applications*, 33(2), pp. 258–275.

Masih, I., Maskey, S., Mussá, F.E.F. & Trambauer, P. (2014) 'A review of droughts on the African continent: a geospatial and long-term perspective', *Hydrology and Earth System Sciences*, 18(9), pp. 3635–3649.

Mathews, R. & Richter, B.D. (2007) 'Application of the Indicators of Hydrologic Alteration Software in Environmental Flow Setting', *JAWRA Journal of the American Water Resources Association*, 43(6), pp. 1400–1413.

Maurer, E.P. & Pierce, D.W. (2014) 'Bias correction can modify climate model simulated precipitation changes without adverse effect on the ensemble mean', *Hydrology and Earth System Sciences*, 18(3), pp. 915–925.

Mburu, N., Rousseau, D.P.L., van Bruggen, J.J.A. & Lens, P.N.L. (2015) *Use of the Macrophyte Cyperus papyrus in Wastewater Treatment BT - The Role of Natural and Constructed Wetlands in Nutrient Cycling and Retention on the Landscape*, in Jan Vymazal (ed.) [Online]. Cham: Springer International Publishing. pp. 293–314.

McMillan, H.K., Westerberg, I.K. & Krueger, T. (2018) 'Hydrological data uncertainty and its implications', *WIREs Water* , 5(6), p. e1319.

Mehdi, B., Dekens, J. & Herrnegger, M. (2021) 'Climatic impacts on water resources in a tropical catchment in Uganda and adaptation measures proposed by resident stakeholders', *Climatic Change*, 164(1), p. 10.

Mekonnen, M.M. & Hoekstra, A.Y. (2010) *The green, blue and grey water footprint of crops and derived crop products. Value of Water Research Report Series No. 47*.

Mileham, L., Taylor, R.G., Todd, M., Tindimugaya, C. & Thompson, J. (2009) 'The impact of climate change on groundwater recharge and runoff in a humid, equatorial catchment: sensitivity of projections to rainfall intensity', *Hydrological Sciences Journal*, 54(4), pp. 727–738.

Millennium Ecosystem Assessment (2005a) *Ecosystems and Human Well-being: Synthesis*.

Millennium Ecosystem Assessment (2005b) *Ecosystems and human well-being: wetlands and water synthesis*.

Mitsch, W.J. & Day, J.W. (2006) 'Restoration of wetlands in the Mississippi–Ohio–Missouri (MOM) River Basin: Experience and needed research', *Ecological Engineering*, 26(1), pp. 55–69.

Mitsch, W.J. & Gosselink, J.G. (2000) *Wetlands*. Third. New York: Wiley & Sons.

Monteith, J.L. (1965) 'Evaporation and environment. In: State and movement of water in living Organisms', *Symposia of the Society for Experimental Biology*, 19(Swansea. Cambridge University Press, London), pp. 205–234.

Moomaw, W.R., Chmura, G.L., Davies, G.T., Finlayson, C.M., Middleton, B.A., Natali, S.M., Perry, J.E., Roulet, N. & Sutton-Grier, A.E. (2018) 'Wetlands In a Changing Climate: Science, Policy and Management', *Wetlands*, 38(2), pp. 183–205.

Moriasi, D.N., Arnold, J.G., Liew, M.W. Van, Bingner, R.L., Harmel, R.D. & Veith, T.L. (2007) 'Model Evaluation Guidelines for Systematic Quantification of Accuracy in Watershed Simulations', *American Society of Agricultural and Biological Engineers*, 50(3), p. 885−900.

Mushet, D.M., Euliss Jr., N.H. & Stockwell, C.A. (2012) 'A conceptual model to facilitate amphibian conservation in the northern Great Plains', *Great Plains Research*, 22(1), pp. 45–58.

Mutai, C.C. & Ward, M.N. (2000) 'East African Rainfall and the Tropical Circulation/Convection on Intraseasonal to Interannual Timescales', *Journal of Climate*, 13(22), pp. 3915–3939.

Mutai, C.C., Ward, M.N. & Colman, A.W. (1998) 'Towards the prediction of the East Africa short rains based on sea-surface temperature – atmosphere coupling', *Int. J. Climatol.*, 18pp. 975–997.

Mutenyo, I., Nejadhashemi, A.P., Woznicki, S.A. & Giri, S. (2013) 'Evaluation of SWAT performance on a mountainous watershed in tropical Africa.', *Hydrology: Current Research*, 6(3), p. 7.

Mwakubo, S.M. & Obare, G.A. (2009) *Vulnerability, livelihood assets and institutional dynamics in the management of wetlands in Lake Victoria watershed basin*, 17(6), pp. 613–626.

MWE (2019) *Catchment Management Plan Guidelines 2019. Popular Version*.

MWE (2018) *Mpologoma Catchment Management Plan*.

MWE (1995) *National Wetland Policies - Uganda. National Policy for the Conservation and Management of Wetland Resources.*

MWE (2016) *Uganda Wetlands Atlas. Volume two - Popular version*. 2.

MWE and UN-WWAP (2006) *Uganda National Water Development Report. Prepared for the 2nd UN World Water Development Report 'Water, a shared responsibility'.*

Naghettini, M. (ed.) (2017) *Fundamentals of Statistical Hydrology*. Springer, Cham.

Naigaga, S. (2021) *Assessment of the adequacy of the regulatory framework for*

wetlands management in Uganda. [Online]. Makerere University.

Namutebi, J. & Sekanjako, H. (2013) 'Food security: Govt to borrow sh187b', *New Vision*, p. 32.

NASA/Japan Space Systems (2018) *ASTER global digital elevation model V003*. [Online] [online]. Available from: https://asterweb.jpl.nasa.gov/gdem.asp (Accessed 5 March 2020).

Negri, C., Chiaradia, E., Rienzner, M., Mayer, A., Gandolfi, C., Romani, M. & Facchi, A. (2020) 'On the effects of winter flooding on the hydrological balance of rice areas in northern Italy', *Journal of Hydrology*, 590p. 125401.

Neumann, J. von (1941) 'Distribution of the Ratio of the Mean Square Successive Difference to the Variance', *The Annals of Mathematical Statistics*, 12(4), pp. 367–395.

Ngoma, H., Wen, W., Ayugi, B., Babaousmail, H., Karim, R. & Ongoma, V. (2021) 'Evaluation of precipitation simulations in CMIP6 models over Uganda', *International Journal of Climatology*, 41(9), pp. 4743–4768.

Nikulin, G., Lennard, C., Dosio, A., Kjellström, E., Chen, Y., Hänsler, A., Kupiainen, M., Laprise, R., Mariotti, L., Maule, C.F., van Meijgaard, E., Panitz, H.-J., Scinocca, J.F. & Somot, S. (2018) 'The effects of 1.5 and 2 degrees of global warming on Africa in the CORDEX ensemble', *Environmental Research Letters*, 13(6), p. 65003.

NOAA-CPC (2001) *RFE 2.0 Technical Description Summary*.

Novella, N.S. & Thiaw, W.M. (2013) 'African Rainfall Climatology Version 2 for Famine Early Warning Systems', *Journal of Applied Meteorology and Climatology*, 52(3), pp. 588–606.

Nyenje, P.M. & Batelaan, O. (2009) 'Estimating the effects of climate change on groundwater recharge and baseflow in the upper Ssezibwa catchment, Uganda', *Hydrological Sciences Journal*, 54(4), pp. 713–726.

Ogden, J.C., Davis, S.M., Jacobs, K.J., Barnes, T. & Fling, H.E. (2005) 'The use of conceptual ecological models to guide ecosystem restoration in South Florida', *Wetlands*, 25(4), pp. 795–809.

Olden, J.D. & Poff, N.L. (2003) 'Redundancy and the choice of hydrologic indices for characterizing streamflow regimes', *River Research and Applications*, 19(2), pp. 101–121.

Opio, A., Jones, M., Kansiime, F. & Otiti, T. (2014) 'Growth and Development of Cyperus papyrus in a Tropical Wetland', *Open Journal of Ecology*, 04pp. 113–123.

Orasen, G., De Nisi, P., Lucchini, G., Abruzzese, A., Pesenti, M., Maghrebi, M., Kumar, A., Nocito, F.F., Baldoni, E., Morgutti, S., Negrini, N., Valè, G. & Sacchi, G.A. (2019) 'Continuous Flooding or Alternate Wetting and Drying Differently Affect the Accumulation of Health-Promoting Phytochemicals and Minerals in Rice Brown Grain'. Agronomy 9 (10).

Orlowsky, B. & Seneviratne, S.I. (2014) 'On the spatial representativeness of temporal

dynamics at European weather stations', *International Journal of Climatology*, 34(10), pp. 3154–3160.

Oweis, T. (1997) *Supplemental Irrigation. A Highly Efficient Water-Use Practice*.

Oyarmoi, A., Birkinshaw, S., Hewett, C.J.M. & Fowler, H.J. (2023) 'The Effect of Papyrus Wetlands on Flow Regulation in a Tropical River Catchment', *Land*, 12(12), p. 2158.

Pacini, N., Hesslerová, P., Pokorný, J., Mwinami, T., Morrison, E.H.J., Cook, A.A., Zhang, S. & Harper, D.M. (2018) 'Papyrus as an ecohydrological tool for restoring ecosystem services in Afrotropical wetlands', *Ecohydrology & Hydrobiology*, 18(2), pp. 142–154.

Pardo-Loaiza, J., Solera, A., Bergillos, R.J., Paredes-Arquiola, J. & Andreu, J. (2021) 'Improving Indicators of Hydrological Alteration in Regulated and Complex Water Resources Systems: A Case Study in the Duero River Basin', *Water*, 13(19), p. 17.

Parkin, G. (1996) *A three-dimensional variably-saturated subsurface modelling system for river basins*. [Online]. University of Newcastle upon Tyne, UK.

Penvenne, L.J. (1996) 'Disappearing delta', *American Scientist*, 84(5), pp. 439–441.

Pettitt, A.N. (1979) 'A Non-Parametric Approach to the Change-Point Problem', *Journal of the Royal Statistical Society. Series C (Applied Statistics)*, 28(2), pp. 126–135.

Pierce, D.W., Cayan, D.R., Maurer, E.P., Abatzoglou, J.T. & Hegewisch, K.C. (2015) 'Improved Bias Correction Techniques for Hydrological Simulations of Climate Change', *Journal of Hydrometeorology*, 16(6), pp. 2421–2442.

Pimentel, D., Berger, B., Filiberto, D., Newton, M., Wolfe, B., Karabinakis, E., Clark, S., Poon, E., Abbett, E. & Nandagopal, S. (2004) 'Water Resources: Agricultural and Environmental Issues', *BioScience*, 54(10), pp. 909–918.

Poff, N.L., Allan, J.D., Bain, M.B., Karr, J.R., Prestegaard, K.L., Richter, B.D., Sparks, R.E. & Stromberg, J.C. (1997) 'The Natural Flow Regime: a paradigm for river conservation and restoration', *BioScience*, 47(11), pp. 769–784.

Poff, N.L., Richter, B.D., Arthington, A.H., Bunn, S.E., Naiman, R.J., Kendy, E., Acreman, M., Apse, C., Bledsoe, B.P., Freeman, M.C., Henriksen, J., Jacobson, R.B., Kennen, J.G., Merritt, D.M., O'keeffe, J.A.Y.H., Olden, J.D., Rogers, K., Tharme, R.E. & Warner, A. (2010) 'The ecological limits of hydrologic alteration (ELOHA): a new framework for developing regional environmental flow standards', *Freshwater Biology*, 55(1), pp. 147–170.

Pompeu, C.R., Peñas, F.J., Goldenberg-Vilar, A., Álvarez-Cabria, M. & Barquín, J. (2022) 'Assessing the effects of irrigation and hydropower dams on river communities using taxonomic and multiple trait-based approaches', *Ecological Indicators*, 145p. 109662.

Pörtner, H.-O., Roberts, D.C., Adams, H., Adelekan, I., Adler, C., Adrian, R., Aldunce, P., Ali, E., Begum, R.A., Bednar-Friedl, B., Kerr, R.B., Biesbroek, R., Birkmann, J., Bowen, K., Caretta, M.A., Carnicer, J., Castellanos, E., Chow, T.S.C.W., G.

Cissé, S.C., et al. (2022) ‘Technical Summary’, in Portner H.-O., Roberts D.C., Tignor M., Poloczanska E.S., Mintenbeck K., Alegria A., Craig M., Langsdorf S., Loschke S., Moller V., Okem A., & Rama B. (eds.) *Climate Change 2022: Impacts, Adaptation and Vulnerability. Contribution of Working Group II to the Sixth Assessment Report of the Intergovernmental Panel on Climate Change*. [Online]. Cambridge, UK and New York, NY, USA: Cambridge University Press. pp. 37–118.

Postel, S. & Richter, B.D. (2003) *Rivers for life - managing water for people and nature*. Island Press.

Principato, G. & Viggiani, G. (2012) *Analysis of Hydrologic Alteration Due to River Diversion*, in Mahamane Ali (ed.) [Online]. Rijeka: IntechOpen. p. Ch. 16.

Prudhomme, C., Jakob, D. & Svensson, C. (2003) ‘Uncertainty and climate change impact on the flood regime of small UK catchments’, *Journal of Hydrology*, 277(1), pp. 1–23.

Quemada, M., Baranski, M., Nobel-de Lange, M.N.J., Vallejo, A. & Cooper, J.M. (2013) ‘Meta-analysis of strategies to control nitrate leaching in irrigated agricultural systems and their effects on crop yield’, *Agriculture, Ecosystems & Environment*, 174pp. 1–10.

Quin, A. & Destouni, G. (2018) ‘Large-scale comparison of flow-variability dampening by lakes and wetlands in the landscape’, *Land Degradation & Development*, 29(10), pp. 3617–3627.

Raes, D. (2022) *AquaCrop training handbooks. Book I - Understanding AquaCrop*.

Raes, D., Steduto, P., Hsiao, T.C. & Fereres, E. (2022) *AquaCrop Version 7.0 reference manual*.

Rains, M.C., Leibowitz, S.G., Cohen, M.J., Creed, I.F., Golden, H.E., Jawitz, J.W., Kalla, P., Lane, C.R., Lang, M.W. & McLaughlin, D.L. (2016) ‘Geographically isolated wetlands are part of the hydrological landscape’, *Hydrological Processes*, 30(1), pp. 153–160.

Raise the River (2013) *Raise the River - Reconnect the Colorado. Restoring the Colorado River Delta. Restoration Opportunity Guide. The Colorado River Delta, Circa 1905*.

Raju, K.S. & Kumar, D.N. (2020) ‘Review of approaches for selection and ensembling of GCMs’, *Journal of Water and Climate Change*, 11(3), pp. 577–599.

Ramalho, Q., Vale, M.M., Manes, S., Diniz, P., Malecha, A. & Prevedello, J.A. (2023) ‘Evidence of stronger range shift response to ongoing climate change by ectotherms and high-latitude species’, *Biological Conservation*, 279p. 109911.

Ramsar Convention (1971) *Convention on Wetlands of International Importance especially as Waterfowl Habitat Ramsar, 2.2.1971 as amended by the Protocol of 3.12.1982*.

Ramsar Convention Secretariat (2016) *The Fourth Ramsar Strategic Plan 2016-2024. Ramsar handbooks for the wise use of wetlands*. 5th editio. Gland, Switzerland: Ramsar Convention Secretariat.

Ramsar Convention Secretariat (2018) *Wetlands and the SDGs. Scaling up wetland conservation, wise use and restoration to achieve the Sustainable Development Goals. Ramsar Convention On Wetlands.*

Ramsar Convention Secretariat (2010) *Wise use of wetlands: Concepts and approaches for the wise use of wetlands. Ramsar handbooks for the wise use of wetlands, 4th edition, vol. 1.*

Rangecroft, S., Birkinshaw, S., Rohse, M., Day, R., McEwen, L., Makaya, E. & Van Loon, A.F. (2018) 'Hydrological modelling as a tool for interdisciplinary workshops on future drought', *Progress in Physical Geography*, 42(2), pp. 237–256.

Räty, O., Räisänen, J. & Ylhäisi, J.S. (2014) 'Evaluation of delta change and bias correction methods for future daily precipitation: intermodel cross-validation using ENSEMBLES simulations', *Climate Dynamics*, 42(9), pp. 2287–2303.

Reddy, K.R. & DeLaune, R.D. (2008) *Biogeochemistry of Wetlands: Science and Applications*. 1st edition. CRC Press.

Ree, W.O., Wimberley, F.L. & Crow, F.R. (1977) 'Manning's n and the Overland Flow Equation', *Transactions, ASAE*, 20(1), pp. 89–95.

Rezanezhad, F., McCarter, C.P.R. & Lennartz, B. (2020) 'Editorial: Wetland Biogeochemistry: Response to Environmental Change', *Frontiers in Environmental Science*, 8.

Richards, M.B. & Sander, B.O. (2014) *Alternate wetting and drying in irrigated rice. Climate-Smart Agriculture Practice Brief*.

Richter, B., Baumgartner, J., Wigington, R. & Braun, D. (1997) 'How much water does a river need?', *Freshwater Biology*, 37(1), pp. 231–249.

Richter, B.D., Baumgartner, J. V, Braun, D.P. & Powell, J. (1998) 'A spatial assessment of hydrologic alteration within a river network', *Regulated Rivers: Research & Management*, 14(4), pp. 329–340.

Richter, B.D., Baumgartner, J. V, Powell, J. & Braun, D.P. (1996) 'A Method for Assessing Hydrologic Alteration within Ecosystems', *Conservation Biology*, 10(4), pp. 1163–1174.

Richter, B.D., Warner, A.T., Meyer, J.L. & Lutz, K. (2006) 'A collaborative and adaptive process for developing environmental flow recommendations', *River Research and Applications*, 22(3), pp. 297–318.

Romilly, T.G. & Gebremichael, M. (2011) 'Evaluation of satellite rainfall estimates over Ethiopian river basins', *Hydrology and Earth System Sciences*, 15(5), pp. 1505–1514.

Rosa, L. (2022) 'Adapting agriculture to climate change via sustainable irrigation: biophysical potentials and feedbacks', *Environmental Research Letters*, 17(6), p. 63008.

Rosa, L., Chiarelli, D.D., Rulli, M.C., Dell'Angelo, J. & D'Odorico, P. (2020) 'Global agricultural economic water scarcity', *Science Advances*, 6(18), p. eaaz6031.

Rosa, L., Chiarelli, D.D., Sangiorgio, M., Beltran-Peña, A.A., Rulli, M.C., D'Odorico, P.

& Fung, I. (2020) ‘Potential for sustainable irrigation expansion in a 3 °C warmer climate.’, *Proceedings of the National Academy of Sciences of the United States of America*, 117(47), pp. 29526–29534.

RUBADA (2001) *Sustainable Management of the Usangu Wetland and its Catchment. Final Report - Water Resources*.

Russi, D., ten Brink, P., Farmer, A., Badura, T., Coates, D., Förster, J., Kumar, R. & Davidson, N. (2013) *The Economics of Ecosystems and Biodiversity for Water and Wetlands*.

Rutter, A.J., Kershaw, K.A., Robins, P.C. & Morton, A.J. (1971) ‘A predictive model of rainfall interception in forests, 1. Derivation of the model from observations in a plantation of Corsican pine’, *Agricultural Meteorology*, 9pp. 367–384.

Rutter, A.J., Morton, A.J. & Robins, P.C. (1975) ‘A Predictive Model of Rainfall Interception in Forests. II. Generalization of the Model and Comparison with Observations in Some Coniferous and Hardwood Stands’, *Journal of Applied Ecology*, 12(1), pp. 367–380.

Salimi, S., Almuktar, S.A.A.A.N. & Scholz, M. (2021) ‘Impact of climate change on wetland ecosystems: A critical review of experimental wetlands’, *Journal of Environmental Management*, 286p. 112160.

Saunders, M.J., Kansiime, F. & Jones, M.B. (2014) ‘Reviewing the carbon cycle dynamics and carbon sequestration potential of Cyperus papyrus L. wetlands in tropical Africa’, *Wetlands Ecology and Management*, 22(2), pp. 143–155.

Savva, A.P. & Frenken, K. (2002) *Irrigation Manual Module 1: Irrigation development - a multifaceted process*.

Saxton, K.E. & Rawls, W. (2018) *Soil Water Characteristics - Hydraulic Properties Calculator*.

Scholte, P., de Kort, S. & van Weerd, M. (2000) ‘Floodplain rehabilitation in Far North Cameroon: expected impact on bird life’, *Ostrich*, 71(1–2), pp. 112–117.

Seibert, J. & McDonnell, J.J. (2002) ‘On the dialog between experimentalist and modeler in catchment hydrology: Use of soft data for multicriteria model calibration’, *Water Resources Research*, 38(11), pp. 14–23.

Semeniuk, C.A. & Semeniuk, V. (2011) ‘A comprehensive classification of inland wetlands of Western Australia using the geomorphic-hydrologic approach’, *Journal of the Royal Society of Western Australia*, 94(3), pp. 449–464.

Semeniuk, C.A. & Semeniuk, V. (1995) ‘A geomorphic approach to global classification for inland wetlands’, *Vegetatio*, 118(1), pp. 103–124.

Semeniuk, V. & Semeniuk, C.A. (1997) ‘A geomorphic approach to global classification for natural inland wetlands and rationalization of the system used by the Ramsar Convention – a discussion’, *Wetlands Ecology and Management*, 5(2), pp. 145–158.

Sen, P.K. (1968) ‘Estimates of the Regression Coefficient Based on Kendall’s Tau’, *Journal of the American Statistical Association*, 63(324), pp. 1379–1389.

Sheikh, V., Sadoddin, A., Najafinejad, A., Zare, A., Hollisaz, A., Siroosi, H., Tajiki, M., Gholipouri, M. & Sheikh, J. (2022) 'The density difference and weighted RVA approaches for assessing hydrologic regime alteration', *Journal of Hydrology*, 613p. 128450.

Shivanna, K.R. (2022) 'Climate change and its impact on biodiversity and human welfare', *Proceedings of the Indian National Science Academy*, 88(2), pp. 160–171.

Shrestha, M., Acharya, S.C. & Shrestha, P.K. (2017) 'Bias correction of climate models for hydrological modelling – are simple methods still useful?', *Meteorological Applications*, 24(3), pp. 531–539.

Siad, S.M., Iacobellis, V., Zdruli, P., Gioia, A., Stavi, I. & Hoogenboom, G. (2019) 'A review of coupled hydrologic and crop growth models', *Agricultural Water Management*, 224p. 105746.

Siebert, S., Henrich, V., Frenken, K. & Burke, J. (2013) *Update of the digital global map of irrigation areas to version 5.*

Singh, R., Subramanian, K. & Refsgaard, J.C. (1999) 'Hydrological modelling of a small watershed using MIKE SHE for irrigation planning', *Agricultural Water Management*, 41(3), pp. 149–166.

Singh, S.K., Ibbitt, R., Srinivasan, M.S. & Shankar, U. (2017) 'Inter-comparison of experimental catchment data and hydrological modelling', *Journal of Hydrology*, 550pp. 1–11.

Smakhtin, V.U. & Batchelor, A.L. (2005) 'Evaluating wetland flow regulating functions using discharge time-series', *Hydrological Processes*, 19(6), pp. 1293–1305.

Sørland, S.L., Schär, C., Lüthi, D. & Kjellström, E. (2018) 'Bias patterns and climate change signals in GCM-RCM model chains', *Environmental Research Letters*, 13(7), p. 74017.

Sreedevi, S. & Eldho, T.I. (2019) 'A two-stage sensitivity analysis for parameter identification and calibration of a physically-based distributed model in a river basin', *Hydrological Sciences Journal*, 64(6), pp. 701–719.

Sreedevi, S. & Eldho, T.I. (2021) 'Effects of grid-size on effective parameters and model performance of SHETRAN for estimation of streamflow and sediment yield', *International Journal of River Basin Management*, 19(4), pp. 535–551.

Ssanyu, G.A., Kipkemboi, J., Mathooko, J.M. & Balirwa, J. (2014) 'Land-use impacts on small-scale Mpologoma wetland fishery, eastern Uganda: A socio-economic perspective', *Lakes & Reservoirs: Science, Policy and Management for Sustainable Use*, 19(4), pp. 280–292.

Stanley, D.J. & Warne, A.G. (1998) 'Nile Delta in Its Destruction Phase', *Journal of Coastal Research*, 14(3), pp. 795–825.

Stefanidis, K., Panagopoulos, Y., Psomas, A. & Mimikou, M. (2016) 'Assessment of the natural flow regime in a Mediterranean river impacted from irrigated agriculture.', *The Science of the total environment*, 573pp. 1492–1502.

Steinfeld, C.M.M., Sharma, A., Mehrotra, R. & Kingsford, R.T. (2020) 'The human

dimension of water availability: Influence of management rules on water supply for irrigated agriculture and the environment', *Journal of Hydrology*, 588p. 125009.

Stewart, R.I.A., Dossena, M., Bohan, D.A., Jeppesen, E., Kordas, R.L., Ledger, M.E., Meerhoff, M., Moss, B., Mulder, C., Shurin, J.B., Suttle, B., Thompson, R., Trimmer, M. & Woodward, G. (2013) 'Chapter Two - Mesocosm Experiments as a Tool for Ecological Climate-Change Research', in Guy Woodward & Eoin J B T - Advances in Ecological Research O'Gorman (eds.) *Global Change in Multispecies Systems: Part 3*. [Online]. Academic Press. pp. 71–181.

Stisen, S. & Sandholt, I. (2010) 'Evaluation of Remote-Sensing-Based Rainfall Products through Predictive Capability in Hydrological Runoff Modeling', *Hydrological Processes*, 24pp. 879–891.

Sun, G.-Q., Li, L., Li, J., Liu, C., Wu, Y.-P., Gao, S., Wang, Z. & Feng, G.-L. (2022) 'Impacts of climate change on vegetation pattern: Mathematical modeling and data analysis', *Physics of Life Reviews*, 43pp. 239–270.

Sun, G., Lei, G., Qu, Y., Zhang, C. & He, K. (2020) 'The Operation of the Three Gorges Dam Alters Wetlands in the Middle and Lower Reaches of the Yangtze River', *Frontiers in Environmental Science*, 8.

Sutcliffe, J. V & Parks, Y.P. (1989) 'Comparative water balances of selected African wetlands', *Hydrological Sciences Journal*, 34(1), pp. 49–62.

Sutcliffe, J. V & Parks, Y.P. (1987) 'Hydrological modelling of the Sudd and Jonglei Canal', *Hydrological Sciences Journal*, 32(2), pp. 143–159.

Talbot, C.J., Bennett, E.M., Cassell, K., Hanes, D.M., Minor, E.C., Paerl, H., Raymond, P.A., Vargas, R., Vidon, P.G., Wollheim, W. & Xenopoulos, M.A. (2018) 'The impact of flooding on aquatic ecosystem services', *Biogeochemistry*, 141(3), pp. 439–461.

Tan, M.L., Ficklin, D.L., Dixon, B., Ibrahim, A.L., Yusop, Z. & Chaplot, V. (2015) 'Impacts of DEM resolution, source, and resampling technique on SWAT-simulated streamflow', *Applied Geography*, 63pp. 357–368.

Tani, S. & Gobiet, A. (2019) 'Quantile mapping for improving precipitation extremes from regional climate models', *Journal of Agrometeorology*, 21(4), pp. 434–443.

Taylor, V., Schulze, R. & Jewitt, G. (2003) 'Application of the Indicators of Hydrological Alteration method to the Mkomazi River, KwaZulu-Natal, South Africa', *African Journal of Aquatic Science*, 28(1), pp. 1–11.

Terer, T., Muasya, A.M., Higgins, S., Gaudet, J.J. & Triest, L. (2014) 'Importance of seedling recruitment for regeneration and maintaining genetic diversity of Cyperus papyrus during drawdown in Lake Naivasha, Kenya', *Aquatic Botany*, 116pp. 93–102.

Teutschbein, C. & Seibert, J. (2012) 'Bias correction of regional climate model simulations for hydrological climate-change impact studies: Review and evaluation of different methods', *Journal of Hydrology*, 456–457pp. 12–29.

The Nature Conservancy (2009) *Indicators of Hydrologic Alteration. Version 7.1 User's Manual. The Nature Conservancy (TNC).* p.p. 81.

Theil, H. (1950) ‘A rank-invariant method of linear and polynomial regression analysis, 1-2; confidence regions for the parameters of linear regression equations in two, three and more variables’, *Indagationes Mathematicae*, 1(2), .

Themeßl, M.J., Gobiet, A. & Heinrich, G. (2012) ‘Empirical-statistical downscaling and error correction of regional climate models and its impact on the climate change signal’, *Climatic Change*, 112(2), pp. 449–468.

Thiemig, V., Rojas, R., Zambrano-Bigiarini, M. & De Roo, A. (2013) ‘Hydrological evaluation of satellite-based rainfall estimates over the Volta and Baro-Akobo Basin’, *Journal of Hydrology*, 499pp. 324–338.

Thom, H.C.S. (1958) ‘A note on the gamma distribution’, *Monthly Weather Review*, 86(4), pp. 117–122.

Thompson, J.R., Gosling, S.N., Zaherpour, J. & Laizé, C.L.R. (2021) ‘Increasing Risk of Ecological Change to Major Rivers of the World With Global Warming’, *Earth’s Future*, 9(11), p. e2021EF002048.

Thompson, K. & Grime, J.P. (1979) ‘Seasonal Variation in the Seed Banks of Herbaceous Species in Ten Contrasting Habitats’, *Journal of Ecology*, 67(3), pp. 893–921.

Thorslund, J., Jarsjo, J., Jaramillo, F., Jawitz, J.W., Manzoni, S., Basu, N.B., Chalov, S.R., Cohen, M.J., Creed, I.F., Goldenberg, R., Hylin, A., Kalantari, Z., Koussis, A.D., Lyon, S.W., Mazi, K., Mard, J., Persson, K., Pietro, J., Prieto, C., et al. (2017) ‘Wetlands as large-scale nature-based solutions: Status and challenges for research, engineering and management’, *Ecological Engineering*, 108pp. 489–497.

Tockner, K. (2002) ‘Riverine flood plains: Present state and future trends’, *Environmental conservation.*, 29(3), pp. 308–330.

Tong, Y., Gao, X., Han, Z., Xu, Y.Y., Xu, Y.Y. & Giorgi, F. (2021) ‘Bias correction of temperature and precipitation over China for RCM simulations using the QM and QDM methods’, *Climate Dynamics*, 57(5), pp. 1425–1443.

Torma, C., Giorgi, F. & Coppola, E. (2015) ‘Added value of regional climate modeling over areas characterized by complex terrain—Precipitation over the Alps’, *Journal of Geophysical Research: Atmospheres*, 120(9), pp. 3957–3972.

Tsuchiya, R., Kato, T., Jeong, J. & Arnold, J.G. (2018) ‘Development of SWAT-Paddy for Simulating Lowland Paddy Fields’. Sustainability 10 (9).

Tucker, M.R. & Sear, C.B. (2001) ‘A comparison of Meteosat rainfall estimation techniques in Kenya’, *Meteorological Applications*, 8(1), pp. 107–117.

Turyahabwe, N., Tumusiime, D., Kakuru, W. & Barasa, B. (2013) ‘Wetland Use/Cover Changes and Local Perceptions in Uganda’, *Sustainable Agriculture Research*, 2.

UBOS (2015) *“Statistical abstract 2015.” Uganda Bureau of Statistcs*.

UNESCO-WWAP (2012) *Facts and figures. Managing water under uncertainty and risk. The United Nations World Water Development Report 4*.

UNESCO (2000) *Water-related vision for the Aral Sea Basin for the year 2025*.

UNFCCC (2013) *Decision 1/CP.18 Report of the Conference of the Parties on its eighteenth session, held in Doha from 26 November to 8 December 2012.*

UNFCCC (2015) *Paris Agreement*.

UNPA (2020) *Third National Development Plan (NDPIII) 2020/21 – 2024/25*.

Valyrakis, M., Liu, D., Turker, U. & Yagci, O. (2021) 'The role of increasing riverbank vegetation density on flow dynamics across an asymmetrical channel', *Environmental Fluid Mechanics*, 21(3), pp. 643–666.

Vaughan, G. (2011) *Cyperus papyrus L. Record from PROTA4U. Brink, M. & Achigan-Dako, E.G. (Editors). PROTA (Plant Resources of Tropical Africa / Ressources végétales de l'Afrique tropicale), Wageningen, Netherlands*. [Online] [online]. Available from: https://uses.plantnet-project.org/en/Cyperus_papyrus_(PROTA) (Accessed 10 November 2022).

Vautard, R., Gobiet, A., Sobolowski, S., Kjellström, E., Stegehuis, A., Watkiss, P., Mendlik, T., Landgren, O., Nikulin, G., Teichmann, C. & Jacob, D. (2014) 'The European climate under a 2 °C global warming', *Environmental Research Letters*, 9(3), p. 34006.

Velásquez-Tibatá, J., Salaman, P. & Graham, C.H. (2013) 'Effects of climate change on species distribution, community structure, and conservation of birds in protected areas in Colombia', *Regional Environmental Change*, 13(2), pp. 235–248.

Verhoeven, J.T.A., Arheimer, B., Yin, C. & Hefting, M.M. (2006) 'Regional and global concerns over wetlands and water quality', *Trends in Ecology & Evolution*, 21(2), pp. 96–103.

Vila-Traver, J., González de Molina, M., Infante-Amate, J. & Aguilera, E. (2022) 'Disentangling the effect of climate and cropland changes on the water performance of agroecosystems (Spain, 1922–2016)', *Journal of Cleaner Production*, 344p. 130811.

Di Vittorio, C.A. & Georgakakos, A.P. (2021) 'Hydrologic Modeling of the Sudd Wetland using Satellite-based Data', *Journal of Hydrology: Regional Studies*, 37p. 100922.

Vogel, E., Johnson, F., Marshall, L., Bende-Michl, U., Wilson, L., Peter, J.R., Wasko, C., Srikanthan, S., Sharples, W., Dowdy, A., Hope, P., Khan, Z., Mehrotra, R., Sharma, A., Matic, V., Oke, A., Turner, M., Thomas, S., Donnelly, C., et al. (2023) 'An evaluation framework for downscaling and bias correction in climate change impact studies', *Journal of Hydrology*, 622p. 129693.

Wagener, T. & Kollat, J. (2007) 'Numerical and Visual Evaluation of Hydrological and Environmental Models Using the Monte Carlo Analysis Toolbox', *Environ. Model. Softw.*, 22(7), pp. 1021–1033.

Walther, G.-R. (2010) 'Community and ecosystem responses to recent climate change', *Philosophical Transactions of the Royal Society B: Biological Sciences*, 365(1549), pp. 2019–2024.

Wang, H., Xu, S. & Sun, L. (2006) ‘Effects of climatic change on evapotranspiration in Zhalong Wetland, Northeast China’, *Chinese Geographical Science*, 16(3), pp. 265–269.

Wang, X., Ma, W., Lv, J., Li, H., Liu, H., Mu, G. & Bian, D. (2022) ‘Analysis of changes in the hydrological regime in Lalin River basin and its impact on the ecological environment’, *Frontiers in Earth Science*, 10.

Wanyama, J., Ssegane, H., Kisekka, I., Komakech, A.J., Banadda, N., Zziwa, A., Ebong, T.O., Mutumba, C., Kiggundu, N., Kayizi, R.K., Mucunguzi, D.B. & Kiyimba, F.L. (2017) ‘Irrigation development in Uganda: Constraints, lessons learned, and future perspectives’, *Journal of Irrigation and Drainage Engineering*, 143(5), p. 10.

Ward, D.P., Hamilton, S.K., Jardine, T.D., Pettit, N.E., Tews, E.K., Olley, J.M. & Bunn, S.E. (2013) ‘Assessing the seasonal dynamics of inundation, turbidity, and aquatic vegetation in the Australian wet–dry tropics using optical remote sensing’, *Ecohydrology*, 6(2), pp. 312–323.

Wassmann, R., Jagadish, S.V.K., Heuer, S., Ismail, A.M., Redoña, E.D., Serraj, R., Singh, R.K., Howell, G., Pathak, H. & Sumfleth, K. (2009) ‘Climate change affecting rice production: the physiological and agronomic basis for possible adaptation strategies’, *Advances in Agronomy*, 101pp. 59–122.

WEF (2023) *The Global Risks Report 2023*.

Weiler, M. & Beven, K. (2015) ‘Do we need a Community Hydrological Model?’, *Water Resources Research*, 51(9), pp. 7777–7784.

Weltz, M.A., Arslan, A.B. & Lane, L.J. (1992) ‘Hydraulic Roughness Coefficients for Native Rangelands’, *Journal of Irrigation and Drainage Engineering-asce - J IRRIG DRAIN ENG-ASCE*, 118.

White, K.D. (2013) ‘Nature–society linkages in the Aral Sea region’, *Journal of Eurasian Studies*, 4(1), pp. 18–33.

Wijngaard, J.B., Klein Tank, A.M.G. & Können, G.P. (2003) ‘Homogeneity of 20th century European daily temperature and precipitation series’, *International Journal of Climatology*, 23(6), pp. 679–692.

Wilby, R.L., Clifford, N.J., De Luca, P., Harrigan, S., Hillier, J.K., Hodgkins, R., Johnson, M.F., Matthews, T.K.R., Murphy, C., Noone, S.J., Parry, S., Prudhomme, C., Rice, S.P., Slater, L.J., Smith, K.A. & Wood, P.J. (2017) ‘The “dirty dozen” of freshwater science: detecting then reconciling hydrological data biases and errors’, *WIREs Water* , 4(3), p. e1209.

Wildemeersch, S., Goderniaux, P., Orban, P., Brouyère, S. & Dassargues, A. (2014) ‘Assessing the effects of spatial discretization on large-scale flow model performance and prediction uncertainty’, *Journal of Hydrology*, 510pp. 10–25.

Willems, P. (2009) ‘A time series tool to support the multi-criteria performance evaluation of rainfall-runoff models’, *Environmental Modelling & Software*, 24(3), pp. 311–321.

Winkler, K., Fuchs, R., Rounsevell, M. & Herold, M. (2021) ‘Global land use changes

are four times greater than previously estimated', *Nature Communications*, 12(1), p. 2501.

Winrock International (2018) *Environmental flows technical guidance manual*.

Woodhouse, P., Veldwisch, G.J., Venot, J.-P., Brockington, D., Komakech, H. & Manjichi, Â. (2017) 'African farmer-led irrigation development: re-framing agricultural policy and investment?', *The Journal of Peasant Studies*, 44(1), pp. 213–233.

Woodward, R.T. & Wui, Y.-S. (2001) 'The economic value of wetland services: a meta-analysis', *Ecological Economics*, 37(2), pp. 257–270.

World Bank (2013) *Uganda Economic Update: Jobs: Key to prosperity*.

World Bank (2016) *Unleashing the power of public investment management*. (April).

WRSRU/TR/9510/61.0 (2001) *SHETRAN Water Flow Component, Equations and Algorithms*.

WTTC (2014) *World Travel & Tourism. Economic Impact 2014*.

Wu, Y., Sun, J., Jun Xu, Y., Zhang, G. & Liu, T. (2022) 'Projection of future hydrometeorological extremes and wetland flood mitigation services with different global warming levels: A case study in the Nenjiang river basin', *Ecological Indicators*, 140p. 108987.

Wu, Y., Zhang, G., Rousseau, A.N., Xu, Y.J. & Foulon, É. (2020) 'On how wetlands can provide flood resilience in a large river basin: A case study in Nenjiang river Basin, China', *Journal of Hydrology*, 587p. 125012.

WWRP/WGNE (2009) *Forecast Verification - Issues, Methods and FAQ*. [Online] [online]. Available from: https://www.cawcr.gov.au/projects/verification/verif_web_page.html#Contributors_to_this_site (Accessed 23 February 2022).

Xia, Q., Liu, P., Fan, Y., Cheng, L., An, R., Xie, K. & Zhou, L. (2022) 'Representing Irrigation Processes in the Land Surface-Hydrological Model and a Case Study in the Yangtze River Basin, China', *Journal of Advances in Modeling Earth Systems*, 14(7), p. e2021MS002653.

Xie, P. & Arkin, P.A. (1996) 'Analyses of Global Monthly Precipitation Using Gauge Observations, Satellite Estimates, and Numerical Model Predictions', *Journal of Climate*, 9(4), pp. 840–858.

Xie, P., Joyce, R. & Wu, S. (2018) *Bias-Corrected CMORPH - Climate Algorithm Theoretical Basis Document. NOAA Climate Data Record Program. CDRP-ATBD-0812, Rev. 0*.

Xu, T., Weng, B., Yan, D., Wang, K., Li, X., Bi, W., Li, M., Cheng, X. & Liu, Y. (2019) 'Wetlands of International Importance: Status, Threats, and Future Protection.', *International journal of environmental research and public health*, 16(10), .

Xu, X., Wang, Y.-C., Kalcic, M., Muenich, R.L., Yang, Y.C.E. & Scavia, D. (2019) 'Evaluating the impact of climate change on fluvial flood risk in a mixed-use watershed', *Environmental Modelling & Software*, 122p. 104031.

Xue, L., Zhang, H., Yang, C., Zhang, L. & Sun, C. (2017) 'Quantitative Assessment of Hydrological Alteration Caused by Irrigation Projects in the Tarim River basin, China', *Scientific Reports*, 7(1), p. 4291.

Yang, W., Wang, X., Liu, Y., Gabor, S., Boychuk, L. & Badiou, P. (2010) 'Simulated environmental effects of wetland restoration scenarios in a typical Canadian prairie watershed', *Wetlands Ecology and Management*, 18(3), pp. 269–279.

Yang, Z., Yan, Y. & Liu, Q. (2012) 'Assessment of the flow regime alterations in the Lower Yellow River, China', *Ecological Informatics*, 10pp. 56–64.

Yasarer, L.M.W., Taylor, J.M., Rigby, J.R. & Locke, M.A. (2020) 'Trends in Land Use, Irrigation, and Streamflow Alteration in the Mississippi River Alluvial Plain', *Frontiers in Environmental Science*, 8.

Yoshida, S. (1979) 'A simple evapotranspiration model of a paddy field in tropical Asia', *Soil Science and Plant Nutrition*, 25(1), pp. 81–91.

Yue, S., Pilon, P., Phinney, B. & Cavadias, G. (2002) 'The influence of autocorrelation on the ability to detect trend in hydrological series', *Hydrological Processes*, 16(9), pp. 1807–1829.

Zeng, Q., Chen, H., Xu, C.-Y., Jie, M.-X., Chen, J., Guo, S.-L. & Liu, J. (2018) 'The effect of rain gauge density and distribution on runoff simulation using a lumped hydrological modelling approach', *Journal of Hydrology*, 563pp. 106–122.

Zhang, R. (2015) *Integrated modelling for evaluation of climate change impacts on agricultural dominated basin*. [Online]. University of Évora.

Zhang, R., Corte-Real, J., Moreira, M., Kilsby, C., Birkinshaw, S., Burton, A., Fowler, H.J., Forsythe, N., Nunes, J.P., Sampaio, E., dos Santos, F.L. & Mourato, S. (2019) 'Downscaling climate change of water availability, sediment yield and extreme events: Application to a Mediterranean climate basin', *International Journal of Climatology*, 39(6), pp. 2947–2963.

Zhou, X., Huang, X., Zhao, H. & Ma, K. (2020) 'Development of a revised method for indicators of hydrologic alteration for analyzing the cumulative impacts of cascading reservoirs on flow regime', *Hydrology and Earth System Sciences*, 24(8), pp. 4091–4107.

Zolfagharpour, F., Saghafian, B. & Delavar, M. (2022) 'Hydrological alteration and biodiversity change along the river network caused by anthropogenic activities and climate variability', *Ecological Processes*, 11(1), p. 19.

APPENDIX 1: SUPPLEMENTARY FIGURES

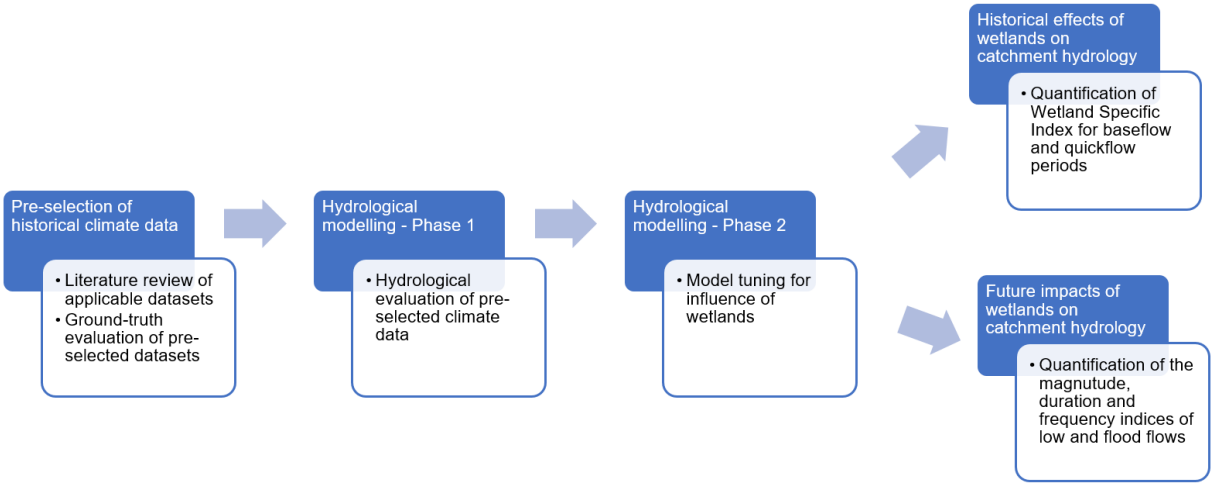

Figure 4 - 9: Schematisation of steps followed in the study.

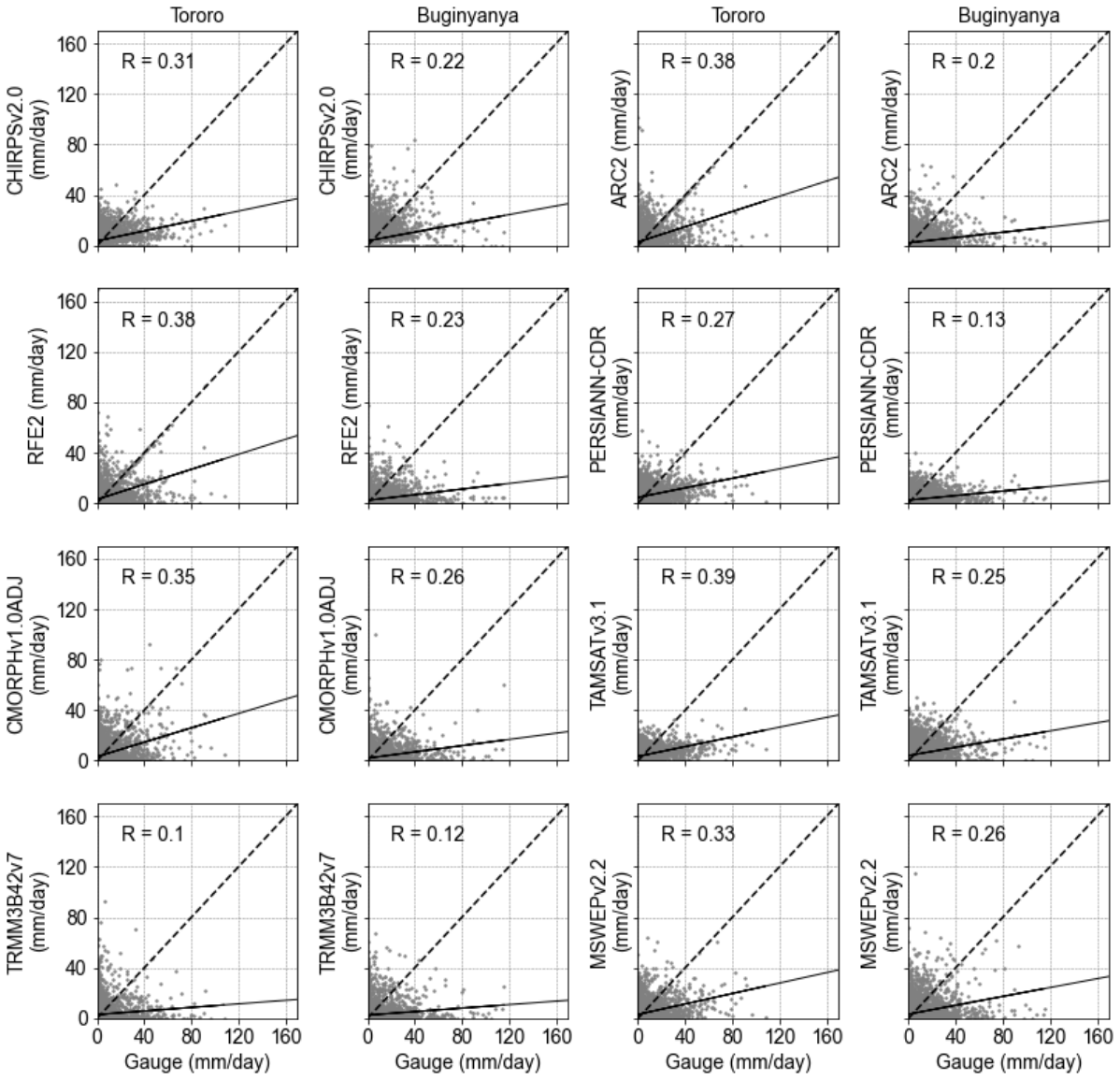

Figure 4 - 10: Scatter plots of daily rainfall total of SPPs and rain gauge data at Tororo (columns 1 and 3) and Buginyanya (columns 2 and 4). The dashed line shows the perfect fit that could be attained if the gauge and SPP data were equal.

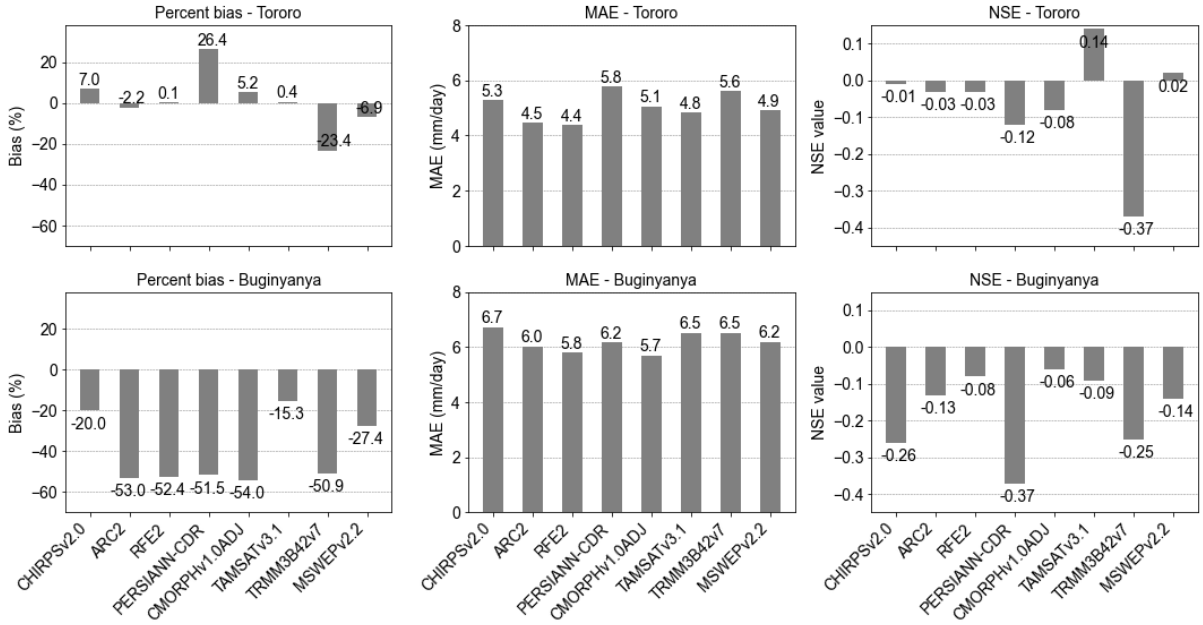

Figure 4 - 11: Bar graphs of percent bias (column 1), mean absolute error (column 2), and Nash-Sutcliffe efficiency (column 3) at daily timescale for the various SPPs at Tororo and Buginyanya.

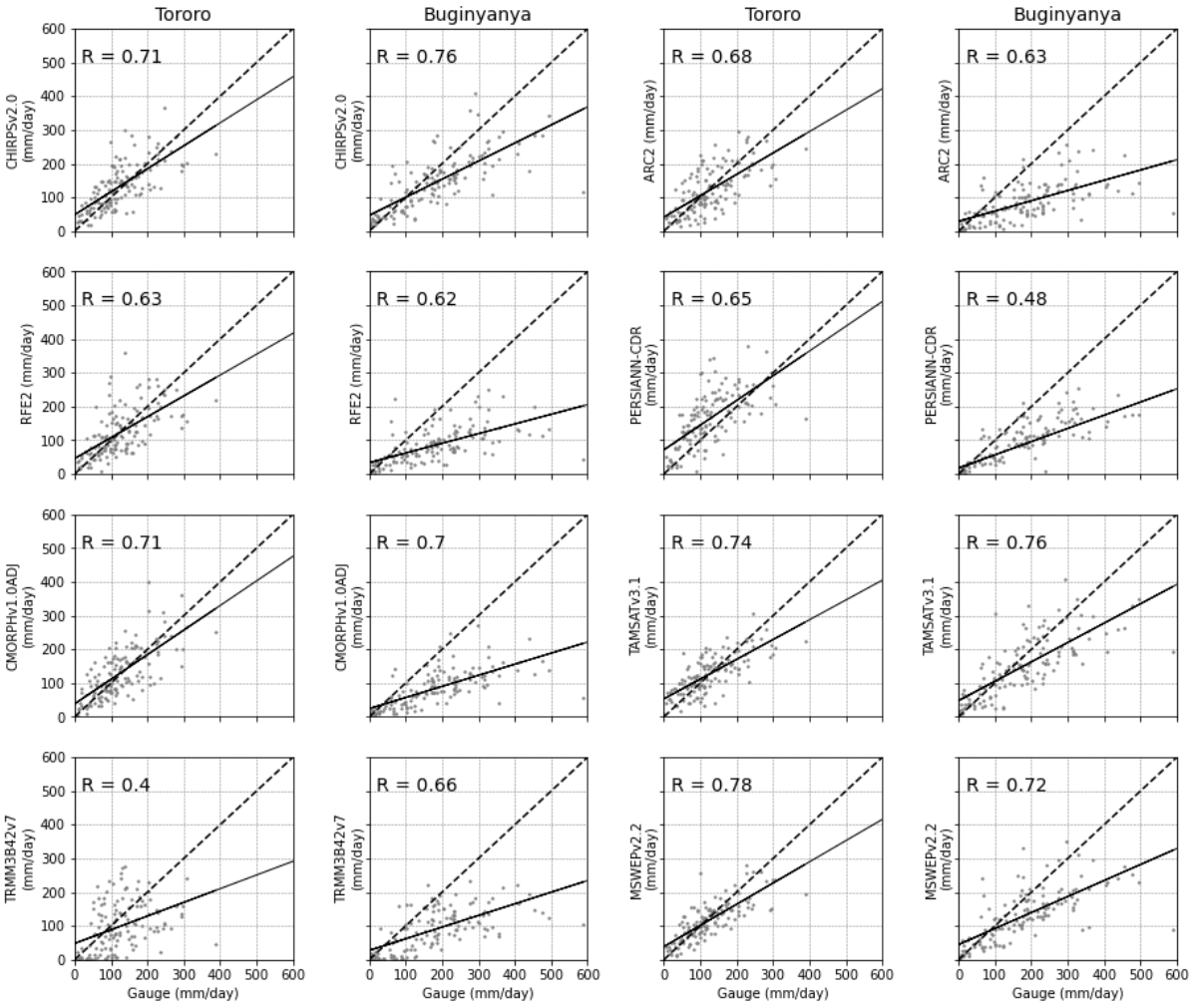

Figure 4 - 12: Scatter plots of monthly rainfall totals (satellite products against gauge) at Tororo (columns 1 and 3) and Buginyanya (columns 2 and 4). The dashed line shows the perfect fit that could be attained if the gauge and SPP data were equal.

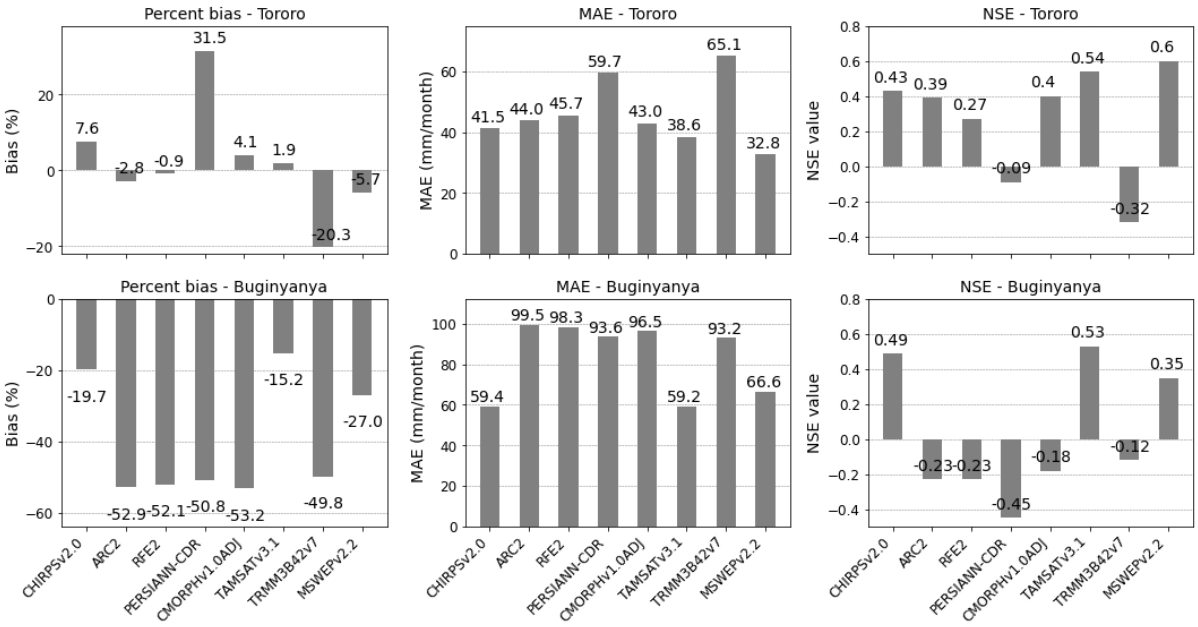

Figure 4 - 13: Bar graphs of percent bias (column 1), mean absolute error (column 2), and Nash-Sutcliffe efficiency (column 3) at monthly timescale for the various SPPs at Tororo and Buginyanya.

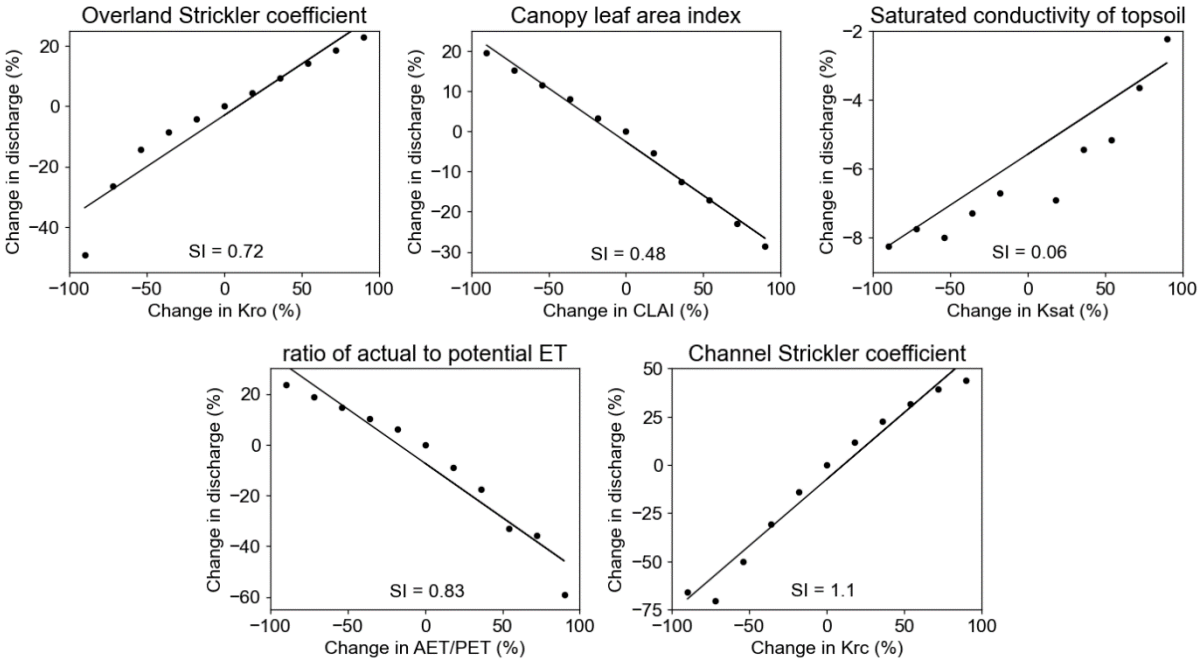

Figure 4 - 14: Scatter plots of model response to changes in key parameters. Inset is the sensitivity index (SI).

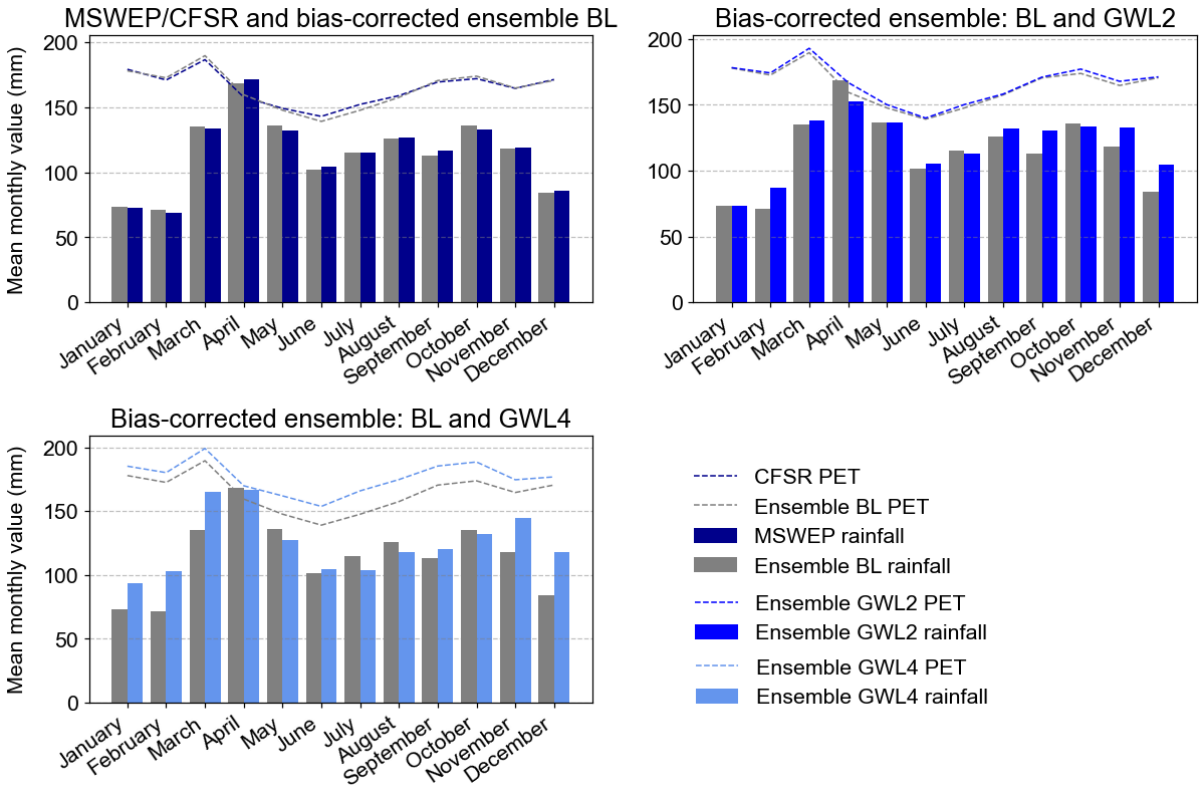

Figure 4 - 15: 30-year ensemble mean of 'observed' (MSWEP and CFSR) and bias-corrected CMIP6 models over the Mpologoma catchment. The plots show mean monthly rainfall and potential evapotranspiration (PET) at baseline (BL, top left), global warming level 2 (GWL2, top right), and global warming level 4 (GWL2, bottom left).

APPENDIX 2: SUPPLEMENTARY TABLES

Table 4 - 6: Key satellite-based precipitation products (SPPs) often applied over Africa.

S. No.	SPP	Description	Resolution (km)	Reference
1	TAMSATv3.1	Tropical Applications of Meteorology using SATellite (TAMSAT) and ground-based observations version 3.1; developed by the University of Reading, UK.	4	Maidment et al. (2017)
2	CHIRPSv2.0	Rainfall Estimates from Rain Gauge and Satellite Observations version 2.0; developed by the U.S. Geological Survey Earth Resources Observation and Science Centre, in collaboration with Santa Barbara Climate Hazards Group of the University of California.	6	Funk et al. (2015)
3	ARC2	Africa Rainfall Climatology (ARC) version 2.0; developed by NOAA Climate Prediction Centre.	11	Novella and Thiaw (2013)
4	RFE2	African Rainfall Estimation Algorithm (RFE) version 2.0; developed by NOAA Climate Prediction Centre.	11	NOAA-CPC (2001); Xie and Arkin (1996)
5	MSWEPv2.2	Multi-Source Weighted-Ensemble Precipitation (MSWEP) version 2.2.	11	Beck et al. (2019)
6	PERSIANN-CDR	Precipitation Estimation from Remotely Sensed Information using Artificial Neural Networks (PERSIANN-CDR); developed by UCI Centre for Hydrometeorology & Remote Sensing.	28	Ashouri et al. (2015)

S. No.	SPP	Description	Resolution (km)	Reference
7	CMORPHv1.0ADJ	Climate Prediction Centre (CPC) morphing technique (CMORPH) bias corrected with gauge data (ADJ) version 1.0; developed by NOAA Climate Prediction Centre.	8	Xie et al. (2018)
8	TRMM 3B42v7	Tropical Rainfall Measuring Mission (TRMM) Multi-satellite Precipitation Analysis (TMPA) version 7; developed by NASA and Japan's National Space Development Agency.	28	Huffman et al. (2011)

Table 4 - 7: FAR, POD, FB and HSS at Tororo and Buginyanya rain gauge stations over January 2001 and December 2016.

Statistical measure	Satellite Precipitation Product							
	CHIRPSv2.0	ARC2	RFE2	PERSIANN-CDR	CMORPHv1.0ADJ	TAMSATv3.1	TRMM3B42v7	MSWEPv2.2
Tororo (1,183 m above sea level)								
FAR (%)	44.76	37.76	41.82	52.93	43.49	47.68	53.71	48.35
POD (%)	73.3	70.11	79.89	92.2	77.69	86.81	49.4	78.9
FB	1.33	1.13	1.37	1.96	1.37	1.66	1.07	1.53
HSS	0.35	0.43	0.41	0.21	0.33	0.35	0.11	0.23
Buginyanya (1,889 m above sea level)								
FAR (%)	32.59	33.12	34.85	37.85	30.88	34.49	38.29	33.66
POD (%)	48.21	48.81	68.02	78.51	63.19	66.72	49.46	72.98

Statistical measure	Satellite Precipitation Product							
	CHIRPSv2.0	ARC2	RFE2	PERSIANN-CDR	CMORPHv1.0ADJ	TAMSATv3.1	TRMM3B42v7	MSWEPv2.2
FB	0.72	0.73	1.04	1.26	0.91	1.02	0.8	1.1
HSS	0.29	0.28	0.37	0.37	0.28	0.36	0.21	0.3

Table 4 - 8: List of best-performing CMIP6 GCM models over the Uganda region. The list is based on the findings of Ayugi, Zhihong, et al. (2021) and Ngoma et al. (2021).

S. No.	GCM Model	Institution	Resolution (km) for ensemble members r1i1p1f1
1	CanESM5	Canadian Centre for Climate Modelling and Analysis, Environment and Climate Change Canada, Victoria, Canada.	500
2	CESM2-WACCM	National Centre for Atmospheric Research, USA.	100
3	CNRM-CM6-1	Centre National de Recherches Météorologiques (CNRM); Centre Européen de Recherches et de Formation Avancéeen Calcul Scientifique, France.	157
4	GFDL-ESM4	Geophysical Fluid Dynamics Laboratory (GFDL), USA.	100
5	MPI-ESM1-2-LR	Max Planck Institute for Meteorology, Germany.	250

S. No.	GCM Model	Institution	Resolution (km) for ensemble members r1i1p1f1
6	MRI-ESM2-0	Meteorological Research Institute, Japan.	100
7	NorESM2-LM	Norwegian Climate Centre, Norway.	250
8	NorESM2-MM	Norwegian Climate Centre, Norway.	100
9	UKESM1-0-LL	UK Met Office Hadley Centre, UK.	209 × 139

Table 6 - 7: IHA-RVA analysis over 30 years showing the degrees of climate- and irrigation-induced alterations with no irrigation in the baseline. Results are based on an ensemble average.

IHA metric	The median annual value of the IHA metric					Degree of alteration, D (%)					
	Baseline, BL (no irrigation)	Climate-induced		Climate- and irrigation-induced		Climate-induced		Climate- and irrigation-induced		Irrigation-induced	
		GWL2	GWL4	GWL2	GWL4	GWL2	GWL4	GWL2	GWL4	GWL2	GWL4
Group 1: Magnitude of monthly water conditions											
March	0.973	0.961	1.509	2.374	2.525	-37.5	-50	-93.8	-93.8	-56.3	-43.8
April	1.151	1.016	1.846	1.819	2.048	-50	-43.8	-50	-75	0	-31.3
May	1.94	1.679	2.907	1.701	2.517	-12.5	12.5	25	31.3	37.5	18.8
June	2.891	2.617	2.944	2.425	2.526	-25	-6.3	-18.8	-6.3	6.3	0
July	2.199	2.696	2.177	2.352	1.878	-37.5	-37.5	-31.3	-37.5	6.3	0
August	1.703	2.15	1.37	2.884	2.427	0	-25	-50	0	-50	25
September	1.665	1.81	1.267	2.188	1.729	-6.3	-37.5	-43.8	6.3	-37.5	43.8
October	1.501	1.793	1.378	1.821	1.44	-12.5	-18.8	-25	-18.8	-12.5	0
November	1.935	1.942	1.641	2.048	1.587	-37.5	-31.3	-43.8	-37.5	-6.3	-6.3
December	2.079	3.923	2.404	3.328	2.3	-81.3	-56.3	-87.5	-37.5	-6.3	18.8

IHA metric	The median annual value of the IHA metric					Degree of alteration, D (%)					
	Baseline, BL (no irrigation)	Climate-induced		Climate- and irrigation-induced		Climate-induced		Climate- and irrigation-induced		Irrigation-induced	
		GWL2	GWL4	GWL2	GWL4	GWL2	GWL4	GWL2	GWL4	GWL2	GWL4
January	1.372	3.089	1.926	2.377	1.658	-68.8	-31.3	-68.8	-31.3	0	0
February	0.961	1.535	1.673	1.272	1.394	-43.8	-56.3	-6.3	-37.5	37.5	18.8
Group 1 overall degree of alteration, D_o (%)						**41.8**	**37.3**	**52.1**	**43.2**	**29.1**	**23.3**
Group 2: Magnitude and duration of annual extreme water conditions											
1-day minimum	0.743	0.812	0.82	0.889	0.835	-37.5	-31.3	-75	-50	-37.5	-18.8
3-day minimum	0.759	0.816	0.824	0.9	0.844	-37.5	-25	-68.8	-50	-31.3	-25
7-day minimum	0.773	0.823	0.835	0.942	0.882	-37.5	-31.3	-68.8	-56.3	-31.3	-25
30-day minimum	1.16	0.851	0.899	1.133	1.003	-62.5	-50	-6.3	-31.3	56.3	18.8
90-day minimum	1.416	1.188	1.096	1.51	1.291	-68.8	-50	-50	-56.3	18.8	-6.3
1-day maximum	5.213	5.303	5.12	4.759	4.573	-68.8	-56.3	-56.3	-50	12.5	6.3
3-day maximum	4.964	5.3	5.115	4.75	4.564	-37.5	-25	-6.3	-6.3	31.3	18.8
7-day maximum	4.753	5.28	5.098	4.709	4.544	-37.5	-25	-6.3	-6.3	31.3	18.8
30-day maximum	3.591	5.037	4.713	4.275	4.024	-50	-50	-12.5	-25	37.5	25
90-day maximum	2.899	4.132	3.914	3.521	3.282	-68.8	-56.3	-37.5	-31.3	31.3	25
Base flow index	0.413	0.371	0.44	0.358	0.396	-12.5	-31.3	-37.5	6.3	-25	37.5
Group 2 overall degree of alteration, D_o (%)						**48.1**	**39.4**	**44.6**	**37.1**	**31.6**	**21.2**
Group 3: Timing of annual extreme water conditions											
Date of minimum	66	76	52	58	44	25	-12.5	37.5	-25	12.5	-12.5
Date of maximum	37	326	157	345	87	-12.5	43.8	18.8	50	31.3	6.3
Group 3 overall degree of alteration, D_o (%)						**19.8**	**32.2**	**29.6**	**39.5**	**23.8**	**9.9**
Group 4: Frequency and duration of high and low pulses											
Low pulse count	17	1	2	2	1	-100	-100	-100	-100	0	0
Low pulse duration	3	76	40	12	32	-88	-84	-92	-88	-4	-4
High pulse count	18	1	2	2	3	-100	-100	-100	-100	0	0

IHA metric	The median annual value of the IHA metric					Degree of alteration, D (%)					
	Baseline, BL (no irrigation)	Climate-induced		Climate- and irrigation-induced		Climate-induced		Climate- and irrigation-induced		Irrigation-induced	
		GWL2	GWL4	GWL2	GWL4	GWL2	GWL4	GWL2	GWL4	GWL2	GWL4
High pulse duration	2	84	72	45	35	-100	-100	-100	-87	0	13.3
Group 4 overall degree of alteration, D_o (%)						**97.1**	**96.2**	**98.1**	**93.9**	**2**	**7**
Group 5: Rate and frequency of water condition changes											
Rise rate	0.057	0.027	0.029	0.04	0.033	-56.3	-81.3	-37.5	-75	18.8	6.3
Fall rate	-0.043	-0.023	-0.021	-0.035	-0.028	-62.5	-68.8	-18.8	-37.5	43.8	31.3
Number of reversals	88	36	38	46	50	-100	-94.4	-94.4	-94.4	5.6	0
Group 5 overall degree of alteration, D_o (%)						**75.4**	**82.2**	**59.7**	**72.9**	**27.7**	**18.4**
The overall degree of alteration of all metrics, D_{on} (%)						**56.2**	**53.6**	**57**	**53.2**	**27.9**	**20.1**

Table 6 - 8: IHA-RVA analysis over 30 years showing the degrees of climate- and irrigation-induced alterations with irrigation in the baseline. Results are based on an ensemble average.

IHA metric	The median value of the IHA metric					Degree of alteration, D (%)					
	Baseline, BL (with irrigation)	Climate-induced		Climate- and irrigation-induced		Climate-induced		Climate- and irrigation-induced		Irrigation-induced	
		GWL2	GWL4	GWL2	GWL4	GWL2	GWL4	GWL2	GWL4	GWL2	GWL4
Group 1: Magnitude of monthly water conditions											
March	1.85	0.961	1.509	2.374	2.525	-87.5	-68.8	-50	-62.5	37.5	6.3
April	1.391	1.016	1.846	1.819	2.048	-81.3	-56.3	-68.8	-68.8	12.5	-12.5
May	1.908	1.679	2.907	1.701	2.517	-12.5	0	12.5	25	25	25
June	2.638	2.617	2.944	2.425	2.526	-43.8	-31.3	-18.8	-18.8	25.0	12.5
July	2.036	2.696	2.177	2.352	1.878	-37.5	-50	-37.5	-31.3	0	18.8
August	2.711	2.15	1.37	2.884	2.427	-18.8	-50	-12.5	0	6.3	50
September	1.859	1.81	1.267	2.188	1.729	-6.3	-62.5	-31.3	-18.8	-25.0	43.8

IHA metric	The median value of the IHA metric					Degree of alteration, D (%)					
	Baseline, BL (with irrigation)	Climate-induced		Climate- and irrigation-induced		Climate-induced		Climate- and irrigation-induced		Irrigation-induced	
		GWL2	GWL4	GWL2	GWL4	GWL2	GWL4	GWL2	GWL4	GWL2	GWL4
October	1.548	1.793	1.378	1.821	1.44	-31.3	-25	-25	-18.8	6.3	6.3
November	1.798	1.942	1.641	2.048	1.587	-31.3	-37.5	-31.3	-37.5	0	0
December	1.773	3.923	2.404	3.328	2.3	-75	-56.3	-87.5	-62.5	-12.5	-6.3
January	1.23	3.089	1.926	2.377	1.658	-93.8	-50	-75	-43.8	18.8	6.3
February	0.863	1.535	1.673	1.272	1.394	-68.8	-43.8	-31.3	-56.3	37.5	-12.5
Group 1 overall degree of alteration, D_o (%)						**57.2**	**47.8**	**46.7**	**42.5**	**21.3**	**22.4**
Group 2: Magnitude and duration of annual extreme water conditions											
1-day minimum	0.706	0.812	0.82	0.889	0.835	-43.8	-56.3	-93.8	-43.8	-50	12.5
3-day minimum	0.746	0.816	0.824	0.9	0.844	-25	-25	-68.8	-43.8	-43.8	-18.8
7-day minimum	0.768	0.823	0.835	0.942	0.882	-25	-18.8	-68.8	-50	-43.8	-31.3
30-day minimum	1.205	0.851	0.899	1.133	1.003	-75	-56.3	-31.3	-37.5	43.8	18.8
90-day minimum	1.463	1.188	1.096	1.51	1.291	-75	-50	-50	-43.8	25	6.3
1-day maximum	4.236	5.303	5.12	4.759	4.573	-75	-68.8	-68.8	-62.5	6.3	6.3
3-day maximum	4.066	5.3	5.115	4.75	4.564	-62.5	-75	-56.3	-37.5	6.3	37.5
7-day maximum	3.907	5.28	5.098	4.709	4.544	-62.5	-68.8	-56.3	-37.5	6.3	31.3
30-day maximum	3.203	5.037	4.713	4.275	4.024	-75	-75	-62.5	-50	12.5	25
90-day maximum	2.628	4.132	3.914	3.521	3.282	-68.8	-68.8	-62.5	-50	6.3	18.8
Base flow index	0.405	0.371	0.44	0.358	0.396	-18.8	-37.5	-50	-18.8	-31.3	18.8
Group 2 overall degree of alteration, D_o (%)						**56.7**	**55.3**	**59.9**	**42.5**	**29.1**	**21.7**
Group 3: Timing of annual extreme water conditions											
Date of minimum	54	76	52	58	44	81	0	43.8	-25	-37.5	-25
Date of maximum	37	326	157	345	87	-13	44	12.5	50	25	6.3
Group 3 overall degree of alteration, D_o (%)						**58.1**	**30.9**	**32.2**	**39.5**	**31.9**	**18.2**
Group 4: Frequency and duration of high and low pulses											
Low pulse count	22	1	1	2	2	-100	-100	-100	-100	0	0
Low pulse duration	2	69	60	24	25	-100	-100	-95.8	-100	4.2	0

IHA metric	The median value of the IHA metric					Degree of alteration, D (%)					
	Baseline, BL (with irrigation)	Climate-induced		Climate- and irrigation-induced		Climate-induced		Climate- and irrigation-induced		Irrigation-induced	
		GWL2	GWL4	GWL2	GWL4	GWL2	GWL4	GWL2	GWL4	GWL2	GWL4
High pulse count	15	1	2	2	3	-100	-100	-100	-100	0	0
High pulse duration	2	84	72	45	35	-100	-100	-100	-90.9	0	9.1
Group 4 overall degree of alteration, D_o (%)						**100.0**	**100.0**	**99.0**	**97.8**	**2.1**	**4.5**
Group 5: Rate and frequency of water condition changes											
Rise rate	0.098	0.027	0.029	0.04	0.033	-100	-100	-93.8	-87.5	6.3	12.5
Fall rate	-0.044	-0.023	-0.021	-0.035	-0.028	-62.5	-81.3	-43.8	-75	18.8	6.3
Number of reversals	115	36	38	46	50	-100	-100	-100	-100	0	0
Group 5 overall degree of alteration, D_o (%)						**89.3**	**94.2**	**83.1**	**88.1**	**11.4**	**8.1**
The overall degree of alteration of all metrics, D_{on} (%)						**67.1**	**63.4**	**63**	**57.2**	**23.4**	**19.5**

Table 7 - 1: How wetlands achieve select SDGs (Adapted from Ramsar Convention Secretariat (2018)).

SDG No.	Name of SDG	Example of how SDG is achieved
1	No poverty	One of the aims for achieving this goal is to help the poor and vulnerable become more resilient. In this regard, wetlands play a crucial role by providing a safe and dependable water source for cattle, agriculture, and human consumption, especially during dry periods. As an illustration, the Waza floodplain restoration project in Cameroon, a Ramsar Site, contributed to the restoration of the flooding regime, thus enhancing grazing, fishing, and agricultural productivity to the tune of USD 2.3 million per year (Russi et al., 2013).

SDG No.	Name of SDG	Example of how SDG is achieved
2	Zero hunger	Human food production relies on nature and its resources, such as water for irrigation and fish ponds from natural wetlands. Further, wetlands are crucial for many people worldwide as a source of protein. For instance, populations in Cambodia acquire 60 - 80% of their animal protein from fish from the Tonle Sap Lake and its accompanying floodplains (Millennium Ecosystem Assessment, 2005b).
5	Gender equality	In the developing world, such as rural Africa, where the largest area of wetlands of international importance exists (T. Xu et al., 2019), access to and control over natural resources are gender-based. This affects users' rights and information transfer on wetland conservation and management. Thus, paying attention to how women and men exploit and manage wetlands may enhance effective and efficient protection, sustainable use and equitable access to the benefits of protected areas.
6	Clean water and sanitation	As natural filters, wetland vegetation traps nutrients, pollutants, and sediments, thus purifying and improving water quality. For example, Nakivubo wetlands in Uganda act as a natural filter preventing pollution from reaching Lake Victoria, a critical source of drinking water for Kampala, a city of 1.5 million inhabitants (Kaggwa et al., 2009). The purification potential of Navikubo wetlands is valued at USD 1.3 million per year.
8	Decent work and economic growth	Historically, economic growth was mainly linked to the level of exploitation of natural resources. However, in recent times, ideas like the "green economy", "green growth", and "natural capital", among others, are established in economic growth models that conserve and exploit natural resources sustainably. Globally, wetlands are known to sustain 266 million jobs in wetland tourism and travel (WTTC, 2014). Additionally, there is the possibility for a sizable amount of this tourism to be centred on ecotourism through visitor fees and ecotourism-related income, giving local populations much-needed income.
9	Industry, innovation and infrastructure	Infrastructure needs better protection from extremes and increasing climate uncertainty, such as floods. As a nature-based solution, wetlands can provide efficient, cost-effective mitigation and adaptation to these escalating hazards. For example, South Africa’s “Working for Wetlands” programme aims to restore degraded wetlands to enhance the country’s water supply, flood control and employment for those in need.

SDG No.	Name of SDG	Example of how SDG is achieved
11	Sustainable cities and communities	With nearly 50% of major cities located within 50 kilometres of the coast, populations in coastal areas are about 2.6 times larger than in inland areas. This poses significant flood hazards. Wetlands prevent floods in coastal and inland towns and cities by acting as retention basins. For example, the IPCC identified Alexandria, situated in the low-lying Nile Delta in Egypt and home to over 4 million people, at high risk of climate-induced sea level rise. As a result, the Nile Delta's integrated coastal zone management, which includes wetland protection and restoration, is receiving more attention.
13	Climate action	A comprehensive and multi-pronged strategic approach is necessary to combat climate change. Well-managed and restored wetlands minimise the impacts of climate-induced floods and effectively store carbon that would exacerbate climate change through increased greenhouse gas emissions. Peatlands (such as papyrus-dominated wetlands) account for only 3% of the earth's surface but hold twice as much carbon as the world's forests (Joosten et al., 2016).
14	Life below water	About half of the world's population depends on marine resources as their primary source of protein. Thus, there is a need to minimise the pollution of water resources. In this regard, coastal and inland wetlands protect water resources. Further, wetlands provide spawning areas for fisheries and upstream migratory pathways in rivers.
15	Life on land	Wetland ecosystems and freshwaters are habitats for numerous biodiversity, representing 9.5% of the animal species, which is a disproportionately high number given that freshwaters cover about 0.01% of the earth's surface.

APPENDIX 3: SUPPLEMENTARY EQUATIONS

Equations for calculation of FAR, POD, FB and HSS.

$$FAR = \frac{B}{A+B} \times 100$$

Equation 4 - 2

$$POD = \frac{A}{A+C} \times 100$$

Equation 4 - 3

$$FB = \frac{A+B}{A+C}$$

Equation 4 - 4

$$HSS = \frac{2(AD - BC)}{(A+C)(C+D) + (A+B)(B+D)}$$

Equation 4 - 5

where A, B, C and D represent hits ("event forecast to occur, and did occur"), false alarms ("event forecast to occur, but did not occur"), misses ("event forecast not to occur, but did occur") and correct negatives ("event forecast not to occur, and did not occur"), respectively (WWRP/WGNE, 2009).

APPENDIX 4: EVALUATION OF SATELLITE PRECIPITATION PRODUCTS (SPPs) WITH GAUGE DATA

Quality control of rain gauge data

Basalirwa (1991, 1995) delineated Uganda into 14 climatological rainfall zones using monthly rainfall records from 102-gauge stations from 1940 to 1975. Mpologoma catchment lies primarily within zones D and F (Figure 4 - 16). Daily rainfall records for stations at Kiige (zone D), Jinja (at the boundary of zones B and A2), Tororo (zone D), and Buginyanya (zone F) were acquired from the Uganda National Meteorological Authority. The gauge datasets were quality-controlled, following the approach of Maidment et al. (2013). Firstly, verification of gauge locations and manual checks for suspicious records were carried out. This was followed by the identification of repeated entries and a double mass curve comparative test (Figure 4 - 17). The double mass curve compares data from a single station with a pattern created from several other stations in the area (Langbein et al., 1960). This is carried out by plotting the cumulative data of a station versus the cumulative data of the mean of all stations in the area. A straight line is attained if the relationship between the variables is a fixed ratio. Any nonlinearity is associated with changes in the relation between the variables. In the case of rain gauge data, these changes may be caused by instrument relocation, change in equipment type, etc. A break in linearity appears to occur between the 4^{th} and 5^{th} scatter points of the plot for Buginyanya station (i.e., the years 2005 and 2007, Table 4 - 9). However, the F-test shows that the break is insignificant, with a p-value of 0.14 at the 0.05 significance level.

Zeng et al. (2018) analysed the impacts of rain gauge density and distribution on hydrological modelling uncertainty of different catchment sizes. Their results show that imperfect precipitation inputs measured by sparse and irregular rain gauge networks lead to substantial uncertainty in model parameter estimation and flow simulation. Further, sparse gauge networks generally affect the quality of gauge-corrected SPPs (Gumindoga et al., 2019). Thus, for this study, the rain gauges were not used to drive hydrological models but to evaluate SPPs. The gauges used were restricted to those within the climatic zones of the Mpologoma catchment (Zones D and F) and no more than 100 km from the boundary of the catchment.

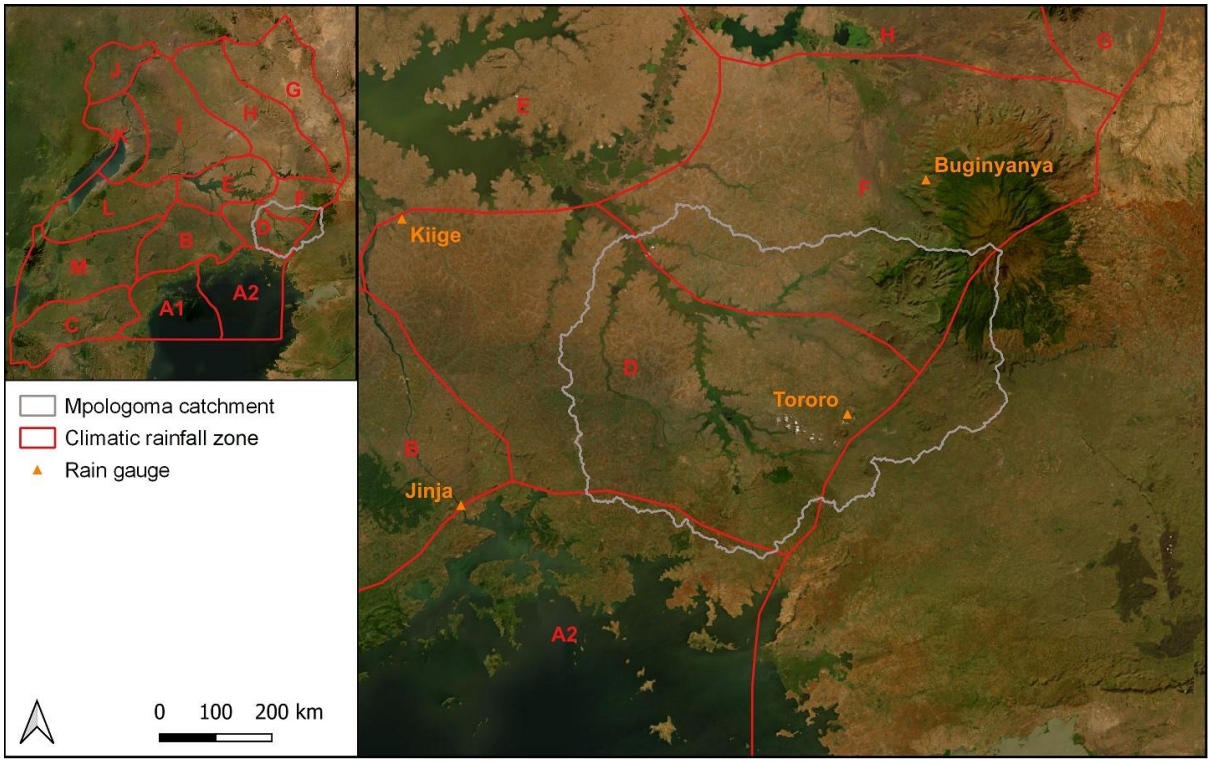

Figure 4 - 16: Climatic rainfall zones in Uganda as defined by Basalirwa (1995, 1991), including locations of rain gauges in and at the vicinity of the Mpologoma catchment.

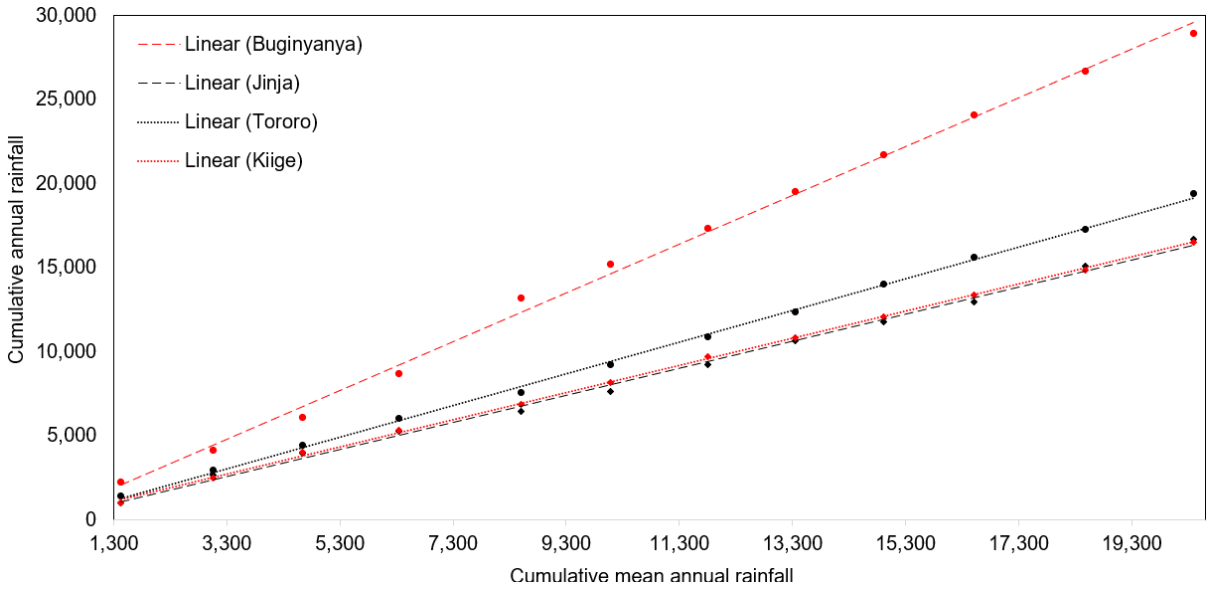

Figure 4 - 17: Double-mass curve of rain gauge data at Buginyanya, Jinja, Tororo and Kiige.

Table 4 - 9: Rain gauge annual precipitation for the double mass curve. The analysis is restricted to years with no missing data.

Year	Annual precipiatation (mm)					Cummmulative annual precipiatation (mm)				
	Kiige	Jinja	Tororo	Buginyanya	Mean	Kiige	Jinja	Tororo	Buginyanya	Mean
2000	996.9	1029.7	1420.1	2265.9	1428.2	996.9	1029.7	1420.1	2265.9	1428.2
2001	1496.1	1650.2	1516.9	1884.1	1636.8	2493.0	2679.9	2937.0	4150.0	3065.0
2003	1559.6	1304.7	1501.7	1945.7	1577.9	4052.6	3984.6	4438.7	6095.7	4642.9
2005	1296.3	1264.1	1616.7	2594.2	1692.8	5348.9	5248.7	6055.4	8689.9	6335.7
2007	1490.3	1178.3	1508.6	4514.0	2172.8	6839.2	6427.0	7564.0	13203.9	8508.5
2010	1344.0	1227.0	1678.1	2016.5	1566.4	8183.2	7654.0	9242.1	15220.4	10074.9
2011	1542.9	1588.8	1639.3	2136.2	1726.8	9726.1	9242.8	10881.4	17356.6	11801.7
2014	1120.0	1416.6	1499.2	2139.5	1543.8	10846.1	10659.4	12380.6	19496.1	13345.5
2017	1227.9	1134.3	1649.8	2235.2	1561.8	12074.0	11793.7	14030.4	21731.3	14907.3
2018	1295.3	1168.4	1573.2	2368.0	1601.2	13369.3	12962.1	15603.6	24099.2	16508.6
2019	1507.4	2129.5	1683.9	2554.1	1968.7	14876.7	15091.6	17287.5	26653.4	18477.3
2020	1659.4	1602.3	2138.6	2258.2	1914.6	16536.1	16693.9	19426.1	28911.6	20391.9

Accuracy of SPPs in Daily Rainfall Identification

The statistics of daily rainfall identification for each SPP and rain gauge location are summarised in Table 4 - 7 in APPENDIX 2. Overall, Probability of Detection (POD) statistics show that SPPs perform better in detecting rain at low altitudes (Tororo) than at high altitudes (Buginyanya). This is because rain detection by satellites is heavily dependent on the presence of ice at cloud tops (Asadullah et al., 2008), which both infrared and passive microwave algorithms weakly detect in the relatively warm orographic rains that dominate mountainous regions (Dinku et al., 2007). This weakness in rain detection could explain the relatively lower False Alarm Ratio (FAR) at a high altitude. Similar to findings by Diem et al. (2014) for a study in the north-western region of Uganda, high POD and Frequency Bias (FB) are generally linked with larger FAR. In general, though all assessed products utilise gauge data for calibration, those that ingest gauge data at longer timescales (e.g., TRMM and PERSIANN-CDR at monthly scale) performed worst.

Accuracy of SPPs in Capturing Daily and Monthly Rainfall Totals

Most satellite precipitation products performed weakly in capturing daily rain totals, with correlation coefficient (R) and Nash-Sutcliffe efficiency (NSE) varying from 0.1 to 0.39 (Figure 4 - 10, APPENDIX 1) and -0.37 to 0.14 (Figure 4 - 11, APPENDIX 1), respectively. However, significant improvement was attained on aggregation to monthly totals (Figure 4 - 12 and Figure 4 - 13, respectively, in APPENDIX 1), with MSWEP, TAMSAT, and CHIRPS performing best. Their monthly R and NSE vary from 0.71 to 0.78 and 0.35 to 0.6, respectively.

SPPs have inherent detection, systematic, and random errors (AghaKouchak et al., 2012; Maggioni & Massari, 2018). However, systematic errors increase slightly for aggregation windows greater than 15 days, while random errors have a negligible effect upon aggregation (Bhatti et al., 2016). Some of the studies over Africa that have reported improvement of SPPs on aggregation include Bhatti et al. (2016), Dembélé & Zwart (2016), Dinku et al. (2018) and Gebrechorkos et al. (2018).

Satellite precipitation estimates are derived from geostationary and polar-orbiting (or low earth orbit) satellite observations (Asadullah et al., 2008; Romilly & Gebremichael, 2011). A critical difference between the two satellite systems lies in their retrieval mechanisms. The relatively stationary (relative to Earth) geostationary satellites

employ thermal infrared (TIR) channels to detect cloud-top temperatures; meanwhile, polar-orbiting satellites use passive microwave (PMW) channels to monitor the scattering of naturally emitted (passive) microwaves within clouds (Asadullah et al., 2008; Romilly & Gebremichael, 2011). An optimum cold cloud threshold temperature, distinguishing rain from non-rain clouds, is established for TIR-derived data (Tucker & Sear, 2001). A simple linear regression is then applied to relate cloud-top temperature and 'cold cloud duration' (CCD) to rain rate. Key strengths of geostationary satellites include their wide coverage (Tucker & Sear, 2001), high-resolution and continuous temporal coverage (hourly or less) (Thiemig et al., 2013), and the ability to discriminate between rain and no rain days, including identification of days with rain below or above relatively small thresholds (Tucker & Sear, 2001). A fundamental weakness is estimating rainfall amounts (Tucker & Sear, 2001) because the sensor signal does not penetrate clouds (Dembélé & Zwart, 2016). Further, given the empirical nature of the CCD method, its applicability beyond the validation period, which is often carried out with scarce gauge data, is questionable (Kummerow, 1998).

Due to the direct physical relationship between the sensor signal and rainfall rate, polar-orbiting satellites give better rainfall estimates than geostationary satellites (Thiemig et al., 2013). However, they pass over a given location only once or twice a day and have a coarser spatial resolution (Thiemig et al., 2013), leading to data gaps. Sensed brightness temperature, obtained from radiance scattered by cloud water and ice droplets, is theoretically related to rain rate (Kummerow, 1998). The theoretical relation depends on the assumption in describing cloud properties such as its horizontal and vertical structures and hydrometeor shapes and sizes. Further, PMW precipitation retrieval is primarily based on scattering by ice, which can result in rain underestimation due to less ice production in orographic systems (Dinku et al., 2007; Romilly & Gebremichael, 2011). On the other hand, overestimation can also occur in PMW retrievals in mountainous regions due to misinterpretation of very cold surfaces and ice over mountains as precipitation (Dinku et al., 2007).

In general, the above-average performance of TAMSAT and CHIRPS could be attributed to the assimilation of gauge datasets from local and regional meteorological authorities. Meanwhile, MSWEP's performance could be due to ingesting multiple datasets, including gauge and reanalysis products.

APPENDIX 5: MODEL SENSITIVITY ANALYSIS

Model sensitivity is usually assessed using local (e.g., the 'one parameter at a time' method) or global methods (e.g., GLUE (Beven & Binley, 2014, 1992)) (Borgonovo & Plischke, 2016). By estimating the local impact of a parameter, local techniques focus on the effects of changes in a particular parameter value (mean, default, or optimum value) on the model output. Thus, they are intrinsically deterministic and preclude assigning a probability distribution to the model inputs. This makes them useful when the state of knowledge does not allow the analyst to confidently assign distributions to the model inputs (Van Groenendaal & Kleijnen, 1997). Meanwhile, global techniques assign probability distributions to model inputs, thus enabling the whole parameter space analysis simultaneously. However, they require the assessment of model input distributions. The advantage of global sensitivity algorithms is that the effects of parameter variation are sampled over one or more centre points in parameter space rather than along a single dimension as in local methods. This facilitates decision-making under uncertainty.

Though unreliable for high-dimensional and non-linear models (Wagener & Kollat, 2007), local approaches are simple and computationally less expensive. Further, they have been applied in numerous hydrological modelling studies (Sreedevi & Eldho, 2019), including SHETRAN (Op de Hipt et al., 2017). Birkinshaw (2008a) gives a detailed description of SHETRAN parameters, including the applicable range. Some of these parameters are not very sensitive. For this study, the 'one parameter at a time' approach was employed in assessing the sensitivity of overland (Kro) and channel (Krc) Strickler coefficients (the Strickler coefficient is the inverse of Manning's coefficient), canopy leaf area index (CLAI), topsoil saturated conductivity (Ksat) and the ratio of actual to potential evapotranspiration at field capacity (AET/PET ratio). Each parameter was evaluated over the range of ±90% by plotting the change in catchment discharge against the change in parameter base value. The sensitivity index (SI) for each parameter was also calculated using Equation 4 - 6, where O_0 is catchment discharge at base value, and O_{90} and O_{-90} are catchment discharge at +90 and -90% change in base value.

$$SI_{90} = \frac{|O_{90} - O_{-90}|}{O_0}$$

Equation 4 - 6

This study's sensitivity analysis was carried out only for the Phase 1 model driven by MSWEP precipitation product.

Results of Model Sensitivity Analysis

Sensitivity indices for overland (Kro) and channel (Krc) Strickler coefficients, canopy leaf area index (CLAI), topsoil saturated conductivity (Ksat), and the ratio of actual to potential evapotranspiration at field capacity (AET/PET) are shown in Figure 4 - 14, APPENDIX 1. The most sensitive parameters, in descending order, are Krc, AET/PET and Kro, with SI values of 1.1, 0.83 and 0.72, respectively. Ksat was the least sensitive, with SI = 0.06. As expected, larger values of Kro, Krc and Ksat increase catchment outflow. On the contrary, increments in CLAI and AET/PET lower outflows. The sensitivity results are similar to findings by Mutenyo et al. (2013) for a SWAT model of the Manafwa sub-catchment in the Mpologoma catchment, in which parameters that control overland and channel flow, canopy cover, evapotranspiration, and flow in soil were found to be most sensitive.

APPENDIX 6: QUALITY CONTROL OF MEASURED FLOW DATA

Following Crochemore et al. (2020), measured flow data were quality controlled by analysing for data availability (i.e., the length and spatial distribution of time series) and quality checks for outliers, homogeneity, and trend. Data availability reflects the extent to which the stations were maintained for the duration under consideration. It was assessed in terms of overall and longest availability and continuity of data. The overall availability (proportion of total time series with data) was 92.77, 95.09 and 89.98% for stations 82212, 82217, and 82218, respectively. Longest availability (the most extended portion of the time series with no data gap) was at 15.75% (11/04/2008 to 14/12/2010), 36.25% (01/01/2000 to 28/02/2006), 35.73% (01/02/2004 to 27/02/2010), respectively. Similarly, the extent of data fragmentation indicated by data continuity (ratio of longest to overall availability) was at 17, 38 and 40%, respectively.

Outliers, an outcome of gross observational error or extraordinary single events, are time series values that deviate substantially from the pattern of variation shown by other elements (Naghettini, 2017). An event was considered a high or low flow outlier if it were larger than ($Q_3 + 1.5[Q_3 - Q_1]$) or smaller than ($Q_1 - 1.5[Q_3 - Q_1]$), respectively, where Q_1 and Q_3 are the first and third quartile. Further, an outlier was assumed to be an observational error if it were at least ten days from the nearest outlier. No outliers were detected in the low flow periods of all the stations. Meanwhile, one outlier (43.99 m^3/s on 08/11/2014) and twenty-three outliers were detected in the high flows of stations 82217 and 82212, respectively.

Inhomogeneity in flow data can be triggered by natural variability (e.g., flows generated by ordinary rainfall events in comparison to extraordinary circumstances), anthropogenic shifts (through damming and flow diversion), or changes in observational routines (e.g., gauge relocation, and changes in rating curves and observational devices) (Naghettini, 2017; Crochemore et al., 2020). All the years, except one in Station 82212, had data gaps. Thus, the homogeneity test was carried out on a monthly timescale for all stations. Table 4 - 10 shows the months at each station with complete daily flow records. Four test methods were applied, including the standard normal homogeneity test (Alexandersson, 1986), the Buishand range test (Buishand, 1982), the Pettitt test (Pettitt, 1979), and the rank version of the von Neumann ratio test (Neumann, 1941), with significance level set at 0.05. Following

Wijngaard et al. (2003), a series is considered homogeneous if one or none of the tests reject the null hypothesis and the possible presence of inhomogeneity if two tests reject the null hypothesis. Otherwise, it is inhomogeneous if three or all tests reject the null hypothesis. None of the tests rejected the null hypothesis at station 82212. For station 82218, the Pettitt test rejected the null hypothesis from February to December. Meanwhile, at station 82217, the standard (March to April and November to December) and Pettitt (February to December) tests rejected the null hypothesis.

Flow series trend reflects nonstationary due to long-term changes in essential statistical properties (Naghettini, 2017), which could be triggered by natural or anthropogenic changes in the catchment or gradual movement of the gauge location (Crochemore et al., 2020). The modified version of the Mann-Kendall nonparametric test (Kendall, 1975; Mann, 1945) proposed by Yue et al. (2002) was employed for trend analysis at the 0.05 significance level. The slope was estimated using the Theil-Sen slope estimator (Theil, 1950; Sen, 1968) for any detected trend. No trend was detected at station 82212. For station 82218, an increasing trend was detected in September and October. Similarly, for station 82217, increasing trends were detected in more than half of the months, except January, February, May, and December.

Table 4 - 10: Number of months at each station with complete daily flow records.

Month	Number of months with complete daily data		
	82212	82217	82218
January	16	15	15
February	15	16	15
March	11	16	15
April	11	16	16
May	12	16	13
June	12	16	16
July	14	15	15
August	12	14	14
September	14	16	15
October	12	14	14
November	14	14	15
December	14	16	15

APPENDIX 7: PROCESSING OF FUTURE PRECIPITATION PRODUCTS

Selection of suitable bias correction approach

In hydrology, climate change impacts are commonly assessed using climate variables from global and regional climate models (Teutschbein & Seibert, 2012; Pierce et al., 2015; Shrestha et al., 2017). Global climate models (GCMs) are mostly coarse in resolution, limiting their application in regional studies (Sørland et al., 2018). To gain high-resolution climate data and enhance the representation of small-scale features, including underlying physical processes, GCMs are often dynamically downscaled using regional climate models (RCMs) (Torma et al., 2015). However, they are simplifications of reality, and their outputs are biased (Räty et al., 2014). The biases are often systematic and emanate from weaknesses in conceptualization, discretization, and spatial averaging (Teutschbein & Seibert, 2012). Bias correction through simple mechanisms (e.g., delta change) to the more robust and effective quantile mapping approaches (Teutschbein & Seibert, 2012; Johnson & Sharma, 2011; Maraun et al., 2010) are often performed on climate model outputs before application in climate change impact studies. These mechanisms apply statistical transfer functions, established between historical model and observed data, to future model data (Maraun & Widmann, 2018).

Quantile mapping (QM) based methods are either parametric, non-parametric (Gudmundsson et al., 2012) or a combination of the two (Tani & Gobiet, 2019; Holthuijzen et al., 2022). In parametric QM, such as distribution mapping (DM), known distributions are employed to fit observed and model datasets (Holthuijzen et al., 2022). Some commonly used distributions include Bernoulli and Gamma for precipitation occurrence and intensity, respectively (Cannon 2008; Maraun and Widmann 2018), and Gaussian for temperature (Teutschbein & Seibert, 2012). Non-parametric QM, such as empirical quantile mapping (EQM), generally outperforms DM (Gudmundsson et al., 2012). Unlike DM, no prior distributional assumptions are made in the relatively flexible EQM (Gudmundsson et al., 2012; Holthuijzen et al., 2022), in which the aid of a quantile-quantile plot establishes a transfer function. Quantile-quantile plots are scatterplots of sorted values between empirical quantiles of modelled and observed data of the same timeframe (Cannon et al., 2015). EQM can

correct model mean, standard deviation, and higher-order distributional moments (Gudmundsson et al., 2012).

However, like all QM methods, EQM has drawbacks. Firstly, all QM methods assume stationarity, in which distributions defining the relation between the historical climate model output and observations remain unchanged in the future (Tong et al., 2021; Maraun, 2012). This can result in distortion of climate change signals (Hagemann et al., 2011), including extremes (Dosio, 2016), given that climate distributions tend to change with time, even on 30-year timescales (Maraun & Widmann, 2018). Secondly, EQM tends to overfit extremes on calibration data (Maraun & Widmann, 2018; Holthuijzen et al., 2022), yet extreme periods are often poorly represented due to few data points and increased variability (Holthuijzen et al., 2022). This usually leads to instability of transfer functions at extremes, such as exaggeration or deflation of trends in projected climate change signals (Themeßl et al., 2012; Maurer & Pierce, 2014), thus undermining models' climate sensitivity.

Overfit in EQM is often minimised by employing a hybrid of parametric and non-parametric QM approaches in which extremes are corrected based on a defined threshold using DM. At the same time, EQM is applied to the rest of the datasets (Holthuijzen et al., 2022). The challenge is that it is difficult to select large enough thresholds to approximate a known DM, which is often a heavy-tailed distribution (Gutjahr & Heinemann, 2013; Holthuijzen et al., 2022). Further, region-specific studies are required to determine the optimal distribution (Li et al., 2021).

Tong et al. (2021) assessed the performance of EQM and quantile delta mapping (QDM), a hybrid QM, in correcting daily temperature and precipitation in China. QDM (Cannon et al., 2015) preserved future temperature change signals' magnitude and spatial distribution. Both methods preserved the change signal for precipitation but amplified precipitation increases, especially EQM. Precipitation increases of 14 to 20% were observed for EQM compared to QDM’s 3 to 10%. These increases were more pronounced in the dry season (winter). Similarly, Cannon et al. (2015) show that QDM outperforms EQM over Canada in preserving the magnitude of relative trends in precipitation extremes. EQM inflated the maximum change signal by a factor greater than four compared to 1.2 for QDM.

The superiority of QDM, a two-step process, over EQM is due to its algorithm that accounts for climate change signals. Firstly, relative changes to model projections are detrended by quantiles, a concept referred to as detrended quantile mapping (DQM), and the filtered simulation is bias-corrected by a QM transfer function (e.g., EQM) developed during the calibration stage (Cannon et al., 2015; Tong et al., 2021). Finally, the detrended relative changes in quantiles, which are absolute for temperature and relative for precipitation, are superimposed on the bias-corrected model outputs by adding or multiplying, respectively. A possible weakness is that detrended climate change signals are generally limited to the mean of climate models and thus do not capture all quantiles, including tails of distributions that often describe extremes (Cannon et al., 2015).

Framework for evaluation of the success/appropriateness of bias correction

This thesis did not evaluate the appropriateness of the bias correction method employed in the study; however, this section describes the approach that can be adopted.

Climate risk assessments that aim to translate future climate changes into impact information rely on bias correction methods that preserve statistics critical for the selected impact modelling approach. For instance, it is crucial to maintain cross-correlations, the interannual and multiannual variability of precipitation, and other hydro-climate factors, such as temperature, solar radiation, and wind speed, to comprehend the danger of severe, multiannual drought under future climate change (Vogel et al., 2023). Thus, many studies have focused on evaluating bias correction methods for the climate variables they aim to correct. Most of these evaluations are carried out in the climate domain (i.e., on post-processed GCM outputs), while fewer studies assess it in the impact domain (i.e., focusing on impact model outputs driven by GCM inputs) (Vogel et al., 2023). These evaluations focus on a single target variable (i.e., univariate evaluation, e.g., rainfall only) or a range of connected variables (i.e., multivariate evaluation), as illustrated in Table 4 - 11. These approaches range from simpler evaluations, such as in Category A, to more complex evaluation methods, such as in Category D.

Several studies that examine the influence of bias correction on derived impacts (e.g., hydrology) vary considerably between studies and are rarely performed comprehensively (Vogel et al., 2023). Upon synthesizing existing approaches, Vogel et al. (2023) developed an impacts-centric evaluation framework, ensuring robust evaluation of impact studies. The framework (Figure 4 - 18), which falls into category D (Table 4 - 11), identifies downscaling and bias correction methods that minimise biases in impacts across a range of variables, key statistical domains, and temporal and regional aggregations. The approach comprises the following steps:

a) Part 1 - Climate data processing:
   Step 1: selection of reference climate datasets (e.g., rain gauge observations, SPP data, or reanalysis data); Step 2: selection of a variety of downscaling and bias correction approaches; and Step 3: generation of downscaled and bias-corrected climate forcings including interpolation or spatial disaggregation before or after bias correction (depending on the method) to the resolution of the observed data.
b) Part 2 - Impact simulations:
   Step 4: selection or formulation of an impact model (e.g., statistical or process-based hydrological model) that describes impacts for the system of interest (see Step 1); and Step 5: generation of impacts simulations for the historical reference period using observed climate inputs and GCM-based impacts simulation using downscaled and bias corrected climate forcings (see Step 3).
c) Part 3 - Evaluation in impacts domain:
   Step 6: selection of appropriate performance metrics in impacts space that are of relevance to stakeholders (e.g., relating to the mean, variability, and extremes); Step 7: selection of spatial and temporal scales of relevance to stakeholders (e.g., spatial: regional aggregations relevant to the impact domain such as eco-climatic zones, major river basins, etc.; temporal: time scales of relevance for end-user applications such as wet/dry season, 3-month seasons, monthly, annual, etc.); Step 8: computation of bias in impacts space, for all impact variables (Step 5), performance metrics (Step 6), spatial and temporal aggregations (Step 7) of interest; Step 9: ranking of bias correction and downscaling methods per performance metric; and Step 10: calculation of overall ranking (as average with or without weighting).

Vogel et al. (2023) applied the above steps in a hydrological application. They concluded that multi-variate bias correction that considers cross-correlations, temporal auto-correlations, and biases at multiple time scales (daily to annual) performs best in reducing biases in hydrological output variables.

Table 4 - 11: Evaluation approaches for bias correction methods (source: Vogel et al. (2023)).

Number of Climate Variables Evaluated	Evaluation in the Climate Domain	Evaluation in the Impact Domain
Univariate evaluation	**Category A:** evaluation of bias correction for individual climate variables	**Category C:** evaluation of bias correction for climate impacts for individual variables
Multivariate evaluation	**Category B:** evaluation of bias correction for multiple climate variables	**Category D:** evaluation of bias correction for climate impacts for multiple impact variables - capturing various aspects of impacts

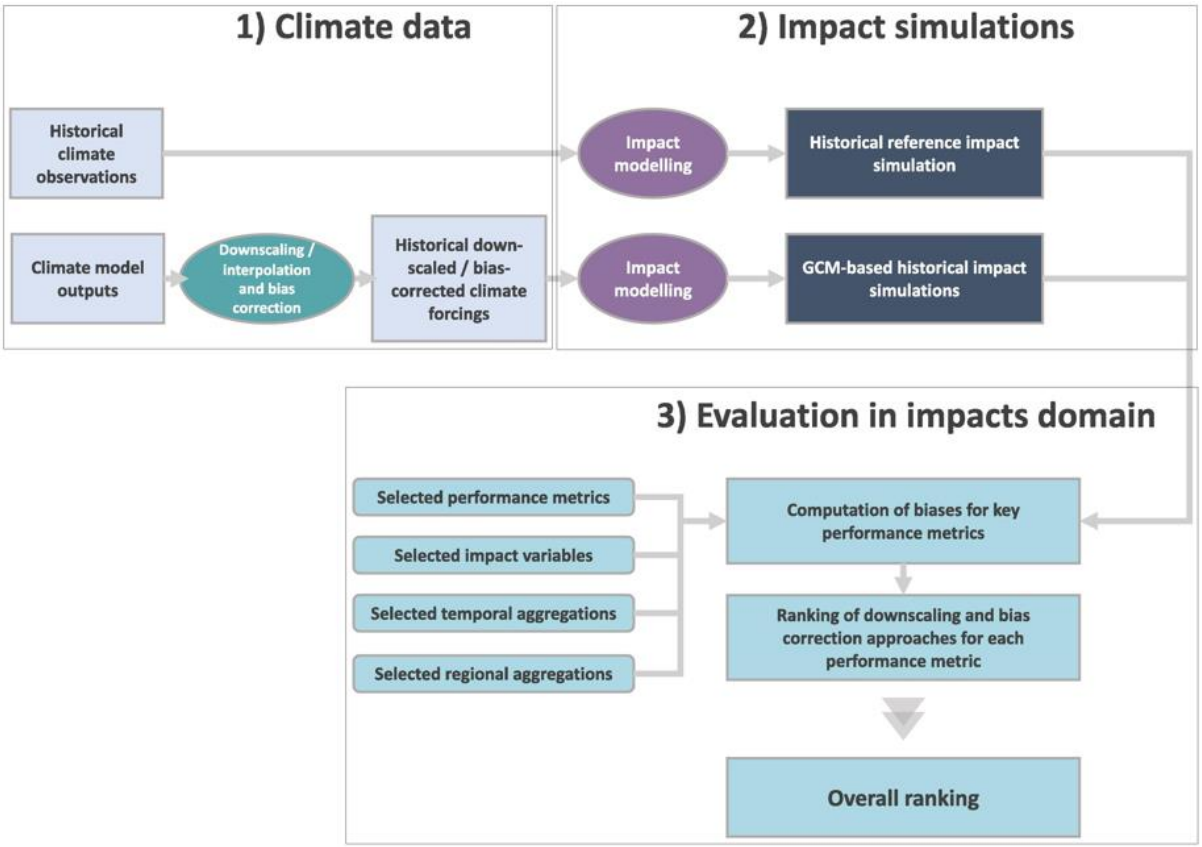

Figure 4 - 18: Impacts-centric evaluation framework for assessing bias correction methods (source: Vogel et al. (2023)).